



**Ollscoil
Mhá Nuad**

Ollscoil na hÉireann
Má Nuad

Towards Anyonic Quantum Computation in
Spinor Bose-Einstein Condensates

Nathan Fox B.Sc.

A thesis submitted for the degree of

Masters by Research

to the

National University of Ireland Maynooth

Department of Theoretical Physics

October 2022

Department Head: Dr. Joost Slingerland

Supervisor: Dr. Joost Slingerland

Contents

1	The Gross-Pitaevskii Equation for a Spinless Condensate	1
2	Hydrodynamic Equations for a Spinless Condensate	9
3	Spinor Bose-Einstein condensates	13
3.1	Hamiltonian for a Spinor Bose-Einstein Condensate	13
3.1.1	General Setup for Spin-n Condensate	13
3.1.2	Interaction Hamiltonian for Spin-1 Condensate	18
3.1.3	Interaction Hamiltonian for spin-2 Condensate	19
3.2	Gross-Pitaevskii Equation for a Spinor Condensate	20
3.2.1	Mean field theory: Spin 1 condensate	25
3.2.2	Mean field theory: Spin 2 condensate	29
4	Ground state phases	33
4.1	Spin One Ground State Phases	33
4.2	Spin 2 Ground State Phases	34
4.3	Graphical Representation of a Bose-Einstein Condensate	35
5	Vortices in Spinor Bose-Einstein Condensates	39
5.1	Symmetries of spinor bose-einstein condensates	39
5.2	Describing vortices in a certain phase	42
5.3	Examples of vortices in Bose-Einstein condensates	44
5.3.1	Vortices in a spinless condensate	44
5.3.2	Vortices in a spin one condensate	45
5.3.3	Vortices in a spin two condensate	46
6	Numerical Methods	57
6.1	Spin One Ground State Code	57
6.1.1	Equation setup	57
6.1.2	Solving the Spin One Gross-Pitaevskii Equations using Gradient Descent	64
6.1.3	Code implementation	70
6.1.4	Periodic Boundary Conditions	76
6.1.5	Code files	80
6.2	Spin Two Ground State Code	81
6.2.1	Equation setup	82
6.2.2	Code files	85
6.3	Spin Two Vortices	86
6.3.1	General setup	86
6.3.2	Numerical Implementation	88
6.4	Spin One Bogoliubov Excitations	92
6.4.1	Equation setup	93
6.4.2	Code implementation	95
6.5	Spin Two Bogoliubov Excitations	98

7	Results	107
7.1	Spin One Vortex Simulation	107
7.2	Spin One Bogoliubov Spectrum	128
7.3	Running the spin one codes	133
7.4	Spin Two Vortex Simulation	135
7.5	Spin Two Bogoliubov Spectrum	145
7.6	Bogoliubov Excitations of Vortex States	148
7.7	Running the spin two codes	157
7.8	Limitations of our code	158

Acknowledgements

I acknowledge financial support from the Irish Research Council Government of Ireland Postgraduate Scholarship GOIPG/2020/536.

I would like to thank the people that have both directly and indirectly helped me throughout the time that I have been working on this thesis. Hopefully they already know that I am grateful even if this does not reflect it well.

Firstly, I would like to thank my supervisor, Dr. Joost Slingerland. He has gone above and beyond the remit of supervisor on many occasions throughout this research project, especially within the last few months. Without his help, I would surely not have succeeded in completing this thesis.

I would like to thank the people that I spent most of my time with within the department (on the odd occasion that I was in with all the working from home that I did). Aoibhinn, Aonghus, Dale, Phillip, Hannah, Joe and Saoirse. The chats that we had did the world of good for me, both work related and otherwise, especially during the past two years when it was very easy to feel isolated.

I would like to thank the broader department, including lecturers who taught me and Suzie who, alongside Dr. Peter Coles, has kept the department going during the two years of my research masters.

I would like to mention the people within the research group that I was a part of: Aaron, Darragh, Babatunde, Domenico, Gert, Alex and Kevin. To have a close network of people doing work related to mine was of great benefit when I needed a bit of help in understanding something.

I would like to thank my friend group, known as the Nerd Network, for the support and friendship they have given me throughout my years at college. They have made Maynooth a much happier place to be and our zoom calls throughout the pandemic are a big reason that I found the motivation to push through very isolating weeks of work.

Finally, I would like to thank my family. My Mam, Dad and sister Shauna. They have been my biggest support right throughout my life, getting me through some pretty tough times and encouraging me to be the best version of myself that I can be. During this thesis, they have supported me in too many ways to mention, however I am keenly aware of all that they have done for me and am very grateful to them.

Abstract

The main objective of this thesis is to describe the codes that we have developed in order to simulate the ground state of a spin one and spin two Bose-Einstein condensate as well as codes that we have developed to solve the Bogoliubov equations used to examine the elementary excitations of these ground states. Motivated by viewing non-abelian vortices within a spin two condensate as anyons that can be used for quantum computation, we also look at introducing vortices into our codes by means of suitable initial conditions. To do this, we have developed methods for setting up and looking at vortices in our ground state systems. Finally, we will put all our code together by numerically solving the Bogoliubov equations for a ground state system with a vortex present and provide analysis of these results.

Introduction

Bose-Einstein condensates were first predicted in the 1920's by Einstein [1], when he generalized work carried out by Bose [2] regarding photons to atoms. The general idea is that under a certain temperature, a system of bosons will undergo a phase transition where a significant fraction of the bosons will sit in the ground state of the system. This is what is known as a Bose-Einstein condensate [3].

It was not until the mid 1990's that experimental realizations of this predicted phase of matter were seen, with three separate groups managing to cool the atoms in rubidium-87, sodium and lithium into a condensed state [4, 5, 6], using techniques such as laser and evaporative cooling as well as confining atoms in magnetic traps [3].

As a result of these experiments, this area of research grew explosively with studies directly related to understanding the theory behind these systems [7, 8], as well as theoretical papers building on initial experiments [9, 10]. As knowledge grew in this field, it was not long before both theoretical and experimental studies of spinor Bose-Einstein condensates, where the particles have spin degrees of freedom and hence multiple components, appeared [11, 12].

An interesting area of study to look at regarding Bose-Einstein condensates is that of vortex formation. Vortices are regions of circulation within a condensate that can be described by homotopy theory. For a spinless condensate, we see only one type of vortex occur due to the single-valuedness of the order parameter. However, for spinor condensates, there is a much richer variety of vortex types that can occur due to the presence of spin degrees of freedom. Many studies have been carried out in relation to vortices in spinless [13], two-component [14], and spinor condensates [15, 16, 17]. In recent years, there have been experimental realizations of vortices in both spin one and spin two condensates [18, 19, 20].

Of particular interest to us and what has served as the inspiration for this thesis is treating the non-abelian vortices that can occur in a spin two condensate as anyons, which can be used for topological quantum computation [21]. Anyons are quasiparticles that exist in two dimensions due to the wider variety of exchange statistics present [22, 23]. Certain anyon models can be used to represent qubits and the braiding and fusion of these anyons can be seen as acting with quantum gates on these qubits [24].

The main work of this thesis is to describe the codes that we have developed to simulate the ground state of a spin one and spin two condensate as well as codes that we have developed to look at Bogoliubov excitations on top of these ground states. Since we have a particular interest in vortices within these systems, we have also developed code that allows for vortices to be imprinted in the ground state of these condensates. We have published these codes online for public use [25].

The layout of this thesis is as follows. We first give a brief introduction to spinless Bose-Einstein condensates, describing the mean field approach used to model them which leads to the Gross-Pitaevskii equation. This is followed by a short section on describing a

condensate using the hydrodynamic approach and connecting this to the single vortex type that can be realized in a spinless condensate. We then turn our attention to introducing spinor condensates, focusing on the Hamiltonian used to describe these systems and how we arrive at the coupled Gross-Pitaevskii equations for spinor condensates in a mean-field approach. We also give a brief description of the different phases that can occur in spinor condensates based on the interaction that is occurring. Once we have introduced the systems of interest, we will look at how the symmetry of a spinor condensate is described and how this, along with homotopy theory, is used to describe the different types of vortices that can occur in these systems. Here, we will provide examples of these vortex types. We will then turn to describing how we have developed the codes used to simulate the ground state of a spin one and spin two condensate along with the codes for looking at Bogoliubov excitations on top of these states. This will include looking at how we set up the code in such a way that we can introduce vortices into our systems. Finally, we will provide results from this code, demonstrating its validity. Since we are particularly interested in the non-abelian vortex types seen in a spin two condensate, we will focus our attention here, not only showing some of the vortices that our code can hold in our systems, but also looking at excited states of these vortex states using our Bogoliubov code where we will provide analysis of results shown.

1 The Gross-Pitaevskii Equation for a Spinless Condensate

In order to describe a system of interacting bosons, some simplifications must be made. To arrive at a description of this system, let's first start by considering the most simple case and build up to the more complicated one. One of the simplest systems we can consider is that of a single particle trapped in some potential. The Hamiltonian for this system is given by the following:

$$H = \frac{\vec{P}^2}{2m} + V(\vec{r}), \quad (1.1)$$

where $\vec{P} = -i\hbar\nabla_r$ is the momentum operator, $V(\vec{r})$ is the potential that the particle is in and m is the mass of the particle.

The equation of motion for this system is governed by the time-dependent Schrodinger equation:

$$H\Psi(\vec{r}, t) = i\hbar\frac{\partial}{\partial t}\Psi(\vec{r}, t). \quad (1.2)$$

If we only wish to look at stationary states of the above equation, namely those of the form:

$$\Psi(\vec{r}, t) = e^{-iEt/\hbar}\psi(\vec{r}), \quad (1.3)$$

where E is the energy of the state in question and $\psi(\vec{r}) = \Psi(\vec{r}, 0)$, then the Schrodinger equation takes the following form for $\psi(\vec{r})$:

$$H\psi(\vec{r}) = E\psi(\vec{r}). \quad (1.4)$$

The ground state of this system, $\phi_0(\vec{r})$, is the state that minimizes the energy of equation (1.4).

Taking this one step further, let's now consider N non-interacting bosons in the same potential. The Hamiltonian for this system is:

$$H = \sum_{i=1}^N \left[\frac{\vec{P}_i^2}{2m} + V(\vec{r}_i) \right]. \quad (1.5)$$

If this system is in the condensed state where all particles occupy the lowest energy ground state, then, following [26], we can take the ground state of the full system to be a symmetrized product of single particle ground states.

$$\Psi(\vec{r}_1, \vec{r}_2, \dots, \vec{r}_N) = \prod_{i=1}^N \psi(\vec{r}_i). \quad (1.6)$$

As a result of this, (1.6) also satisfies the time-independent Schrodinger equation given by equation (1.4) with H now given by (1.5). The ground state will again minimize the

energy of (1.4).

With the above groundwork, we can now turn to the system of interest: N interacting bosons in a potential $V(\vec{r})$. In the same way that a system of N non-interacting bosons was described above; we would like to describe a state of this system using a single wave function. To do this, we need a simplified way of describing the interactions between the particles in the system. One such way of doing this is by adding an extra potential to the Hamiltonian that accounts for the force that a particle feels due to all other particles in the system and then adding over all pairs of particles to account for the entire system.

For our purposes, we will take the system to be dilute and therefore can take the potential that a particle at position \vec{r}_i feels due to interaction with a particle at \vec{r}_j to be of the form:

$$U = U_0 \delta(\vec{r}_i - \vec{r}_j), \quad (1.7)$$

where:

$$U_0 = \frac{4\pi\hbar^2 a}{m}, \quad (1.8)$$

and a is the s-wave scattering length between the two particles.

The full interaction potential, V_{int} is then given by summing over all pairs of particles:

$$V_{\text{int}} = U_0 \sum_{i < j} \delta(\vec{r}_i - \vec{r}_j). \quad (1.9)$$

Therefore, the Hamiltonian for this system of N interacting bosons is:

$$H = \sum_{i=1}^N \left[\frac{\vec{P}_i^2}{2m} + V(\vec{r}_i) \right] + U_0 \sum_{i < j} \delta(\vec{r}_i - \vec{r}_j). \quad (1.10)$$

We now try to find the energy of this system by taking a trial wavefunction where all particles occupy the same state. As a result, we again take our trial wavefunction to be a product of single particle states.

$$\Phi(\vec{r}_1, \vec{r}_2, \dots, \vec{r}_N) = \prod_{i=1}^N \phi(\vec{r}_i), \quad (1.11)$$

where $\phi(\vec{r}_i)$ is the single particle wave function for the particle at position \vec{r}_i in the system described by the Hamiltonian as in (1.10). We also take the normalization:

$$\int |\phi(\vec{r})|^2 d\vec{r} = 1 \quad (1.12)$$

The energy of the system in state Φ is then given by:

$$\begin{aligned}
E &= \langle \Phi | H | \Phi \rangle \\
&= \int \prod_i d\vec{r}_i \prod_p \phi^*(\vec{r}_p) \left[\sum_{i=1}^N \left[\frac{\vec{P}_i^2}{2m} + V(\vec{r}_i) \right] + U_0 \sum_{i<j} \delta(\vec{r}_i - \vec{r}_j) \right] \prod_q \phi(\vec{r}_q), \tag{1.13}
\end{aligned}$$

where $\phi^*(\vec{r})$ is the complex conjugate of $\phi(\vec{r})$.

We can work out each term of (1.13) individually, the first of these being:

$$\begin{aligned}
E_1 &= \int \prod_i d\vec{r}_i \prod_p \phi^*(\vec{r}_p) \sum_{i=1}^N \frac{\vec{P}_i^2}{2m} \prod_q \phi(\vec{r}_q), \\
&= \int \prod_i d\vec{r}_i \prod_p \phi^*(\vec{r}_p) \sum_{i=1}^N -\frac{\hbar^2}{2m} \nabla_{\vec{r}_i}^2 \prod_q \phi(\vec{r}_q), \\
&= -\frac{\hbar^2 N}{2m} \int \phi^*(\vec{r}) \nabla_{\vec{r}}^2 \phi(\vec{r}) d\vec{r}, \tag{1.14} \\
&= -\frac{\hbar^2 N}{2m} \left[\int \phi^*(\vec{r}) \nabla_{\vec{r}}^2 \phi(\vec{r}) d\vec{r} - \int \nabla_{\vec{r}} \phi^*(\vec{r}) \nabla_{\vec{r}} \phi(\vec{r}) d\vec{r} \right], \\
&= -\frac{\hbar^2 N}{2m} \left[\int_{\Sigma} \phi^*(\vec{r}) (\nabla \phi(\vec{r}) \cdot \hat{n}) d\vec{S} - \int |\nabla \phi(\vec{r})|^2 d\vec{r} \right], \\
&= \frac{\hbar^2 N}{2m} \int |\nabla \phi(\vec{r})|^2 d\vec{r}.
\end{aligned}$$

In going from the second to third line, we have used that the normalization (1.12) holds for all except the i th term. We integrate by parts to go from line three to four and use the divergence theorem to integrate the first term on the boundary of the system. Since all particles are confined by the potential $V(\vec{r})$, the first term on line five vanishes and so we are left with the final expression.

The second term of (1.13) is:

$$\begin{aligned}
E_2 &= \int \prod_i d\vec{r}_i \prod_p \phi^*(\vec{r}_p) \sum_i V(\vec{r}_i) \prod_q \phi(\vec{r}_q), \\
&= N \int |\phi(\vec{r})|^2 V(\vec{r}) d\vec{r}, \tag{1.15}
\end{aligned}$$

where (1.12) has again been used here going from the first to second line.

The third and final term of (1.13) is the interaction term:

$$\begin{aligned}
E_3 &= \int \prod_i d\vec{r}_i \prod_p \phi^*(\vec{r}_p) U_0 \sum_{i<j} \delta(\vec{r}_i - \vec{r}_j) \prod_q \phi(\vec{r}_q), \\
&= \sum_{i<j} \int d\vec{r}_i d\vec{r}_j |\phi(\vec{r}_i)|^2 |\phi(\vec{r}_j)|^2 U_0 \delta(\vec{r}_i - \vec{r}_j), \\
&= \frac{U_0 N(N-1)}{2} \int |\phi(\vec{r})|^4 d\vec{r},
\end{aligned} \tag{1.16}$$

where we have used (1.12) on all terms except the i th and j th term, and have then integrated over r_j . We then sum over the number of pairs of particles to get the final expression.

All in all, this means that the expression for the energy in (1.13) becomes:

$$E = N \int d\vec{r} \left[\frac{\hbar^2}{2m} |\nabla\phi(\vec{r})|^2 + V(\vec{r}) |\phi(\vec{r})|^2 + \frac{U_0(N-1)}{2} |\phi(\vec{r})|^4 \right]. \tag{1.17}$$

Now that we have an expression for the energy of this system, we can vary this to find the wavefunction $\phi(\vec{r})$ that minimizes it, hence finding an expression for the condensed state of the system.

Before minimizing the energy, let's take $\psi(\vec{r})$ to be the wave function of the condensed state which is given by:

$$\psi(\vec{r}) = \sqrt{N}\phi(\vec{r}), \tag{1.18}$$

which means that ψ is normalized in the following way:

$$\int |\psi(\vec{r})|^2 = N. \tag{1.19}$$

This means that we get the following expression for the energy functional by subbing (1.18) into (1.17) and dropping terms of order $1/N$:

$$E[\psi] = \int d\vec{r} \left[\frac{\hbar^2}{2m} |\nabla\psi(\vec{r})|^2 + V(\vec{r}) |\psi(\vec{r})|^2 + \frac{U_0}{2} |\psi(\vec{r})|^4 \right]. \tag{1.20}$$

It is this energy functional that we now wish to minimize in order to find an equation for the the condensed state ψ . Since ψ is a complex wave function, we must minimize (1.20) with respect to both ψ and its complex conjugate, ψ^* . This means that we will get an equation with two components, one for ψ and one for ψ^* . It turns out, however that these equations are identical and so we will just focus on minimizing (1.20) with respect to ψ^* which will give the equation for ψ .

The problem of minimizing (1.20) under the constraint (1.19) is a constrained variation problem. We can solve this by defining the following functional:

$$K[\psi] = \int \left[\tilde{E}(\vec{r}, \psi, \psi') - \mu G(\vec{r}, \psi, \psi') \right] d\vec{r}, \tag{1.21}$$

where \tilde{E} is the integrand of (1.20), ψ' is equal to $\nabla_{\vec{r}}\psi$, μ is a Lagrange multiplier and

$$G(\vec{r}, \psi, \psi') = |\psi(\vec{r})|^2 \quad (1.22)$$

To find the equation for ψ which minimizes K , we apply the Euler-Lagrange equation with respect to ψ^* :

$$\begin{aligned} & \frac{\partial}{\partial \psi^*}(\tilde{E} - \mu G) - \frac{d}{d\vec{r}} \left[\frac{\partial}{\partial (\psi^*)'}(\tilde{E} - \mu G) \right] = 0 \\ \implies & \frac{\partial \tilde{E}}{\partial \psi^*} - \frac{d}{d\vec{r}} \left(\frac{\partial \tilde{E}}{\partial (\psi^*)'} \right) - \mu \left[\frac{\partial G}{\partial \psi^*} - \frac{d}{d\vec{r}} \left(\frac{\partial G}{\partial (\psi^*)'} \right) \right] = 0 \end{aligned} \quad (1.23)$$

Working out the above, we are left with the following equation for the wave function of the condensed state:

$$-\frac{\hbar^2}{2m}\nabla^2\psi(\vec{r}) + V(\vec{r})\psi(\vec{r}) + U_0|\psi(\vec{r})|^2\psi(\vec{r}) = \mu\psi(\vec{r}). \quad (1.24)$$

This is the Gross-Pitaevskii equation which describes the stationary states of a Bose-Einstein condensate.

We see from the above that the Lagrange multiplier μ is the chemical potential that keeps the number of particles in the condensate fixed.

We can look at time-dependent states of Bose-Einstein condensates by generalizing equation (1.24) to the time-dependent Gross-Pitaevskii equation:

$$-\frac{\hbar^2}{2m}\nabla^2\psi(\vec{r}, t) + V(\vec{r})\psi(\vec{r}, t) + U_0|\psi(\vec{r}, t)|^2\psi(\vec{r}, t) = i\hbar\frac{\partial\psi(\vec{r}, t)}{\partial t} \quad (1.25)$$

Motivation for (1.25) comes from noting that (1.24) is essentially a non-linear Schrodinger equation where μ has replaced the energy per particle. Then in going from a time independent regime to a time-dependent one, we replace the chemical potential by a time derivative acting on ψ which now also depends on time. For consistency between equation (1.24) and (1.25), we must have that $\psi(\vec{r}, t)$ evolves in time as:

$$\psi(\vec{r}, t) = e^{-i\mu t/\hbar}\psi(\vec{r}). \quad (1.26)$$

Healing Length of the condensate An important length scale that we will have to consider throughout this research is the healing length of the condensate. This will determine the scale over which changes can occur in the condensate and is important when looking at the size of vortices.

In order to arrive at an expression for this length, we will look at a condensate in one dimension, in the region $x > 0$. That is, we will assume that we have an infinite potential in the region $x < 0$ and zero potential otherwise. The Gross-Pitaevskii equation for this

system is:

$$-\frac{\hbar^2}{2m} \frac{d^2\psi(x)}{dx^2} + U_0|\psi(x)|^2\psi(x) = \mu\psi(x). \quad (1.27)$$

For this system, we will have the following boundary conditions. We require $\psi(0) = 0$ and $\psi(\infty) = \psi_0$, where ψ_0 is a constant. What this means is that as we move away from the wall at $x = 0$, $\psi(x)$ approaches its bulk value, ψ_0 , at which the derivative of $\psi(x)$ is zero. As a result we can find a value for the chemical potential for this system by looking at the system when $\psi(x) = \psi_0$ and the derivative of $\psi(x)$ is zero. Plugging this into equation (1.27) gives the following for μ .

$$\mu = U_0|\psi_0|^2 = U_0n. \quad (1.28)$$

Here we approximate the absolute value of the condensate's bulk value, $|\psi_0|^2$ as the particle density, n .

Rearranging (1.27) and subbing in for μ , we get:

$$\frac{\hbar^2}{2m} \frac{d^2\psi(x)}{dx^2} = -U_0(|\psi_0|^2 - |\psi(x)|^2)\psi(x). \quad (1.29)$$

We will solve this equation in order to look at the wavefunction of this condensate, from which we arrive at the healing length.

First we will multiply across by ψ' . By this notation, we mean the derivative of $\psi(x)$ with respect to x . We will also, for now, use ψ'' to denote the second derivative with respect to x . For our case here, we will also assume that $\psi(x)$ is real and $\psi'(x) > 0$.

$$\psi''\psi' = -\frac{2mU_0}{\hbar^2}(\psi_0^2 - \psi^2)\psi'\psi. \quad (1.30)$$

We now integrate both sides with respect to ψ to get:

$$\frac{1}{2}(\psi')^2 = -\frac{2mU_0}{\hbar^2} \left[\frac{1}{2}\psi_0^2\psi^2 - \frac{1}{4}\psi^4 + C \right]. \quad (1.31)$$

In order to determine the constant of integration, C , we must use the boundary conditions of this system. Here, we will use that $\psi(\infty) = \psi_0$ which means that $\psi'(\infty) = 0$. Plugging this into (1.31) gives the following for C :

$$C = -\frac{1}{4}\psi_0^4. \quad (1.32)$$

We can then sub this back into (1.31) and simplify:

$$\begin{aligned}
\frac{1}{2}(\psi')^2 &= -\frac{2mU_0}{\hbar^2} \left[\frac{1}{2}\psi_0^2\psi^2 - \frac{1}{4}\psi^4 - \frac{1}{4}\psi_0^4 \right], \\
&= -\frac{mU_0}{\hbar^2} \left[\psi_0^2\psi^2 - \frac{1}{2}\psi^4 - \frac{1}{2}\psi_0^4 \right] \\
&= \frac{mU_0}{2\hbar^2} (\psi^2 - \psi_0^2)^2 \\
\implies \frac{d\psi}{dx} &= \sqrt{\frac{mU_0}{\hbar^2}} (\psi^2 - \psi_0^2). \tag{1.33}
\end{aligned}$$

We can rearrange this further and integrate both sides as shown below:

$$\begin{aligned}
-\int \frac{d\psi}{(\psi_0^2 - \psi^2)} &= \int \sqrt{\frac{mU_0}{\hbar^2}} dx \\
-\frac{1}{\psi_0} \operatorname{arctanh} \left(\frac{\psi}{\psi_0} \right) &= \sqrt{\frac{mU_0}{\hbar^2}} x + D. \tag{1.34}
\end{aligned}$$

To determine the constant of integration, D, we use the other boundary condition that we have not yet used, which is that $\psi(0) = 0$. When we sub this into (1.34), we get that $D = 0$. We can then rearrange (1.34) for $\psi(x)$.

$$-\frac{1}{\psi_0} \operatorname{arctanh} \left(\frac{\psi}{\psi_0} \right) = \sqrt{\frac{mU_0}{\hbar^2}} x \tag{1.35}$$

$$\implies \psi(x) = \psi_0 \operatorname{tanh} \left(-\psi_0 \sqrt{\frac{mU_0}{\hbar^2}} x \right) \tag{1.36}$$

$$= -\psi_0 \operatorname{tanh} \left(\psi_0 \sqrt{\frac{mU_0}{\hbar^2}} x \right) \tag{1.37}$$

We can suppress the minus sign into ψ_0 out front. We also now substitute for $n = |\psi_0|^2$ inside the hyperbolic tangent function.

$$\psi(x) = \psi_0 \operatorname{tanh} \left(\sqrt{\frac{mnU_0}{\hbar^2}} x \right). \tag{1.38}$$

If we define $\xi^2 = \frac{\hbar^2}{2mnU_0}$, we can rewrite (1.38) in the following way:

$$\psi(x) = \psi_0 \operatorname{tanh} \left(\frac{x}{\sqrt{2}\xi} \right). \tag{1.39}$$

We see that the general behaviour of this wavefunction is given by the hyperbolic tan function. If $x = 0$, we see that the wavefunction is zero. However, if $x \gg \xi$, then we see that $\tanh \left(\frac{x}{\sqrt{2}\xi} \right)$ approaches one and so the condensate wavefunction approaches its bulk

value. Since this is happening on a scale of some number of lengths ξ , we say that ξ is the healing length of the condensate over which the condensate reaches its bulk value.

2 Hydrodynamic Equations for a Spinless Condensate

In order to gain some intuition for how vortices arise in Bose-Einstein condensates, let's first draw some parallels with fluid dynamics by formulating the Gross-Pitaevskii equation in terms of hydrodynamic equations [26].

The starting point for this section is the time-dependent Gross-Pitaevskii equation given by equation (1.25). If we multiply this by $\psi^*(\vec{r}, t)$ and subtract the complex conjugate of the resulting equation, we are left with:

$$\frac{\partial |\psi|^2}{\partial t} + \nabla \cdot \left[\frac{\hbar}{2mi} (\psi^* \nabla \psi - \psi \nabla \psi^*) \right] = 0, \quad (2.1)$$

where we have used the product rule for differentiation and the identity:

$$\nabla^2 \psi = \nabla \cdot (\nabla \psi). \quad (2.2)$$

We have also suppressed the spatial and time dependence of ψ for notational convenience.

By inspecting equation (2.1), we see that it has the form of a continuity equation:

$$\frac{\partial n}{\partial t} + \nabla \cdot (n \vec{v}) = 0, \quad (2.3)$$

where $n = |\psi|^2$ is the particle density and \vec{v} is the velocity of the condensate given by:

$$\vec{v} = \frac{\hbar}{2mi} \frac{(\psi^* \nabla \psi - \psi \nabla \psi^*)}{|\psi|^2}. \quad (2.4)$$

Using the above, we can obtain two useful physical observables of the condensate by rewriting the wave function in polar form:

$$\psi = f e^{i\phi}, \quad (2.5)$$

where $f = |\psi|$ and ϕ is the phase of the complex wave function.

From this, we get expressions for the particle density and velocity of the condensate:

$$n = f^2, \quad (2.6)$$

$$\vec{v} = \frac{\hbar}{m} \nabla \phi, \quad (2.7)$$

where we have obtained the second expression by subbing (2.5) into (2.4).

From equation (2.7), we immediately see that the motion of the condensate corresponds to potential flow and as a result the motion of the condensate is irrotational.

We can find equations of motion for the particle density and velocity of the condensate by substituting (2.5) into the time-dependent Gross-Pitaevskii equation, (1.25):

$$-\frac{\hbar^2}{2m}\nabla^2[f e^{i\phi}] + V(\vec{r})f e^{i\phi} + U_0|f e^{i\phi}|^2 f e^{i\phi} = i\hbar\frac{\partial}{\partial t}[f e^{i\phi}], \quad (2.8)$$

$$\begin{aligned} \implies \frac{\hbar^2}{2m}[-\nabla^2 f + (\nabla\phi)^2 f - i f \nabla^2 \phi - 2i \nabla\phi \cdot \nabla f] e^{i\phi} \\ + V(\vec{r})f e^{i\phi} + U_0 f^3 e^{i\phi} = i\hbar\frac{\partial f}{\partial t} e^{i\phi} - \hbar\frac{\partial\phi}{\partial t} f e^{i\phi}. \end{aligned} \quad (2.9)$$

Splitting (2.9) into its real and imaginary components gives us the equations of motion we are looking for. The imaginary part of (2.9) is:

$$\begin{aligned} -\frac{\hbar^2}{2m}[f \nabla^2 \phi + 2 \nabla\phi \cdot \nabla f] &= \hbar\frac{\partial f}{\partial t}, \\ -\frac{\hbar^2}{m}[f^2 \nabla^2 \phi + 2 f \nabla\phi \cdot \nabla f] &= 2f\hbar\frac{\partial f}{\partial t}, \\ -\frac{\hbar}{m}\nabla \cdot (f^2 \nabla\phi) &= \frac{\partial(f^2)}{\partial t}, \end{aligned} \quad (2.10)$$

where, in going from the second to third line, we have used the chain rule for differentiation on the right hand side. On the left hand side, we have used the product rule identity for the divergence operator:

$$\nabla \cdot (\psi \vec{A}) = \psi \nabla \cdot \vec{A} + \vec{A} \cdot \nabla \psi, \quad (2.11)$$

where ψ is a scalar field and \vec{A} is a vector field.

Equation (2.10) is the continuity equation rewritten in terms of the scalar field ϕ and particle density f^2 . The real part component of (2.9) is:

$$\begin{aligned} \frac{\hbar^2}{2m}[-\nabla^2 f + (\nabla\phi)^2 f] + fV(\vec{r}) + U_0 f^3 &= -\hbar\frac{\partial\phi}{\partial t} f \\ -\frac{\hbar^2}{2mf}\nabla^2 f + \frac{1}{2}mv^2 + V(\vec{r}) + U_0 f^2 &= -\hbar\frac{\partial\phi}{\partial t}. \end{aligned} \quad (2.12)$$

Equation (2.12) gives an equation of motion for the scalar potential ϕ . In order to get an equation of motion for the velocity of the condensate, we take the gradient of this:

$$m\frac{\partial\vec{v}}{\partial t} = -\nabla \left(V(\vec{r}) + nU_0 - \frac{\hbar^2}{2m\sqrt{n}}\nabla^2\sqrt{n} + \frac{1}{2}mv^2 \right). \quad (2.13)$$

In order to rewrite (2.13) in a form that is more familiar, we note that, for a uniform condensate, the chemical potential is given as $\mu = nU_0$. To see this, examine the Gross-Pitaevskii equation for a stationary state as given by (1.24), neglecting the kinetic and potential energy terms but keeping the interaction potential. We can then use the Gibbs-Duhem relation relating changes to the chemical potential of a system to changes in pressure

at zero temperature, $dp = nd\mu$.

Using this, we can rewrite (2.13):

$$\frac{\partial \vec{v}}{\partial t} = -\frac{1}{mn} \nabla p - \nabla \left(\frac{v^2}{2} \right) + \frac{1}{m} \nabla \left(\frac{\hbar^2}{2m\sqrt{n}} \nabla^2 \sqrt{n} \right) - \frac{1}{m} \nabla V(\vec{r}). \quad (2.14)$$

This equation is the analogue of the Euler equation for fluid dynamics. The usual form of the Euler equation for a perfect fluid with irrotational flow is:

$$\frac{\partial \vec{v}}{\partial t} = -\frac{1}{mn} \nabla p - \nabla \left(\frac{v^2}{2} \right) - \frac{1}{m} \nabla V(\vec{r}). \quad (2.15)$$

The only difference between equations (2.14) and (2.15) is the third term on the right hand side of (2.14). This term is called the quantum pressure term and accounts for forces due to spatial variations of the wave function of the condensed state.

We saw earlier in this section from equation (2.7) that the motion of the condensate is irrotational and as such we would normally conclude from this that no vortices are present. However, this is not the case here. Let's consider the circulation of the condensate around a closed loop, C .

$$\tau = \oint_C \vec{v} \cdot d\vec{l} = \frac{\hbar}{m} \nabla \phi \cdot d\vec{l}. \quad (2.16)$$

We can calculate this circulation by taking into account that the wavefunction of the condensate must be single-valued. This means that if we go around a loop in the condensate and end at the same point that we started, we must get the same value for the condensate wavefunction at this point. This means that the change in the phase of the wavefunction, $\nabla \phi$, must be a multiple of 2π along a closed loop.

$$\oint_C \nabla \phi \cdot d\vec{l} = 2\pi l. \quad (2.17)$$

Subbing this into (2.16) gives:

$$\tau = \frac{2\pi \hbar l}{m} = \frac{\hbar}{m} l. \quad (2.18)$$

Therefore we see that the circulation is quantized in units of $\frac{\hbar}{m}$. This means that we can get one type of vortex in a spinless condensate. This vortex consists of a winding of the phase of the wavefunction where the phase winds from zero to 2π an integer number of times. We will arrive at this result again when we consider vortices in a condensate from the point of view of homotopy theory in section (5).

3 Spinor Bose-Einstein condensates

With the formalism of a spinless condensate set up in the previous sections; we can now take a similar approach in order to deal with a system of bosons with spin. To do this, we will follow the approach taken in [27] and first consider the Hamiltonian for this system. From this, we will derive the Gross-Pitaevskii equation for a spinor Bose-Einstein condensate coming from a mean-field approach. We note that some of the formalism here has been previously dealt with for spin two in [28] and the interaction Hamiltonian for spin one has been originally looked at in [29, 30].

3.1 Hamiltonian for a Spinor Bose-Einstein Condensate

3.1.1 General Setup for Spin-n Condensate

To start, consider a system of identical bosons with mass M and spin f . This system is described by field operators $\hat{\Psi}_m(\vec{r})$, where m is the magnetic quantum number running from $-f$ to f and the field operators satisfy the canonical commutation relations:

$$\left[\hat{\Psi}_m(\vec{r}), \hat{\Psi}_{m'}^\dagger(\vec{r}') \right] = \delta_{mm'} \delta(\vec{r} - \vec{r}'), \quad (3.1)$$

$$\left[\hat{\Psi}_m(\vec{r}), \hat{\Psi}_{m'}(\vec{r}') \right] = \left[\hat{\Psi}_m^\dagger(\vec{r}), \hat{\Psi}_{m'}^\dagger(\vec{r}') \right] = 0. \quad (3.2)$$

As was done in the spinless case, we will first look at the non-interacting system. The Hamiltonian for this is given by:

$$\hat{H}_0 = \int d\vec{r} \sum_{m, m'=-f}^f \hat{\Psi}_m^\dagger \left[-\frac{\hbar^2 \nabla^2}{2M} + V(\vec{r}) - p(f_z)_{mm'} + q(f_z^2)_{mm'} \right] \hat{\Psi}_{m'}, \quad (3.3)$$

which has the usual kinetic energy term and potential that the particles are in. The linear and quadratic Zeeman terms, p and q , are included to allow for the presence of external fields such as a magnetic field. Within these terms we are using the (m, m') components of the f_z and f_z^2 spin matrices, the spin matrices f_ν where $\nu = (x, y, z)$ for spin one and spin two are listed below:

$$f_x = \frac{1}{\sqrt{2}} \begin{pmatrix} 0 & 1 & 0 \\ 1 & 0 & 1 \\ 0 & 1 & 0 \end{pmatrix}, \quad f_y = \frac{i}{\sqrt{2}} \begin{pmatrix} 0 & -1 & 0 \\ 1 & 0 & -1 \\ 0 & 1 & 0 \end{pmatrix}, \quad f_z = \begin{pmatrix} 1 & 0 & 0 \\ 0 & 0 & 0 \\ 0 & 0 & -1 \end{pmatrix}. \quad (3.4)$$

$$\begin{aligned}
f_x &= \begin{pmatrix} 0 & 1 & 0 & 0 & 0 \\ 1 & 0 & \sqrt{\frac{3}{2}} & 0 & 0 \\ 0 & \sqrt{\frac{3}{2}} & 0 & \sqrt{\frac{3}{2}} & 0 \\ 0 & 0 & \sqrt{\frac{3}{2}} & 0 & 1 \\ 0 & 0 & 0 & 1 & 0 \end{pmatrix}, \\
f_y &= \begin{pmatrix} 0 & -i & 0 & 0 & 0 \\ i & 0 & -i\sqrt{\frac{3}{2}} & 0 & 0 \\ 0 & i\sqrt{\frac{3}{2}} & 0 & -i\sqrt{\frac{3}{2}} & 0 \\ 0 & 0 & i\sqrt{\frac{3}{2}} & 0 & -i \\ 0 & 0 & 0 & i & 0 \end{pmatrix}, \\
f_z &= \begin{pmatrix} 2 & 0 & 0 & 0 & 0 \\ 0 & 1 & 0 & 0 & 0 \\ 0 & 0 & 0 & 0 & 0 \\ 0 & 0 & 0 & -1 & 0 \\ 0 & 0 & 0 & 0 & -2 \end{pmatrix}.
\end{aligned} \tag{3.5}$$

Neglecting the Zeeman terms, the Hamiltonian in (3.3) has the same form as that of the spinless case, however, we now sum over the different values of spin that the magnetic quantum number can take.

Now, let's include interactions in this system. Just like in the spinless case, we will assume that the system is dilute and as a result, we will only consider interactions where a particle at position \vec{r} feels a force due to a particle at position \vec{r}' . This interaction is spin conserving.

If we think of this interaction as the exchange of two particles, each with spin f , at positions \vec{r} and \vec{r}' , we can gain some insight into the form that the interaction Hamiltonian should take. Following [27], consider two identical particles of spin f . If we exchange these particles, the many body wave function picks up a phase factor of $(-1)^{2f}$. At the same time, the spin and orbital parts of the wave function will also change by $(-1)^{F+2f}$ and $(-1)^L$ respectively, where F is the total spin of the two particles in question and L is the relative orbital angular momentum of the particles. In order for the changes in the wave function to be consistent, we must have that the changes in the many body wave function equate to the combined changes in the spin and orbital parts of the wave function:

$$\begin{aligned}
(-1)^{2f} &= (-1)^{F+2f} \cdot (-1)^L \\
\implies (-1)^{F+L} &= 1,
\end{aligned} \tag{3.6}$$

which tells us that the sum of the total spin and orbital angular momentum must be even. Since we are considering a dilute system, we will only look at S -wave scattering between the particles ($L = 0$) which means that the total spin, F , between the two interacting particles must be even. Since the interaction is spin conserving, we can split the interaction Hamiltonian into different spin channels:

$$\hat{U} = \sum_{F=0,2,\dots,2f} \hat{U}^{(F)}, \quad (3.7)$$

where $\hat{U}^{(F)}$ is the interaction Hamiltonian between two bosons whose total spin is F .

This means that we can find the full interaction Hamiltonian, \hat{U} , by examining the form of the interaction Hamiltonian for each separate spin channel and then adding these together.

To determine the form of $\hat{U}^{(F)}$, consider the following operator that annihilates a pair of bosons at positions \vec{r} and \vec{r}' :

$$\hat{A}_{F\mathcal{M}}(\vec{r}, \vec{r}') = \sum_{m, m'=-f}^f \langle F, \mathcal{M} | f, m; f, m' \rangle \hat{\Psi}_m(\vec{r}) \hat{\Psi}_{m'}(\vec{r}'). \quad (3.8)$$

This operator contains the Clebsch-Gordon coefficients for transforming from an uncoupled two-particle state, where both particles have spin f , to a coupled single particle state with total spin F and magnetic quantum number \mathcal{M} .

It can be shown that, since the field operators $\hat{\Psi}_m(\vec{r})$ and $\hat{\Psi}_{m'}(\vec{r}')$ commute, $\hat{A}_{F\mathcal{M}}(\vec{r}, \vec{r}') = 0$ when F is odd. This is due to the fact that odd F will give antisymmetric Clebsch-Gordon coefficients when f is an integer. Therefore since m and m' run through all values from $-f$ to f , we will get sums of pairs that are summing to zero. This suggests that we can use (3.8) to construct $\hat{U}^{(F)}$. Since we are thinking of this interaction as an exchange of particles, we will need both creation and annihilation operators to remove particles with a given spin, and then replace these particles with some possibly different spin after interaction. This exchange should also contain a prefactor describing the strength of interaction between the two particles. All in all, this means that we can take the following form for the interaction Hamiltonian between two particles with total spin F :

$$\hat{U}^{(F)} = \frac{1}{2} \int d\vec{r} \int d\vec{r}' U^{(F)}(\vec{r}, \vec{r}') \sum_{\mathcal{M}=-F}^F \hat{A}_{F\mathcal{M}}^\dagger(\vec{r}, \vec{r}') \hat{A}_{F\mathcal{M}}(\vec{r}, \vec{r}'). \quad (3.9)$$

We have seen, from examining a spinless condensate, that this prefactor should take the form of (1.7), where we again take a delta function interaction due to the system being dilute. The only difference made to the prefactor we will take in this case is that we have to account for the spin channel we are considering which is done by taking different S -wave scattering lengths, a_F , for each total spin F channel.

$$U^{(F)}(\vec{r}, \vec{r}') = g_F \delta(\vec{r} - \vec{r}'), \quad (3.10)$$

where:

$$g_F = \frac{4\pi\hbar^2}{M} a_F. \quad (3.11)$$

Putting all of this together, we find the full interaction Hamiltonian:

$$\hat{U} = \frac{1}{2} \int d\vec{r} \sum_{m_1 m_2 m'_1 m'_2} C_{m'_1 m'_2}^{m_1 m_2} \hat{\Psi}_{m_1}^\dagger(\vec{r}) \hat{\Psi}_{m_2}^\dagger(\vec{r}) \hat{\Psi}_{m'_2}(\vec{r}) \hat{\Psi}_{m'_1}(\vec{r}), \quad (3.12)$$

where:

$$C_{m'_1 m'_2}^{m_1 m_2} = \frac{4\pi\hbar^2}{M} \sum_{F=0,2,\dots,2f} a_F \langle f, m_1; f, m_2 | \hat{P}_F | f, m'_1; f, m'_2 \rangle \quad (3.13)$$

$$\hat{P}_F = \sum_{\mathcal{M}=-F}^F |F, \mathcal{M}\rangle \langle F, \mathcal{M}|, \quad (3.14)$$

\hat{P}_F is a projection operator onto a two body state with total spin F .

Before we work out the interaction hamiltonian for the specific examples of a spin one and spin two condensate, we first introduce the following physical observables that we can relate to (3.8) and as such write the interaction hamiltonian in terms of these physical observables of the condensate. These are the total density operator:

$$\hat{n}(\vec{r}) = \sum_{m=-f}^f \hat{\Psi}_m^\dagger(\vec{r}) \hat{\Psi}_m(\vec{r}), \quad (3.15)$$

the singlet-pair operator:

$$\hat{A}_{00}(\vec{r}, \vec{r}') = \frac{1}{\sqrt{2f+1}} \sum_{m=-f}^f (-1)^{f-m} \hat{\Psi}_m(\vec{r}) \hat{\Psi}_{-m}(\vec{r}'), \quad (3.16)$$

and the spin density operator:

$$\hat{F}_\nu(\vec{r}) = \sum_{m, m'=-f}^f (f_\nu)_{mm'} \hat{\Psi}_m^\dagger(\vec{r}) \hat{\Psi}_{m'}(\vec{r}'), \quad (3.17)$$

where, in (3.17), $(f_\nu)_{mm'}$ are the (m, m') components of the spin matrices f_ν , where $\nu = x, y, z$. In (3.16), the Clebsch-Gordon coefficient for $F = \mathcal{M} = 0$ has been used:

$$\langle 0, 0 | f, m; f, m' \rangle = \delta_{m+m', 0} \frac{(-1)^{f-m}}{\sqrt{2f+1}}. \quad (3.18)$$

In order to relate these physical observables to $\hat{A}_{F\mathcal{M}}(\vec{r}, \vec{r}')$, we start with the complete-

ness relation for the projection operator given by (3.14):

$$\hat{1} = \sum_F \hat{P}_F, \quad (3.19)$$

and act the following operator on the left and right hand sides of (3.19):

$$\sum_{m_1 m_2 m'_1 m'_2} \hat{\Psi}_{m_1}^\dagger(\vec{r}) \hat{\Psi}_{m_2}^\dagger(\vec{r}') \langle f, m_1; f, m_2 | \cdot | f, m'_1; f, m'_2 \rangle \hat{\Psi}_{m'_2}(\vec{r}') \hat{\Psi}_{m'_1}(\vec{r}), \quad (3.20)$$

where \cdot denotes the left and right hand sides of (3.19). After acting with this on (3.19) and using (3.15) and (3.8), we get:

$$: \hat{n}(\vec{r}) \hat{n}(\vec{r}') : = \sum_{F=0,2,\dots,2f} \sum_{\mathcal{M}=-F}^F \hat{A}_{F\mathcal{M}}^\dagger(\vec{r}, \vec{r}') \hat{A}_{F\mathcal{M}}(\vec{r}, \vec{r}'), \quad (3.21)$$

where $::$ represents normal ordering which puts annihilation operators to the right of creation operators.

This gives us a relation between the total density operator and (3.8). In order to obtain a relation between (3.8) and the spin density operator, we consider the inner product for angular momentum:

$$\begin{aligned} \vec{f}_1 \cdot \vec{f}_2 &= \frac{1}{2} [(\vec{f}_1 + \vec{f}_2)^2 - f_1^2 - f_2^2] \\ &= \frac{1}{2} \vec{f}_{tot}^2 - f(f+1) \\ &= \frac{1}{2} F(F+1) - f(f+1), \end{aligned} \quad (3.22)$$

where \vec{f}_i is the total spin angular momentum vector for particle i , f is the spin quantum number for \vec{f}_i which in this case is the same for each \vec{f}_i as we are considering identical particles. F is the spin quantum number of the total spin angular momentum vector, \vec{f}_{tot} .

Acting this on the completeness relation expression (3.19) gives:

$$\vec{f}_1 \cdot \vec{f}_2 = \sum_F \left[\frac{1}{2} F(F+1) - f(f+1) \right] \hat{P}_F. \quad (3.23)$$

We then find the relation we are looking for by acting again with (3.20) on the left and right hand side of (3.23). Substituting in for (3.17) and (3.8) in the resultant expression gives:

$$: \hat{F}(\vec{r}) \cdot \hat{F}(\vec{r}') : = \sum_{F=0,2,\dots,2f} \left[\frac{1}{2} F(F+1) - f(f+1) \right] \sum_{\mathcal{M}=-F}^F \hat{A}_{F\mathcal{M}}^\dagger(\vec{r}, \vec{r}') \hat{A}_{F\mathcal{M}}(\vec{r}, \vec{r}'), \quad (3.24)$$

where in obtaining the above, we used the following expression:

$$\langle f, m_1; f, m_2 | \vec{f}_1 \cdot \vec{f}_2 | f, m'_1; f, m'_2 \rangle = \sum_{\nu=x,y,z} (f_\nu)_{m_1 m'_1} \cdot (f_\nu)_{m_2 m'_2}. \quad (3.25)$$

This gives us an expression relating the spin density operator and annihilation operator, $\hat{A}_{F\mathcal{M}}(\vec{r}, \vec{r}')$.

3.1.2 Interaction Hamiltonian for Spin-1 Condensate

We can now write out the relations above specifically for a spin-1 Bose-Einstein condensate by filling in $f = 1$ in equations (3.21) and (3.24):

$$: \hat{n}(\vec{r}) \cdot \hat{n}(\vec{r}') : = \sum_{\mathcal{M}} \hat{A}_{2\mathcal{M}}^\dagger(\vec{r}, \vec{r}') \hat{A}_{2\mathcal{M}}(\vec{r}, \vec{r}') + \hat{A}_{00}^\dagger(\vec{r}, \vec{r}') \hat{A}_{00}(\vec{r}, \vec{r}'), \quad (3.26)$$

$$: \hat{F}(\vec{r}) \cdot \hat{F}(\vec{r}') : = \sum_{\mathcal{M}} \hat{A}_{2\mathcal{M}}^\dagger(\vec{r}, \vec{r}') \hat{A}_{2\mathcal{M}}(\vec{r}, \vec{r}') - 2\hat{A}_{00}^\dagger(\vec{r}, \vec{r}') \hat{A}_{00}(\vec{r}, \vec{r}'). \quad (3.27)$$

If we subtract (3.27) from (3.26) and rearrange, we find an expression involving all three of our physical observables:

$$: \hat{n}(\vec{r}) \cdot \hat{n}(\vec{r}') : = : \hat{F}(\vec{r}) \cdot \hat{F}(\vec{r}') : + 3\hat{A}_{00}^\dagger(\vec{r}, \vec{r}') \hat{A}_{00}(\vec{r}, \vec{r}') \quad (3.28)$$

This equation shows that we only have two independent operators describing the interaction in a spin-1 condensate.

Using the above relations, we can work out the interaction Hamiltonian given by (3.7) and (3.9). Since we are looking at spin-1 ($f=1$), (3.7) reduces to:

$$\hat{U} = \hat{U}^0 + \hat{U}^2. \quad (3.29)$$

We then get expressions for \hat{U}^0 and \hat{U}^2 from (3.9):

$$\hat{U}^{(0)} = \frac{g_0}{2} \int d\vec{r} \hat{A}_{00}^\dagger(\vec{r}) \hat{A}_{00}(\vec{r}) \quad (3.30)$$

$$\begin{aligned} \hat{U}^{(2)} &= \frac{g_2}{2} \int d\vec{r} \sum_{\mathcal{M}=-2}^2 \hat{A}_{2\mathcal{M}}^\dagger(\vec{r}) \hat{A}_{2\mathcal{M}}(\vec{r}) \\ &= \frac{g_2}{2} \int d\vec{r} \left[: \hat{n}^2(\vec{r}) : - \hat{A}_{00}^\dagger(\vec{r}) \hat{A}_{00}(\vec{r}) \right]. \end{aligned} \quad (3.31)$$

Here, we have integrated over \vec{r}' which sets $\vec{r}' = \vec{r}$ due to the delta function interaction as described by the expression for the interaction prefactor, (3.10). For conciseness, we adopt the notation $\hat{A}_{F\mathcal{M}}(\vec{r}) = \hat{A}_{F\mathcal{M}}(\vec{r}, \vec{r})$. In going from the first to second line of (3.31) we have

used equation (3.26).

Substituting (3.30) and (3.31) back into (3.29), we get the full expression for the interaction Hamiltonian of a spin-1 Bose-Einstein condensate:

$$\begin{aligned}\hat{U} &= \int d\vec{r} \left[\frac{g_2}{2} : \hat{n}^2(\vec{r}) : + \frac{g_0 - g_2}{2} \hat{A}_{00}^\dagger(\vec{r}) \hat{A}_{00}(\vec{r}) \right], \\ \implies \hat{U} &= \frac{1}{2} \int d\vec{r} \left[c_0 : \hat{n}^2(\vec{r}) : + c_1 : \hat{F}^2(\vec{r}) : \right].\end{aligned}\tag{3.32}$$

Here, we have used (3.28) and have defined c_0 and c_1 in the following way:

$$\begin{aligned}c_0 &= \frac{g_0 + 2g_2}{3}, \\ c_1 &= \frac{g_2 - g_0}{3}.\end{aligned}\tag{3.33}$$

The strength of interaction parameters, g_F , are defined in (3.11).

3.1.3 Interaction Hamiltonian for spin-2 Condensate

In the same way that was done for a spin-1 condensate, we now find the interaction Hamiltonian for a spin-2 condensate by first evaluating equations (3.21) and (3.24) for $f = 2$:

$$\begin{aligned}: \hat{n}(\vec{r}) \cdot \hat{n}(\vec{r}') : &= \sum_{\mathcal{M}} \hat{A}_{4\mathcal{M}}^\dagger(\vec{r}, \vec{r}') \hat{A}_{4\mathcal{M}}(\vec{r}, \vec{r}') + \sum_{\mathcal{M}} \hat{A}_{2\mathcal{M}}^\dagger(\vec{r}, \vec{r}') \hat{A}_{2\mathcal{M}}(\vec{r}, \vec{r}') \\ &+ \hat{A}_{00}^\dagger(\vec{r}, \vec{r}') \hat{A}_{00}(\vec{r}, \vec{r}'),\end{aligned}\tag{3.34}$$

$$\begin{aligned}: \hat{F}(\vec{r}) \cdot \hat{F}(\vec{r}') : &= 4 \sum_{\mathcal{M}} \hat{A}_{4\mathcal{M}}^\dagger(\vec{r}, \vec{r}') \hat{A}_{4\mathcal{M}}(\vec{r}, \vec{r}') - 3 \sum_{\mathcal{M}} \hat{A}_{2\mathcal{M}}^\dagger(\vec{r}, \vec{r}') \hat{A}_{2\mathcal{M}}(\vec{r}, \vec{r}') \\ &- 6 \hat{A}_{00}^\dagger(\vec{r}, \vec{r}') \hat{A}_{00}(\vec{r}, \vec{r}').\end{aligned}\tag{3.35}$$

In a similar manner to the spin-1 case, we can combine the two equations above to obtain a third relation. Here, we multiply (3.34) by four and subtract this from (3.35). Rearranging this gives:

$$4 : \hat{n}(\vec{r}) \cdot \hat{n}(\vec{r}') : = : \hat{F}(\vec{r}) \cdot \hat{F}(\vec{r}') : + 7 \sum_{\mathcal{M}} \hat{A}_{2\mathcal{M}}^\dagger(\vec{r}, \vec{r}') \hat{A}_{2\mathcal{M}}(\vec{r}, \vec{r}') + 10 \hat{A}_{00}^\dagger(\vec{r}, \vec{r}') \hat{A}_{00}(\vec{r}, \vec{r}').\tag{3.36}$$

Comparing to the spin-1 case, where the interaction was described by two independent operators, we see here from equation (3.36) that the interaction is described by three independent operators.

Using these relations along with (3.7) and (3.9), we find the interaction Hamiltonian for a spin-2 condensate:

$$\begin{aligned}
\hat{U} &= \hat{U}^{(0)} + \hat{U}^{(2)} + \hat{U}^{(4)}, \\
&= \frac{1}{2} \int d\vec{r} \left[g_0 \hat{A}_{00}^\dagger(\vec{r}) \hat{A}_{00}(\vec{r}) + g_2 \sum_{\mathcal{M}=-2}^2 \hat{A}_{2\mathcal{M}}^\dagger(\vec{r}) \hat{A}_{2\mathcal{M}}(\vec{r}) + g_4 \sum_{\mathcal{M}=-4}^4 \hat{A}_{4\mathcal{M}}^\dagger(\vec{r}) \hat{A}_{4\mathcal{M}}(\vec{r}) \right], \\
&= \frac{1}{2} \int d\vec{r} \left[c_0 : \hat{n}^2(\vec{r}) : + c_1 : \hat{F}^2(\vec{r}) : + c_2 \hat{A}_{00}^\dagger(\vec{r}) \hat{A}_{00}(\vec{r}) \right],
\end{aligned} \tag{3.37}$$

where:

$$\begin{aligned}
c_0 &= \frac{4g_2 + 3g_4}{7}, \\
c_1 &= \frac{g_4 - g_2}{7}, \\
c_2 &= \frac{7g_0 - 10g_2 + 3g_4}{7}.
\end{aligned} \tag{3.38}$$

In going from line two to line three of (3.37), we have used (3.34) and (3.36) to eliminate the expressions involving $\hat{A}_{4\mathcal{M}}(\vec{r}, \vec{r}')$ and $\hat{A}_{2\mathcal{M}}(\vec{r}, \vec{r}')$ in favour of the physical observables.

3.2 Gross-Pitaevskii Equation for a Spinor Condensate

Now that we have worked out the full Hamiltonian for a spinor condensate, we can do the same thing as in the spinless case, and determine the energy for the system. Once we have done this, we again minimize this energy, resulting in the time-independent Gross-Pitaevskii equation for the ground state of the system.

To start, we need to expand the bosonic field operators, $\hat{\Psi}_m(\vec{r})$, in the Hamiltonian in terms of a complete orthonormal set of basis functions, $\{\phi_{mi}(\vec{r})\}$, describing the spin degree of freedom using the magnetic quantum number m running from $-f$ to f in integer steps and the spatial mode, i .

$$\hat{\Psi}_m(\vec{r}) = \sum_i \hat{a}_{mi} \phi_{mi}(\vec{r}). \tag{3.39}$$

Here, $\{\hat{a}_{mi}\}$ are annihilation operators satisfying the canonical commutation relations:

$$\begin{aligned}
[\hat{a}_{mi}, \hat{a}_{m'j}^\dagger] &= \delta_{mm'} \delta_{ij}, \\
[\hat{a}_{mi}, \hat{a}_{m'j}] &= [\hat{a}_{mi}^\dagger, \hat{a}_{m'j}^\dagger] = 0.
\end{aligned} \tag{3.40}$$

This setup ensures that the bosonic field operators still satisfy the canonical commutation

relations given by (3.1) and (3.2).

As mentioned, the basis functions are orthogonal and satisfy the completeness relation:

$$\begin{aligned} \int d\vec{r} \phi_{mi}^*(\vec{r}) \phi_{mj}(\vec{r}) &= \delta_{ij}, \\ \sum_i \phi_{mi}(\vec{r}) \phi_{mi}^*(\vec{r}') &= \delta(\vec{r} - \vec{r}'). \end{aligned} \quad (3.41)$$

We consider a state vector that creates N bosons in a single spatial mode ($i = 0$), superposed over all magnetic sublevels of the condensate:

$$|\zeta\rangle = \frac{1}{\sqrt{N!}} \left(\sum_{m=-f}^f \zeta_m \hat{a}_{m0}^\dagger \right)^N |vac\rangle \quad (3.42)$$

We will find the general expression for the energy of a system in the state given by (3.42). Once we find this, we will vary the prefactors ζ_m in order to minimize the energy and find an equation for the ground state of the system.

In order to find the energy for the state $|\zeta\rangle$, we will need the following relations:

$$\langle \zeta | \hat{\Psi}_m^\dagger(\vec{r}) \hat{\Psi}_{m'}(\vec{r}') | \zeta \rangle = \psi_m^*(\vec{r}) \psi_{m'}(\vec{r}'), \quad (3.43)$$

$$\langle \zeta | \hat{\Psi}_{m_1}^\dagger(\vec{r}_1) \hat{\Psi}_{m_2}^\dagger(\vec{r}_2) \hat{\Psi}_{m_2}(\vec{r}_3) \hat{\Psi}_{m_1}(\vec{r}_4) | \zeta \rangle = \left(1 - \frac{1}{N} \right) \psi_{m_1}^*(\vec{r}_1) \psi_{m_2}^*(\vec{r}_2) \psi_{m_2}(\vec{r}_3) \psi_{m_1}(\vec{r}_4), \quad (3.44)$$

where $\psi_m(\vec{r}) = \sqrt{N} \zeta_m \phi_{m0}(\vec{r})$.

To see where these two relations come from, we will derive the second of the two as it contains all the steps required to work out the first one along with steps only needed for the second one.

Starting with the left hand side of equation (3.44), we expand this out into its full form using (3.42) and (3.39):

$$\begin{aligned}
\langle \zeta | \hat{\Psi}_{m_1}^\dagger(\vec{r}_1) \hat{\Psi}_{m_2}^\dagger(\vec{r}_2) \hat{\Psi}_{m_2'}(\vec{r}_3) \hat{\Psi}_{m_1'}(\vec{r}_4) | \zeta \rangle &= \frac{1}{N!} \langle vac \left| \left(\sum_{m=-f}^f \zeta_m^* \hat{a}_{m0} \right)^N \right. \\
&\quad \sum_i \hat{a}_{m_1 i}^\dagger \phi_{m_1 i}^*(\vec{r}_1) \sum_i \hat{a}_{m_2 i}^\dagger \phi_{m_2 i}^*(\vec{r}_2) \sum_i \hat{a}_{m_3 i} \phi_{m_3 i}(\vec{r}_3) \\
&\quad \left. \sum_i \hat{a}_{m_4 i} \phi_{m_4 i}(\vec{r}_4) \left| \left(\sum_{m=-f}^f \zeta_m \hat{a}_{m0}^\dagger \right)^N \right| vac \right\rangle. \quad (3.45)
\end{aligned}$$

We will evaluate this expression by breaking it down into a series of steps, the first of these being:

$$\sum_i \hat{a}_{m_4 i} \phi_{m_4 i}(\vec{r}_4) \left| \left(\sum_{m=-f}^f \zeta_m \hat{a}_{m0}^\dagger \right)^N \right| vac \rangle \quad (3.46)$$

This first creates N particles, followed by an annihilation of any particle with magnetic quantum number m_4 . We can see from (3.46) that since we only created particles in spatial mode $i = 0$, the only nonzero contribution from this expression will be from the $i = 0$ term of the sum acting on the N particle state. This means that the above expression is equivalent to computing:

$$\hat{a}_{m_4 0} \phi_{m_4 0}(\vec{r}_4) \left| \left(\sum_{m=-f}^f \zeta_m \hat{a}_{m0}^\dagger \right)^N \right| vac \rangle. \quad (3.47)$$

To help calculate the above, we will relabel the terms in the following way and substitute back after:

$$\hat{A} = \hat{a}_{m_4 0} \phi_{m_4 0}(\vec{r}_4), \quad (3.48)$$

$$\hat{B} = \left(\sum_{m=-f}^f \zeta_m \hat{a}_{m0}^\dagger \right). \quad (3.49)$$

This now reduces (3.47) to:

$$\hat{A} \hat{B}^N | vac \rangle \quad (3.50)$$

We would like to have \hat{A} acting on the vacuum before \hat{B} and so we must commute A through each of the N \hat{B} operators.

To start, let's rewrite (3.50):

$$\begin{aligned}
\hat{A}\hat{B}^N|vac\rangle &= \hat{A}\hat{B}\hat{B}^{N-1}|vac\rangle, \\
&= \hat{B}\hat{A}\hat{B}^{N-1}|vac\rangle + [\hat{A}, \hat{B}] \hat{B}^{N-1}|vac\rangle, \\
&= \hat{B}\hat{A}\hat{B}\hat{B}^{N-2}|vac\rangle + [\hat{A}, \hat{B}] \hat{B}^{N-1}|vac\rangle, \\
&= \hat{B}^2\hat{A}\hat{B}^{N-2}|vac\rangle + \hat{B} [\hat{A}, \hat{B}] \hat{B}^{N-2}|vac\rangle + [\hat{A}, \hat{B}] \hat{B}^{N-1}|vac\rangle, \\
&\vdots \\
&= \hat{B}^N \hat{A}|vac\rangle + \sum_{n=1}^N \hat{B}^{n-1} [\hat{A}, \hat{B}] \hat{B}^{N-n}|vac\rangle.
\end{aligned} \tag{3.51}$$

In order to move the \hat{A} operator through each of the \hat{B} operators, we have used the definition of the commutator and rearranged for $\hat{A}\hat{B}$:

$$\hat{A}\hat{B} = \hat{B}\hat{A} + [\hat{A}, \hat{B}]. \tag{3.52}$$

Since \hat{A} is actually an annihilation operator as defined by (3.48), the first term in the last line of (3.51) goes to zero. We can express the second term of (3.51) by calculating the commutator:

$$[\hat{A}, \hat{B}] = \left[\hat{a}_{m_4 0}, \sum_{m=-f}^f \zeta_m \hat{a}_{m 0}^\dagger \right]. \tag{3.53}$$

We can expand out the commutator on the right hand side as a sum of commutators of the form:

$$\left[\hat{a}_{m_4 0} \phi_{m_4 0}(\vec{r}_4), \zeta_m \hat{a}_{m 0}^\dagger \right].$$

The only one of these that is nonzero is where $m = m_4$:

$$\left[\hat{a}_{m_4 0} \phi_{m_4 0}(\vec{r}_4), \zeta_{m_4} \hat{a}_{m_4 0}^\dagger \right] = \phi_{m_4 0}(\vec{r}_4) \zeta_{m_4} \left[\hat{a}_{m_4 0}, \hat{a}_{m_4 0}^\dagger \right] = \phi_{m_4 0}(\vec{r}_4) \zeta_{m_4}. \tag{3.54}$$

Subbing this into the last line of (3.51) gives:

$$\begin{aligned}
\hat{A}\hat{B}^N|vac\rangle &= \phi_{m_4 0}(\vec{r}_4) \zeta_{m_4} \sum_{n=1}^N \hat{B}^{n-1} \hat{B}^{N-n}|vac\rangle, \\
&= \phi_{m_4 0}(\vec{r}_4) \zeta_{m_4} \sum_{n=1}^N \hat{B}^{N-1}|vac\rangle \\
&= N \phi_{m_4 0}(\vec{r}_4) \zeta_{m_4} \hat{B}^{N-1}|vac\rangle.
\end{aligned} \tag{3.55}$$

Subbing back in for the operator \hat{B} gives us the expression for the first step of (3.45) given

by (3.46):

$$\sum_i \hat{a}_{m_4 i} \phi_{m_4 i}(\vec{r}_4) \left| \left(\sum_{m=-f}^f \zeta_m \hat{a}_{m0}^\dagger \right)^N \right| vac \rangle = N \zeta_{m_4} \phi_{m_4 0}(\vec{r}_4) \left(\sum_{m=-f}^f \zeta_m \hat{a}_{m0}^\dagger \right)^{N-1} |vac \rangle. \quad (3.56)$$

The next step from (3.45) is to compute

$$\begin{aligned} & \sum_i \hat{a}_{m_3 i} \phi_{m_3 i}(\vec{r}_3) \sum_i \hat{a}_{m_4 i} \phi_{m_4 i}(\vec{r}_4) \left| \left(\sum_{m=-f}^f \zeta_m \hat{a}_{m0}^\dagger \right)^N \right| vac \rangle, \\ &= \sum_i \hat{a}_{m_3 i} \phi_{m_3 i}(\vec{r}_3) N \zeta_{m_4} \phi_{m_4 0}(\vec{r}_4) \left(\sum_{m=-f}^f \zeta_m \hat{a}_{m0}^\dagger \right)^{N-1} |vac \rangle, \\ &= N(N-1) \zeta_{m_3} \phi_{m_3 0}(\vec{r}_3) \zeta_{m_4} \phi_{m_4 0}(\vec{r}_4) \left(\sum_{m=-f}^f \zeta_m \hat{a}_{m0}^\dagger \right)^{N-2} |vac \rangle. \end{aligned} \quad (3.57)$$

In going from the first to second line, we used (3.56). Then to go from the second to third line, we again used (3.56), but this time replace N with $N-1$, m_4 with m_3 and \vec{r}_4 with \vec{r}_3 .

The remaining section of (3.45) is:

$$\langle vac \left| \left(\sum_{m=-f}^f \zeta_m^* \hat{a}_{m0} \right)^N \right| \sum_i \hat{a}_{m_1 i}^\dagger \phi_{m_1 i}^*(\vec{r}_1) \sum_i \hat{a}_{m_2 i}^\dagger \phi_{m_2 i}^*(\vec{r}_2). \quad (3.58)$$

This can be calculated by using the same steps as above, however, now acting operators to the left instead of the right. Doing this and subbing back in for the full expression gives:

$$\begin{aligned} \langle \zeta | \hat{\Psi}_{m_1}^\dagger(\vec{r}_1) \hat{\Psi}_{m_2}^\dagger(\vec{r}_2) \hat{\Psi}_{m_2}(\vec{r}_3) \hat{\Psi}_{m_1}(\vec{r}_4) | \zeta \rangle &= \frac{1}{N!} \langle vac \left| \left(\sum_{m=-f}^f \zeta_m^* \hat{a}_{m0} \right)^{N-2} \right. \\ & (N(N-1))^2 \zeta_{m_1}^* \phi_{m_1 0}^*(\vec{r}_1) \zeta_{m_2}^* \phi_{m_2 0}^*(\vec{r}_2) \zeta_{m_3} \phi_{m_3 0}(\vec{r}_3) \zeta_{m_4} \phi_{m_4 0}(\vec{r}_4) \\ & \left. \left(\sum_{m=-f}^f \zeta_m \hat{a}_{m0}^\dagger \right)^{N-2} \right| vac \rangle. \end{aligned} \quad (3.59)$$

In the above expression, we can calculate the following inner product:

$$\langle vac | \left(\sum_{m=-f}^f \zeta_m^* \hat{a}_{m0} \right)^{N-2} \left(\sum_{m=-f}^f \zeta_m \hat{a}_{m0}^\dagger \right)^{N-2} | vac \rangle = (N-2)! \quad (3.60)$$

This can be seen by looking at the expression for the condensed state, $|\zeta\rangle$, given by (3.42). This creates N particles and has a normalization factor of $\frac{1}{\sqrt{N!}}$ so that $\langle \zeta | \zeta \rangle = 1$. In this case we are taking an inner product of a state creating $N-2$ particles but with no normalization factor. If our condensed state $|\zeta\rangle$ did not have the normalization factor, then $\langle \zeta | \zeta \rangle$ would equal $N!$. By this reasoning, we can see that the inner product we are looking at here must evaluate to $(N-2)!$.

Therefore, we can rewrite (3.59) as:

$$\begin{aligned} \langle \zeta | \hat{\Psi}_{m_1}^\dagger(\vec{r}_1) \hat{\Psi}_{m_2}^\dagger(\vec{r}_2) \hat{\Psi}_{m'_2}(\vec{r}_3) \hat{\Psi}_{m'_1}(\vec{r}_4) | \zeta \rangle &= (N(N-1))^2 \frac{(N-2)!}{N!} \\ &\quad \zeta_{m_1}^* \phi_{m_1 0}^*(\vec{r}_1) \zeta_{m_2}^* \phi_{m_2 0}^*(\vec{r}_2) \zeta_{m_3} \phi_{m_3 0}(\vec{r}_3) \zeta_{m_4} \phi_{m_4 0}(\vec{r}_4), \\ &= N(N-1) \zeta_{m_1}^* \phi_{m_1 0}^*(\vec{r}_1) \zeta_{m_2}^* \phi_{m_2 0}^*(\vec{r}_2) \zeta_{m_3} \phi_{m_3 0}(\vec{r}_3) \zeta_{m_4} \phi_{m_4 0}(\vec{r}_4), \\ &= \left(1 - \frac{1}{N}\right) \psi_{m_1}^*(\vec{r}_1) \psi_{m_2}^*(\vec{r}_2) \psi_{m'_2}(\vec{r}_3) \psi_{m'_1}(\vec{r}_4), \end{aligned} \quad (3.61)$$

where, on the last line, we have made the substitution $\psi_m(\vec{r}) = \sqrt{N} \zeta_m \phi_{m0}(\vec{r})$.

An extension which follows from (3.43) by a similar argument, that will be used in finding the energy in the state $|\zeta\rangle$ is the following:

$$\langle \zeta | \hat{\Psi}_m^\dagger(\vec{r}) \left(-\frac{\hbar^2 \nabla^2}{2M} \right) \hat{\Psi}_{m'}(\vec{r}') | \zeta \rangle = \psi_m^*(\vec{r}) \left(-\frac{\hbar^2 \nabla^2}{2M} \right) \psi_{m'}(\vec{r}') \quad (3.62)$$

3.2.1 Mean field theory: Spin 1 condensate

Now that we have relations (3.43), (3.44) and (3.62), we can calculate the energy of the system in the state $|\zeta\rangle$ by taking the expectation value of the Hamiltonian of the spin one condensate with this state. The full Hamiltonian for the spin one system is the sum of the non-interacting Hamiltonian, given by equation (3.3) with $f=1$, and the interaction Hamiltonian for spin one given by (3.32):

$$\begin{aligned} \hat{H} &= \hat{H}_0 + \hat{U}, \\ &= \int d\vec{r} \sum_{m,m'=-1}^1 \hat{\Psi}_m^\dagger \left[-\frac{\hbar^2 \nabla^2}{2M} + V(\vec{r}) - p(f_z)_m m' + q(f_z)_m m' \right] \hat{\Psi}_{m'} \\ &\quad + \frac{1}{2} \int d\vec{r} \left[c_0 : \hat{n}^2(\vec{r}) : + c_1 : \hat{F}^2(\vec{r}) : \right]. \end{aligned} \quad (3.63)$$

The energy of this system in the state $|\zeta\rangle$ is therefore:

$$E[\psi_m] = \langle \zeta | \hat{H} | \zeta \rangle, \\ = \int d\vec{r} \left\{ \sum_{m=-1}^1 \psi_m^* \left[-\frac{\hbar^2 \nabla^2}{2M} + V(\vec{r}) - pm + qm^2 \right] \psi_m + \frac{c_0}{2} n^2 + \frac{c_1}{2} |\vec{F}|^2 \right\}, \quad (3.64)$$

where n is the particle density given by:

$$n = n(\vec{r}) = \langle \zeta | \hat{n}(\vec{r}) | \zeta \rangle = \sum_{m=-1}^1 |\psi_m(\vec{r})|^2, \quad (3.65)$$

and $\vec{F} = (F_x, F_y, F_z)$ is the spin density vector where:

$$F_\nu(\vec{r}) = \langle \zeta | \hat{F}_\nu(\vec{r}) | \zeta \rangle, \\ = \sum_{m, m'=-1}^1 \psi_m^*(\vec{r}) (f_\nu)_{mm'} \psi_{m'}(\vec{r}). \quad (3.66)$$

As mentioned earlier, f_ν are the spin matrices for $\nu = x, y, z$. For spin one, the spin matrices are given by the following irreducible representation:

$$f_x = \frac{1}{\sqrt{2}} \begin{pmatrix} 0 & 1 & 0 \\ 1 & 0 & 1 \\ 0 & 1 & 0 \end{pmatrix}, \quad f_y = \frac{i}{\sqrt{2}} \begin{pmatrix} 0 & -1 & 0 \\ 1 & 0 & -1 \\ 0 & 1 & 0 \end{pmatrix}, \quad f_z = \begin{pmatrix} 1 & 0 & 0 \\ 0 & 0 & 0 \\ 0 & 0 & -1 \end{pmatrix}. \quad (3.67)$$

Using these and (3.66), we can work out the components of the spin density vector:

$$F_x = \frac{1}{2} [\psi_1^* \psi_0 + \psi_0^* (\psi_1 + \psi_{-1}) + \psi_{-1}^* \psi_0], \quad (3.68)$$

$$F_y = \frac{i}{\sqrt{2}} [-\psi_1^* \psi_0 + \psi_0^* (\psi_1 - \psi_{-1}) + \psi_{-1}^* \psi_0], \quad (3.69)$$

$$F_z = |\psi_1|^2 - |\psi_{-1}|^2. \quad (3.70)$$

With all of this, we can now find an equation for the ground state of the system in a similar way to what was done in section 1. Again, we will find the equation for the full wavefunction by noting that minimizing with respect to either of ψ_m or ψ_m^* will give an equivalent form of equation and so we choose to minimize with respect to ψ_m^* and to get an equation for ψ_m .

An important note to make is that what we are really varying is ζ_m , the coefficient governing the distribution of bosons in each magnetic sublevel as introduced in the condensate

state vector (3.42). This can be seen by looking at the definition of $\psi_m(\vec{r})$ defined from equation (3.44).

In order to conserve particle number, we take the following constraint on the wavefunction:

$$G[\psi] = \int (|\psi_1|^2 + |\psi_0|^2 + |\psi_{-1}|^2) d\vec{r} = N. \quad (3.71)$$

Above, we use $\psi = (\psi_1, \psi_0, \psi_{-1})$.

Therefore, the expression we wish to minimize is the following functional:

$$K[\psi] = \int [\bar{E}(\vec{r}, \psi, \psi') - \mu \bar{G}(\vec{r}, \psi, \psi')] d\vec{r}, \quad (3.72)$$

where μ is a lagrange multiplier used to keep the number of particles constant. \bar{E} is the integrand of the energy functional given by (3.64) and \bar{G} is the integrand of the constraint given by (3.71).

To minimize this, we use the Euler-Lagrange equation for each ψ_m , $m \in (1, 0, -1)$:

$$\frac{\partial}{\partial \psi_m^*} (\bar{E} - \mu \bar{G}) - \frac{d}{d\vec{r}} \left[\frac{\partial}{\partial (\psi_m^*)'} (\bar{E} - \mu \bar{G}) \right] = 0. \quad (3.73)$$

To work out the Euler-Lagrange equation for each ψ_m , it is useful to break up the integrand, $\bar{E} - \mu \bar{G}$ into the following three parts:

$$\bar{E} - \mu \bar{G} = \sum_{m=-1}^1 \psi_m^* \left[-\frac{\hbar^2 \nabla^2}{2M} + V(\vec{r}) - pm + qm^2 \right] \psi_m - \mu \sum_{m=-1}^1 |\psi_m|^2 \quad (3.74)$$

$$+ \frac{c_0}{2} \left(\sum_{m=-1}^1 \psi_m \psi_m^* \right)^2 \quad (3.75)$$

$$+ \frac{c_1}{2} [F_x^2 + F_y^2 + F_z^2]. \quad (3.76)$$

Looking at the full expression for the above integrand, we can see that there is no $(\psi_m^*)'$ dependence and so the second term in (3.73) is zero. This means that the Euler-Lagrange equations reduce to the following:

$$\frac{\partial}{\partial \psi_m^*} (\bar{E} - \mu \bar{G}) = 0. \quad (3.77)$$

We now work out this derivative for each part of the integrand $(\bar{E} - \mu \bar{G})$, starting with

(3.74):

$$\begin{aligned} \frac{\partial}{\partial \psi_m^*} \left(\sum_{m=-1}^1 \psi_m^* \left[-\frac{\hbar^2 \nabla^2}{2M} + V(\vec{r}) - pm + qm^2 \right] \psi_m - \mu \sum_{m=-1}^1 |\psi_m|^2 \right) \\ = \left[-\frac{\hbar^2 \nabla^2}{2M} + V(\vec{r}) - pm + qm^2 \right] \psi_m - \mu \psi_m, \end{aligned} \quad (3.78)$$

where $m \in (1, 0, -1)$. The derivative with respect to ψ_m^* of (3.75) is:

$$\frac{\partial}{\partial \psi_m^*} \left[\frac{c_0}{2} \left(\sum_{m=-1}^1 \psi_m \psi_m^* \right)^2 \right] = c_0 \left(\sum_{m=-1}^1 |\psi_m|^2 \right) \psi_m = c_0 n \psi_m. \quad (3.79)$$

Finally, we need to compute the derivative of (3.76) with respect to ψ_m . We will first calculate this derivative for one component of the spin density vector:

$$\begin{aligned} \frac{\partial F_\nu^2(\vec{r})}{\partial \psi_m^*} &= \frac{\partial}{\partial \psi_m^*} \left[\left(\sum_{m,m'=-1}^1 \psi_m^*(\vec{r}) (f_\nu)_{mm'} \psi_{m'}(\vec{r}) \right)^2 \right], \\ &= 2 \left(\sum_{m,m'=-1}^1 \psi_m^*(\vec{r}) (f_\nu)_{mm'} \psi_{m'}(\vec{r}) \right) \left(\sum_{m'=-1}^1 (f_\nu)_{mm'} \psi_{m'} \right), \\ &= 2 \sum_{m'=-1}^1 F_\nu (f_\nu)_{mm'} \psi_{m'}. \end{aligned} \quad (3.80)$$

Again, this holds for each component of $m \in (1, 0, -1)$. With this we can write out the full derivative of (3.76) with respect to ψ_m :

$$\begin{aligned} \frac{\partial}{\partial \psi_m^*} \left(\frac{c_1}{2} [F_x^2 + F_y^2 + F_z^2] \right) &= c_1 \left[\sum_{m'=-1}^1 F_x (f_x)_{mm'} \psi_{m'} + \sum_{m'=-1}^1 F_y (f_y)_{mm'} \psi_{m'} \right. \\ &\quad \left. + \sum_{m'=-1}^1 F_z (f_z)_{mm'} \psi_{m'} \right] = c_1 \sum_{m'=-1}^1 \vec{F} \cdot \vec{f}_{mm'} \psi_{m'}. \end{aligned} \quad (3.81)$$

Now that we have calculated the derivatives for each part of the integrand, K , we can sub these back into the Euler-Lagrange equation (3.77) to obtain the multi-component Gross-Pitaevskii equation for $m \in (1, 0, -1)$, describing the ground state of a spin-one Bose-Einstein condensate:

$$\left[-\frac{\hbar^2 \nabla^2}{2M} + V(\vec{r}) - pm + qm^2 \right] \psi_m + c_0 n \psi_m + c_1 \sum_{m'=-1}^1 \vec{F} \cdot \vec{f}_{mm'} \psi_{m'} = \mu \psi_m. \quad (3.82)$$

We can fill in for $m \in (1, 0, -1)$ to write out the time-independent Gross-Pitaevskii

equation for each ψ_m :

$$\mu\psi_1 = \left[-\frac{\hbar^2\nabla^2}{2M} + V(\vec{r}) - p + q + c_0n + c_1F_z \right] \psi_1 + \frac{c_1}{\sqrt{2}}F_-\psi_0, \quad (3.83)$$

$$\mu\psi_0 = \left[-\frac{\hbar^2\nabla^2}{2M} + V(\vec{r}) + c_0n \right] \psi_0 + \frac{c_1}{\sqrt{2}}F_+\psi_1 + \frac{c_1}{\sqrt{2}}F_-\psi_{-1}, \quad (3.84)$$

$$\mu\psi_{-1} = \left[-\frac{\hbar^2\nabla^2}{2M} + V(\vec{r}) + p + q + c_0n - c_1F_z \right] \psi_{-1} + \frac{c_1}{\sqrt{2}}F_+\psi_0. \quad (3.85)$$

In the above expressions we have used:

$$F_{\pm} = F_x \pm iF_y. \quad (3.86)$$

In the same way as was done for the spinless case, we can generalize (3.82) to the time-dependent Gross-Pitaevskii equations.

$$i\hbar\frac{\partial\psi_1}{\partial t} = \left[-\frac{\hbar^2\nabla^2}{2M} + V(\vec{r}) - p + q + c_0n + c_1F_z \right] \psi_1 + \frac{c_1}{\sqrt{2}}F_-\psi_0, \quad (3.87)$$

$$i\hbar\frac{\partial\psi_0}{\partial t} = \frac{c_1}{\sqrt{2}}F_+\psi_1 + \left[-\frac{\hbar^2\nabla^2}{2M} + V(\vec{r}) + c_0n \right] \psi_0 + \frac{c_1}{\sqrt{2}}F_-\psi_{-1} \quad (3.88)$$

$$i\hbar\frac{\partial\psi_{-1}}{\partial t} = \frac{c_1}{\sqrt{2}}F_+\psi_0 + \left[-\frac{\hbar^2\nabla^2}{2M} + V(\vec{r}) + p + q + c_0n - c_1F_z \right] \psi_{-1}. \quad (3.89)$$

3.2.2 Mean field theory: Spin 2 condensate

The procedure for arriving at the Gross-Pitaevskii equation for a spin 2 condensate is the exact same as in the spin 1 case, detailed in section 3.2.1. As such, the steps will be given here without as much detail as to why each step is carried out.

The hamiltonian for the spin 2 system is obtained from (3.3) with $f = 2$ and (3.37):

$$\begin{aligned} \hat{H} &= \hat{H}_0 + \hat{U}, \\ &= \int d\vec{r} \sum_{m,m'=-2}^2 \hat{\Psi}_m^\dagger \left[-\frac{\hbar^2\nabla^2}{2M} + V(\vec{r}) - p(f_z)_m m' + q(f_z^2)_m m' \right] \psi \\ &\quad + \frac{1}{2} \int d\vec{r} \left[c_0 : \hat{n}^2(\vec{r}) : + c_1 : \hat{F}^2(\vec{r}) : + c_2 \hat{A}_{00}^\dagger(\vec{r}) \hat{A}_{00}(\vec{r}) \right]. \end{aligned} \quad (3.90)$$

The energy of the system in the state $|\zeta\rangle$ is given by the expectation value of the Hamiltonian

(3.90) in the state $|\zeta\rangle$:

$$\begin{aligned}
E[\psi_m] &= \langle \zeta | \hat{H} | \zeta \rangle, \\
&= \int d\vec{r} \left\{ \sum_{m=-2}^2 \psi_m^* \left[-\frac{\hbar^2 \nabla^2}{2M} + V(\vec{r}) - pm + qm^2 \right] \psi_m + \frac{c_0}{2} n^2 + \frac{c_1}{2} |\vec{F}|^2 + \frac{c_2}{2} |A_{00}|^2 \right\}.
\end{aligned} \tag{3.91}$$

Here we have used $A_{00} = \langle \zeta | \hat{A}_{00}(\vec{r}) | \zeta \rangle = \frac{1}{\sqrt{5}} [2\psi_2(\vec{r})\psi_{-2}(\vec{r}) - 2\psi_1(\vec{r})\psi_{-1}(\vec{r}) + \psi_0^2(\vec{r})]$. The particle density and spin density vector are defined in a similar manner to the spin one case:

$$n = n(\vec{r}) = \langle \zeta | \hat{n}(\vec{r}) | \zeta \rangle = \sum_{m=-2}^2 |\psi_m(\vec{r})|^2. \tag{3.92}$$

$\vec{F} = (F_x, F_y, F_z)$, where:

$$\begin{aligned}
F_\nu(\vec{r}) &= \langle \zeta | \vec{F}_\nu(\vec{r}) | \zeta \rangle \\
&= \sum_{m, m'=-2}^2 \psi_m^*(\vec{r}) (f_\nu)_{mm'} \psi_{m'}(\vec{r}).
\end{aligned} \tag{3.93}$$

For spin two, the spin matrices, f_ν , are given by the following matrices:

$$\begin{aligned}
f_x &= \begin{pmatrix} 0 & 1 & 0 & 0 & 0 \\ 1 & 0 & \sqrt{\frac{3}{2}} & 0 & 0 \\ 0 & \sqrt{\frac{3}{2}} & 0 & \sqrt{\frac{3}{2}} & 0 \\ 0 & 0 & \sqrt{\frac{3}{2}} & 0 & 1 \\ 0 & 0 & 0 & 1 & 0 \end{pmatrix}, \\
f_y &= \begin{pmatrix} 0 & -i & 0 & 0 & 0 \\ i & 0 & -i\sqrt{\frac{3}{2}} & 0 & 0 \\ 0 & i\sqrt{\frac{3}{2}} & 0 & -i\sqrt{\frac{3}{2}} & 0 \\ 0 & 0 & i\sqrt{\frac{3}{2}} & 0 & -i \\ 0 & 0 & 0 & i & 0 \end{pmatrix}, \\
f_z &= \begin{pmatrix} 2 & 0 & 0 & 0 & 0 \\ 0 & 1 & 0 & 0 & 0 \\ 0 & 0 & 0 & 0 & 0 \\ 0 & 0 & 0 & -1 & 0 \\ 0 & 0 & 0 & 0 & -2 \end{pmatrix}.
\end{aligned} \tag{3.94}$$

Using these and equation (3.93), we can work out the components of the spin density vector:

$$\begin{aligned}
F_x = & \psi_2^* \psi_1 + \psi_1^* \psi_2 + \sqrt{\frac{3}{2}} \psi_1^* \psi_0 + \sqrt{\frac{3}{2}} \psi_0^* \psi_1 + \sqrt{\frac{3}{2}} \psi_0^* \psi_{-1} \\
& + \sqrt{\frac{3}{2}} \psi_{-1}^* \psi_0 + \psi_{-1}^* \psi_{-2} + \psi_{-2}^* \psi_{-1}, \quad (3.95)
\end{aligned}$$

$$\begin{aligned}
F_y = & i \left[-\psi_2^* \psi_1 + \psi_1^* \psi_2 - \sqrt{\frac{3}{2}} \psi_1^* \psi_0 + \sqrt{\frac{3}{2}} \psi_0^* \psi_1 - \sqrt{\frac{3}{2}} \psi_0^* \psi_{-1} \right. \\
& \left. + \sqrt{\frac{3}{2}} \psi_{-1}^* \psi_0 - \psi_{-1}^* \psi_{-2} + \psi_{-2}^* \psi_{-1} \right], \quad (3.96)
\end{aligned}$$

$$F_z = 2|\psi_2|^2 + |\psi_1|^2 - |\psi_{-1}|^2 - 2|\psi_{-2}|^2. \quad (3.97)$$

We again compute the Euler-Lagrange equations in order to minimize the energy functional. We still want to conserve particle number and so we minimize subject to the following constraint:

$$G[\psi] = \int (|\psi_2|^2 + |\psi_1|^2 + |\psi_0|^2 + |\psi_{-1}|^2 + |\psi_{-2}|^2) d\vec{r} = N. \quad (3.98)$$

The Euler-Lagrange equation is then given by equation (3.73) but now with $\psi = (\psi_2, \psi_1, \psi_0, \psi_{-1}, \psi_{-2})$, \bar{E} being the integrand of (3.91) and \bar{G} being the integrand of (3.98).

Like in the spin one case, since there is no $(\psi_m^*)'$ dependence, the Euler-Lagrange equation reduces to setting the derivative of $\bar{E} - \mu\bar{G}$ to zero.

From the spin one case, we have already worked out general expressions for most of these derivatives. The only difference here is that the sums over m now run from -2 to 2 and the components of the spin matrix are now given by (3.94). The only term that we have left to work out is the spin singlet interaction term:

$$\begin{aligned}
\frac{\partial}{\partial \psi_m^*} |A_{00}|^2 &= \frac{\partial}{\partial \psi_m^*} \left[A_{00} \left(\frac{1}{\sqrt{5}} \sum_{m=-2}^2 (-1)^{f-m} \psi_m^* \psi_{-m} \right) \right], \\
&= \frac{2}{\sqrt{5}} A_{00} (-1)^{f-m} \psi_{-m}^*. \quad (3.99)
\end{aligned}$$

Subbing in for all of the derivative terms and setting to zero gives the components of the Gross-Pitaevskii equation for a spin two condensate, listed in the order $m = 2, 1, 0, -1, -2$:

$$\mu\psi_2 = \left[-\frac{\hbar^2\nabla^2}{2M} + V(\vec{r}) - 2p + 4q + c_0n + 2c_1F_z \right] \psi_2 + c_1F_-\psi_1 + \frac{c_2}{\sqrt{5}}A_{00}\psi_{-2}^*, \quad (3.100)$$

$$\begin{aligned} \mu\psi_1 = & \left[-\frac{\hbar^2\nabla^2}{2M} + V(\vec{r}) - p + q + c_0n + c_1F_z \right] \psi_1 \\ & + c_1 \left(\sqrt{\frac{3}{2}}F_-\psi_0 + F_+\psi_2 \right) - \frac{c_2}{\sqrt{5}}A_{00}\psi_{-1}^*, \end{aligned} \quad (3.101)$$

$$\mu\psi_0 = \left[-\frac{\hbar^2\nabla^2}{2M} + V(\vec{r}) + c_0n \right] \psi_0 + c_1 \left(\sqrt{\frac{3}{2}}F_+\psi_1 + \sqrt{\frac{3}{2}}F_-\psi_{-1} \right) + \frac{c_2}{\sqrt{5}}A_{00}\psi_0^*, \quad (3.102)$$

$$\begin{aligned} \mu\psi_{-1} = & \left[-\frac{\hbar^2\nabla^2}{2M} + V(\vec{r}) + p + q + c_0n - c_1F_z \right] \psi_{-1} \\ & + c_1 \left(\sqrt{\frac{3}{2}}F_+\psi_0 + F_-\psi_{-2} \right) - \frac{c_2}{\sqrt{5}}A_{00}\psi_1^*, \end{aligned} \quad (3.103)$$

$$\mu\psi_{-2} = \left[-\frac{\hbar^2\nabla^2}{2M} + V(\vec{r}) + 2p + 4q + c_0n - 2c_1F_z \right] \psi_{-2} + c_1F_+\psi_{-1} + \frac{c_2}{\sqrt{5}}A_{00}\psi_2^*. \quad (3.104)$$

In these expressions, we have again used the expression given by (3.86), however in this case, the expressions for F_x and F_y are the spin 2 forms given by (3.95) and (3.96).

Again, these can be generalized to the time dependent Gross Pitaevskii equations for spin two:

$$i\hbar\frac{\partial\psi_2}{\partial t} = \left[-\frac{\hbar^2\nabla^2}{2M} + V(\vec{r}) - 2p + 4q + c_0n + 2c_1F_z \right] \psi_2 + c_1F_-\psi_1 + \frac{c_2}{\sqrt{5}}A_{00}\psi_{-2}^*, \quad (3.105)$$

$$\begin{aligned} i\hbar\frac{\partial\psi_1}{\partial t} = & \left[-\frac{\hbar^2\nabla^2}{2M} + V(\vec{r}) - p + q + c_0n + c_1F_z \right] \psi_1 \\ & + c_1 \left(\sqrt{\frac{3}{2}}F_-\psi_0 + F_+\psi_2 \right) - \frac{c_2}{\sqrt{5}}A_{00}\psi_{-1}^*, \end{aligned} \quad (3.106)$$

$$i\hbar\frac{\partial\psi_0}{\partial t} = \left[-\frac{\hbar^2\nabla^2}{2M} + V(\vec{r}) + c_0n \right] \psi_0 + c_1 \left(\sqrt{\frac{3}{2}}F_+\psi_1 + \sqrt{\frac{3}{2}}F_-\psi_{-1} \right) + \frac{c_2}{\sqrt{5}}A_{00}\psi_0^*, \quad (3.107)$$

$$\begin{aligned} i\hbar\frac{\partial\psi_{-1}}{\partial t} = & \left[-\frac{\hbar^2\nabla^2}{2M} + V(\vec{r}) + p + q + c_0n - c_1F_z \right] \psi_{-1} \\ & + c_1 \left(\sqrt{\frac{3}{2}}F_+\psi_0 + F_-\psi_{-2} \right) - \frac{c_2}{\sqrt{5}}A_{00}\psi_1^*, \end{aligned} \quad (3.108)$$

$$i\hbar\frac{\partial\psi_{-2}}{\partial t} = \left[-\frac{\hbar^2\nabla^2}{2M} + V(\vec{r}) + 2p + 4q + c_0n - 2c_1F_z \right] \psi_{-2} + c_1F_+\psi_{-1} + \frac{c_2}{\sqrt{5}}A_{00}\psi_2^*. \quad (3.109)$$

4 Ground state phases

In this section, we will list some of the different types of phases that can be observed in a spinor Bose-Einstein condensate based on the magnetization of the system. These results have been obtained from [27].

We will first look at this for a spin one condensate; considering the phases that arise with and without the presence of an external magnetic field. Building on this, we will look at the different types of phases present in a spin two condensate without the presence of an external magnetic field, which is more varied than the spin one analogue. It will be particularly important to understand the phases for both spin one and spin two condensates without an external magnetic field as it will be these phases that we consider when we look at the different types of vortices that can be hosted within these systems.

4.1 Spin One Ground State Phases

We first start by looking at the ground state phases of a spin one condensate without an external magnetic field. The governing factor for deciding the magnetization of the system and thus the phase that the condensate is in is the energy functional for a spin one condensate, which is shown here again for convenience:

$$E[\hat{\Psi}_m] = \int d\vec{r} \left\{ \sum_{m=-1}^1 \psi_m^* \left[-\frac{\hbar^2 \nabla^2}{2M} + V(\vec{r}) - pm + qm^2 \right] \psi_m + \frac{c_0}{2} n^2 + \frac{c_1}{2} |\vec{F}|^2 \right\}. \quad (4.1)$$

The ground state of the system will minimize this energy and so we can use this result to decide what the phase of the condensate is for different values of c_1 . We will look at this first for a uniform system ($V(\vec{r}) = 0$, $\nabla^2 \psi_m = 0$). Since we are first only considering the condensate without an external magnetic field, we also have that the Zeeman terms are zero ($p = q = 0$). Since we are looking at a uniform system with a fixed number density n , we can renormalize the order parameter in the following way:

$$\psi_m = \sqrt{n} \zeta_m, \quad (4.2)$$

where ζ_m is a normalized spinor. Furthermore, since we are looking at a uniform system, where we are neglecting the potential and kinetic energy terms, the entire normalized spinor becomes constant in space, leaving us with the following to minimize:

$$\frac{c_0}{2} n^2 + \frac{c_1}{2} |\vec{F}|^2 \quad (4.3)$$

With this, we can define the spin expectation value per particle:

$$\vec{f} = \sum_{mm'} \zeta_m^* \vec{f}_{mm'} \zeta_{m'}, \quad (4.4)$$

where this is related to the spin density (3.66) through $\vec{F} = n\vec{f}$ and $\vec{f}_{mm'}$ is a vector whose components are the spin one matrices given by (3.67).

Since we are dealing with a spin one condensate, we can see that the maximum value that $|\vec{f}|$ can take is $|\vec{f}| = 1$ and the minimum value it can take is $|\vec{f}| = 0$. With this we can see that there are two different phases for a spin one condensate with no external magnetic field that depend on what value is assigned to c_1 (ie: whether or not the spin interaction is attractive or repulsive):

$$\begin{array}{llll} c_1 < 0 & |\vec{f}| = 1 & \text{Ferromagnetic} & \zeta = (1, 0, 0)^T \text{ or } \zeta = (0, 0, 1)^T \\ c_1 > 0 & |\vec{f}| = 0 & \text{Antiferromagnetic} & \zeta = (1, 0, 1)^T/\sqrt{2} \text{ or } \zeta = (0, 1, 0)^T. \end{array}$$

The final column above lists a representative spinor for the phase in question where the general format is $\zeta = (\zeta_1, \zeta_0, \zeta_{-1})^T$ for a spin one condensate.

We will briefly revisit the ferromagnetic phase of a spin one condensate later when we look at vortices for this system.

Now, we consider the different phases that are possible for a spin one condensate in the presence of an external magnetic field. Here, we will just summarize what these phases are rather than derive them as we will not be working with them past this section and will only use them when discussing different phases in the cores of some vortices present in a spin one condensate. This is described in section (5). The procedure for finding these phases is well documented between [27] and [31].

For a spin one condensate in the presence of an external magnetic field, we get the following five phases:

Phase	Order Parameter	f_z
Ferromagnetic (1)	$(e^{i\chi_1}, 0, 0)$	1
Ferromagnetic (2)	$(0, 0, e^{i\chi_{-1}})$	-1
Antiferromagnetic	$\left(e^{i\chi_1} \sqrt{\frac{1}{2} \left(1 + \frac{p}{c_1 n} \right)}, 0, e^{i\chi_{-1}} \sqrt{\frac{1}{2} \left(1 - \frac{p}{c_1 n} \right)} \right)$	$\frac{p}{c_1 n}$
Polar	$(0, e^{i\chi_0}, 0)$	0
Broken Axisymmetry	See Ref. [31]	$\frac{p(-p^2 + q^2 + 2qc_1 n)}{2c_1 n q^2}$

4.2 Spin 2 Ground State Phases

We will now look at the ground state phases for a spin two condensate without the presence of an external magnetic field. Comparing with the spin one case, we have a wider array of phases possible due to both the spin density and spin singlet density varying. This means that the phase of the condensate depends on the values of the interaction parameters c_1 and c_2 . We list the phase that the condensate lies in when these parameters take on different values, as well as the representative order parameter for each phase.

Phase	Order Parameter	Interaction Parameters
Ferromagnetic	$(1, 0, 0, 0, 0)^T$	$c_1 < 0, c_2 > 0$
Uniaxial Nematic	$(0, 0, 1, 0, 0)^T$	$c_1 > 0, c_2 < 0$
Biaxial Nematic	$(1, 0, 0, 0, 1)^T/\sqrt{2}$	$c_1 > 0, c_2 < 0$
Cyclic	$(1/2, 0, i/\sqrt{2}, 0, 1/2)^T$	$c_1 > 0, c_2 > 0$

Note that the uniaxial and biaxial nematic phases of the condensate occur in the same space of interaction parameter values, however we can see by using the graphical representation described in the next section that these phases have different symmetries and are therefore different. Since the method described for finding these states is for a uniform system, we are here only minimizing:

$$\frac{c_0}{2}n^2 + \frac{c_1}{2}|\vec{F}|^2 + \frac{c_2}{2}|A_{00}|^2. \quad (4.5)$$

When we only look at the minimization of this part of the energy functional, it is difficult to see how the system chooses between which of these phases to be in when the interaction parameters are set appropriately. However, since a simplified approach of a uniform system has been taken here as well as looking at a condensate through mean field theory, we note that going beyond these simplifications must cause one of these two phases to be favoured in certain situations.

4.3 Graphical Representation of a Bose-Einstein Condensate

In certain cases it is useful to have some sort of graphical representation of the condensate. Two such reasons that will be used in this research are to see what phase of the wavefunction we are in and to determine whether there is a winding within the condensate in spin space and phase space, suggesting the presence of a vortex. We will see more on this later in section (5), however for now we will just detail the spherical harmonic representation of a spinor condensate which gives a nice graphical picture [27].

The motivation for using spherical harmonics comes from the fact that they are used to describe integer spin states. In our case, since we have different spin channels, we can take the following expression to describe the state of the system:

$$\Psi(\theta, \phi) = \sum_m \psi_m Y_f^m(\theta, \phi), \quad (4.6)$$

where f is the spin of the particles in the condensate, for us we will only be looking at spin $f = 1$ and $f = 2$ condensates; m is the magnetic quantum number describing the spin channel the particles are in, for example, for a spin two condensate, m runs from -2 to 2 . ψ_m is the wavefunction for the spin m state. $Y_f^m(\theta, \phi)$ is the spherical harmonic for spin quantum number f and magnetic quantum number m that depends on the spherical coordinate angles θ and ϕ .

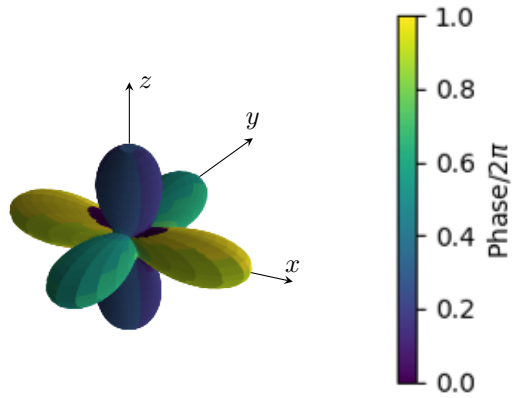


Figure 1: Spherical harmonic representation for cyclic representative order parameter.

We can use this expression to get a graphical representation of what phase of the condensate we are in by taking surface plots of $|\Psi(\theta, \phi)|^2$ on top of which we plot the complex phase of $\Psi(\theta, \phi)$ as a representation of the phase of the condensate. We show some examples of this graphical representation for some of the phases of a spin two condensate in figures (1) and (2).

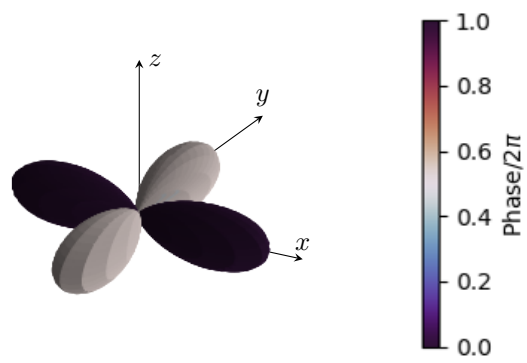


Figure 2: Spherical harmonic representation for biaxial nematic representative order parameter.

5 Vortices in Spinor Bose-Einstein Condensates

When reviewing the setup and properties of spinless condensates in the first two sections, we briefly discussed the possibility of vortices being hosted. Although we saw that the spinless condensate was irrotational from the hydrodynamic equations, we could still get a vortex that caused an integer winding in the complex phase of the wavefunction due to its single-valuedness. Similarly in spinor condensates, we can discuss the possibility of vortices being hosted. However, here, the variety of vortices that can be realized is much more diverse where we see both mass and spin circulation can occur. As we will see, this variety comes from the fact that we now have spin degrees of freedom that were not present in the spinless condensate. A hydrodynamic approach can be taken to look at spinor condensates which can then be used to obtain information about vortices, however we will not look at this here. Details of the hydrodynamic approach for spinor condensates can be found in [27]. Instead we will study vortices in different phases of a spinor condensate through homotopy theory as well as group theory. Before doing this, we will look at how we can describe different phases of the condensate by using symmetry considerations which will be useful when we go to classifying vortices in these different phases.

5.1 Symmetries of spinor bose-einstein condensates

In order to describe the vortices that can be hosted in a spinor condensate, we first need a way of describing the different phases of the relevant condensate that were discussed earlier. We follow [27] for this discussion and the sections to follow. To do this we will consider what symmetries remain when we restrict ourselves to the phase in question.

First of all, let's consider the full space that describes a spin f condensate. We have seen previously that we can describe a state in this space with an order parameter Ψ that is made up of a set of $2f + 1$ complex amplitudes:

$$\Psi = (\psi_{-f}, \psi_{-f+1}, \dots, \psi_f)^T \quad (5.1)$$

As an example, we know that the order parameter for a spin one condensate is $\Psi = (\psi_1, \psi_0, \psi_{-1})$.

We can see that this general order parameter can move in a space $\mathcal{M} = \mathbb{C}^{2f+1}$. We call this space, \mathcal{M} , the order parameter manifold for a spin f condensate.

With this, we can look at the symmetries that are present in this system. We do this by finding a group, G , that acts on \mathcal{M} and leaves the energy of the system invariant.

This is done by noting that the energy functional of a spin f condensate, with no external magnetic field, is invariant under the following:

1. SO(3) rotations in spin space.
2. U(1) gauge transformations.

This means that the full symmetry group of a spin f condensate is $G = SO(3) \times U(1)$. With this, we see that any element, $g \in G$ has the following form:

$$g = e^{i\phi} e^{-if_z\alpha} e^{-if_y\beta} e^{-if_z\gamma}, \quad (5.2)$$

where α, β and γ are the Euler angles in ZYZ format [32], and f_ν are the spin matrices with $\nu = (x, y, z)$. We will discuss the Euler angles in more detail when we look at how to implement specific vortices numerically.

Now, let's restrict ourselves to a certain phase of the condensate and look at how to describe its order parameter manifold. We restrict ourselves by only considering certain spinors, $\zeta \in \mathcal{M}$. How can we classify this phase? If we take a representative order parameter from this phase, say ζ_0 , and act with a group element of G , we should reach another order parameter that also describes the phase of the condensate that we have restricted ourselves to since the group G leaves the energy of the system invariant. Looking at all elements that we can obtain by acting different elements of G on our representative order parameter, ζ_0 is called the orbit of ζ_0 :

$$\mathcal{M}_0(\zeta_0) = \{g\zeta_0 | g \in G\}. \quad (5.3)$$

As an example, we can look at the ferromagnetic phase of a spin one condensate. A representative order parameter for this phase is $\Psi = (1, 0, 0)$. By using the orbit of this spinor, we can obtain a general spin vector representing the ferromagnetic phase of a spin one condensate:

$$\begin{aligned} \zeta &= e^{i\phi} e^{-if_z\alpha} e^{-if_y\beta} e^{-if_z\gamma} \begin{pmatrix} 1 \\ 0 \\ 0 \end{pmatrix}, \\ &= e^{i(\phi-\gamma)} \begin{pmatrix} e^{-i\alpha} \cos^2(\frac{\beta}{2}) \\ \frac{1}{\sqrt{2}} \sin(\beta) \\ e^{i\alpha} \sin^2(\frac{\beta}{2}) \end{pmatrix}. \end{aligned} \quad (5.4)$$

Here, we have used the 3-dimensional $SU(3)$ spin matrix to represent $e^{-if_z\alpha} e^{-if_y\beta} e^{-if_z\gamma}$ which is given by [32].

$$U_3(\alpha, \beta, \gamma) = \begin{pmatrix} e^{-i(\alpha+\gamma)} \cos^2(\frac{\beta}{2}) & -\frac{e^{-i\alpha}}{\sqrt{2}} \sin(\beta) & e^{-i(\alpha-\gamma)} \sin^2(\frac{\beta}{2}) \\ \frac{e^{-i\gamma}}{\sqrt{2}} \sin(\beta) & \cos(\beta) & -\frac{e^{i\gamma}}{\sqrt{2}} \sin(\beta) \\ e^{i(\alpha-\gamma)} \sin^2(\frac{\beta}{2}) & \frac{e^{i\alpha}}{\sqrt{2}} \sin(\beta) & e^{i(\alpha+\gamma)} \cos^2(\frac{\beta}{2}) \end{pmatrix} \quad (5.5)$$

We will list the five-dimensional matrix for spin two, in a later section.

From this, we see that we can describe the order parameter manifold of a certain phase of the condensate if we know the orbit of the representative spinor for this phase.

Can we find a nice, tidy expression for the orbit of ζ_0 ? One way to do this is by introducing the stabilizer or isotropy group of ζ_0 , written H_{ζ_0} which is the group of elements, $g \in G$ that, when acted on ζ_0 , leave it invariant.

$$H_{\zeta_0} = \{g \in G | g\zeta_0 = \zeta_0\}. \quad (5.6)$$

Next, we consider a map from the full symmetry group G to the orbit of ζ_0 defined by:

$$\phi : G \rightarrow M_0(\zeta_0), \quad (5.7)$$

$$\phi(g) = g\zeta_0. \quad (5.8)$$

It is clear that this map is onto by definition of the map ϕ and by definition of the orbit.

We now note that this map is constant on cosets of the stabilizer, H_{ζ_0} . We can see this by taking two elements, $h_1, h_2 \in H_{\zeta_0}$ and acting gh_1 and gh_2 on ζ_0 for $g \in G$. Since h_1 and h_2 leave ζ_0 invariant. We see that acting with gh_1 or gh_2 on ζ_0 just leaves us with $g\zeta_0$ for $g \in G$, therefore showing that the map ϕ is constant on cosets of the stabilizer.

This means that every coset of H_{ζ_0} gets sent to an element of the orbit, $M_0(\zeta_0)$ and so we choose to look at this map instead.

$$\phi' : G/H_{\zeta_0} \rightarrow M_0(\zeta_0), \quad (5.9)$$

$$\phi'(gH_{\zeta_0}) = g\zeta_0, \quad g \in G. \quad (5.10)$$

It follows from the map ϕ that ϕ' is onto. if we can show that ϕ' is 1-1 then we will have a bijective correspondence between the orbit of ζ_0 and the cosets of the stabilizer group of ζ_0 . We can do this by taking two elements $g_1, g_2 \in G$ and assume that ϕ' sends g_1 and g_2 to the same element of the orbit of ζ_0 , that is:

$$g_1\zeta_0 = g_2\zeta_0, \quad (5.11)$$

$$\implies g_1^{-1}g_2\zeta_0 = \zeta_0, \quad (5.12)$$

$$\implies g_1^{-1}g_2 \in H_{\zeta_0}, \quad (5.13)$$

$$\implies g_1H_{\zeta_0} = g_2H_{\zeta_0}. \quad (5.14)$$

As we can see, if we assume that two elements in G are sent to the same element of the orbit, the only way that this can happen is if those two elements belong to the same coset of the stabilizer and so we see that the map ϕ' is 1-1 and since we already know this map is onto, we can conclude that we have the following bijection:

$$\mathcal{M}_0(\zeta_0) \sim G/H_{\zeta_0}. \quad (5.15)$$

From this, we see that we can write the order parameter manifold for a certain phase of the condensate, described by the representative order parameter, ζ_0 , as:

$$\mathcal{R} = G/H_{\zeta_0}. \quad (5.16)$$

5.2 Describing vortices in a certain phase

Now that we have a way of describing the order parameter manifold for a certain phase of a condensate, we can look at how we describe vortices within such a phase. We will classify vortices using loops within the condensate. A loop is defined as the image of a map from a loop in real space to the order parameter manifold, \mathcal{R} . For example, in 2-dimensional space, the map would be from the circle to the order parameter manifold, $f : S^1 \rightarrow \mathcal{R}$. Put more rigorously, a loop l is a map from the interval $[0, 1]$ to the order parameter manifold, \mathcal{R} where $l(0) = l(1) = x_0 \in \mathcal{R}$. x_0 is called the base point of a loop. If two loops l_1 and l_2 share the same base point, x_0 , and one can be deformed into the other, then the two loops are said to be homotopic to each other. We can already see how these loops might describe a vortex in two-dimensions. If we look at how the order parameter is changing along a closed loop, we can think of that as looking at how the condensate is circulating around this loop, whether this be a spin or mass circulation. We know that we could have two vortices that are the same but at different regions in the condensate. In this case we would like to be able to identify these as the same vortex using the loop classification given above. To do this we will say that two loops that can be continuously deformed into each other without sharing a base point are freely homotopic to one another. We will use this in a few moments where we will not specify the base point we are using. For now though we will keep the base point and consider loops that are homotopic to each other. We can easily see that homotopy forms an equivalence relation by checking the conditions of reflexivity, symmetry and transitivity. This means that we can classify loops into equivalence classes known as homotopy classes in which we consider all loops in a certain homotopy class to be essentially the same. The homotopy class of a loop, l , is denoted as $[l]$.

What if we want to know what happens if we bring two vortices together. To do this, we need to have some idea of what happens if we traverse one loop and then another. This idea is depicted in figure (3) where we start at a base point x_0 , traverse a loop in the homotopy class $[l_1]$ and then traverse a loop in the homotopy class $[l_2]$. We can describe this operation by taking the product $[l_1] \cdot [l_2] = [l_1 \cdot l_2]$. It is worth noting that we do not need to return to the base point when traversing a loop within the homotopy group $[l_1 \cdot l_2]$.

We see that this set has an identity element given by $[e]$, in which all points on the circle map to the base point x_0 . We also have an inverse loop $[l^{-1}]$ where we traverse a loop in $[l]$ in the opposite direction.

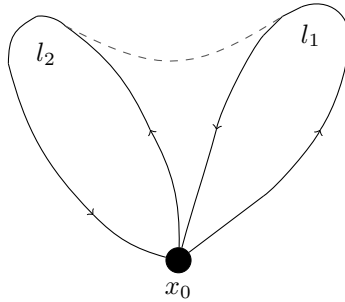


Figure 3: Demonstration of taking a product of two loops $[l_1] \cdot [l_2]$.

We see that since the set of homotopy classes has a closed product, an identity element and an inverse, this set and product form a group known as the fundamental group or first homotopy group of \mathcal{R} at x_0 , $\pi_1(\mathcal{R}, x_0)$. Since we will be working in two-dimensions, we need only concern ourselves with this group, however there are other homotopy groups that can be considered when working in higher dimensions such as $\pi_2(\mathcal{R}, x_0)$ where points on a sphere are mapped to an order parameter manifold.

As stated earlier, we want to be able to identify vortices that are the same even if they are in different regions of space and as a result we will refrain from choosing a specific base point from here on out and just consider the fundamental group of \mathcal{R} , $\pi_1(\mathcal{R})$. We can do this due to the fact that any fundamental group at some base point is isomorphic to the fundamental group at \mathcal{R} as shown in [33]. Another fact that we will use that is shown in [33], is that if the fundamental group of \mathcal{R} is non-abelian, then freely homotopic classes correspond to the conjugacy classes of the fundamental group. That is, two non-abelian vortices that are conjugate to each other are indistinguishable as far as homotopy theory is concerned. It is worth noting that if we wish to merge two vortices together, we will have to consider the exact base point for this operation again in order to use the group product discussed above, however, if we are just looking at a single vortex type, it is permissible to not specify the base point.

We will now look at how we can obtain the fundamental group for different phases of a condensate and how we can then use that to classify vortices. First, we will discuss this in general, followed by examples in both spin one and spin two.

We know that in order to describe vortices, we want to look at the fundamental group of the order parameter manifold for a certain phase of the condensate. Recall from section (5.1) that the order parameter manifold for the phase of a condensate with stabilizer group H is given by $\mathcal{R} = G/H$ where G is the full symmetry group of a spin f condensate and H is the symmetry group left in the system when we restrict to a certain phase. So we would like to find the fundamental group of G/H , given by $\pi_1(G/H)$. Its elements of this group that represent the different types of vortices present in the current phase of the condensate. As mentioned above, if this group is non-abelian, then it is conjugacy classes of this group

that describe the different types of vortices that can be hosted.

We can write the fundamental group, $\pi_1(G/H)$ in a way that will be nicer to deal with by using a key identity which is stated and proved in [33]. If G is both connected and simply connected, and H is a subgroup of G , then the following holds:

$$\pi_1(G/H) \sim \pi_0(H) \tag{5.17}$$

If H is a discrete group then it follows that $\pi_0(H) = H$.

This means that as long as the conditions above hold, we can characterize vortices by the elements of the symmetry group H of a particular phase. We will use this in some of the examples given in the next section.

5.3 Examples of vortices in Bose-Einstein condensates

We will now provide some examples, illustrating how the above is used practically in describing the different types of vortices that can be observed in both spinless and spinor condensates. Some of these examples, particularly in spin two, will be used in later sections and so this section also serves as an introduction to some background material for upcoming sections.

5.3.1 Vortices in a spinless condensate

Here, we revisit looking at the different types of vortices that can be hosted in a spinless condensate. As we have already seen, it turns out that only one type of vortex can be realized in this system. We will again come to this conclusion by considering the different types of vortices accommodated by a spinless condensate from the viewpoint of homotopy theory described above. To do this we follow the series of steps described below.

First, we need to determine the order parameter manifold for a spinless condensate. We have seen previously that the order parameter for a spinless condensate takes the form $\psi = |\psi|e^{i\phi}$ and as such we can easily see that the order parameter manifold for a spinless condensate is given by $\mathcal{R} = U(1)$.

Once we know this, we want to classify loops within this system which will then correspond to the different types of vortices the system can host. To do this, we need to find the fundamental group of $U(1)$. Since we know that $U(1) \sim S^1$ and $\pi_1(S^1) = \mathbb{Z}$, it follows that $\pi_1(U(1)) = \mathbb{Z}$.

We see that this gives us exactly the same result as was discussed in section (2). Namely, the one type of vortex is characterized by a winding number that tells us how many times we have wound around the unit circle. Linking this back to our previous discussion, it tells us that the circulation of a vortex in a spinless condensate is quantized which is exactly what we observed earlier.

5.3.2 Vortices in a spin one condensate

Once we introduce spin degrees of freedom, there is a much wider variety of vortices that can be obtained other than just those with quantized mass circulation as observed in a spinless condensate. Here we will show an example of the vortex types that can be observed in a spin one ferromagnetic condensate. As discussed earlier, a representative order parameter for the spin one ferromagnetic phase is $\zeta_0 = (1, 0, 0)$. In order to find the order parameter manifold for this phase, we need to find the stabilizer group for this order parameter. Since this order parameter is restricted to one component in spin space, we see that the only symmetry that occurs is that of rotating the complex phase of the nonzero spin component, similar to a spinless condensate. As a result, we see that the stabilizer group is $H = U(1)$. Therefore, to get the order parameter manifold, we take $\mathcal{R} = G/H$ where G is the full symmetry group of a spin one condensate given by $G = SO(3) \times U(1)$. Therefore, the order parameter manifold for a spin one ferromagnetic condensate is:

$$\mathcal{R} = \frac{SO(3) \times U(1)}{U(1)} = SO(3). \quad (5.18)$$

To classify vortices in this phase, we need to find the fundamental group for this order parameter manifold which is $\pi_1(SO(3)) = \mathbb{Z}_2$. Therefore we see that we have two cases to deal with here that correspond to the two elements of $\mathbb{Z}_2 = \{0, 1\}$.

To see what these cases correspond to, it is useful to compare to the general order parameter for a spin one ferromagnetic condensate which is given by (5.4) and listed here again for convenience:

$$\zeta = e^{i(\phi')} \begin{pmatrix} e^{-i\alpha} \cos^2(\frac{\beta}{2}) \\ \frac{1}{\sqrt{2}} \sin(\beta) \\ e^{i\alpha} \sin^2(\frac{\beta}{2}) \end{pmatrix}. \quad (5.19)$$

Following [27], we can write $\phi' = \phi - \gamma$ as a single variable due to the spin-gauge symmetry displayed. Recall, that γ is one of the Euler angles. In order to satisfy the single-valuedness of the wave function, we vary α and ϕ' in terms of the azimuthal angle φ as $\alpha = n\varphi$ and $\phi' = m\varphi$ where $n, m \in \mathbb{Z}$.

With this, we can see what vortices the elements 0 and 1 in \mathbb{Z}_2 correspond to. First let's look at $0 \in \mathbb{Z}_2$. This corresponds to $n + m$ being an even integer. As an example, let's take $n = -n_\alpha$ and $m = n_\alpha$ where $n_\alpha \in \mathbb{Z}$. If we do this the order parameter (5.19) becomes:

$$\zeta = \begin{pmatrix} e^{2in_\alpha\varphi} \cos^2(\frac{\beta}{2}) \\ \frac{1}{\sqrt{2}} \sin(\beta) \\ \sin^2(\frac{\beta}{2}) \end{pmatrix} \quad (5.20)$$

To ensure that we don't have any singularities at the origin, we require that $\beta(r = 0, \varphi) =$

π . We can then have circulation far away from the origin, say at r_0 with $\beta(r = r_0, \varphi) = 0$. However, this vortex is unstable. To see this we can follow a continuous path in the order parameter manifold from $\beta = 0$ to $\beta = \pi$. If we do this, we see that the order parameter goes from $(e^{2in_\alpha\varphi}, 0, 0)^T$ to $(0, 0, 1)^T$. Therefore there is no vortex present under stable conditions.

Next, we can look at what type of vortex corresponds to $1 \in \mathbb{Z}_2$. In this case, we will have $n + m$ being an odd integer. As an example, let's take $n = -n_\alpha$ and $m = n_\alpha + 1$. The order parameter for this is:

$$\zeta = \begin{pmatrix} e^{i(2n_\alpha+1)\varphi} \cos^2(\frac{\beta}{2}) \\ \frac{1}{\sqrt{2}} \sin(\beta) \\ e^{i\varphi} \sin^2(\frac{\beta}{2}) \end{pmatrix} \quad (5.21)$$

Again, to avoid singularities at the origin, we require the $m = 1$ and $m = -1$ components of the order parameter to go to zero. The difference in this case to the previous one is that the number density in the $m = 0$ case need not vanish at $r = 0$ and so the core of the vortex is filled with a polar state, leading to this vortex being called the polar-core vortex. Far away from the vortex core we are still in a ferromagnetic phase and as a result, we have the following variational order parameter that describes the situation, both at and far away from the core, given by [27]:

$$\zeta = \begin{pmatrix} e^{-i\varphi} g_1(\vec{r}) \cos^2(\frac{\beta}{2}) \\ \sqrt{1 - g_1^2(\vec{r}) \cos^4(\frac{\beta}{2}) - g_2^2(\vec{r}) \sin^4(\frac{\beta}{2})} \\ e^{i\varphi} g_2(\vec{r}) \sin^2(\frac{\beta}{2}) \end{pmatrix}, \quad (5.22)$$

where $g_1(\vec{r})$ and $g_2(\vec{r})$ are variational functions such that $g_1(0) = g_2(0) = 0$ and $g_1(\infty) = g_2(\infty) = 1$.

As with the previous example, we can check to see if the vortex far away from the origin, given by (5.21), is stable. Again, we can take a continuous path in the order parameter manifold from $\beta = 0$ to $\beta = \pi$. If we do this we see that the aforementioned order parameter changes from $(e^{i(2n_\alpha+1)\varphi}, 0, 0)^T$ to $(0, 0, e^{i\varphi})^T$. This shows that a vortex with winding $2n_\alpha + 1$ decays into a singly quantized vortex which is stable. This shows that the singly quantized polar-core vortex is stable in the ferromagnetic phase. More details of this can be found in [27, 30].

We can also have other types of vortices that occur in different phases of a spin one condensate such as the polar phase. Details of this are discussed in [27].

5.3.3 Vortices in a spin two condensate

Just as there was a wider variety of vortices present in a spin one condensate when compared to the spinless case, so too is the case between a spin one and spin two condensate. One of the interesting types of vortices that can show up in a spin two condensate that is not

present at spin one is that of non-abelian vortices. This occurs when the stabilizer group that is describing the phase of the condensate is non-abelian. Both of the examples that we will look at here are examples of non-abelian vortices.

Cyclic phase vortices We follow the same steps outlined in sections (5.1) and (5.2). These steps for cyclic phase vortices can be found in [27], however are listed here with further explanation to serve as an introduction for upcoming sections. Just like in all the previous examples we have shown so far, we would first like to find the order parameter manifold for this phase. To do this, we need to determine the stabilizer group for this phase. That is, we want to find the group that leaves the representative order parameter for this phase invariant. As we have seen earlier in section (4), the representative order parameter for the cyclic phase is given by:

$$\zeta = \begin{pmatrix} \frac{1}{2} \\ 0 \\ \frac{i}{\sqrt{2}} \\ 0 \\ \frac{1}{2} \end{pmatrix}. \quad (5.23)$$

The easiest way to determine the stabilizer group for this order parameter is geometrically. That is, by looking at the spherical harmonic representation for this order parameter and investigating its symmetries in spin space. The spherical harmonic representation for (5.23) is shown in figure (4). We see that the spherical harmonic depicting the representative order parameter of the cyclic phase is characterized by three lobes emanating from each of the coordinate axes. The colour of each lobe characterizes the phase of the spherical harmonic representation as discussed in section (4). The difference between the phase at a point on one lobe and the corresponding point on the next lobe going anticlockwise is $\frac{2\pi}{3}$.

We would now like to look at what symmetries are present. Figure (5) reveals the underlying symmetry for the cyclic phase is rotations of the tetrahedron. We obtain figure (5) by rotating the (1,1,1) axis onto the z-axis. This means we can generate the tetrahedral group using rotations of $\frac{2\pi}{3}$ about the (1,1,1) axis and rotations of π about the z-axis. There is one addition that we must make here which is different to the usual tetrahedral group. Since the full condensate has a $U(1)$ gauge degree of freedom which is broken when we restrict ourselves to a certain phase, we need to account for this when looking at symmetries in a certain phase. We can clearly see this in figure (5) where if we perform a $\frac{2\pi}{3}$ rotation about the (1,1,1) axis by itself, this will not be a symmetry of the system as the phase colours of the lobes have not been shifted. For example, the rotation described above will send the yellow lobe onto green lobe, the green lobe onto the blue and the blue lobe onto the yellow. To correct for this we need to make a phase shift of $\frac{2\pi}{3}$ together with this rotation to preserve the symmetry. We therefore see that the generators for the remaining symmetry group of the cyclic phase are the following:

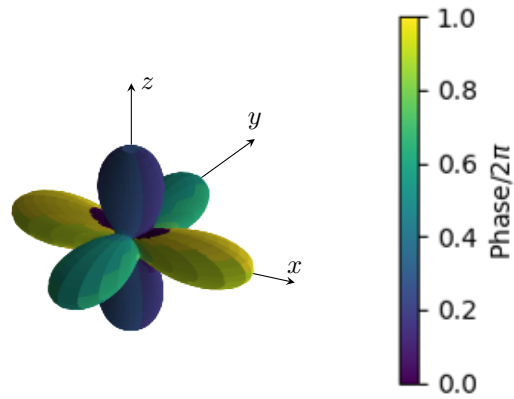


Figure 4: Spherical harmonic representation for cyclic representative order parameter.

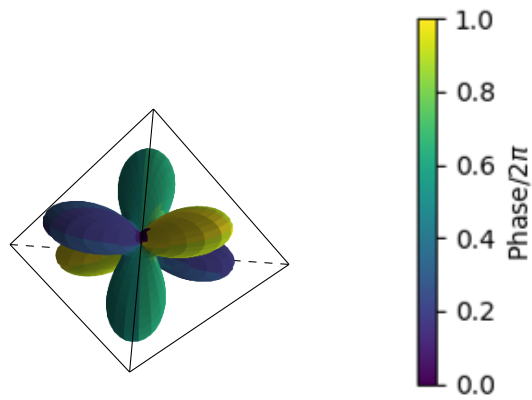


Figure 5: Rotated spherical harmonic representation of cyclic phase. We see that this phase has the rotational symmetry of a tetrahedron.

$$\bar{C} = e^{2\pi i/3} C_{3,x+y+z} \quad (5.24)$$

$$f_z = C_{2,z}. \quad (5.25)$$

Here, we are using the notation that $C_{n,\Omega_x x + \Omega_y y + \Omega_z z}$ is a $\frac{2\pi}{n}$ rotation about the $(\Omega_x, \Omega_y, \Omega_z)$ axis. We see that the two generators correspond to a rotation of $\frac{2\pi}{3}$ of the tetrahedron and a flip of π . The modification for the gauge angle has been accounted for in (5.24). From these two generators, we can obtain our modified tetrahedral group.

$$T = \{1, f_x, f_y, f_z, \bar{C}, f_x \bar{C}, f_y \bar{C}, f_z \bar{C}, f_x \bar{C}^2, f_y \bar{C}^2, f_z \bar{C}^2, \bar{C}^2\}. \quad (5.26)$$

Now that we have found the stabilizer group for the cyclic phase, we can use it to construct the order parameter manifold by subbing this into equation (5.16).

$$\mathcal{R} = \frac{SO(3) \times U(1)}{T}. \quad (5.27)$$

We can now classify the types of vortices that can be hosted in the cyclic phase by looking at the fundamental group of the above order parameter manifold, $\pi_1(SO(3) \times U(1)/T)$. In order to find this fundamental group, we would like to be able to use the expression given by (5.17). However, at the moment, we cannot use this as $SO(3)$ is not simply connected. To fix this issue, we need to lift $SO(3)$ to $SU(2)$ which is a double cover space of $SO(3)$ and is both connected and simply connected. The connection between $SO(3)$ and $SU(2)$ can be seen by thinking of both groups as rotations in space. $SO(3)$ gives all rotations in three-dimensional space. We can also view $SU(2)$ as describing rotations in three-dimensional space through the isomorphism with the unit quaternions [34]. The unit quaternions give rotations in the following way. If we take a unit quaternion $q = a\mathbf{1} + b\mathbf{i} + c\mathbf{j} + d\mathbf{k}$, we can construct \mathbb{R}^3 as the span of $(\mathbf{i}, \mathbf{j}, \mathbf{k})$ and can therefore rotate an element $v \in \mathbb{R}^3$ through the conjugation qvq^{-1} . However, we can get the same rotation by taking $q \rightarrow -q$ which means that one element in $SO(3)$ corresponds to two elements in $SU(2)$.

When we perform this lift, we must also lift the stabilizer group of the phase of the condensate we are looking at which, in this case, is the tetrahedral group given by (5.26). To do this, we need to consider what elements of $SU(2)$ correspond to our elements in T . This is a particularly easy task as all elements of T correspond to a simple rotation about some axis, neglecting the gauge angle shift. Therefore, we can link our elements of T to those in $SU(2)$ using the Pauli matrices, σ_x, σ_y and σ_z , which describe a rotation by an angle π about the x, y and z axes respectively. A general rotation in $SU(2)$ is given by [35]:

$$R(\hat{n}, \theta) = \mathbf{1} \cos\left(\frac{\theta}{2}\right) - i\vec{\sigma} \cdot \hat{n} \sin\left(\frac{\theta}{2}\right) \quad (5.28)$$

With this, we can see how the generator elements of T lift to elements of $SU(2)$:

$$\begin{aligned}
f_z &\rightarrow \pm i\sigma_z \\
e^{2\pi i/3} C_{3,x+y+z} &\rightarrow \pm \frac{1}{2} e^{2\pi i/3} (\mathbf{1} + i\sigma_x + i\sigma_y + i\sigma_z) = \pm \tilde{\sigma}.
\end{aligned} \tag{5.29}$$

From this, we can lift all elements of T to their corresponding elements in $SU(2)$ given by T^* :

$$T^* = \left\{ \begin{array}{cccc} \pm \mathbf{1}, & \pm i\sigma_x, & \pm i\sigma_y, & \pm i\sigma_z, \\ \pm i\sigma_x \tilde{\sigma}, & \pm i\sigma_y \tilde{\sigma}, & \pm i\sigma_z \tilde{\sigma}, & \pm \tilde{\sigma}, \\ \pm i\sigma_x \tilde{\sigma}^2, & \pm i\sigma_y \tilde{\sigma}^2, & \pm i\sigma_z \tilde{\sigma}^2, & \pm \tilde{\sigma}^2 \end{array} \right\}. \tag{5.30}$$

We still cannot use (5.17) as we have not yet accounted for the $U(1)$ symmetry contained within the full symmetry group of the condensate, G . Here, we see that $U(1)$ is not simply connected. However, the lift that we must perform is very easy to see and is $U(1) \rightarrow \mathbb{R}$.

We again must account for this lift when we lift the stabilizer group T . Since the $U(1)$ component of the symmetry group G describes what happens to the gauge angle ϕ , we expect that accounting for this lift in the stabilizer group will similarly affect the portion of the element affecting the gauge angle. This is indeed the case and can be determined by looking at the homomorphism between $U(1)$ and \mathbb{R} given by $e^{2\pi i\phi} \rightarrow \phi$. Since the kernel of the inverse map is \mathbb{Z} , we can just consider $\phi \rightarrow n_w + t$ where $n_w \in \mathbb{Z}$ and $t \in [0, 1)$. n_w tells us how many times the gauge angle winds around the unit circle. We saw, in the case of a spinless condensate, that this winding of the gauge angle was the only vortex present. However, in this case, we can have fractional vortices which is accounted for by t . We see this in elements of T^* such as $\tilde{\sigma}$ where we get a phase shift of $\frac{2\pi}{3}$, or $\tilde{\sigma}^2$ where there is a phase shift of $\frac{4\pi}{3}$. We can make the same change in the gauge angle of these elements as is done above. Namely, send $\phi = 0 \rightarrow 2\pi n_w$, $\phi = \frac{2\pi}{3} \rightarrow 2\pi(n_w + \frac{1}{3})$ and $\phi = \frac{4\pi}{3} \rightarrow 2\pi(n_w + \frac{2}{3})$.

With this full lift, we see that the elements of T go to the following, note that an alternative view to classifying the closed paths in the cyclic order parameter manifold is given in [34]:

$$\tilde{T} = \left\{ \begin{array}{cccc} (n_w, \mathbf{1}), & (n_w, -\mathbf{1}), & (n_w, i\sigma_\alpha), & (n_w, -i\sigma_\alpha), \\ (n_w + \frac{1}{3}, \tilde{\sigma}), & (n_w + \frac{1}{3}, -\tilde{\sigma}), & (n_w + \frac{1}{3}, i\sigma_\alpha \tilde{\sigma}), & (n_w + \frac{1}{3}, -i\sigma_\alpha \tilde{\sigma}), \\ (n_w + \frac{2}{3}, \tilde{\sigma}^2), & (n_w + \frac{2}{3}, -\tilde{\sigma}^2), & (n_w + \frac{2}{3}, i\sigma_\alpha \tilde{\sigma}^2), & (n_w + \frac{2}{3}, -i\sigma_\alpha \tilde{\sigma}^2) \end{array} \right\}, \tag{5.31}$$

Now that we have fully lifted the full symmetry group $G = SO(3) \times U(1)$ to $SU(2) \times \mathbb{R}$ which is both connected and simply connected, and we have accounted for how this lift affects the tetrahedral group, T ; we can now use the expression given by (5.17).

$$\pi_1 \left(\frac{SO(3) \times U(1)}{T} \right) \sim \pi_1 \left(\frac{SU(2) \times \mathbb{R}}{\tilde{T}} \right) \sim \pi_0(\tilde{T}). \tag{5.32}$$

Further to this, if \tilde{T} is a discrete group, which it is in this case, then we have $\pi_0(\tilde{T}) = \tilde{T}$. Therefore the vortices in the cyclic phase of a spin two condensate are described by the elements of the group \tilde{T} above. As mentioned earlier, for non-abelian groups, homotopy theory cannot distinguish between two vortices that are conjugate to each other and therefore, to be fully correct, we must say that the vortex types that can be hosted by the cyclic phase of a spin two condensate are given by the conjugacy classes of \tilde{T} . The group \tilde{T} splits into seven conjugacy classes [21]:

$$(1)\{(n_w, \mathbf{1})\} \tag{5.33}$$

$$(2)\{(n_w, -\mathbf{1})\} \tag{5.34}$$

$$(3)\{(n_w, i\sigma_\nu), (n_w, -i\sigma_\nu)\} \tag{5.35}$$

$$(4)\{(n_w + 1/3, \tilde{\sigma}), (n_w + 1/3, -i\sigma_\nu\tilde{\sigma})\} \tag{5.36}$$

$$(5)\{(n_w + 1/3, -\tilde{\sigma}), (n_w + 1/3, i\sigma_\nu\tilde{\sigma})\} \tag{5.37}$$

$$(6)\{(n_w + 2/3, -\tilde{\sigma}^2), (n_w + 2/3, -i\sigma_\nu\tilde{\sigma}^2)\} \tag{5.38}$$

$$(7)\{(n_w + 2/3, \tilde{\sigma}^2), (n_w + 2/3, i\sigma_\nu\tilde{\sigma}^2)\}. \tag{5.39}$$

From this, we see that we get seven different vortex types that can be hosted in the cyclic phase of a spin two condensate. Class (1) is the vacuum state of the system and class (2) is the integer spin vortex that we have seen in a spinless condensate where we just get a winding of the U(1) phase of the wavefunction. Class (3) is the first vortex in this phase where we see a winding in the spin degree of freedom. This vortex is called the half quantum vortex as the elements cause a rotation of π in spin space. Classes (4) to (7) are the first examples of fractional winding in the gauge degree of freedom. Due to the accompanying rotation in spin space, these elements still represent a closed loop in the order parameter manifold. Due to the extra $\frac{1}{3}$ or $\frac{2}{3}$ winding of the phase of the condensate order parameter, vortices classed by (4) and (5) are known as $\frac{1}{3}$ fractional vortices and vortices classed by (6) and (7) are known as $\frac{2}{3}$ fractional vortices. We see that we get two different types of these vortices corresponding to the amount of rotation that occurs in spin space. This difference between two vortices with the same fractional winding in the gauge degree of freedom is shown in figures (6) and (7) for vortices described by class (4) and (5) respectively.

Biaxial Nematic phase vortices We will follow the exact same procedure as detailed in (5.3.3) to study the types of vortices that can occur in the biaxial nematic phase of a spin two condensate. The representative order parameter for this phase of the condensate is given by:

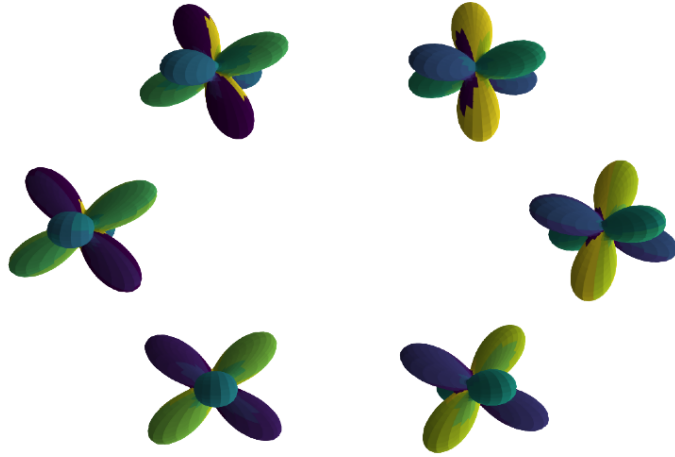


Figure 6: A class 4 vortex. A $\frac{1}{3}$ fractional vortex with a rotation of $\frac{2\pi}{3}$ in spin space.

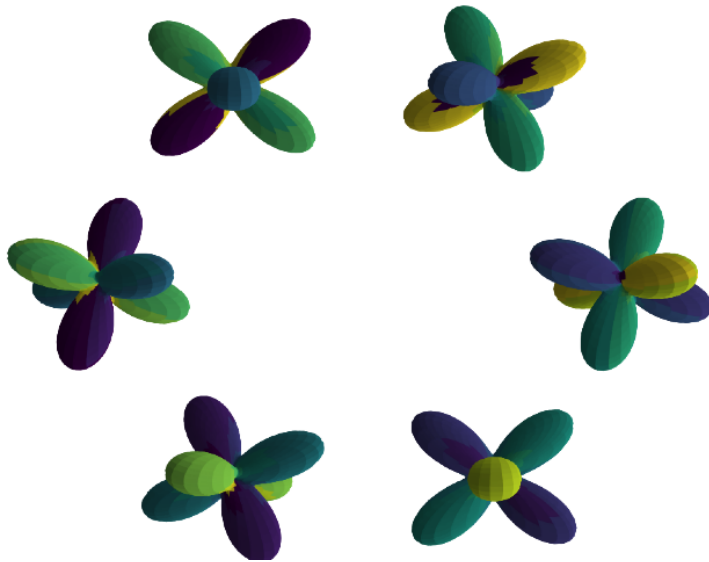


Figure 7: A class 5 vortex. A $\frac{1}{3}$ fractional vortex with a rotation of $\frac{4\pi}{3}$ in spin space.

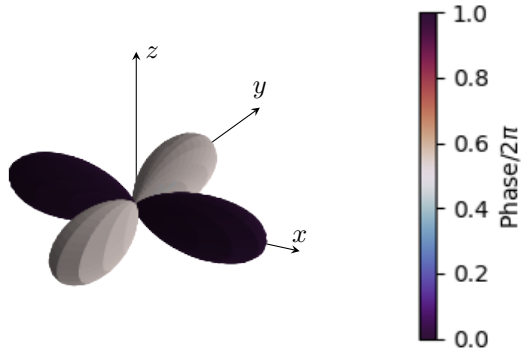


Figure 8: Spherical harmonic representation for biaxial nematic representative order parameter.

$$\zeta = \begin{pmatrix} \frac{1}{\sqrt{2}} \\ 0 \\ 0 \\ 0 \\ \frac{1}{\sqrt{2}} \end{pmatrix}. \quad (5.40)$$

We can again determine the stabilizer group for this phase by looking at the symmetries of the spherical harmonic representation of the representative order parameter. This is shown in figure (8) where we can clearly see that this spherical harmonic possesses the symmetry of a square and so we can describe the stabilizer group using the dihedral four group D_4 .

Just as was the case for the cyclic phase, we need to slightly modify the dihedral-4 group in order to account for the phase of the spherical harmonic representation. We see that the difference in phase between the x-lobe and y-lobe in figure (8) is π and so when we make a rotation of $\frac{\pi}{2}$ about the z-axis, we have to include a phase shift of π . This means that the generators for the symmetry group are:

$$\bar{C} = e^{i\pi} C_{4,z}, \quad (5.41)$$

$$f_y = C_{2,y}. \quad (5.42)$$

We will again need to lift these elements to their $SU(2)$ counterparts in order to account for lifting $SO(3) \times U(1) \rightarrow SU(2) \times \mathbb{R}$. Here we will just lift the generators and then use them to generate the remaining group elements.

$$\begin{aligned} f_y &\rightarrow \pm i\sigma_y \\ e^{i\pi} C_{4,z} &\rightarrow \pm e^{i\pi} (\mathbf{1} + i\sigma_z) / \sqrt{2} = \pm e^{i\pi} \tilde{\sigma}. \end{aligned} \quad (5.43)$$

Note that we have redefined $\tilde{\sigma}$ here from what it represented when discussing the cyclic phase.

Just as was done previously, we must also lift the gauge angle part of each element. This is done by sending the gauge angle $\phi = \frac{2\pi}{m}$ to $2\pi(n_w + 1/m)$. Once we do this and use the generators described above, we get the following lifted stabilizer group, \tilde{D}_4 for the biaxial nematic phase, which is split into its conjugacy classes [21]:

$$(1)\{(n_w, \mathbf{1})\} \quad (5.44)$$

$$(2)\{(n_w, -\mathbf{1})\} \quad (5.45)$$

$$(3)\{(n_w, \pm i\sigma_x), (n_w, \pm i\sigma_y)\} \quad (5.46)$$

$$(4)\{(n_w, i\sigma_z), (n_w, -i\sigma_z)\} \quad (5.47)$$

$$(5)\{(n_w + 1/2, \tilde{\sigma}), (n_w + 1/2, -i\sigma_z \tilde{\sigma})\} \quad (5.48)$$

$$(6)\{(n_w + 1/2, -\tilde{\sigma}), (n_w + 1/2, i\sigma_z \tilde{\sigma})\} \quad (5.49)$$

$$(7)\{(n_w + 1/2, \pm i\sigma_x \tilde{\sigma}), (n_w + 1/2, \pm i\sigma_y \tilde{\sigma})\}. \quad (5.50)$$

Here, we see that we get a different type of fractional vortex, the half quantum vortex with a corresponding spin rotation. We get three different types of this vortex which correspond to spin rotations of $\frac{\pi}{2}$, $\frac{3\pi}{2}$ and π for classes (5), (6) and (7) respectively. These vortices are shown in figures (9) to (11).

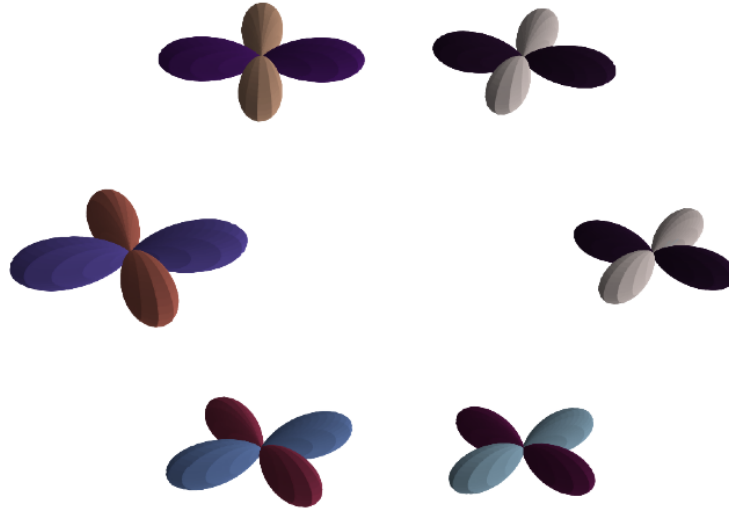


Figure 9: A class 5 vortex. A $\frac{1}{2}$ fractional vortex with a rotation of $\frac{\pi}{2}$ in spin space

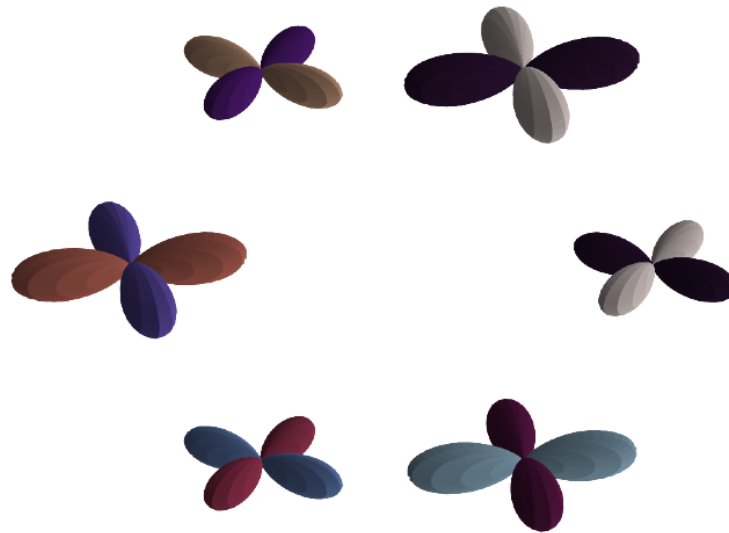


Figure 10: A class 6 vortex. A $\frac{1}{2}$ fractional vortex with a rotation of $\frac{3\pi}{2}$ in spin space

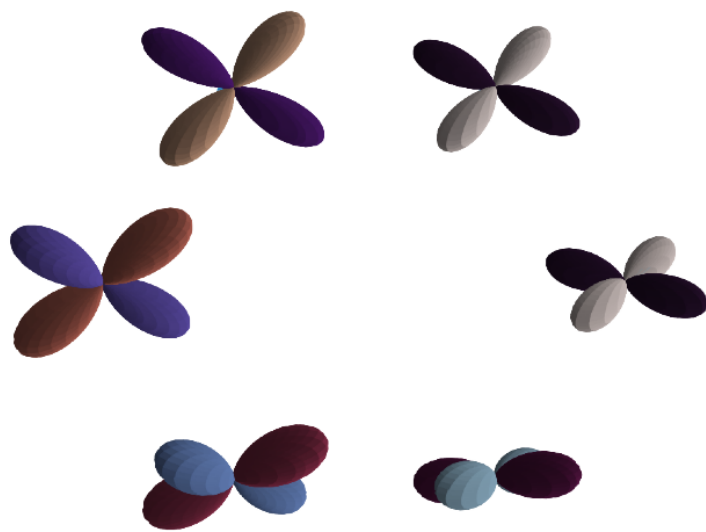


Figure 11: A class 7 vortex. A $\frac{1}{2}$ fractional vortex with a rotation of π in spin space

6 Numerical Methods

This section details how the code involved in this thesis works, which includes ground state solvers for spin one and spin two condensates and code to solve the Bogoliubov equations for a spin one and spin two condensate [25]. The Bogoliubov equations allow us to look at elementary excitations over ground states of the Gross-Pitaevskii equation whose eigenvalues give the energy of these elementary excitations. These are useful in further analysing ground states. We will see more about these equations in section (6.4).

The details for this section will be laid out in the following way. For each piece of code, we will describe how the equations are set up and formatted to be fed into the algorithm that performs the particular function, whether that be finding the ground state of the system or solving the Bogoliubov equations. Once this has been done, we will move on to describe the algorithm to do these tasks. Finally, for task, we will describe the actual code, how it is setup, and the different files involved.

Ultimately, the aim of this section is to provide a detailed understanding of how the code used is setup.

We include a reference to a review paper on numerical methods that has been instructive on developing our own codes for solving the Gross Pitaevskii equations for the ground state as well as setting up the Bogoliubov equations for a spin one and spin two condensate [36].

6.1 Spin One Ground State Code

6.1.1 Equation setup

In order to solve for the ground state of a spin one condensate, we need to find a wavefunction that minimizes the energy functional for this system which is again given by:

$$E[\psi_m] = \int d\vec{r} \left\{ \sum_{m=-1}^1 \psi_m^* \left[-\frac{\hbar^2 \nabla^2}{2M} + V(\vec{r}) - pm + qm^2 \right] \psi_m + \frac{c_0}{2} n^2 + \frac{c_1}{2} |\vec{F}|^2 \right\}. \quad (6.1)$$

The terms in this equation are described in section (3.2.1). As seen in section (3.2.1), if we want to find equations for the wavefunction that minimizes this energy, we end up with the time-independent Gross-Pitaevskii equations which are listed here again for convenience:

$$\mu\phi_1 = \left[-\frac{\hbar^2 \nabla^2}{2M} + V(\vec{r}) - p + q + c_0 n + c_1 F_z \right] \phi_1 + \frac{c_1}{\sqrt{2}} F_- \phi_0, \quad (6.2)$$

$$\mu\phi_0 = \left[-\frac{\hbar^2 \nabla^2}{2M} + V(\vec{r}) + c_0 n \right] \phi_0 + \frac{c_1}{\sqrt{2}} F_+ \phi_1 + \frac{c_1}{\sqrt{2}} F_- \phi_{-1}, \quad (6.3)$$

$$\mu\phi_{-1} = \left[-\frac{\hbar^2 \nabla^2}{2M} + V(\vec{r}) + p + q + c_0 n - c_1 F_z \right] \phi_{-1} + \frac{c_1}{\sqrt{2}} F_+ \phi_0. \quad (6.4)$$

Here, we have introduced $\phi = (\phi_1, \phi_0, \phi_{-1})$ as the ground state of the condensate which minimizes the energy functional instead of just looking at an arbitrary stationary state. When reading these equations now, we are thinking of the ground state wavefunction replacing the arbitrary stationary state in all terms of these equations, including terms such as n , F_x , F_y and F_z which, for spin one, are given by equations (3.65), (3.68), (3.69) and (3.70) respectively.

Equations (6.2) to (6.4) are what we wish to solve numerically. Recall that we have the following constraint on the wavefunctions in order to conserve particle number N :

$$\int (|\psi_1|^2 + |\psi_0|^2 + |\psi_{-1}|^2) d\vec{r} = N. \quad (6.5)$$

To start, we would like to work with dimensionless versions of these equations. To do this we will scale the full time-dependent equations and then apply this to the time independent ones. The time dependent Gross-Pitaevskii equations for spin one are easily obtained from the time dependent ones listed in (6.2) to (6.4):

$$i\hbar \frac{\partial \psi_1}{\partial t} = \left[-\frac{\hbar^2 \nabla^2}{2M} + V(\vec{r}) - p + q + c_0 n + c_1 F_z \right] \psi_1 + \frac{c_1}{\sqrt{2}} F_- \psi_0, \quad (6.6)$$

$$i\hbar \frac{\partial \psi_0}{\partial t} = \frac{c_1}{\sqrt{2}} F_+ \psi_1 + \left[-\frac{\hbar^2 \nabla^2}{2M} + V(\vec{r}) + c_0 n - \mu \right] \psi_0 + \frac{c_1}{\sqrt{2}} F_- \psi_{-1} \quad (6.7)$$

$$i\hbar \frac{\partial \psi_{-1}}{\partial t} = \frac{c_1}{\sqrt{2}} F_+ \psi_0 + \left[-\frac{\hbar^2 \nabla^2}{2M} + V(\vec{r}) + p + q + c_0 n - c_1 F_z - \mu \right] \psi_{-1}. \quad (6.8)$$

Here we are again using $\psi = (\psi_1, \psi_0, \psi_{-1})$ for the wavefunction as we are dealing with the time dependent Gross-Pitaevskii equations and so are not considering the ground state at this moment.

Before moving to a dimensionless form, we would like to reduce the dimension of these equations by one. We do this as we will be working with two dimensional systems in this research. Here, we will reduce the dimension of this problem by one by considering a system with periodic boundary conditions such that we are sitting on a torus as the procedure for this is simpler. A procedure for reducing the dimension of a system in a harmonic trap is given in [37].

We will start by assuming that nothing interesting happens in the z -direction of the system. That is, that the z -direction of the condensate is so thin that the system lies in the ground state in that direction which on the torus means that the wavefunction in the z -direction is a constant. We will call the length of the z -direction L_z .

Seeing as the wavefunction in the z -direction is constant, we can factorise the wavefunction for the condensate in the following way:

$$\psi_m(\vec{r}, z) = \psi_m(\vec{r}) \psi_m(z). \quad (6.9)$$

where now we have a wavefunction that just depends on the x and y direction and a wavefunction that depends on the z-direction which is a constant. We can determine this constant by subbing (6.9) into our constraint, (6.5):

$$\int |\psi_1(\vec{r})\psi_1(z)|^2 + |\psi_0(\vec{r})\psi_0(z)|^2 + |\psi_{-1}(\vec{r})\psi_{-1}(z)|^2 d\vec{r}dz = N, \quad (6.10)$$

$$\int |\psi(z)|^2 (|\psi_1(\vec{r})|^2 + |\psi_0(\vec{r})|^2 + |\psi_{-1}(\vec{r})|^2) d\vec{r}dz = N, \quad (6.11)$$

$$\int |\psi(z)|^2 \int |\psi_1(\vec{r})|^2 + |\psi_0(\vec{r})|^2 + |\psi_{-1}(\vec{r})|^2 d\vec{r}dz = N. \quad (6.12)$$

In the second line, we are assuming that the wavefunction in the z-direction is the same constant solution in all spin components and so we call it $\psi(z)$ and factor it out.

We now have a choice of how to set the normalization. We will choose the following:

$$\int |\psi(z)|^2 dz = 1, \quad (6.13)$$

$$\int |\psi_1(\vec{r})|^2 + |\psi_0(\vec{r})|^2 + |\psi_{-1}(\vec{r})|^2 d\vec{r} = N. \quad (6.14)$$

Using (6.13), we can get an expression for the constant $\psi(z)$ by taking the integral over the length L_z .

$$L_z |\psi(z)|^2 = 1, \quad (6.15)$$

$$\implies |\psi(z)|^2 = \frac{1}{L_z}, \quad (6.16)$$

$$\implies \psi(z) = \frac{1}{\sqrt{L_z}}. \quad (6.17)$$

In going from the second to third line, we have made another choice to put the complex phase of the wavefunction into $\psi(\vec{r})$ and choose $\phi(z)$ to be real and positive.

We can now substitute this constant into expression (6.9) and in turn substitute this into the time dependent Gross-Pitaevskii equations, (6.6) to (6.8), in order to reduce the dimension of the problem from three to two. We will just show the working for (6.6), as the procedure is the exact same for all other equations. First, write out (6.6) after expanding out the spin density terms using equations (3.68), (3.69), (3.70) and (3.86) and tidying up the resulting equation.

$$i\hbar \frac{\partial}{\partial t} \psi_1 = \left[-\frac{\hbar^2}{2M} \frac{\partial^2}{\partial \vec{r}^2} + V(\vec{r}) - p + q + c_0 n + c_1(n_1 + n_0 - n_{-1}) \right] \psi_1 + c_1 \psi_{-1}^* \psi_0^2, \quad (6.18)$$

$$\begin{aligned} \frac{i\hbar}{\sqrt{L_z}} \frac{\partial}{\partial t} \psi_1 = & \left[-\frac{\hbar^2}{2M\sqrt{L_z}} \frac{\partial^2}{\partial \vec{r}^2} + \frac{1}{\sqrt{L_z}}(V - p + q) + \frac{c_0}{L_z^{3/2}} n \right. \\ & \left. + \frac{c_1}{L_z^{3/2}}(n_1 + n_0 - n_{-1}) \right] \psi_1 + \frac{c_1}{L_z^{3/2}} \psi_{-1}^* \psi_0^2, \end{aligned} \quad (6.19)$$

$$i\hbar \frac{\partial}{\partial t} \psi_1 = \left[-\frac{\hbar^2}{2M} \frac{\partial^2}{\partial \vec{r}^2} + V - p + q + \frac{c_0}{L_z} n + \frac{c_1}{L_z}(n_1 + n_0 - n_{-1}) \right] \psi_1 + \frac{c_1}{L_z} \psi_{-1}^* \psi_0^2. \quad (6.20)$$

Here, we are redefining $\psi_1 = \psi_1(\vec{r})$ where \vec{r} now only depends on x and y. We are also redefining the particle densities n and n_m to be the sum of the absolute values squared of the wavefunctions that only depend on x and y.

We can now get a dimensionless form of (6.20) by taking the following scaling:

$$\tilde{t} = \frac{t}{t_s}, \quad \tilde{r} = \frac{\vec{r}}{r_s}, \quad \tilde{L}_z = \frac{L_z}{r_s}, \quad \tilde{\psi} = \frac{\psi r_s}{N^{1/2}}. \quad (6.21)$$

If we sub these into (6.20) and multiply across by $\frac{N^{1/2}}{r_s}$, we get the following:

$$\frac{i\hbar}{t_s} \frac{\partial}{\partial \tilde{t}} \tilde{\psi}_1 = \left[-\frac{\hbar^2}{2M r_s^2} \nabla^2 + V - p + q + \frac{c_0 N}{\tilde{L}_z r_s^3} \tilde{n} + \frac{c_1 N}{\tilde{L}_z r_s^3} (\tilde{n}_1 + \tilde{n}_0 - \tilde{n}_{-1}) \right] \tilde{\psi}_1 + \frac{c_1 N}{\tilde{L}_z r_s^3} \tilde{\psi}_{-1}^* \tilde{\psi}_0^2. \quad (6.22)$$

We can now choose a scaling to use for t_s and r_s , here we will discuss this in terms of periodic boundary conditions on a finite lattice for completeness of this discussion and will move afterwards to the system of interest, namely a system in a harmonic potential.

It is useful to briefly discuss the setup and parameters involved with this lattice. Note that for periodic boundary conditions, the value we choose for the number of lattice points is slightly different to that for Dirichlet boundary conditions which is what we will mainly be working with in the ground state code, whereas for the Bogoliubov code, we will be using Dirichlet boundary conditions. As a result, here, we will discuss the setup of both so as to point out the subtle differences. We will use L to denote the number of lattice spacings along a side length of the square lattice. For both the x and y direction, the side length of the square lattice will be bounded between a and b such that the lattice spacing, $h = (b - a)/L$. With this setup, we will have $L + 1$ points along a side length of a lattice including the two boundary points a and b . This gives an $(L + 1) \times (L + 1)$ lattice.

For Dirichlet boundary conditions, we will choose to ignore the boundary points and so our grid will be of dimension $(L - 1) \times (L - 1)$ in the number of lattice points.

For periodic boundary conditions, we will identify the boundary points a and b with each

other and so we will just drop one of them, leaving us with a grid of dimension $L \times L$ in the number of lattice points. Note that in both cases, the lattice spacing, h , for both of these grids remains the same.

If we are working on a lattice with periodic boundary conditions and lattice spacing h (not to be confused with the reduced Planck constant, \hbar) along with boundaries at a and b so that the length of the lattice is $(b - a)$; we can choose the following scaling:

$$t_s = \frac{Mr_s^2}{\hbar}, \quad (6.23)$$

$$r_s = h. \quad (6.24)$$

Note that this means we are choosing to take all units of distance in terms of our lattice spacing, h .

When we substitute in for t and \vec{r} in terms of t_s and r_s in equation (6.22), we get the following:

$$\begin{aligned} \frac{i\hbar^2}{Mr_s^2} \frac{\partial}{\partial t} \tilde{\psi}_1 = & \left[-\frac{\hbar^2 \nabla^2}{2Mr_s^2} + V + q - p + \frac{c_0 N}{\tilde{L}_z r_s^3} \tilde{n} \right. \\ & \left. + \frac{c_1 N}{\tilde{L}_z r_s^3} (\tilde{n}_1 + \tilde{n}_0 - \tilde{n}_{-1}) \right] \tilde{\psi}_1 + \frac{c_1 N}{\tilde{L}_z r_s^3} \tilde{\psi}_{-1}^* \tilde{\psi}_0^2, \end{aligned} \quad (6.25)$$

$$\begin{aligned} i \frac{\partial}{\partial t} \tilde{\psi}_1 = & \left[-\frac{1}{2} \nabla^2 + (V + q - p) \frac{Mh^2}{\hbar^2} + \frac{c_0 MN}{\tilde{L}_z \hbar^2 h} \tilde{n} \right. \\ & \left. + \frac{c_1 MN}{\tilde{L}_z \hbar^2 h} (\tilde{n}_1 + \tilde{n}_0 - \tilde{n}_{-1}) \right] \tilde{\psi}_1 + \frac{c_1 MN}{\tilde{L}_z \hbar^2 h} \tilde{\psi}_{-1}^* \tilde{\psi}_0^2. \end{aligned} \quad (6.26)$$

From this we can define dimensionless interaction parameters:

$$\beta_\nu = \frac{c_\nu MN}{\tilde{L}_z \hbar^2 h} \quad (6.27)$$

We can then substitute this into (6.26) to get the form of equation that we will be using. We also drop the $\tilde{}$ on all symbols as we know we are working with dimensionless quantities.

$$i \frac{\partial}{\partial t} \psi_1 = \left[-\frac{1}{2} \nabla^2 + (V + q - p) \frac{Mh^2}{\hbar^2} + \beta_0 n + \beta_1 (n_1 + n_0 - n_{-1}) \right] \psi_1 + \beta_1 \psi_{-1}^* \psi_0^2. \quad (6.28)$$

We will also perform the same procedure for a condensate in three dimensions, subject to a potential, which we will use for our discussion throughout the rest of this section so as to include the potential and Zeeman terms for generality.

We will assume that we are working with an isotropic harmonic potential with frequency

ω for convenience.

$$V(\vec{r}) = \frac{1}{2}M\omega^2\vec{r}^2. \quad (6.29)$$

In order to obtain dimensionless versions of the above equations, we define the following scaling:

$$\tilde{t} = \frac{t}{t_s}, \quad \tilde{\vec{r}} = \frac{\vec{r}}{r_s}, \quad \tilde{\psi} = \frac{\psi}{r_s^{3/2}N^{1/2}}, \quad (6.30)$$

where

$$t_s = \frac{1}{\omega}, r_s = \sqrt{\frac{\hbar}{M\omega}}. \quad (6.31)$$

We then substitute these scaled variables into equations (6.2) - (6.4). We will just show the working for (6.2), as the procedure is the exact same for all other equations. First write out (6.2) after expanding out the spin density terms using equations (3.68), (3.69), (3.70) and (3.86) and tidying up the resulting equation.

$$i\hbar \frac{\partial}{\partial t} \psi_1 = \left[-\frac{\hbar^2}{2M} \frac{\partial^2}{\partial \vec{r}^2} + V(\vec{r}) - p + q + c_0 n + c_1(n_1 + n_0 - n_{-1}) \right] \psi_1 + c_1 \psi_{-1}^* \psi_0^2, \quad (6.32)$$

$$i\hbar \omega \frac{\partial}{\partial \tilde{t}} \tilde{\psi}_1 N^{1/2} r_s^{-3/2} = \left[-\frac{\hbar^2}{2Mr_s^2} \frac{\partial^2}{\partial \tilde{\vec{r}}^2} + V(\vec{r}) - p + q + \frac{c_0 N \tilde{n}}{r_s^3} + \frac{c_1 N}{r_s^3} (\tilde{n}_1 + \tilde{n}_0 - \tilde{n}_{-1}) \right] r_s^{-3/2} N^{1/2} \tilde{\psi}_1 + c_1 r_s^{-9/2} N^{3/2} \tilde{\psi}_{-1}^* \tilde{\psi}_0^2, \quad (6.33)$$

where $n = \sum_{m=-1}^1 n_m$, $n_m = |\psi_m|^2$. \tilde{n} and \tilde{n}_m are the equivalent of these using $\tilde{\psi}_m$. In the following step, we multiply across by $r_s^{9/2} N^{-3/2}$:

$$i\hbar \omega \frac{\partial}{\partial \tilde{t}} \tilde{\psi}_1 N^{-1} r_s^3 = \left[-\frac{\hbar^2}{2Mr_s^2} \frac{\partial^2}{\partial \tilde{\vec{r}}^2} + V(\vec{r}) - p + q + \frac{c_0 N \tilde{n}}{r_s^3} + \frac{c_1 N}{r_s^3} (\tilde{n}_1 + \tilde{n}_0 - \tilde{n}_{-1}) \right] r_s^3 N^{-1} \tilde{\psi}_1 + c_1 \tilde{\psi}_{-1}^* \tilde{\psi}_0^2. \quad (6.34)$$

Now, multiply across by $t_s^2/Mr_s^{1/2}N^{1/2} = 1/\omega^2 Mr_s^{1/2}N^{1/2}$:

$$i\hbar \frac{\partial}{\partial t} \tilde{\psi}_1 \frac{r^{5/2}}{\omega MN^{3/2}} = \left[-\frac{\hbar^2}{2Mr_s^2} \frac{\partial^2}{\partial \tilde{r}^2} + V(\vec{r}) - p + q + \frac{c_0 N \tilde{n}}{r_s^3} + \frac{c_1 N}{r_s^3} (\tilde{n}_1 + \tilde{n}_0 - \tilde{n}_{-1}) \right] \frac{r_s^{5/2}}{\omega^2 MN^{3/2}} \tilde{\psi}_1 + \frac{c_1}{\omega^2 Mr_s^{1/2} N^{1/2}} \tilde{\psi}_{-1}^* \tilde{\psi}_0^2. \quad (6.35)$$

This is followed by multiplication by $\frac{\omega MN^{3/2}}{\hbar r^{5/2}}$:

$$i \frac{\partial}{\partial t} \tilde{\psi}_1 = \left[-\frac{\hbar^2}{2Mr_s^2} \frac{\partial^2}{\partial \tilde{r}^2} + V(\vec{r}) - p + q + \frac{c_0 N \tilde{n}}{r_s^3} + \frac{c_1 N}{r_s^3} (\tilde{n}_1 + \tilde{n}_0 - \tilde{n}_{-1}) \right] \frac{1}{\hbar \omega} + \frac{c_1 N}{\hbar \omega r_s^3} \tilde{\psi}_{-1}^* \tilde{\psi}_0^2, \quad (6.36)$$

$$i \frac{\partial}{\partial t} \psi_1 = \left[-\frac{1}{2} \nabla^2 + \frac{V(\vec{r})}{\omega \hbar} - \frac{p}{\omega \hbar} + \frac{q}{\omega \hbar} + \beta_0 n + \beta_1 (n_1 + n_0 - n_{-1}) \right] \psi_1 + \beta_1 \psi_{-1}^* \psi_0^2. \quad (6.37)$$

In the last line above, we have defined:

$$\beta_m = \frac{c_m N}{\omega r_s^3 \hbar}. \quad (6.38)$$

We have also dropped the $\tilde{}$ on all symbols as we now know we are working with this dimensionless form. We will also suppress the $\omega \hbar$ into all of V , p and q to get the following:

$$i \frac{\partial}{\partial t} \psi_1 = \left[-\frac{1}{2} \nabla^2 + V(\vec{r}) - p + q + \beta_0 n + \beta_1 (n_1 + n_0 - n_{-1}) \right] \psi_1 + \beta_1 \psi_{-1}^* \psi_0^2. \quad (6.39)$$

In the exact same way, we also give the following dimensionless equations for the $m = 0$ and $m = -1$ components of the Gross-Pitaevskii equation:

$$i \frac{\partial}{\partial t} \psi_0 = \left[-\frac{1}{2} \nabla^2 + V(\vec{r}) + \beta_0 n + \beta_1 (n_1 + n_{-1}) \right] \psi_0 + 2\beta_1 \psi_{-1} \psi_0^* \psi_1, \quad (6.40)$$

$$i \frac{\partial}{\partial t} \psi_{-1} = \left[-\frac{1}{2} \nabla^2 + V(\vec{r}) + p + q + \beta_0 n + \beta_1 (n_{-1} + n_0 - n_1) \right] \psi_{-1} + \beta_1 \psi_1^* \psi_0^2. \quad (6.41)$$

If we were to use an isotropic harmonic potential for $V(\vec{r})$, it would become $V(\vec{r}) = \frac{1}{2} \vec{r}^2$ in our dimensionless format. Note that due to our re-scaling of the wavefunction, the normalization condition (6.5) becomes:

$$\int (|\psi_1|^2 + |\psi_0|^2 + |\psi_{-1}|^2) d\vec{r} = 1. \quad (6.42)$$

where this is an integral over three-dimensions for the harmonic oscillator example we showed above and over two-dimensions for the torus system earlier.

6.1.2 Solving the Spin One Gross-Pitaevskii Equations using Gradient Descent

Now that we have this dimensionless form for the Gross-Pitaevskii equations, we can use this to write down the energy functional in the same way, where we are switching back to writing the wavefunction as ϕ again as we are interested in finding the ground state.

$$E[\phi_m] = \int d\vec{r} \left\{ \sum_{m=-1}^1 \phi_m^* \left[-\frac{1}{2} \nabla^2 + V(\vec{r}) - pm + qm^2 \right] \phi_m + \frac{\beta_0}{2} n^2 + \frac{\beta_1}{2} |\vec{F}|^2 \right\}. \quad (6.43)$$

We want to find the wavefunction ϕ which minimizes the energy. We saw previously that we could get equations for this by using the Euler-Lagrange equations to minimize the energy with respect to each component of ϕ , which resulted in the time-independent Gross-Pitaevskii equations.

To solve these, we can look at minimizing the energy functional numerically for ϕ using the method of gradient descent and then renormalizing ϕ at each gradient descent step. For a function $f(\vec{x})$, where $\vec{x} \in \mathbb{R}^3$, we move towards the minimum of f with the following gradient descent step:

$$\vec{x}_{i+1} = \vec{x}_i - \lambda \nabla f(\vec{x}_i). \quad (6.44)$$

We interpret the above as having moved a small step λ from \vec{x}_i in the direction of the negative gradient of f to arrive at the point \vec{x}_{i+1} . This point will give a lower value of the function, f , than the point \vec{x}_i and so iterating this step should give us the minimum of the function f .

For our purposes, we will take an implicit, backward Euler step in which we will substitute the value of x at the next gradient descent step, x_{i+1} , into the gradient of the function and then solve this equation for x_{i+1} . Doing this gives a similar equation to (6.44).

$$\vec{x}_{i+1} = \vec{x}_i - \lambda \nabla f(\vec{x}_{i+1}). \quad (6.45)$$

Backward Euler methods are known to be more stable than explicit methods and so we will use (6.45) instead.

In a similar way, we can do the same thing here with the energy functional to find the ground state of the spin one system. Before taking the gradient of the energy functional with respect to the different components of the wavefunction ϕ , let's set up the problem on a finite grid so that it can be solved numerically. We do this by discretizing the energy functional:

$$\begin{aligned}
E[\phi_{i,j}] = \sum_i \sum_j \left\{ \sum_{m=-1}^1 \phi_{m,i,j}^* \left[- \left(\frac{\phi_{m,i+1,j} - 2\phi_{m,i,j} + \phi_{m,i-1,j}}{2h^2} \right. \right. \right. \\
+ \left. \left. \frac{\phi_{m,i,j+1} - 2\phi_{m,i,j} + \phi_{m,i,j-1}}{2h^2} \right) + [V_{i,j} - pm + qm^2]\phi_{m,i,j} \right] \\
+ \left. \frac{\beta_0}{2} n_{i,j}^2 + \frac{\beta_1}{2} |\vec{F}_{i,j}|^2 \right\}. \tag{6.46}
\end{aligned}$$

Here, we are using i and j to describe a 2D grid where i describes the y component of a coordinate in space and j describes the x component. Depending on the problem we are looking at, we will change how many lattice points we use and the side length of the grid. h is the lattice spacing which we are taking to be the same in both the x and y direction for the duration of this thesis. With this setup, we see that $\phi_{m,i,j}$ is the value of the m^{th} component of our ground state wavefunction at the position (i, j) in our grid. $n_{i,j}$ and $\vec{F}_{i,j}$ are defined in the same way as (3.65) and (3.66) respectively. However, here we are again subbing $\phi_{m,i,j}$ into these definitions to look at their values at a particular point, (i, j) in our grid.

With this, we can now take the derivative of the energy functional with respect to the conjugate of the components of the wavefunction, $\phi_{m,i,j}^*$. Note that, since we have discretized the energy functional onto a grid, we are now talking about a numerical approximation of the gradient as opposed to the exact analytic gradient. This numerical approximation can then be subbed into the gradient descent formula to find a value for $\phi_{m,i,j}$ that brings the energy functional closer to its minimum value.

$$\phi_{m,i,j}^{n+1} = \phi_{m,i,j}^n - \tau \nabla_{\phi_{m,i,j}} E[\phi_{i,j}^{n+1}]. \tag{6.47}$$

Here, we are using that ϕ^{n+1} is the value of the wavefunction at the next gradient descent step, which we are trying to find and ϕ^n is the value of the wavefunction at the current step which we already know. Notice that we do this for each grid point (i, j) and so each time we take a derivative of $E[\phi_{i,j}]$, we are only interested in the term in the sum that contains $\phi_{i,j}^*$ which will only be one term in the sum.

We have also previously computed the expressions for the derivatives of $n_{i,j}^2$ and $|\vec{F}_{i,j}|^2$ with respect to $\phi_{m,i,j}^*$ for each value of $m = (1, 0, -1)$ which are contained within equations (3.83) to (3.85). Filling in for these, we get the following three gradient descent equations for each of the components of the spin one ground state:

$$\begin{aligned}\phi_{1,i,j}^{n+1} &= \phi_{1,i,j} - \tau \left[-\frac{1}{2h^2} [\phi_{1,i+1,j}^{n+1} + \phi_{1,i-1,j}^{n+1} + \phi_{1,i,j+1}^{n+1} + \phi_{1,i,j-1}^{n+1} - 4\phi_{1,i,j}^{n+1}] \right. \\ &\quad \left. + [V_{i,j} - p + q + \beta_0 n^{i,j} + \beta_1 (F_z)_{i,j}] \phi_{1,i,j}^{n+1} + \frac{\beta_1}{\sqrt{2}} (F_-)_{i,j} \phi_{0,i,j}^n \right],\end{aligned}\quad (6.48)$$

$$\begin{aligned}\phi_{0,i,j}^{n+1} &= \phi_{0,i,j}^n - \tau \left[-\frac{1}{2h^2} [\phi_{0,i+1,j}^{n+1} + \phi_{0,i-1,j}^{n+1} + \phi_{0,i,j+1}^{n+1} + \phi_{0,i,j-1}^{n+1} - 4\phi_{0,i,j}^{n+1}] \right. \\ &\quad \left. + [V_{i,j} + \beta_0 n_{i,j}] \phi_{0,i,j}^{n+1} + \frac{\beta_1}{\sqrt{2}} (F_+)_{i,j} \phi_{1,i,j}^n + \frac{\beta_1}{\sqrt{2}} (F_-)_{i,j} \phi_{-1,i,j}^n \right],\end{aligned}\quad (6.49)$$

$$\begin{aligned}\phi_{-1,i,j}^{n+1} &= \phi_{-1,i,j}^n \\ &\quad - \tau \left[-\frac{1}{2h^2} [\phi_{-1,i+1,j}^{n+1} + \phi_{-1,i-1,j}^{n+1} + \phi_{-1,i,j+1}^{n+1} + \phi_{-1,i,j-1}^{n+1} - 4\phi_{-1,i,j}^{n+1}] \right. \\ &\quad \left. + [V_{i,j} + p + q + \beta_0 n_{i,j} - \beta_1 (F_z)_{i,j}] \phi_{-1,i,j}^{n+1} + \frac{\beta_1}{\sqrt{2}} (F_+)_{i,j} \phi_{0,i,j}^n \right].\end{aligned}\quad (6.50)$$

In the above equations, we have subbed in the value of the wavefunction at the next gradient descent step everywhere that that component shows up in its respective equation, including in the gradient of the energy functional. We will only use the previous value of the wavefunction for components that we are not currently solving for or for terms where the component shows up as $|\phi|^2$ and as a result, we think of terms such as $n_{i,j}$ as being at the previous gradient descent step. As done previously, we can now substitute in for the spin matrices in the above using the expressions given by (3.68), (3.69), (3.70) and (3.86):

$$\begin{aligned}\phi_{1,i,j}^{n+1} &= \phi_{1,i,j} - \tau \left[-\frac{1}{2h^2} [\phi_{1,i+1,j}^{n+1} + \phi_{1,i-1,j}^{n+1} + \phi_{1,i,j+1}^{n+1} + \phi_{1,i,j-1}^{n+1} - 4\phi_{1,i,j}^{n+1}] \right. \\ &\quad \left. + [V_{i,j} - p + q + \beta_0 n_{i,j} + \beta_1 (n_{1,i,j} + n_{0,i,j} - n_{-1,i,j})] \phi_{1,i,j}^{n+1} \right. \\ &\quad \left. + \beta_1 (\phi_{-1,i,j}^n)^* (\phi_{0,i,j}^n)^2 \right],\end{aligned}\quad (6.51)$$

$$\begin{aligned}\phi_{0,i,j}^{n+1} &= \phi_{0,i,j}^n - \tau \left[-\frac{1}{2h^2} [\phi_{0,i+1,j}^{n+1} + \phi_{0,i-1,j}^{n+1} + \phi_{0,i,j+1}^{n+1} + \phi_{0,i,j-1}^{n+1} - 4\phi_{0,i,j}^{n+1}] \right. \\ &\quad \left. + [V_{i,j} + \beta_0 n_{i,j} + \beta_1 (n_{1,i,j} + n_{-1,i,j})] \phi_{0,i,j}^{n+1} + 2\beta_1 \phi_{-1,i,j}^n (\phi_{0,i,j}^n)^* \phi_{1,i,j}^n \right],\end{aligned}\quad (6.52)$$

$$\begin{aligned}\phi_{-1,i,j}^{n+1} &= \phi_{-1,i,j}^n \\ &\quad - \tau \left[-\frac{1}{2h^2} [\phi_{-1,i+1,j}^{n+1} + \phi_{-1,i-1,j}^{n+1} + \phi_{-1,i,j+1}^{n+1} + \phi_{-1,i,j-1}^{n+1} - 4\phi_{-1,i,j}^{n+1}] \right. \\ &\quad \left. + [V_{i,j} + p + q + \beta_0 n_{i,j} + \beta_1 (n_{-1,i,j} + n_{0,i,j} - n_{-1,i,j})] \phi_{-1,i,j}^{n+1} \right. \\ &\quad \left. + \beta_1 (\phi_{1,i,j}^n)^* (\phi_{0,i,j}^n)^2 \right].\end{aligned}\quad (6.53)$$

We are using the notation that $n_{m,i,j} = |\phi_{m,i,j}^n|^2$. Since we are trying to solve for the

respective ground state component at the next gradient descent step, we can rearrange the above expressions to get equations for these components:

$$\begin{aligned}
& (2h^2 + 4\tau + 2h^2\tau [V_{i,j} - p + q + \beta_0 n_{i,j} + \beta_1 (n_{1,i,j} + n_{0,i,j} - n_{-1,i,j})]) \phi_{1,i,j}^{n+1} \\
& \quad - \tau [\phi_{1,i+1,j}^{n+1} + \phi_{1,i-1,j}^{n+1} + \phi_{1,i,j+1}^{n+1} + \phi_{1,i,j-1}^{n+1}] \\
& \quad = 2h^2 \phi_{1,i,j}^n - 2h^2 \tau \beta_1 (\phi_{-1,i,j}^n)^* (\phi_{0,i,j}^n)^2,
\end{aligned} \tag{6.54}$$

$$\begin{aligned}
& (2h^2 + 4\tau + 2h^2\tau [V_{i,j} + \beta_0 n_{i,j} + \beta_1 (n_{1,i,j} + n_{-1,i,j})]) \phi_{0,i,j}^{n+1} \\
& \quad - \tau [\phi_{0,i+1,j}^{n+1} + \phi_{0,i-1,j}^{n+1} + \phi_{0,i,j+1}^{n+1} + \phi_{0,i,j-1}^{n+1}] \\
& \quad = 2h^2 \phi_{0,i,j}^n - 4h^2 \tau \beta_1 \phi_{-1,i,j}^n (\phi_{0,i,j}^n)^* \phi_{1,i,j}^n,
\end{aligned} \tag{6.55}$$

$$\begin{aligned}
& (2h^2 + 4\tau + 2h^2\tau [V_{i,j} + p + q + \beta_0 n_{i,j} + \beta_1 (n_{-1,i,j} + n_{0,i,j} - n_{1,i,j})]) \phi_{-1,i,j}^{n+1} \\
& \quad - \tau [\phi_{-1,i+1,j}^{n+1} + \phi_{-1,i-1,j}^{n+1} + \phi_{-1,i,j+1}^{n+1} + \phi_{-1,i,j-1}^{n+1}] \\
& \quad = 2h^2 \phi_{-1,i,j}^n - 2h^2 \tau \beta_1 (\phi_{1,i,j}^n)^* (\phi_{0,i,j}^n)^2.
\end{aligned} \tag{6.56}$$

These equations can be solved to find $\phi_{i,j}^{n+1} = (\phi_{1,i,j}^{n+1}, \phi_{0,i,j}^{n+1}, \phi_{-1,i,j}^{n+1})$ which will be closer to the minimum value of the energy than the components at the previous step.

Notice that each one of these equations is actually a system of coupled linear equations for the value of ϕ_m at every position in our lattice and so to solve these, we can write each one of them as a matrix equation of the following form:

$$A\vec{\phi}_m = \vec{b} \tag{6.57}$$

To demonstrate how this works, we will show an example of setting up a small lattice and writing out the full matrix equation for this example. After this, we will discuss the general case which will have the exact same format as the example given here.

For our example, we will use the $m = 1$ component equation given by (6.54). The procedure for setting up the other components is the exact same. We will take $L = 4$ lattice spacings which, when we include the boundary points of the lattice, gives us a 5×5 grid as seen in figure (12).

There are different ways to specify the boundary conditions of this problem, however, no matter which regime we choose, we will always approach the problem as if we are only solving for the values on the interior points of the grid. For now we will set up the equations for dirichlet boundary conditions and will look at different boundary conditions later.

As just mentioned, we would like to solve for the values of ϕ on the interior points of the grid and seeing as we are looking at the $m = 1$ component equation, we will get the following $\vec{\phi}_1$ vector in our matrix equation (6.57):

$$\vec{\phi}_1 = \begin{bmatrix} \phi_{22} & \phi_{32} & \phi_{42} & \phi_{23} & \phi_{33} & \phi_{43} & \phi_{24} & \phi_{34} & \phi_{44} \end{bmatrix}^T. \tag{6.58}$$

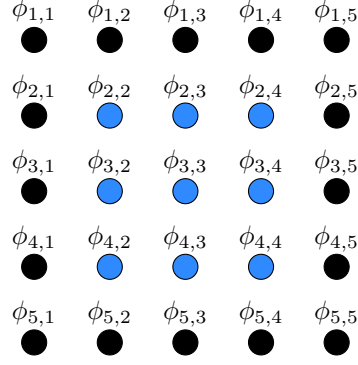


Figure 12: 5×5 lattice.

Here we are setting up our equations, traversing the grid in column major order in which we count the grid values going down one column before moving to the next column.

Next, we write out the A matrix which will represent everything on the left hand side of the coupled equations listed in (6.54). For notational convenience, we will label the term multiplying the $\phi_{1,i,j}^{n+1}$ as $\chi_{1,i,j}$:

$$\chi_{1,i,j} = (2h^2 + 4\tau + 2h^2\tau [V_{i,j} - p + q + \beta_0 n_{i,j} + \beta_1 (n_{1,i,j} + n_{0,i,j} - n_{-1,i,j})]). \quad (6.59)$$

With this, we can write out the A matrix for this example. Since there are 9 interior points, we will have a 9×9 matrix for A which agrees with our general rule of $(L-1) \times (L-1)$ interior points.

$$A = \begin{pmatrix} \chi_{1,2,2} & -\tau & 0 & -\tau & 0 & 0 & 0 & 0 & 0 \\ -\tau & \chi_{1,3,2} & -\tau & 0 & -\tau & 0 & 0 & 0 & 0 \\ 0 & -\tau & \chi_{1,4,2} & 0 & 0 & -\tau & 0 & 0 & 0 \\ -\tau & 0 & 0 & \chi_{1,2,3} & -\tau & 0 & -\tau & 0 & 0 \\ 0 & -\tau & 0 & -\tau & \chi_{1,3,3} & -\tau & 0 & -\tau & 0 \\ 0 & 0 & -\tau & 0 & -\tau & \chi_{1,4,3} & 0 & 0 & -\tau \\ 0 & 0 & 0 & -\tau & 0 & 0 & \chi_{1,2,4} & -\tau & 0 \\ 0 & 0 & 0 & 0 & -\tau & 0 & -\tau & \chi_{1,3,4} & -\tau \\ 0 & 0 & 0 & 0 & 0 & -\tau & 0 & -\tau & \chi_{1,4,4} \end{pmatrix}. \quad (6.60)$$

The \vec{b} vector will contain everything on the right hand side of equation (6.54).

$$\vec{b} = \begin{pmatrix} 2h^2\phi_{1,2,2}^n - 2h^2\tau\beta_1(\phi_{-1,2,2}^n)^*(\phi_{0,2,2}^n)^2 & +\tau\phi_{2,1} + \tau\phi_{1,2} \\ 2h^2\phi_{1,3,2}^n - 2h^2\tau\beta_1(\phi_{-1,3,2}^n)^*(\phi_{0,3,2}^n)^2 & +\tau\phi_{3,1} \\ 2h^2\phi_{1,4,2}^n - 2h^2\tau\beta_1(\phi_{-1,4,2}^n)^*(\phi_{0,4,2}^n)^2 & +\tau\phi_{5,2} + \tau\phi_{4,1} \\ 2h^2\phi_{1,2,3}^n - 2h^2\tau\beta_1(\phi_{-1,2,3}^n)^*(\phi_{0,2,3}^n)^2 & +\tau\phi_{1,3} \\ 2h^2\phi_{1,3,3}^n - 2h^2\tau\beta_1(\phi_{-1,3,3}^n)^*(\phi_{0,3,3}^n)^2 & \\ 2h^2\phi_{1,4,3}^n - 2h^2\tau\beta_1(\phi_{-1,4,3}^n)^*(\phi_{0,4,3}^n)^2 & +\tau\phi_{53} \\ 2h^2\phi_{1,2,4}^n - 2h^2\tau\beta_1(\phi_{-1,2,4}^n)^*(\phi_{0,2,4}^n)^2 & +\tau\phi_{2,5} + \tau\phi_{1,4} \\ 2h^2\phi_{1,3,4}^n - 2h^2\tau\beta_1(\phi_{-1,3,4}^n)^*(\phi_{0,3,4}^n)^2 & +\tau\phi_{3,5} \\ 2h^2\phi_{1,4,4}^n - 2h^2\tau\beta_1(\phi_{-1,4,4}^n)^*(\phi_{0,4,4}^n)^2 & +\tau\phi_{5,4} + \tau\phi_{4,5} \end{pmatrix}. \quad (6.61)$$

We see here that each element of the \vec{b} vector contains terms from the previous gradient descent step that appear on the right hand side of the relevant equation. We also get boundary terms that appear on the left hand side of certain equations, however, since we know what the boundary values are for dirichlet boundary conditions, we can move these over to the right. This pattern of how the boundary points show up in the \vec{b} vector will be the same for the other two component equations ($m = 0, -1$). The change that will occur here is what previous gradient descent step terms appear originally on the right hand side of these equations.

Now we can use this small example to instruct us on how these equations are set up for larger grids. For an arbitrarily large L , the A matrix will have the following form:

$$A = \begin{pmatrix} D & -\tau I & 0 & \dots & 0 & 0 \\ -\tau I & D & -\tau I & 0 & \dots & 0 \\ 0 & -\tau I & \ddots & \ddots & \ddots & \vdots \\ \vdots & 0 & \ddots & \ddots & -\tau I & 0 \\ 0 & \vdots & \ddots & -\tau I & D & -\tau I \\ 0 & 0 & \dots & 0 & -\tau I & D \end{pmatrix}, \quad (6.62)$$

$$D = \begin{pmatrix} \chi & -\tau & 0 & \dots & 0 & 0 \\ -\tau & \chi & -\tau & 0 & \dots & 0 \\ 0 & -\tau & \ddots & \ddots & \ddots & \vdots \\ \vdots & 0 & \ddots & \ddots & -\tau & 0 \\ 0 & \vdots & \ddots & -\tau & \chi & -\tau \\ 0 & 0 & \dots & 0 & -\tau & \chi \end{pmatrix}. \quad (6.63)$$

Here, D is an $(L-1) \times (L-1)$ matrix where τ and 0 are numbers. χ represents the same χ as in our small example for the A matrix, where we have dropped the subscripts detailing what grid values we are looking at for convenience. This means that the A matrix has

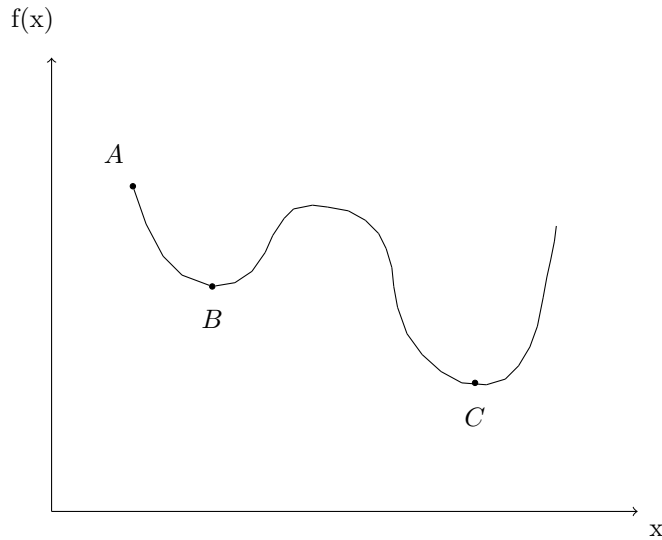


Figure 13: Demonstration of the limitations of gradient descent.

dimension $(L - 1)^2 \times (L - 1)^2$ where I is the $(L - 1) \times (L - 1)$ identity matrix and 0 is the $(L - 1) \times (L - 1)$ zero matrix.

Gradient Descent Limitations As mentioned previously, the main machinery used to arrive at a set of equations that can be solved numerically for the ground state of a spinor condensate is gradient descent. As such, it is worth mentioning the limitations of this approach which will transfer to our code. One of the main limitations of gradient descent is determining whether we have legitimately found the global minimum of a system which, for our purposes, corresponds to whether we have successfully found the ground state wavefunction. The reason for this can be clearly seen by considering figure (13). Here, we see that if we take an initial condition for our gradient descent starting at A , gradient descent will work to bring us to the local minimum at point B . However, we can clearly see that the global minimum of this system is at point C .

To mitigate against this situation occurring, we need to think carefully about the initial condition of our system that we provide to our code. Details surrounding this are discussed in the context of vortices in chapter (7).

6.1.3 Code implementation

In this section, we will detail how the A matrix from the previous section is translated to code so that the matrix equation (6.57) can be solved for the relevant ground state component. After this, we will discuss how we ensure convergence to the ground state along with maintaining a suitable step size, τ for the gradient descent.

First, let's consider writing the A matrix in code. To help illustrate how this is done,

and say that in each block matrix of size $(L - 1) \times (L - 1)$ on the main diagonal, all the elements on the two diagonals just off the main diagonal are filled with nonzero elements. The length of one of these diagonals is one less than the length of the main diagonal in a block matrix which makes this length $(L - 2)$. Since we are looking at two of these diagonals, we get $2(L - 2)$. Finally for these elements, since there are $(L - 1)$ block matrices on the main diagonal, the number of elements from the diagonals just off the main diagonal contributes $2(L - 1)(L - 2)$ nonzero elements to the A matrix.

3. Next, we can look at the block matrices just off the main diagonal block matrices. The main diagonal elements in these block matrices are filled with $-\tau$. This means each block matrix here gives another $(L - 1)$ nonzero elements. Since this happens on either side of the main block diagonal, we get $2(L - 1)$. Finally for these elements, we have $(L - 2)$ block matrices on either side of the main block diagonal, which means the total contribution from these elements is also $2(L - 1)(L - 2)$

Overall this means that the number of nonzero elements in the A matrix for Dirichlet boundary conditions is $(L - 1)^2 + 4(L - 1)(L - 2)$

We have included some pseudo-code to show how the elements discussed above are filled into the A matrix. We are assuming that this code starts with the A matrix being filled with zeros. Note that, in the actual code for this project, this is done using sparse matrices.

Algorithm 1 Filling in the A matrix

```

for (i=0; i < (L - 1)2; i++) do                                ▷ Looping down the main diagonal of A.
  A[i, i] = χ[i]                                                ▷ Set main diagonal elements.
  if i mod (L - 1) != (L - 2) then
    A[i + 1, i] = -τ                                           ▷ Just below main diagonal element.
    A[i, i + 1] = -τ                                           ▷ Just to the right of main diagonal element.
  end if
  if i < (L - 1)(L - 2) then
    A[i, i + (L - 1)] = -τ                                     ▷ Further to right of main diagonal.
    A[i + (L - 1), i] = -τ                                     ▷ Further below main diagonal element.
  end if
end for

```

Once the A matrix has been filled in properly, the next step is to fill in the \vec{b} vector. To visualize how this is done, we write out a general term from the \vec{b} vector.

$$b[(L - 1) * (i - 2) + (j - 2)] = 2h^2\phi_{i,j}^n - 2h^2\tau\beta_1(\phi_{i,j}^n)^*(\phi_{i,j}^n)^2 + \tau(\phi \text{ boundary terms}). \quad (6.64)$$

For our purposes, these boundary values will usually be set to zero for Dirichlet boundary conditions and otherwise will be periodic, in which case they will not be dealt with in the \vec{b} vector, as we shall see later.

With this, we can now fill in the \vec{b} vector as detailed in algorithm (2).

Algorithm 2 Fill in the \vec{b} vector

```

for ( $i = 2; i < (L + 1); i ++$ ) do
  for ( $j = 2; j < (L + 1); j ++$ ) do
     $m \leftarrow (L - 1)(i - 2) + (j - 2)$ 
     $b[m] \leftarrow 2h^2\phi_1[m] - 2h^2\tau\beta_1(\phi_{-1}[m])^*(\phi_0[m])^2$ 
  end for
end for

```

Algorithm (2) describes filling in the \vec{b} vector for the $m = 1$ component equation. The non-boundary terms filled into \vec{b} will change slightly when we look at each component equation, however, the main body of code will not change for each component equation.

Once the A matrix and \vec{b} vector have been set up, we can solve the matrix equation (6.57) for the ϕ component we are looking for. In our code this is achieved using the python library numpy.

The procedure described above for solving one of the component equations is done for all other component equations. Solving for all the components together constitutes as a single gradient descent step. This is due to the fact that all these component equations are coupled together, although it is worth noting that this coupling is done indirectly through the density, spin density and spin-singlet density. The final step we must take to complete the current gradient descent step is to renormalize the condensate wavefunction in order to account for particle conservation which is described by our constraint (6.5).

$$\begin{aligned}
\|\phi\| &= \int (|\phi_1(\vec{r})|^2 + |\phi_0(\vec{r})|^2 + |\phi_{-1}(\vec{r})|^2) d\vec{r}, \\
\phi_1 &\rightarrow \frac{\phi_1}{\|\phi\|}, \\
\phi_0 &\rightarrow \frac{\phi_0}{\|\phi\|}, \\
\phi_{-1} &\rightarrow \frac{\phi_{-1}}{\|\phi\|}.
\end{aligned} \tag{6.65}$$

By taking this normalization explicitly, we don't have to implement the constraint (6.42) using the lagrange multiplier, μ , in our spin one Gross-Pitaevskii equations.

Procedure for choosing an adaptive step size: Now, we want to iterate this procedure to perform multiple gradient descent steps in order to converge to the ground state of the system. Two questions that arise when doing this are: how do we determine if we have converged to the ground state and how do we adjust the gradient descent step size, τ , in order to make sure it is reasonable at each step.

We will answer these questions by considering a one dimensional problem for visualization purposes, however, the logic extends to our case. The situation is shown in figure (15). Here

we see that we are trying to find the value of ϕ that will minimize our energy functional, $E[\phi]$. As stated before, we will do this by gradient descent. We see from figure (15) that the step size in ϕ space that we would like to take between two points, say ϕ_a and ϕ_b , is $\tau = \tau_0$. We can vary this step depending on what the value of the gradient of the energy functional is. We assume that the energy difference varies linearly with respect to τ and as a result we can approximate the derivative of the energy functional to be the following:

$$E'[\phi] = \frac{E_{diff}}{\tau}. \quad (6.66)$$

As a start, we would like to keep the energy difference that we obtain between one step and the next constant by varying the step size τ . We can do this by defining an initial target energy difference, which we call t , and defining the following expression for updating the gradient descent step size τ :

$$\tau_{i+1} = \frac{t}{E_{diff}} \tau_i = \frac{t}{E'[\phi]}. \quad (6.67)$$

Here, we stress again that the second term in the equality in (6.67) only holds when E_{diff} varies linearly with respect to τ . We see that this condition will provide the functionality that we require. If we are in a regime where the derivative of the energy functional is constant (such as in the region between ϕ_a and ϕ_b in figure (15)) and the energy difference is approximately equal to t , then (6.67) keeps our step size approximately the same as it was in the previous gradient descent step. If the gradient changes slightly such that the energy difference diverges slightly from t , then (6.67) will vary τ slightly to continue to keep the same energy difference between one gradient descent step and the next. Note, that we need to ensure that the energy difference is near our starting value of t in the first place which we will discuss momentarily.

We immediately see that we will run into a problem if we take this expression for updating τ by itself with no adjustments. Namely that, if the derivative of the energy functional changes significantly, such as in the region between ϕ_b and ϕ_c , our linear approximation for the energy difference in terms of τ breaks down as quadratic terms begin to dominate and so (6.67) will not be valid, leading to the energy difference not being close to our target energy difference t . Our update expression will also fail if we are approaching the minimum, where the gradient is extremely small, as this will cause τ to grow large, whereas we would like to take small steps in ϕ space if we are near the minimum, defined by ϕ_f in figure (15).

To remedy this situation, when we encounter situations where the energy difference is not within a given tolerance of t , we will reduce the step size by a half, as well as t . We hope that by taking a smaller step size τ and reducing the target energy difference t , that we will be in a linear regime again and can update using (6.67) and use the newly generated step size in our gradient descent.

While doing this remedies our first problem, it brings up another, which can be seen as

we move from the region between ϕ_b and ϕ_c and into the one between ϕ_c and ϕ_d . If we move from a region where the gradient changes, in which case we reduce τ and t , into a region where the gradient becomes constant again, we see that the step size τ and target energy difference t remain small and so it will be time consuming to walk down to the minimum of the energy functional if we do not increase τ and t again. To account for this, we increase these parameters by ten percent when we are in regions where the gradient has become constant again. That is, in regions where we have the energy difference approximately equal to our target difference t .

We now describe the algorithm step by step which we carry out to implement the above actions.

First, define t to be a predefined value that we will compare to the energy difference between the current ϕ and ϕ found at the next gradient descent step. We will use this value throughout to update τ according to our update expression (6.67).

Once we have defined an initial value for both t , τ and have an initial condensate wavefunction, we perform the following steps:

1. Perform one gradient descent step on our initial ϕ and find the energy difference between the value returned and this initial ϕ . Ensure that this energy difference is smaller than t by reducing the value of τ . Keep performing this first step until this condition is met.
2. Once this condition has been met, update τ using (6.67) and repeatedly take gradient descent steps and find the energy difference between the ϕ returned by the current step and the previous ϕ . If this value is within a certain tolerance of the value of t , then accept the wavefunction ϕ returned by the current gradient descent step as the next step towards the ground state of the system. If we have just accepted a wavefunction ϕ or the number of gradient descent steps we have taken is odd, update ϕ according to (6.67) and repeat this step. Note that we update on odd gradient descent steps in order to give extra time to see if the current gradient descent step is sufficient.
3. If the energy difference is not within a given tolerance of t and the number of already taken gradient descent steps is not an odd number, then decrease both t and τ by a factor of two and return to step 3.
4. At each iteration where a wavefunction ϕ has been accepted or the number of gradient descent steps is an odd number, increase the value of τ and t by ten percent.
5. If the value of t becomes less than some constant tolerance that has been set at the start of the code, the system has converged to the ground state.
6. If the number of iterations of the gradient descent step reaches some predefined constant and t has not become less than the predefined tolerance, exit the code and inspect the value of t to determine whether convergence has occurred to a satisfactory value.

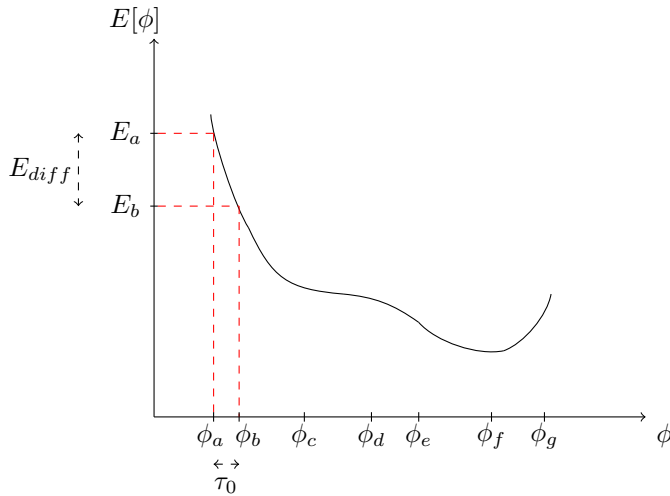


Figure 15: Demonstration of choosing a suitable step τ

6.1.4 Periodic Boundary Conditions

Everything that has been discussed so far has been in relation to Dirichlet boundary conditions. If we wish to use periodic boundary conditions, the only changes that occur are in the A matrix and \vec{b} vector. All other steps discussed above in performing multiple gradient descent steps and the method of varying τ and determining convergence will remain the same. Although we will not be using ground state codes with periodic boundary conditions in this thesis, they were developed as part of this research and the discussion here will be used later to describe how we have implemented our Bogoliubov codes, which do use periodic boundary conditions.

Here, we will show the changes that occur in the A matrix and \vec{b} if we wish to use periodic boundary conditions for our system. First, we will go back to our example on a small lattice and show the changes that occur. Once we have done this, we will again move to the general case and modify the pseudo-code given by algorithms (1) and (2) to show the additions needed for periodic boundary conditions.

As mentioned earlier, for periodic boundary conditions, we think of the grid as being of size $L \times L$ instead of size $(L - 1) \times (L - 1)$ as we only discard one of the boundary points and keep the other one. This would mean that if we wanted to look at the exact same system as in the example for dirichlet boundary conditions above but instead use periodic boundary conditions, we would need to look at a 4×4 lattice. For our purposes here, we will instead just set $L = 3$ so that we can continue to use the example of a 3×3 lattice, however, it is important to note that there is an actual difference that occurs between periodic and dirichlet boundary conditions for the same system.

The modified lattice can be seen in figure (16), where the actual lattice we are working on now is the lower right corner of the original lattice in figure (12) as encircled in red. We

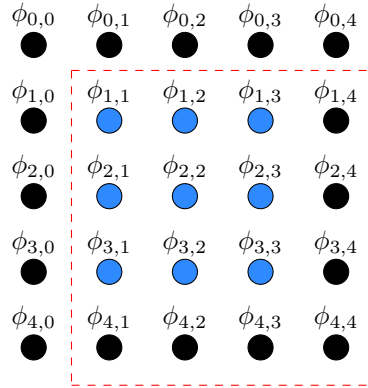


Figure 16: 4×4 lattice encircled in red. The physical boundaries of the lattice are the points just inside this red boundary as opposed to the case for Dirichlet boundary conditions where the boundary was all points coloured in black. Here for periodic boundary conditions, we keep one of the boundaries on the left and top of the lattice and identify the other boundaries on the right and bottom with these.

have changed the indexing to highlight that we are now taking the boundaries of the lattice to be different. This means that the vector of points, $\vec{\phi}_1$, that we wish to solve for is now given by:

$$\vec{\phi}_1 = \left[\phi_{11} \quad \phi_{21} \quad \phi_{31} \quad \phi_{12} \quad \phi_{22} \quad \phi_{32} \quad \phi_{13} \quad \phi_{23} \quad \phi_{33} \right]^T. \quad (6.68)$$

Again, we will write out the A matrix for the coupled equations given by (6.54). We see that these equations are the exact same as before for Dirichlet boundary conditions, however we will now make the following change for periodic boundary conditions.

$$\begin{aligned} \phi_{i,0} &= \phi_{i,L} \\ \phi_{i,L+1} &= \phi_{i,1} \\ \phi_{0,i} &= \phi_{L,i} \\ \phi_{L+1,i} &= \phi_{1,i}. \end{aligned} \quad (6.69)$$

Here, we are taking i to run from 1 to L . This condition essentially means that if a particle tries to leave our lattice on one side, it will re-enter on the other side in both the x and y direction. We see that this condition means that our boundary points are now written in terms of internal points in the grid that we wish to solve for and as a result, we will now have extra terms in the A matrix for each row, corresponding to one of the coupled equations given by (6.54). The extra terms that appear as extra non-zero terms in each row of the A matrix will disappear from the corresponding row in the \vec{b} vector. To make this more clear, let's look at the first equation given by (6.54) which is described by the first row

of the A matrix.

$$\begin{aligned} \chi_{1,1,1}\phi_{1,1,1}^{n+1} - \tau [\phi_{1,2,1}^{n+1} + \phi_{1,0,1}^{n+1} + \phi_{1,1,2}^{n+1} + \phi_{1,1,0}^{n+1}] \\ = 2h^2\phi_{1,1,1}^{n+1} - 2h^2\tau\beta_1(\phi_{-1,1,1}^n)^*(\phi_{0,1,1}^n)^2, \end{aligned} \quad (6.70)$$

$$\begin{aligned} \Rightarrow \chi_{1,1,1}\phi_{1,1,1}^{n+1} - \tau [\phi_{1,2,1}^{n+1} + \phi_{1,3,1}^{n+1} + \phi_{1,1,2}^{n+1} + \phi_{1,1,3}^{n+1}] \\ = 2h^2\phi_{1,1,1}^{n+1} - 2h^2\tau\beta_1(\phi_{-1,1,1}^n)^*(\phi_{0,1,1}^n)^2. \end{aligned} \quad (6.71)$$

In going from the first line to the second line, we have substituted for our periodic boundary conditions, where in this example: $\phi_{1,0,1}^{n+1} = \phi_{1,3,1}^{n+1}$ and $\phi_{1,1,0}^{n+1} = \phi_{1,1,3}^{n+1}$. The two terms $\phi_{1,3,1}^{n+1}$ and $\phi_{1,1,3}^{n+1}$ are now terms in the $\vec{\phi}_1$ vector, given by (6.68), that get multiply by the A matrix and this means that the first row of the A matrix will change in the following way:

$$A_1 = \begin{bmatrix} \chi_{1,1,1} & -\tau & -\tau & -\tau & 0 & 0 & -\tau & 0 & 0 \end{bmatrix}. \quad (6.72)$$

Here, we have coloured any extra terms that come from periodic boundary conditions in the x-direction in blue and any that come from periodic boundary conditions in the y-direction in red.

The procedure for modifying the first component equation of the system of coupled equations given by (6.54) is the exact same for modifying all other component equations. When we do this for all of them, we get the following A matrix and \vec{b} vector for our small lattice example using periodic boundary conditions. We have kept the same colour coding as above to distinguish between additional terms in the A matrix coming from periodic boundary conditions in the x-direction and periodic boundary conditions in the y-direction.

$$A = \begin{pmatrix} \chi_{1,1,1} & -\tau & -\tau & -\tau & 0 & 0 & -\tau & 0 & 0 \\ -\tau & \chi_{1,2,1} & -\tau & 0 & -\tau & 0 & 0 & -\tau & 0 \\ -\tau & -\tau & \chi_{1,3,1} & 0 & 0 & -\tau & 0 & 0 & -\tau \\ -\tau & 0 & 0 & \chi_{1,1,2} & -\tau & -\tau & -\tau & 0 & 0 \\ 0 & -\tau & 0 & -\tau & \chi_{1,2,2} & -\tau & 0 & -\tau & 0 \\ 0 & 0 & -\tau & -\tau & -\tau & \chi_{1,3,2} & 0 & 0 & -\tau \\ -\tau & 0 & 0 & -\tau & 0 & 0 & \chi_{1,1,3} & -\tau & -\tau \\ 0 & -\tau & 0 & 0 & -\tau & 0 & -\tau & \chi_{1,2,3} & -\tau \\ 0 & 0 & -\tau & 0 & 0 & -\tau & -\tau & -\tau & \chi_{1,3,3} \end{pmatrix}. \quad (6.73)$$

$$\vec{b} = \begin{pmatrix} 2h^2 \phi_{1,1,1}^n - 2h^2 \tau \beta_1 (\phi_{-1,1,1}^n)^* (\phi_{0,1,1}^n)^2 \\ 2h^2 \phi_{1,2,1}^n - 2h^2 \tau \beta_1 (\phi_{-1,2,1}^n)^* (\phi_{0,2,1}^n)^2 \\ 2h^2 \phi_{1,3,1}^n - 2h^2 \tau \beta_1 (\phi_{-1,3,1}^n)^* (\phi_{0,3,1}^n)^2 \\ 2h^2 \phi_{1,1,2}^n - 2h^2 \tau \beta_1 (\phi_{-1,1,2}^n)^* (\phi_{0,1,2}^n)^2 \\ 2h^2 \phi_{1,2,2}^n - 2h^2 \tau \beta_1 (\phi_{-1,2,2}^n)^* (\phi_{0,2,2}^n)^2 \\ 2h^2 \phi_{1,3,2}^n - 2h^2 \tau \beta_1 (\phi_{-1,3,2}^n)^* (\phi_{0,3,2}^n)^2 \\ 2h^2 \phi_{1,1,3}^n - 2h^2 \tau \beta_1 (\phi_{-1,1,3}^n)^* (\phi_{0,1,3}^n)^2 \\ 2h^2 \phi_{1,2,3}^n - 2h^2 \tau \beta_1 (\phi_{-1,2,3}^n)^* (\phi_{0,2,3}^n)^2 \\ 2h^2 \phi_{1,3,3}^n - 2h^2 \tau \beta_1 (\phi_{-1,3,3}^n)^* (\phi_{0,3,3}^n)^2 \end{pmatrix}. \quad (6.74)$$

From this example, we can see what changes need to be made to our code to fill in the correct values to a general $L^2 \times L^2$ A matrix. First, let's look at the changes that need to be made to account for the periodic boundary conditions in the y-direction. If we compare the A matrix from our small example for periodic boundary conditions and the expanded out A matrix for Dirichlet boundary conditions given by figure (14), we see that the additional elements for y periodic boundary conditions can be added in each block matrix of size $L \times L$ on the main diagonal of the A matrix. These values will be added in by adding a $-\tau$ value that is $(L-1)$ spaces to the left and above the last main diagonal value in each block matrix on the main diagonal.

For the x-periodic boundary conditions, these are accounted for by adding a $-\tau$ value $(L)(L-1)$ spaces to the right and below each main diagonal element in the first block matrix of size $L \times L$ on the main diagonal.

We have included the expanded out A matrix for periodic boundary conditions, given by figure (17), as well as the modified algorithm for filling in this matrix, given by algorithm (3). We have again colour coded the additional elements being included in the expanded out A matrix in figure (17). The majority of elements in this matrix are zero which is being represented by the zero block matrices in this figure. These matrices repeat along the diagonal and row that they are in until we reach one of the nonzero block matrices.

We again would like to know how many nonzero elements are in the A matrix as we will be using sparse matrices to store A in our code. We will still have the $L^2 + 4(L)(L-1)$ elements from Dirichlet boundary conditions, noting that L has been redefined here as we are taking an $L \times L$ lattice instead of $(L-1) \times (L-1)$ lattice. We now need to see how many extra nonzero elements we have when we introduce periodic boundary conditions in the x and y direction.

1. For the y periodic boundary conditions, we get two extra elements in each block matrix on the main diagonal. Since there are L of these, we get an extra $2L$ nonzero elements.
2. For the x periodic boundary conditions, the main diagonal of the block matrix in the top right hand corner and bottom left hand corner are filled with nonzero elements.

Algorithm 3 Filling in the A matrix (Periodic boundary conditions)

```
for (i=0; i < L2; i++) do                                ▷ Looping down the main diagonal of A.  
  A[i, i] = χ[i]                                          ▷ Set main diagonal elements.  
  if i mod L ≠ (L - 1) then  
    A[i + 1, i] = -τ                                     ▷ Just below main diagonal element.  
    A[i, i + 1] = -τ                                     ▷ Just to the right of main diagonal element.  
  else                                                    ▷ Fill in elements corresponding to y periodic boundary conditions.  
    A[i - (L - 1), i] = -τ   ▷ (L - 1) spaces above last main diagonal element in each  
    main diagonal block matrix.  
    A[i, i - (L - 1)] = -τ   ▷ (L - 1) spaces to the left of the last main diagonal  
    element in each main diagonal block matrix.  
  end if  
  if i < L(L - 1) then  
    A[i, i + L] = -τ                                     ▷ Further to right of main diagonal.  
    A[i + L, i] = -τ                                     ▷ Further below main diagonal element.  
  end if  
  if i < L then     ▷ Fill in elements corresponding to x periodic boundary conditions.  
    A[i, i + L(L - 1)] = -τ   ▷ L(L - 1) spaces to the right of the main diagonal  
    element in the first block matrix on the main diagonal.  
    A[i + L(L - 1), i] = -τ   ▷ L(L - 1) spaces below the main diagonal element in the  
    first block matrix on the main diagonal.  
  end if  
end for
```

- This file is what solves for the ground state of the system by calling the relevant ground state one step code repeatedly. This file also takes care of keeping the gradient descent step at a suitable size and determines whether we have converged to the ground state. This code does not return anything and instead saves a list of condensate wavefunctions at each step that we accepted. If we have converged, the last wavefunction in this list will be the ground state of the system.

4. `groundStateTools.py`:

- This file contains functions that are called throughout all other code files such as a function to compute the energy of the system in its current state. Other functions in this file involve saving and loading wave functions as well as computing relevant quantities associated with the condensate such as its density. This file also has code to plot and animate frames of these quantities.

6.2 Spin Two Ground State Code

We will now discuss the code for solving for the ground state of a spin two condensate. Since the algorithms used for solving the component equations and running gradient descent in spin two are the exact same as those used in spin one, we will not provide details of this here as it has already been covered. We will however provide the component equations that are

fed into the A matrix and \vec{b} vector for spin two. In contrast to spin one where there were three systems of coupled equations to be solved, here, we will have five systems of coupled equations.

6.2.1 Equation setup

As in the spin one case, if we wish to find the ground state of the spin two system, we need to find a wavefunction that minimizes the energy functional which, for spin two, is given by:

$$E[\psi_m] = \int d\vec{r} \left\{ \sum_{m=-2}^2 \psi_m^* \left[-\frac{\hbar^2 \nabla^2}{2M} + V(\vec{r}) - pm + qm^2 \right] \psi_m + \frac{c_0}{2} n^2 + \frac{c_1}{2} |\vec{F}|^2 + \frac{c_2}{2} |A_{00}|^2 \right\}. \quad (6.75)$$

Following the procedure in the spin one case, we would like to perform gradient descent on this energy functional. This will involve taking derivatives of (6.75). Before we do this, however, we would like to write the energy functional in a dimensionless form. We will not show the steps for finding the dimensionless equations in spin two as it is the exact same procedure as in spin one. The only difference when carrying out the procedure here is to account for the extra term given by the spin singlet density term and use the spin two version of the spin matrices which are given by equations (3.95) to (3.97) and equation (3.86). Note that each term in the component equations for spin two that involves ψ terms will have dimensions of ψ^3 just like in the spin one case which is why the procedure is the exact same.

When we perform this procedure, the energy functional becomes:

$$E[\phi_m] = \int d\vec{r} \left\{ \sum_{m=-2}^2 \phi_m^* \left[-\frac{1}{2} \nabla^2 + V(\vec{r}) - pm + qm^2 \right] \phi_m + \frac{\beta_0}{2} n^2 + \frac{\beta_1}{2} |\vec{F}|^2 + \frac{\beta_2}{2} |A_{00}|^2 \right\}. \quad (6.76)$$

We have again moved to writing the energy functional in terms of ϕ as we are trying to minimize this energy functional and will vary ϕ to do this, ultimately, making ϕ the ground state of the system. Note that the changes in dimension made here are the same as those made in spin one using (6.30) and so if we want to return to dimension full quantities, we will have to account for these. We have also dropped the \sim on all terms in (6.76) as we know we are working with this dimensionless form. Terms such as β_m are defined in terms of c_m in the same way as before and are written here for convenience.

$$\beta_m = \frac{c_m N}{\omega r_s^3 \hbar}. \quad (6.77)$$

Once we have this dimensionless form for the energy functional, we can follow the same procedure for discretizing it on a finite grid. Once we have done this, we can take the gradient of this discretized form with respect to the conjugate of each component of the spin two wavefunction on the lattice, $\phi_{m,i,j}^*$, and sub these into the gradient descent formula given in the spin one numerical section by equation (6.47) (now m runs from -2 to 2) in order to obtain the five systems of coupled equations that need to be solved numerically to obtain the spin two ground state, $\phi = (\phi_2, \phi_1, \phi_0, \phi_{-1}, \phi_{-2})$. We omit these steps in detail here as the procedure is the exact same as in the spin one case, details of which can be found in section (6.1.2).

Once these steps have been performed, we end up with the following five coupled systems of linear equations for $m = (2, 1, 0, -1, -2)$:

$$\begin{aligned}
& \left(2h^2 + 4\tau + 2h^2\tau \left[V - 2p + 4q + \beta_0 n \right. \right. \\
& \quad \left. \left. + \beta_1(4n_2 + 4n_1 - 2n_{-1} - 4n_{-2}) + \frac{2}{5}\beta_2 n_{-2} \right] \right) \phi_{2,i,j}^{n+1} \\
& \quad - \tau(\phi_{2,i+1,j}^{n+1} + \phi_{2,i-1,j}^{n+1} + \phi_{2,i,j+1}^{n+1} + \phi_{2,i,j-1}^{n+1}) \\
& = 2h^2\phi_{2,i,j}^n - 2h^2\tau \left[\beta_1 \left(\sqrt{6}[(\phi_{0,i,j}^n)^*(\phi_{1,i,j}^n)^2 + (\phi_{-1,i,j}^n)^*\phi_{0,i,j}^n\phi_{1,i,j}^n] \right. \right. \\
& \quad \left. \left. + 2(\phi_{-2,i,j}^n)^*\phi_{-1,i,j}^n\phi_{1,i,j}^n \right) \right. \\
& \quad \left. + \frac{\beta_2}{5}((\phi_{0,i,j}^n)^2(\phi_{-2,i,j}^n)^* - 2\phi_{1,i,j}^n\phi_{-1,i,j}^n(\phi_{-2,i,j}^n)^*) \right], \tag{6.78}
\end{aligned}$$

$$\begin{aligned}
& \left(2h^2 + 4\tau + 2h^2\tau \left[V - p + q + \beta_0 n \right. \right. \\
& \quad \left. \left. + \beta_1(4n_2 + n_1 - n_{-1} - 2n_{-2} + 3n_0) + \frac{2}{5}\beta_2 n_{-1} \right] \right) \phi_{1,i,j}^{n+1} \\
& \quad - \tau(\phi_{1,i+1,j}^{n+1} + \phi_{1,i-1,j}^{n+1} + \phi_{1,i,j+1}^{n+1} + \phi_{1,i,j-1}^{n+1}) \\
& = 2h^2\phi_{1,i,j}^n - 2h^2\tau \left[\beta_1 \left(2\sqrt{6}(\phi_{1,i,j}^n)^*\phi_{2,i,j}^n\phi_{0,i,j}^n + 3(\phi_{-1,i,j}^n)^*(\phi_{0,i,j}^n)^2 \right. \right. \\
& \quad \left. \left. + \sqrt{6}((\phi_{-2,i,j}^n)^*\phi_{-1,i,j}^n\phi_{0,i,j}^n + (\phi_{0,i,j}^n)^*\phi_{-1,i,j}^n\phi_{2,i,j}^n) \right) \right. \\
& \quad \left. + 2(\phi_{-1,i,j}^n)^*\phi_{-2,i,j}^n\phi_{2,i,j}^n \right) \\
& \quad \left. - \frac{\beta_2}{5}(2\phi_{2,i,j}^n\phi_{-2,i,j}^n(\phi_{-1,i,j}^n)^* + (\phi_{0,i,j}^n)^2(\phi_{-1,i,j}^n)^*) \right], \tag{6.79}
\end{aligned}$$

$$\begin{aligned}
& \left(2h^2 + 4\tau + 2h^2\tau \left[V + \beta_0 n + 3\beta_1(n_1 + n_{-1}) + \frac{\beta_2}{5}n_0 \right] \right) \phi_{0,i,j}^{n+1} \\
& - \tau(\phi_{0,i+1,j}^{n+1} + \phi_{0,i-1,j}^{n+1} + \phi_{0,i,j+1}^{n+1} + \phi_{0,i,j-1}^{n+1}) \\
& = 2h^2\phi_{0,i,j}^n - 2h^2\tau \left[\beta_1 \left(\sqrt{6} \left((\phi_{2,i,j}^n)^* (\phi_{1,i,j}^n)^2 + (\phi_{-1,i,j}^n)^* \phi_{-2,i,j}^n \phi_{1,i,j}^n \right. \right. \right. \\
& \left. \left. \left. + (\phi_{1,i,j}^n)^* \phi_{2,i,j}^n \phi_{-1,i,j}^n + (\phi_{-2,i,j}^n)^* (\phi_{-1,i,j}^n)^2 \right) + 6(\phi_{0,i,j}^n)^* \phi_{1,i,j}^n \phi_{-1,i,j}^n \right) \right. \\
& \left. + \frac{\beta_2}{5} (2\phi_{2,i,j}^n \phi_{-2,i,j}^n (\phi_{0,i,j}^n)^* - 2\phi_{1,i,j}^n \phi_{-1,i,j}^n (\phi_{0,i,j}^n)^*) \right], \tag{6.80}
\end{aligned}$$

$$\begin{aligned}
& \left(2h^2 + 4\tau + 2h^2\tau \left[V + p + q + \beta_0 n \right. \right. \\
& \left. \left. - \beta_1(2n_2 + n_1 - n_{-1} - 4n_{-2} - 3n_0) + \frac{2}{5}\beta_2 n_1 \right] \right) \phi_{-1,i,j}^{n+1} \\
& - \tau(\phi_{-1,i+1,j}^{n+1} + \phi_{-1,i-1,j}^{n+1} + \phi_{-1,i,j+1}^{n+1} + \phi_{-1,i,j-1}^{n+1}) \\
& = 2h^2\phi_{-1,i,j}^n - 2h^2\tau \left[\beta_1 \left(2\sqrt{6}(\phi_{-1,i,j}^n)^* \phi_{0,i,j}^n \phi_{-2,i,j}^n + 3(\phi_{1,i,j}^n)^* (\phi_{0,i,j}^n)^2 \right. \right. \\
& \left. \left. + \sqrt{6}((\phi_{2,i,j}^n)^* \phi_{1,i,j}^n \phi_{0,i,j}^n + (\phi_{0,i,j}^n)^* \phi_{1,i,j}^n \phi_{-2,i,j}^n) \right. \right. \\
& \left. \left. + 2(\phi_{1,i,j}^n)^* \phi_{2,i,j}^n \phi_{-2,i,j}^n \right) \right. \\
& \left. - \frac{\beta_2}{5} (2\phi_{2,i,j}^n \phi_{-2,i,j}^n (\phi_{1,i,j}^n)^* + (\phi_{0,i,j}^n)^2 (\phi_{1,i,j}^n)^*) \right], \tag{6.81}
\end{aligned}$$

$$\begin{aligned}
& \left(2h^2 + 4\tau + 2h^2\tau \left[V + 2p + 4q + \beta_0 n \right. \right. \\
& \left. \left. - \beta_1(4n_2 + 2n_1 - 4n_{-1} - 4n_{-2}) + \frac{2}{5}\beta_2 n_2 \right] \right) \phi_{-2,i,j}^{n+1} \\
& - \tau(\phi_{-2,i+1,j}^{n+1} + \phi_{-2,i-1,j}^{n+1} + \phi_{-2,i,j+1}^{n+1} + \phi_{-2,i,j-1}^{n+1}) \\
& = 2h^2\phi_{-2,i,j}^n - 2h^2\tau \left[\beta_1 \left(\sqrt{6}[(\phi_{0,i,j}^n)^* (\phi_{-1,i,j}^n)^2 + (\phi_{1,i,j}^n)^* \phi_{0,i,j}^n \phi_{-1,i,j}^n] \right. \right. \\
& \left. \left. + 2(\phi_{2,i,j}^n)^* \phi_{1,i,j}^n \phi_{-1,i,j}^n \right) \right. \\
& \left. + \frac{\beta_2}{5} ((\phi_{0,i,j}^n)^2 (\phi_{2,i,j}^n)^* - 2\phi_{-1,i,j}^n \phi_{1,i,j}^n (\phi_{2,i,j}^n)^*) \right]. \tag{6.82}
\end{aligned}$$

We are again using the notation $n = \sum_{m=-2}^2 n_m$ where $n_m = |\phi_m|^2$. Here we assume that all n values are being taken at the relevant position, (i, j) , in our lattice.

These equations are implemented into code in the same way as the spin one equations, given by equations (6.54) to (6.56), by filling in the A matrix and \vec{b} vector for each of the five component equations above and solving the matrix equation, given by (6.57), in sequence for each of the five component equations. The procedure for constructing these matrices

for a discretized system of linear equations has already been given in sections (6.1.2) and (6.1.3).

6.2.2 Code files

Many of the code files in spin one have their equivalent in spin two, however, since there are extra files used in spin two for setting up vortices, we will detail all code files here for completeness.

1. **spinTwoInput.ini:**

- This is an input file that is called by other code files to read in constants and parameters relating to the system such as the parameters involved in setting up our finite lattice and the interaction parameters of the system.

2. **groundStateOneStep.py:**

- This file is called to perform one gradient descent step, which, when called multiple times, works to find the ground state of a spin two condensate. This file is responsible for setting up the A matrix and \vec{b} vector for each component equation in spin two and solves these equations, returning the normalized result.

3. **modularGroundState.py:**

- This file is what solves for the ground state of the system by calling the relevant ground state one step code repeatedly. This file also takes care of keeping the gradient descent step at a suitable size and determines whether we have converged to the ground state. This code does not return anything and instead saves a list of condensate wavefunctions at each step that we accepted. If we have converged, the last wavefunction in this list will be the ground state of the system.

4. **groundStateTools.py:**

- This file contains functions that are called throughout all other code files such as a function to compute the energy of the system in its current state. Other functions in this file involve saving and loading wave functions as well as computing relevant quantities associated with the condensate such as its density. This file also has code to plot and animate frames of these quantities.

5. **loop.py:**

- This file sets up discrete points on a loop within the condensate and returns the value of the condensate at these points. This is used to study the winding of a vortex within the condensate. We will see more details of this in the next section.

6. **graphicalBEC.py:**

- This file produces a plot of the spherical harmonic representation of a point in the condensate.

7. `graphicalVortex.py`:

- This file takes in spherical harmonic plots of points on a loop in the condensate and plots them on a loop to represent a vortex that we are looking at.

8. `axisAngleToEuler.py`:

- Given a rotation in axis angle format, this file will return the corresponding Euler angles for ZYZ format. This is needed as we input vortices in spin two in axis angle format, however, the rotation matrix for acting on the order parameter of the condensate is written in terms of Euler angles. We will again see more details of this in the next section.

9. `createVortex.py`:

- This file just sets up the vortex we are studying by specifying the axis and angle of rotation and passes this in as the initial condition to the ground state code. That is, this file is where we can specify input and run the ground state files above to obtain results.

6.3 Spin Two Vortices

Now that we have discussed how the ground state is numerically found for a spin two condensate, we will discuss how we simulate vortices in these condensates by way of passing in a suitable initial condition. We will first discuss the general procedure for setting up this initial condition and then describe how parts of this procedure are implemented numerically. The code files that perform the tasks mentioned in this section are described in the previous section.

6.3.1 General setup

We have seen in section (5.1) that the order parameter for a general element of a certain phase of the condensate, described by the representative order parameter ζ_0 is given by:

$$\zeta = e^{i\phi} e^{-if_z\alpha} e^{-if_y\beta} e^{-if_z\gamma} \zeta_0 = e^{i\phi} U(\alpha, \beta, \gamma) \zeta_0 \quad (6.83)$$

Here, ϕ is the gauge angle, describing the $U(1)$ phase and α , β and γ are the Euler angles in ZYZ format describing a rotation in spin space. For a spin two condensate with five spin components, $U(\alpha, \beta, \gamma)$ will be a 5×5 matrix or a five dimensional irreducible representation of $SO(3)$. This matrix is called the Wigner D-matrix [32][38]. This matrix is listed below for spin two in the format given in [27]:

$$\begin{aligned}
U(\alpha, \beta, \gamma) = & \tag{6.84} \\
& \left(\begin{array}{ccccc}
e^{-2i(\alpha+\gamma)} C^4 & -2e^{-i(2\alpha+\gamma)} C^3 S & \sqrt{6} e^{-2i\alpha} C^2 S^2 & -2e^{-i(2\alpha-\gamma)} C S^3 & e^{-2i(\alpha-\gamma)} S^4 \\
2e^{-i(\alpha+2\gamma)} C^3 S & e^{-i(\alpha+\gamma)} C^2 (C^2 - 3S^2) & -\sqrt{\frac{3}{8}} e^{-i\alpha} \sin 2\beta & -e^{-i(\alpha-\gamma)} S^2 (S^2 - 3C^2) & -2e^{-i(\alpha-2\gamma)} C S^3 \\
\sqrt{6} e^{-2i\gamma} C^2 S^2 & \sqrt{\frac{3}{8}} e^{-i\gamma} \sin 2\beta & \frac{1}{4} (1+3 \cos 2\beta) & -\sqrt{\frac{3}{8}} e^{i\gamma} \sin 2\beta & \sqrt{6} e^{2i\gamma} C^2 S^2 \\
2e^{i(\alpha-2\gamma)} C S^3 & -e^{i(\alpha-\gamma)} S^2 (S^2 - 3C^2) & \sqrt{\frac{3}{8}} e^{i\alpha} \sin 2\beta & e^{i(\alpha+\gamma)} C^2 (C^2 - 3S^2) & -2e^{i(\alpha+2\gamma)} C^3 S \\
e^{2i(\alpha-\gamma)} S^4 & 2e^{i(2\alpha-\gamma)} C S^3 & \sqrt{6} e^{2i\alpha} C^2 S^2 & 2e^{i(2\alpha+\gamma)} C^3 S & e^{2i(\alpha+\gamma)} C^4
\end{array} \right). \tag{6.85}
\end{aligned}$$

We have already seen in section (5.3.3) that the vortices in spin two are described by elements of a stabilizer group that rotate in both spin space and phase space. Since we have the $SU(2)$ form of these elements, we can find both the axis and angle that describes the rotation that a specific element of the stabilizer group performs in spin space using the expression for a general $SU(2)$ rotation given by (5.28). We also know the phase change in the gauge angle that occurs for each element.

With all of these parameters, we could set up a vortex by considering a closed loop in our system that starts at the representative order parameter for the given phase and, as we go around the loop, we linearly vary the gauge angle and angle of rotation in spin space around the given axis from zero to their final values for the chosen element of the stabilizer group. At each position in our finite grid that we look at the value of the angle of rotation in spin space, we calculate the Euler angles for a rotation by that amount of angle about the axis of rotation that we have already determined. Once we know this, we can say that the order parameter of the condensate at that point in our finite grid is given by (6.83).

We can give an example of this procedure by discussing it in relation to one of the vortices displayed in section (5.3.3). Here, we will take the class 4 vortex in the cyclic phase as shown in figure (6). This particular vortex is a fractional $\frac{1}{3}$ vortex, with a gauge angle of $\frac{2\pi}{3}$, and a rotation of $\frac{2\pi}{3}$ in spin space. The element of the stabilizer group, \tilde{T} , that describes this is $\tilde{\sigma}$. By comparing the expression for $\tilde{\sigma}$ given by (5.29) with (5.28), we see that the axis for the rotation in spin space is the (-1,-1,-1) axis. Note that we have rotated this axis onto the z-axis in figure (6) and so the order parameter at the start of the loop, which is given by the rightmost spherical harmonic in figure (6), is actually a rotation of the representative order parameter. As we follow this loop around anti-clockwise to the next point on the loop, we calculate how much of the spin space rotation should have taken place in order to make the full angle of rotation vary linearly around this loop. We then calculate the Euler angles for this rotation and use this, along with the value the gauge angle should have at this point in the loop in order to vary linearly around the closed loop also, to calculate the order parameter of the condensate at this point in the loop using (6.83). We do this at each point of the loop which when finished will give us the full rotation in spin and phase space describing the vortex. The value of the order parameter calculated in this way at each point in our grid serves as our initial condition for a vortex to be passed into our ground state

code. Note that we will also have to think about how to smooth this wavefunction in order for it to be a good approximation to the ground state of the system. This will be discussed in section (7) for both spin one and spin two condensates.

6.3.2 Numerical Implementation

Now that we have described the general procedure for how a vortex is setup as the initial condition for our ground state code, we will look at how the parts of this procedure are practically implemented. We will first describe the aspects of the procedure that do not depend on the type of boundary conditions used for the ground state code, followed by those that do.

Axis-Angle to Euler angles As mentioned in the previous section, we will first have an axis-angle description of the rotation that a vortex produces. However, in order to write out the order parameter for each point of the vortex in space, we will need to obtain the Euler angles for a given axis-angle rotation that will be substituted into the general order parameter expression, (6.83). We do this with the following steps. We first find the rotation matrix that, when acted on a vector in \mathbb{R}^3 , produces the rotation described by the angle and axis given. The general form of this rotation matrix is given by [39] for a normalized axis of rotation $\vec{a} = (a_x, a_y, a_z)$ and angle θ :

$$R_{\vec{a},\theta} = \tag{6.86}$$

$$\begin{pmatrix} a_x^2 + (a_y^2 + a_z^2) \cos \theta & a_x a_y (1 - \cos \theta) - a_z \sin \theta & a_x a_z (1 - \cos \theta) + a_y \sin \theta \\ a_x a_y (1 - \cos \theta) + a_z \sin \theta & a_y^2 + (a_x^2 + a_z^2) \cos \theta & a_y a_z (1 - \cos \theta) - a_x \sin \theta \\ a_x a_z (1 - \cos \theta) - a_y \sin \theta & a_y a_z (1 - \cos \theta) + a_x \sin \theta & a_z^2 + (a_x^2 + a_y^2) \cos \theta \end{pmatrix}. \tag{6.87}$$

The first, second and third column of this matrix tell us where the x, y and z axes of a coordinate system attached to an object get rotated to if we rotate the object by an angle θ about the (a_x, a_y, a_z) axis. These new axes are given in terms of the fixed coordinate system and as such we can compare the axes of the coordinate system that rotates with the object to the x, y and z axes of the fixed coordinate system in order to determine the Euler angles for the rotation.

In order to do this, it is useful to look at the format of the Euler angles for *ZYZ* format and look at what we are doing when we make each of the rotations by angles of α , β and γ .

This can be seen in figures (18) to (20). In figure (18), we first perform a rotation about the z-axis of the fixed coordinate system by an angle of α . This causes the x and y axes of the object we are rotating to rotate to positions x' and y' . Next we rotate about the y' axis by an angle β which brings the z and x axes of the object being rotated to z_f and x'' respectively. Finally, we rotate about the z_f axis by an angle γ which brings the x and y

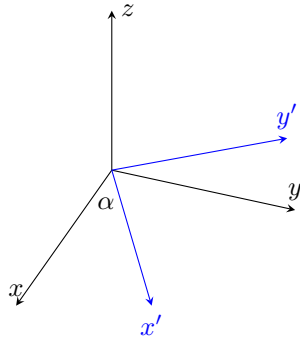


Figure 18: A demonstration of Euler angles for ZYZ format.

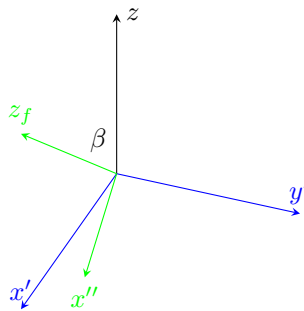


Figure 19: A demonstration of Euler angles for ZYZ format.

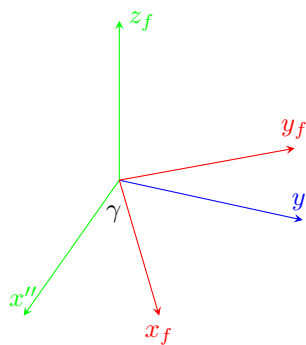


Figure 20: A demonstration of Euler angles for ZYZ format.

axes of the object to their final orientation x_f and y_f . After the full rotation, the coordinate axes of the object we have rotated are at positions x_f , y_f and z_f in terms of the fixed system.

From this procedure, we can easily see how we can obtain the Euler angles for a certain rotation once we have x_f , y_f and z_f . First let's look at how we find α . We can see from figures (18) and (19) that the rotation of α about the fixed z axis causes the original x axis, attached to the rotated object, to be rotated to x' which we can see is the projection of the final z axis, z_f into the xy plane. Therefore we can find α by using the dot product between the original x axis and the projection of the z_f axis into the xy plane. Setting $\vec{z}_p = (z_{fx}, z_{fy}, 0)$, we get the following expression for α :

$$\alpha = \arccos \frac{\vec{z}_p \cdot \vec{x}}{|z_p||x|}. \quad (6.88)$$

We can see from figure (19) that to find β we need only find the angle between the z_f axis and the original fixed z axis.

$$\beta = \arccos \frac{\vec{z}_f \cdot \vec{z}}{|z_f||z|}. \quad (6.89)$$

Finally we can find the angle γ by finding the angle between the y axis after the rotation by α , y' , and the final y axis of the object, y_f .

$$\gamma = \arccos \frac{\vec{y}' \cdot \vec{y}_f}{|y'||y_f|}. \quad (6.90)$$

At each step when we find each of these angles, we must check that we have found the anti-clockwise angle between them with respect to the axis of rotation. This is easy to do by taking the cross product between the old vector and new vector that we have rotated to by α , β or γ . We can then take a dot product between the resulting vector of the cross product and the known axis of rotation. If this dot product is greater than zero, then the orientation is correct and we have found the anti-clockwise angle. Otherwise, we adjust the angle by subtracting it from 2π .

Dirichlet Boundary conditions vortex setup Now that we have a way of finding the Euler angles for a given rotation in spin space, we need to think about how exactly we encode the vortex as an initial condition for the ground state code. As mentioned earlier, the method of implementing (6.83) as the initial condition is slightly different depending on whether we are using Dirichlet or periodic boundary conditions. Here, we will only look at the problem for Dirichlet boundary conditions as these are the conditions used in our ground state codes. We will also look at how to define a loop within the condensate for this case so that we can view if a vortex is present.

The first thing to consider for setting up a vortex in this system is what a closed loop is in this system. Figure (21) shows what a closed loop looks like in a 2-D system with Dirichlet boundary conditions.

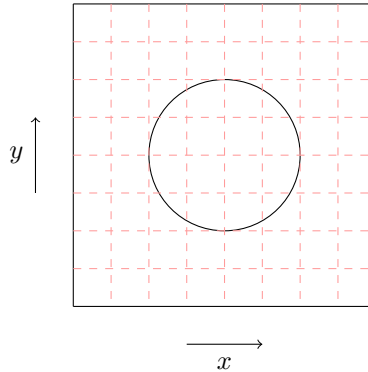


Figure 21: A closed loop in a grid with Dirichlet boundary conditions.

We think of this loop being centered on (0,0) within the grid. We can clearly see that a loop in our grid with Dirichlet boundary conditions can be parameterized using the polar angle φ .

Practically, we do this in the following way. Given a 2d grid of x and y points at which we will store the value of the condensate in space, we make a corresponding grid of the value of the polar angle φ at these points. Once we do this we can parameterize the gauge angle, ϕ , and spin space angle of rotation, θ , for our vortex.

$$\phi_p = \frac{\phi\varphi}{2\pi} \tag{6.91}$$

$$\theta_p = \frac{\theta\varphi}{2\pi}. \tag{6.92}$$

Here, we are thinking of φ as the full two-dimensional grid of polar angle points and as such, ϕ_p and θ_p are also meant to be the corresponding 2D arrays giving the values of the gauge angle and spin space rotation angle for all points on our finite grid. It is these lists that we feed into (6.83) to build our initial condition. Note that by doing it in this way, our initial condition actually imprints the vortex winding at all radii in our grid and not just at one loop at some distance from the origin.

We now have a way of setting up a vortex as an initial condition for our ground state code for Dirichlet boundary conditions, but what if we want to look at the value of the condensate around a closed loop in our grid to search for the presence of a vortex. How do we do that? One method would be to choose a loop at a certain radius in our grid and look at the grid points on that loop where we have data. However, this is not practical by its self as the loop we choose may not coincide with many points in our grid where we actually have the value of the condensate in space. This can be seen in figure (21). We think of the points where the red dashed grid lines cross as points in our grid where we have data on the condensate at that point in space. We can see that the example loop that we have drawn in

this figure only coincides with four data points which is not sufficient for determining what is happening along a closed loop within the condensate. Instead, we would like to be able to choose a loop at any radius in the condensate and specify how many points on that loop we would like to return the value of the condensate at. Since we do not have the value of the condensate at every point in space, we achieve this goal in the following way.

We choose a loop at some radius in our grid, such as the one shown in figure (21) and specify the number of points that we would like to sample the value of the condensate at along this loop. We then position these points along the loop so that they are spaced equally apart from each other in terms of the polar angle φ . For each of these points on the loop, if we have the value of the condensate at that point, then we just return the relevant order parameter there. In the other case where the point on the loop is not a point where we have data in our grid, we perform a weighted average of the value of the condensate at the nearest neighbour points where we do know the value of the condensate. This procedure is shown in figure (22). Here, we are looking at one of the square grids within our full grid and would like to approximate the value of the condensate at a point P , where we know the value of the condensate at points A, B, C and D . We first take the Euclidean distance between each of the points on the vertices of this square grid with P . Once we have done this we find the approximate order parameter of the condensate at the point P using the following expression:

$$\Psi_P = \frac{1}{W_{tot}} \left[\left(1 - \frac{d_A}{d_{Tot}}\right) \Psi_A + \left(1 - \frac{d_B}{d_{Tot}}\right) \Psi_B + \left(1 - \frac{d_C}{d_{Tot}}\right) \Psi_C + \left(1 - \frac{d_D}{d_{Tot}}\right) \Psi_D \right], \quad (6.93)$$

where Ψ_ν is the order parameter of the condensate at a point ν , $d_{Tot} = d_A + d_B + d_C + d_D$ and:

$$W_{tot} = \left(1 - \frac{d_A}{d_{Tot}}\right) + \left(1 - \frac{d_B}{d_{Tot}}\right) + \left(1 - \frac{d_C}{d_{Tot}}\right) + \left(1 - \frac{d_D}{d_{Tot}}\right) \quad (6.94)$$

is the total weight.

If the point P happens to lie on one of the red grid lines between two points, then we just take a weighted average of the order parameter of the condensate at the two points nearest to P along the same grid line.

Once we have a value of the order parameter at each point of the loop we have chosen, we can make graphical images of the condensate along this loop by using the spherical harmonic representation of the condensate as discussed previously.

6.4 Spin One Bogoliubov Excitations

In this section we will detail how we have derived and implemented the Bogoliubov equations for a spin one condensate. The code we implement is for two dimensions and the ground

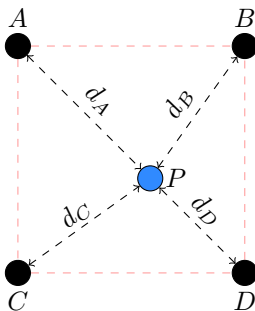


Figure 22: Computing the value of the condensate at a point we do not have data by taking a weighted average of neighbouring points.

states generated by our spin one code can be passed in as input to the Bogoliubov code to look at excitations about the ground state.

6.4.1 Equation setup

The method used here for deriving the Bogoliubov equations is an extension of the method used in [36] for a pseudo-spin half condensate. This method can also be found in [26] for a spinless condensate and has been employed for a spin one condensate with spin-orbit coupling in [40]. We also note that [41] was useful in ensuring our code was working when testing this for spinless cases in the earlier stages of this research.

We will take a perturbative approach to deriving these equations by thinking of the Bogoliubov excitations as slight fluctuations from the ground state. As a result, we will take the full wavefunction of the time-dependent system to be of the following form:

$$\begin{aligned}\vec{\Psi}(\vec{r}, t) &= (\psi_1, \psi_0, \psi_{-1}), \\ \psi_m(\vec{r}, t) &= e^{i\mu t}(\phi_m(\vec{r}) + u_m(\vec{r})e^{-i\omega t} + v_m^*(\vec{r})e^{i\omega^* t}).\end{aligned}\quad (6.95)$$

Here, $\phi_m(\vec{r})$ is the ground state of the system and ω is the frequency of perturbation. $u_m(\vec{r})$ and $v_m(\vec{r})$ are the Bogoliubov excitations and it is these that we wish to find. We will do this by subbing the ansatz (6.95) into the spin one time dependent Gross-Pitaevskii equations given by (6.39), (6.40) and (6.41). Note that, by using these, we are working in the dimensionless form specified before in section (6.1.1).

Once we have done this, we keep linear terms in u_m and v_m and split the terms into two equations where the first is given by all terms that are multiplied by $e^{-i(\mu+\omega)t}$ and the second is given by all terms multiplied by $e^{-i(\mu-\omega^*)t}$. This is why we get two equations from each time dependent Gross-Pitaevskii equation: one for u_m and one for v_m .

To obtain the first of these two equations we can read off the terms being multiplied by $e^{-i(\mu+\omega)t}$. To obtain the second equation, we must read off all terms being multiplied by

$e^{-i(\mu-\omega^*)t}$, conjugate them and multiply the entire equation by a minus sign. This step is to account for the $-\omega^*$ in the exponential and we want each of the equations to be of the form ωu_m or ωv_m on the right hand side of the equation. Without this step, the v_m equations will read $-\omega^* v_m^*$ on the right hand side.

Once we perform these steps for each of the three spin one Gross-Pitaevskii equations, we are left with six coupled equations for $u_1, v_1, u_0, v_0, u_{-1}$ and v_{-1} which are the spin one Bogoliubov equations:

$$\begin{aligned} & \mathcal{L}_1 u_1 + (\beta_0 + \beta_1)(\phi_1)^2 v_1 + [(\beta_0 + \beta_1)\phi_0^* \phi_1 + 2\beta_1 \phi_{-1}^* \phi_0] u_0 \\ & + (\beta_0 + \beta_1)\phi_0 \phi_1 v_0 + (\beta_0 - \beta_1)\phi_{-1}^* \phi_1 u_{-1} \\ & + [(\beta_0 - \beta_1)\phi_{-1} \phi_1 + \beta_1 \phi_0^2] v_{-1} = \omega u_1, \end{aligned} \quad (6.96)$$

$$\begin{aligned} & -(\beta_0 + \beta_1)(\phi_1^*)^2 u_1 - \mathcal{L}_1 v_1 - (\beta_0 + \beta_1)(\phi_0 \phi_1)^* u_0 \\ & + [-(\beta_0 + \beta_1)\phi_0 \phi_1^* - 2\beta_1 \phi_0^* \phi_{-1}] v_0 \\ & + [-(\beta_0 - \beta_1)(\phi_{-1} \phi_1)^* - \beta_1 (\phi_0^*)^2] u_{-1} \\ & - (\beta_0 - \beta_1)\phi_{-1} \phi_1^* v_{-1} = \omega v_1, \end{aligned} \quad (6.97)$$

$$\begin{aligned} & [(\beta_0 + \beta_1)\phi_1^* \phi_0 + 2\beta_1 \phi_{-1} \phi_0^*] u_1 + (\beta_0 + \beta_1)\phi_1 \phi_0 v_1 + \mathcal{L}_2 u_0 \\ & + [\beta_0 \phi_0^2 + 2\beta_1 \phi_{-1} \phi_1] v_0 \\ & + [(\beta_0 + \beta_1)\phi_{-1}^* \phi_0 + 2\beta_1 \phi_0^* \phi_1] u_{-1} \\ & + (\beta_0 + \beta_1)\phi_{-1} \phi_0 v_{-1} = \omega u_0, \end{aligned} \quad (6.98)$$

$$\begin{aligned} & -(\beta_0 + \beta_1)(\phi_1 \phi_0)^* u_1 + [-(\beta_0 + \beta_1)\phi_1 \phi_0^* - 2\beta_1 \phi_{-1}^* \phi_0] v_1 \\ & + [-\beta_0 (\phi_0^*)^2 - 2\beta_1 (\phi_{-1} \phi_1)^*] u_0 - \mathcal{L}_2 v_0 \\ & - (\beta_0 + \beta_1)(\phi_{-1} \phi_0)^* u_{-1} \\ & + [-(\beta_0 + \beta_1)\phi_{-1} \phi_0^* - 2\beta_1 \phi_0 \phi_1^*] v_{-1} = \omega v_0, \end{aligned} \quad (6.99)$$

$$\begin{aligned} & (\beta_0 - \beta_1)\phi_1^* \phi_{-1} u_1 + [(\beta_0 - \beta_1)\phi_1 \phi_{-1} + \beta_1 \phi_0^2] v_1 \\ & + [(\beta_0 + \beta_1)\phi_0^* \phi_{-1} + 2\beta_1 \phi_0 \phi_1^*] u_0 + (\beta_0 + \beta_1)\phi_0 \phi_{-1} v_0 \\ & + \mathcal{L}_3 u_{-1} + (\beta_0 + \beta_1)\phi_{-1}^2 v_{-1} = \omega u_{-1}, \end{aligned} \quad (6.100)$$

$$\begin{aligned} & [-(\beta_0 - \beta_1)(\phi_1 \phi_{-1})^* - \beta_1 (\phi_0^*)^2] u_1 - (\beta_0 - \beta_1)\phi_1 \phi_{-1}^* v_1 \\ & - (\beta_0 + \beta_1)(\phi_0 \phi_{-1})^* u_0 \\ & + [-(\beta_0 + \beta_1)\phi_0 \phi_{-1}^* - 2\beta_1 \phi_0^* \phi_1] v_0 \\ & - (\beta_0 + \beta_1)(\phi_{-1}^*)^2 u_{-1} - \mathcal{L}_3 v_{-1} = \omega v_{-1}, \end{aligned} \quad (6.101)$$

where:

$$\begin{aligned}
\mathcal{L}_1 &= -\frac{1}{2}\nabla^2 + V(\vec{r}) + q - p + 2(\beta_0 + \beta_1)|\phi_1|^2 + (\beta_0 - \beta_1)|\phi_{-1}|^2 + (\beta_0 + \beta_1)|\phi_0|^2 - \mu, \\
\mathcal{L}_2 &= -\frac{1}{2}\nabla^2 + V(\vec{r}) + 2\beta_0|\phi_0|^2 + (\beta_0 + \beta_1)(|\phi_{-1}|^2 + |\phi_1|^2) - \mu, \\
\mathcal{L}_3 &= -\frac{1}{2}\nabla^2 + V(\vec{r}) + q + p + 2(\beta_0 + \beta_1)|\phi_{-1}|^2 + (\beta_0 - \beta_1)|\phi_1|^2 + (\beta_0 + \beta_1)|\phi_0|^2 - \mu,
\end{aligned} \tag{6.102}$$

To use these equations, we need an expression for the chemical potential, μ . This can be obtained from the time-independent Gross-Pitaevskii equations, which we will list in a convenient form for our purpose here.

$$\mu\phi_1 = \left[-\frac{1}{2}\nabla^2 + V - p + q + \beta_0 n + \beta_1 F_z \right] \phi_1 + \frac{\beta_1}{\sqrt{2}} F_- \phi_0, \tag{6.103}$$

$$\mu\phi_0 = \left[-\frac{1}{2}\nabla^2 + V + \beta_0 n \right] \phi_0 + \frac{\beta_1}{\sqrt{2}} F_+ \phi_1 + \frac{\beta_1}{\sqrt{2}} F_- \phi_{-1}, \tag{6.104}$$

$$\mu\phi_{-1} = \left[-\frac{1}{2}\nabla^2 + V + p + q + \beta_0 n - \beta_1 F_z \right] \phi_{-1} + \frac{\beta_1}{\sqrt{2}} F_+ \phi_0. \tag{6.105}$$

We first multiply each of these component equations by their conjugate ψ_m^* and then add them together and integrate over position. Using the normalization constraint (6.42), we see that we just get left with μ on the left hand side which means that the results on the right hand side is an expression for μ . After some manipulation of the right hand side, we get the following expression for μ :

$$\mu = \int \left\{ \sum_{m=-1}^1 \left(\frac{1}{2} |\nabla \phi_m|^2 + (V - pm + qm^2) |\phi_m|^2 \right) + \beta_0 n^2 + \beta_1 |\vec{F}|^2 \right\}. \tag{6.106}$$

6.4.2 Code implementation

We now want to solve these equations numerically. Note that we will do this using periodic boundary conditions which have been described in detail for the ground state code in section (6.1.4). To solve, we will set them up on our finite grid. Each u_m and v_m will be discretized in the same way as the ground state wave function was previously. This means that we will describe these Bogoliubov excitations using L^2 points on a two-dimensional grid. An example of this is shown for u_1 :

$$\vec{u}_1 = \left[u_{1,1,1} \quad u_{1,2,1} \quad \dots \quad u_{1,L,1} \quad u_{1,1,2} \quad \dots \quad u_{1,L,2} \right]^T \tag{6.107}$$

As a result, we need to write the Bogoliubov equations above in the same format where, now, each of the six Bogoliubov equations above will become a system of L^2 linear equations

A_{1,u_1}	A_{1,v_1}	A_{1,u_0}	A_{1,v_0}	$A_{1,u_{-1}}$	$A_{1,v_{-1}}$
A_{2,u_1}	A_{2,v_1}	A_{2,u_0}	A_{2,v_0}	$A_{2,u_{-1}}$	$A_{2,v_{-1}}$
A_{3,u_1}	A_{3,v_1}	A_{3,u_0}	A_{3,v_0}	$A_{3,u_{-1}}$	$A_{3,v_{-1}}$
A_{4,u_1}	A_{4,v_1}	A_{4,u_0}	A_{4,v_0}	$A_{4,u_{-1}}$	$A_{4,v_{-1}}$
A_{5,u_1}	A_{5,v_1}	A_{5,u_0}	A_{5,v_0}	$A_{5,u_{-1}}$	$A_{5,v_{-1}}$
A_{6,u_1}	A_{6,v_1}	A_{6,u_0}	A_{6,v_0}	$A_{6,u_{-1}}$	$A_{6,v_{-1}}$

Figure 23: Format of the M matrix.

that can be solved to give the value of the Bogoliubov excitation at each position in our lattice. Here, we have written the first of six Bogoliubov equations, given by (6.96), in discretized form. The discretized version of the other five equations is similar.

$$\begin{aligned}
& -\frac{1}{2\hbar^2} (u_{1,i+1,j} + u_{1,i-1,j} + u_{1,i,j+1} + u_{1,i,j-1} - 4u_{1,i,j}) \\
& + (V_{i,j} + q - p + 2(\beta_0 + \beta_1)|\phi_{1,i,j}|^2 + (\beta_0 - \beta_1)|\phi_{-1,i,j}|^2 \\
& \quad + (\beta_0 + \beta_1)|\phi_{0,i,j}|^2 - \mu) u_{1,i,j} \\
& + (\beta_0 + \beta_1)(\phi_{1,i,j})^2 v_{1,i,j} \\
& + [(\beta_0 + \beta_1)\phi_{0,i,j}^* \phi_{1,i,j} + 2\beta_1 \phi_{-1,i,j}^* \phi_{0,i,j}] u_{0,i,j} \\
& + (\beta_0 + \beta_1)\phi_{0,i,j} \phi_{1,i,j} v_{0,i,j} + (\beta_0 - \beta_1)\phi_{-1,i,j}^* \phi_{1,i,j} u_{-1,i,j} \\
& + [(\beta_0 - \beta_1)\phi_{-1,i,j} \phi_{1,i,j} + \beta_1 \phi_{0,i,j}^2] v_{-1,i,j} = \omega u_{1,i,j}. \tag{6.108}
\end{aligned}$$

Once we do this for all six Bogoliubov equations, we will end up with $6L^2$ equations. Note that each of the six systems are coupled together and so cannot be solved independently. However, if we write the full $6L^2$ equations as one matrix equation, we see that we are dealing with an eigenvalue equation which we can solve numerically.

$$M\vec{b} = \omega\vec{b}. \tag{6.109}$$

To do this, we need to set up the M matrix and \vec{b} vector in the above equation. First, let's look at the \vec{b} vector. This will be of the following form:

$$\vec{b} = [\vec{u}_1 \quad \vec{v}_1 \quad \vec{u}_0 \quad \vec{v}_0 \quad \vec{u}_{-1} \quad \vec{v}_{-1}]^T, \tag{6.110}$$

where each entry given in the \vec{b} vector is itself a vector whose form is given by (6.107). This means that the \vec{b} vector contains $6L^2$ elements.

The M vector is set up according to figure (23).

Each block matrix in M is of size $L^2 \times L^2$ so that it lines up with the corresponding elements in \vec{b} that it multiplies to represent one of our $6L^2$ equations. For example A_{1,v_1} will store the values of $(\beta_0 + \beta_1)(\phi_{1,i,j})^2$ at each position in our lattice as these are the values that multiply v_1 in (6.108).

We can easily see how each of these block matrices are filled. All block matrices not on the main diagonal of M will have their main diagonal entries filled with the value of the term multiplying the bogoliubov excitation, u_m or v_m , at the corresponding position in our lattice, with all other entries being zero. That is, if we use column major order for our finite grid, then the main diagonal of each block matrix not on the main diagonal of M will contain the value multiplying the relevant $u_{m,i,j}$ or $v_{m,i,j}$ which are assumed to be in column major order in \vec{b} .

An example of how this is filled in can be seen by looking at the main diagonal of (6.73). Instead of filling in $\chi_{i,j}$ along the main diagonal, we will fill in the corresponding (i, j) value of the term multiplying $u_{m,i,j}$ or $v_{m,i,j}$ and all other terms will be zero.

To fill in the elements to the block matrices on the main diagonal of M , we have to take into account that these matrices account for the derivative acting on u_m or v_m in each of the $6L^2$ equations and as such will have terms both on and off the main diagonal. The main diagonal terms will be those that are multiplying u_m or v_m at the current position in our lattice. For example, if we look at A_{1,u_1} , then the main diagonal terms will be of the form:

$$\chi_{i,j} = \frac{2}{\hbar^2} + (V_{i,j} + q - p + 2(\beta_0 + \beta_1)|\phi_{1,i,j}|^2 + (\beta_0 - \beta_1)|\phi_{-1,i,j}|^2 + (\beta_0 + \beta_1)|\phi_{0,i,j}|^2 - \mu). \quad (6.111)$$

We can see this by looking at (6.108).

We still have to account for the coupling of position terms due to the derivative, however, we have seen this before when we filled in the A matrix in section (6.1.4). The A matrix in those sections was of size $L^2 \times L^2$ and so we see that to fill in each of the block matrices in M we can do the exact same procedure as before. The only difference is that the main diagonal χ elements will be slightly different and instead of filling in $-\tau$ for the off diagonal elements, we will now fill in $-\frac{1}{2\hbar^2}$. Since we are using periodic boundary conditions, we also add $-\frac{1}{2\hbar^2}$ in the matrices on the main diagonal of M , corresponding with the $-\tau$ values coloured in blue and red in the A matrix described by equation (6.73) and figure (17). Algorithm (3) describing filling the A matrix in section (6.1.4) can be used here to fill each block matrix in M where the full algorithm is used to fill the block matrices on the main diagonal of M and the start of the algorithm is used to fill in the main diagonal elements of all other block matrices in M , The only adjustment we need to do is substitute the relevant terms as discussed above. Once this is done, the only extra step involved here, is arranging the block matrices in the correct way to construct the M matrix and solving for its eigenvectors and eigenvalues. The eigenvectors of M will be the \vec{b} vector discussed above, from which the

Bogoliubov excitations can be extracted. For example, the first L^2 elements of \vec{b} will be u_1 , the next L^2 values will be v_1 and so on. The eigenvalues of M will be our corresponding frequencies of perturbation, ω .

6.5 Spin Two Bogoliubov Excitations

Below, we will list the Bogoliubov equations for a spin two condensate. The procedure for deriving these is the exact same as the spin one case. We start with the same ansatz (6.95), however, here m runs from -2 to 2 , and we substitute each of these into the relevant m component equation of the time dependent Gross Pitaevskii equations for spin two, given by equations (3.105) to (3.109). Once we do this, we again keep linear terms in u_m and v_m and split the terms in each equation into terms involving $e^{-i(\mu+\omega)t}$ and $e^{-i(\mu-\omega^*)t}$. We then read off the terms multiplying these to obtain two equations for each spin component, remembering to multiply terms with a factor of $e^{-i(\mu-\omega^*)t}$ by a minus sign and conjugate.

$$\begin{aligned}
& \mathcal{L}_1 u_1 + (4\beta_1 + \beta_0)(\phi_2)^2 v_2 \\
& + \left[\beta_0 \phi_1^* \phi_2 + \beta_1 \{ 4\phi_1^* \phi_2 + 2\sqrt{6}\phi_0^* \phi_1 \right. \\
& \left. + \sqrt{6}\phi_{-1}^* \phi_0 + 2\phi_{-2}^* \phi_{-1} \} - \frac{2}{5}\beta_2 \phi_{-2}^* \phi_{-1} \right] u_1 \\
& + [(4\beta_1 + \beta_0)\phi_1 \phi_2] v_1 \\
& + \left[\beta_0 \phi_0^* \phi_2 + \sqrt{6}\beta_1 \phi_{-1}^* \phi_1 + \frac{2}{5}\beta_2 \phi_{-2}^* \phi_0 \right] u_0 \\
& + [\beta_0 \phi_0 \phi_2 + \sqrt{6}\beta_1 (\phi_1)^2] v_0 \\
& + \left[(\beta_0 - 2\beta_1)\phi_{-1}^* \phi_2 + 2\beta_1 \phi_{-2}^* \phi_1 - \frac{2}{5}\beta_2 \phi_{-2}^* \phi_1 \right] u_{-1} \\
& + [(\beta_0 - 2\beta_1)\phi_{-1} \phi_2 + \sqrt{6}\beta_1 \phi_0 \phi_1] v_{-1} \\
& + \left[(\beta_0 - 4\beta_1)\phi_{-2}^* \phi_2 + \frac{2}{5}\beta_2 \phi_{-2}^* \phi_2 \right] u_{-2} \\
& + \left[\left(\beta_0 - 4\beta_1 + \frac{2}{5}\beta_2 \right) \phi_{-2} \phi_2 + \left(2\beta_1 - \frac{2}{5}\beta_2 \right) \phi_1 \phi_{-1} + \frac{\beta_2}{5} (\phi_0)^2 \right] v_{-2} \\
& = \omega u_2, \tag{6.112}
\end{aligned}$$

$$\begin{aligned}
& - [(4\beta_1 + \beta_0)(\phi_2^*)^2] u_2 - \mathcal{L}_1 v_2 - [(4\beta_1 + \beta_0)\phi_1^* \phi_2^*] u_1 \\
& - \left[\beta_0 \phi_1 \phi_2^* + \beta_1 \{4\phi_1 \phi_2^* + 2\sqrt{6}\phi_0 \phi_1^* \right. \\
& \left. + \sqrt{6}\phi_{-1} \phi_0^* + 2\phi_{-2} \phi_{-1}^* \} - \frac{2}{5}\beta_2 \phi_{-2} \phi_{-1}^* \right] v_1 \\
& - \left[\beta_0 \phi_0^* \phi_2^* + \sqrt{6}\beta_1 (\phi_1^*)^2 \right] u_0 \\
& - \left[\beta_0 \phi_0 \phi_2^* + \sqrt{6}\beta_1 \phi_{-1} \phi_1^* + \frac{2}{5}\beta_2 \phi_{-2} \phi_0^* \right] v_0 \\
& - \left[(\beta_0 - 2\beta_1) \phi_{-1}^* \phi_2^* + \sqrt{6}\beta_1 \phi_0^* \phi_1^* \right] u_{-1} \\
& - \left[(\beta_0 - 2\beta_1) \phi_{-1} \phi_2^* + 2\beta_1 \phi_{-2} \phi_1^* - \frac{2}{5}\beta_2 \phi_{-2} \phi_1^* \right] v_{-1} \\
& - \left[\left(\beta_0 - 4\beta_1 + \frac{2}{5}\beta_2 \right) \phi_{-2}^* \phi_2^* + \left(2\beta_1 - \frac{2}{5}\beta_2 \right) \phi_{-1}^* \phi_1^* + \frac{\beta_2}{5} (\phi_0^*)^2 \right] u_{-2} \\
& - \left[\left(\beta_0 - 4\beta_1 + \frac{2}{5}\beta_2 \right) \phi_{-2} \phi_2^* \right] v_{-2} = \omega v_2, \tag{6.113}
\end{aligned}$$

$$\begin{aligned}
& \left[(\beta_0 + 4\beta_1) \phi_2^* \phi_1 + 2\sqrt{6}\beta_1 \phi_1^* \phi_0 \right. \\
& \left. + \sqrt{6}\beta_1 \phi_0^* \phi_{-1} + \left(2\beta_1 - \frac{2}{5}\beta_2 \right) \phi_{-1}^* \phi_{-2} \right] u_2 \\
& + [(\beta_0 + 4\beta_1) \phi_2 \phi_1] v_2 + \mathcal{L}_2 u_1 \\
& + [(\beta_0 + \beta_1) (\phi_1)^2 + 2\sqrt{6}\beta_1 \phi_2 \phi_0] v_1 \\
& + \left[(\beta_0 + 3\beta_1) \phi_0^* \phi_1 + 2\sqrt{6}\beta_1 \phi_1^* \phi_2 \right. \\
& \left. + \sqrt{6}\beta_1 \phi_{-2}^* \phi_{-1} + \left(6\beta_1 - \frac{2}{5}\beta_2 \right) \phi_{-1}^* \phi_0 \right] u_0 \\
& + [(\beta_0 + 3\beta_1) \phi_0 \phi_1 + \sqrt{6}\beta_1 \phi_{-1} \phi_2] v_0 \\
& + \left[\left(\beta_0 - \beta_1 + \frac{2}{5}\beta_2 \right) \phi_{-1}^* \phi_1 + \sqrt{6}\beta_1 (\phi_{-2}^* \phi_0 + \phi_0^* \phi_2) \right] u_{-1} \\
& + \left[\left(\beta_0 - \beta_1 + \frac{2}{5}\beta_2 \right) \phi_1 \phi_{-1} + \left(2\beta_1 - \frac{2}{5}\beta_2 \right) \phi_{-2} \phi_2 \right. \\
& \left. + \left(3\beta_1 - \frac{\beta_2}{5} \right) (\phi_0)^2 \right] v_{-1} \\
& + \left[(\beta_0 - 2\beta_1) \phi_{-2}^* \phi_1 + \left(2\beta_1 - \frac{2}{5}\beta_2 \right) \phi_{-1}^* \phi_2 \right] u_{-2} \\
& + [(\beta_0 - 2\beta_1) \phi_{-2} \phi_1 + \sqrt{6}\beta_1 \phi_{-1} \phi_0] v_{-2} = \omega u_1 \tag{6.114}
\end{aligned}$$

$$\begin{aligned}
& - [(\beta_0 + 4\beta_1)\phi_2^*\phi_1^*] u_2 \\
& - \left[(\beta_0 + 4\beta_1)\phi_2\phi_1^* + 2\sqrt{6}\beta_1\phi_1\phi_0^* \right. \\
& \left. + \sqrt{6}\beta_1\phi_0\phi_{-1}^* + \left(2\beta_1 - \frac{2}{5}\beta_2\right)\phi_{-1}\phi_{-2}^* \right] v_2 \\
& - \left[(\beta_0 + \beta_1)(\phi_1^*)^2 + 2\sqrt{6}\beta_1\phi_2^*\phi_0^* \right] u_1 - \mathcal{L}_2 v_1 \\
& - \left[(\beta_0 + 3\beta_1)\phi_0^*\phi_1^* + \sqrt{6}\beta_1\phi_{-1}^*\phi_2^* \right] u_0 \\
& - \left[(\beta_0 + 3\beta_1)\phi_0\phi_1^* + 2\sqrt{6}\beta_1\phi_1\phi_2^* \right. \\
& \left. + \sqrt{6}\beta_1\phi_{-2}\phi_{-1}^* + \left(6\beta_1 - \frac{2}{5}\beta_2\right)\phi_{-1}\phi_0^* \right] v_0 \\
& - \left[\left(\beta_0 - \beta_1 + \frac{2}{5}\beta_2\right)\phi_1^*\phi_{-1}^* + \left(2\beta_1 - \frac{2}{5}\beta_2\right)\phi_{-2}^*\phi_2^* \right. \\
& \qquad \qquad \qquad \left. + \left(3\beta_1 - \frac{\beta_2}{5}\right)(\phi_0^*)^2 \right] u_{-1} \\
& - \left[\left(\beta_0 - \beta_1 + \frac{2}{5}\beta_2\right)\phi_{-1}\phi_1^* + \sqrt{6}\beta_1(\phi_{-2}\phi_0^* + \phi_0\phi_2^*) \right] v_{-1} \\
& - \left[(\beta_0 - 2\beta_1)\phi_{-2}^*\phi_1^* + \sqrt{6}\beta_1\phi_{-1}^*\phi_0^* \right] u_{-2} \\
& - \left[(\beta_0 - 2\beta_1)\phi_{-2}\phi_1^* + \left(2\beta_1 - \frac{2}{5}\beta_2\right)\phi_{-1}\phi_2^* \right] v_{-2} = \omega v_1, \tag{6.115}
\end{aligned}$$

$$\begin{aligned}
& \left[\beta_0 \phi_2^* \phi_0 + \sqrt{6} \beta_1 \phi_1^* \phi_{-1} + \frac{2}{5} \beta_2 \phi_0^* \phi_{-2} \right] u_2 \\
& + \left[\beta_0 \phi_2 \phi_0 + \sqrt{6} \beta_1 (\phi_1)^2 \right] v_2 \\
& + \left[(\beta_0 + 3\beta_1) \phi_1^* \phi_0 + 2\sqrt{6} \beta_1 \phi_2^* \phi_1 \right. \\
& \left. + \sqrt{6} \beta_1 \phi_{-1}^* \phi_{-2} + \left(6\beta_1 - \frac{2}{5} \beta_2 \right) \phi_0^* \phi_{-1} \right] u_1 \\
& + \left[(\beta_0 + 3\beta_1) \phi_1 \phi_0 + \sqrt{6} \beta_1 \phi_2 \phi_{-1} \right] v_1 + \mathcal{L}_3 u_0 \\
& + \left[\left(\beta_0 + \frac{\beta_2}{5} \right) (\phi_0)^2 + \left(6\beta_1 - \frac{2}{5} \beta_2 \right) \phi_1 \phi_{-1} + \frac{2}{5} \beta_2 \phi_{-2} \phi_2 \right] v_0 \\
& + \left[(\beta_0 + 3\beta_1) \phi_{-1}^* \phi_0 + \left(6\beta_1 - \frac{2}{5} \beta_2 \right) \phi_0^* \phi_1 \right. \\
& \left. + \sqrt{6} \beta_1 \phi_1^* \phi_2 + 2\sqrt{6} \beta_1 \phi_{-2}^* \phi_{-1} \right] u_{-1} \\
& + \left[(\beta_0 + 3\beta_1) \phi_{-1} \phi_0 + \sqrt{6} \beta_1 \phi_{-2} \phi_1 \right] v_{-1} \\
& + \left[\beta_0 \phi_{-2}^* \phi_0 + \sqrt{6} \beta_1 \phi_{-1}^* \phi_1 + \frac{2}{5} \beta_2 \phi_0^* \phi_2 \right] u_{-2} \\
& + \left[\beta_0 \phi_{-2} \phi_0 + \sqrt{6} \beta_1 (\phi_{-1})^2 \right] v_{-2} = \omega u_0,
\end{aligned} \tag{6.116}$$

$$\begin{aligned}
& - [\beta_0 \phi_2^* \phi_0^* + \sqrt{6} \beta_1 (\phi_1^*)^2] u_2 \\
& - \left[\beta_0 \phi_2 \phi_0^* + \sqrt{6} \beta_1 \phi_1 \phi_{-1}^* + \frac{2}{5} \beta_2 \phi_0 \phi_{-2}^* \right] v_2 \\
& - \left[(\beta_0 + 3\beta_1) \phi_1^* \phi_0^* + \sqrt{6} \beta_1 \phi_2^* \phi_{-1}^* \right] u_1 \\
& - \left[(\beta_0 + 3\beta_1) \phi_1 \phi_0^* + 2\sqrt{6} \beta_1 \phi_2 \phi_1^* \right. \\
& \left. + \sqrt{6} \beta_1 \phi_{-1} \phi_{-2}^* + \left(6\beta_1 - \frac{2}{5} \beta_2 \right) \phi_0 \phi_{-1}^* \right] v_1 \\
& - \left[\left(\beta_0 + \frac{\beta_2}{2} \right) (\phi_0^*)^2 + \left(6\beta_1 - \frac{2}{5} \beta_2 \right) \phi_1^* \phi_{-1}^* + \frac{2}{5} \beta_2 \phi_{-2}^* \phi_2^* \right] u_0 \\
& - \mathcal{L}_3 v_0 - \left[(\beta_0 + 3\beta_1) \phi_{-1}^* \phi_0^* + \sqrt{6} \beta_1 \phi_{-2}^* \phi_1^* \right] u_{-1} \\
& - \left[(\beta_0 + 3\beta_1) \phi_{-1} \phi_0^* + \left(6\beta_1 - \frac{2}{5} \beta_2 \right) \phi_0 \phi_1^* \right. \\
& \left. + \sqrt{6} \beta_1 \phi_1 \phi_2^* + 2\sqrt{6} \beta_1 \phi_{-2} \phi_{-1}^* \right] v_{-1} \\
& - \left[\beta_0 \phi_{-2}^* \phi_0^* + \sqrt{6} \beta_1 (\phi_{-1}^*)^2 \right] u_{-2} \\
& - \left[\beta_0 \phi_{-2} \phi_0^* + \sqrt{6} \beta_1 \phi_{-1} \phi_1^* + \frac{2}{5} \beta_2 \phi_0 \phi_2^* \right] v_{-2} = \omega v_0, \tag{6.117}
\end{aligned}$$

$$\begin{aligned}
& \left[(\beta_0 - 2\beta_1)\phi_2^*\phi_{-1} + \left(2\beta_1 - \frac{2}{5}\beta_2 \right) \phi_1^*\phi_{-2} \right] u_2 \\
& + \left[(\beta_0 - 2\beta_1)\phi_2\phi_{-1} + \sqrt{6}\beta_1\phi_1\phi_0 \right] v_2 \\
& + \left[\left(\beta_0 - \beta_1 + \frac{2}{5}\beta_2 \right) \phi_1^*\phi_{-1} + \sqrt{6}\beta_1\phi_2^*\phi_0 + \sqrt{6}\beta_1\phi_0^*\phi_{-2} \right] u_1 \\
& + \left[\left(\beta_0 - \beta_1 + \frac{2}{5}\beta_2 \right) \phi_1\phi_{-1} + \left(3\beta_1 - \frac{\beta_2}{5} \right) (\phi_0)^2 \right. \\
& \qquad \qquad \qquad \left. + \left(2\beta_1 - \frac{2}{5}\beta_2 \right) \phi_2\phi_{-2} \right] v_1 \\
& + \left[(\beta_0 + 3\beta_1)\phi_0^*\phi_{-1} + 2\sqrt{6}\beta_1\phi_{-1}^*\phi_{-2} \right. \\
& \left. + \sqrt{6}\beta_1\phi_2^*\phi_1 + \left(6\beta_1 - \frac{2}{5}\beta_2 \right) \phi_1^*\phi_0 \right] u_0 \\
& + \left[(\beta_0 + 3\beta_1)\phi_0\phi_{-1} + \sqrt{6}\beta_1\phi_1\phi_{-2} \right] v_0 + \mathcal{L}_4 u_{-1} \\
& + \left[(\beta_0 + \beta_1)(\phi_{-1})^2 + 2\sqrt{6}\beta_1\phi_0\phi_{-2} \right] v_{-1} \\
& + \left[(\beta_0 + 4\beta_1)\phi_{-2}^*\phi_{-1} + 2\sqrt{6}\beta_1\phi_{-1}^*\phi_0 \right. \\
& \left. + \sqrt{6}\beta_1\phi_0^*\phi_1 + \left(2\beta_1 - \frac{2}{5}\beta_2 \right) \phi_1^*\phi_2 \right] u_{-2} \\
& + [(\beta_0 + 4\beta_1)\phi_{-2}\phi_{-1}] v_{-2} = \omega u_{-1}, \tag{6.118}
\end{aligned}$$

$$\begin{aligned}
& -[(\beta_0 - 2\beta_1)\phi_2^*\phi_{-1}^* + \sqrt{6}\beta_1\phi_1^*\phi_0^*]u_2 \\
& - \left[(\beta_0 - 2\beta_1)\phi_2\phi_{-1}^* + \left(2\beta_1 - \frac{2}{5}\beta_2\right)\phi_1\phi_{-2}^* \right] v_2 \\
& - \left[\left(\beta_0 - \beta_1 + \frac{2}{5}\beta_2\right)\phi_1^*\phi_{-1}^* + \left(3\beta_1 - \frac{\beta_2}{5}\right)(\phi_0^*)^2 \right. \\
& \quad \left. + \left(2\beta_1 - \frac{2}{5}\beta_2\right)\phi_{-2}^*\phi_2^* \right] u_1 \\
& - \left[\left(\beta_0 - \beta_1 + \frac{2}{5}\beta_2\right)\phi_1\phi_{-1}^* + \sqrt{6}\beta_1\phi_2\phi_0^* + \sqrt{6}\beta_1\phi_0\phi_{-2}^* \right] v_1 \\
& - [(\beta_0 + 3\beta_1)\phi_0^*\phi_{-1}^* + \sqrt{6}\beta_1\phi_1^*\phi_{-2}^*] u_0 \\
& - [(\beta_0 + 3\beta_1)\phi_0\phi_{-1}^* + 2\sqrt{6}\beta_1\phi_{-1}\phi_{-2}^* \\
& + \sqrt{6}\beta_1\phi_2\phi_1^* + \left(6\beta_1 - \frac{2}{5}\beta_2\right)\phi_1\phi_0^*] v_0 \\
& - [(\beta_0 + \beta_1)(\phi_{-1}^*)^2 + 2\sqrt{6}\beta_1\phi_0^*\phi_{-2}^*] u_{-1} - \mathcal{L}_4 v_{-1} \\
& - [(\beta_0 + 4\beta_1)\phi_{-2}^*\phi_{-1}^*] u_{-2} \\
& - [(\beta_0 + 4\beta_1)\phi_{-2}\phi_{-1}^* + 2\sqrt{6}\beta_1\phi_{-1}\phi_0^* \\
& + \sqrt{6}\beta_1\phi_0\phi_1^* + \left(2\beta_1 - \frac{2}{5}\beta_2\right)\phi_1\phi_2^*] v_{-2} \\
& = \omega v_{-1}, \tag{6.119}
\end{aligned}$$

$$\begin{aligned}
& \left[\left(\beta_0 - 4\beta_1 + \frac{2}{5}\beta_2 \right) \phi_2^* \phi_{-2} \right] u_2 \\
& + \left[\left(\beta_0 - 4\beta_1 + \frac{2}{5}\beta_2 \right) \phi_2 \phi_{-2} + \left(2\beta_1 - \frac{2}{5}\beta_2 \right) \phi_1 \phi_{-1} + \frac{\beta_2}{5} (\phi_0)^2 \right] v_2 \\
& + \left[(\beta_0 - 2\beta_1) \phi_1^* \phi_{-2} + \left(2\beta_1 - \frac{2}{5}\beta_2 \right) \phi_2^* \phi_{-1} \right] u_1 \\
& + \left[(\beta_0 - 2\beta_1) \phi_1 \phi_{-2} + \sqrt{6}\beta_1 \phi_0 \phi_{-1} \right] v_1 \\
& + \left[\beta_0 \phi_0^* \phi_{-2} + \sqrt{6}\beta_1 \phi_1^* \phi_{-1} + \frac{2}{5}\beta_2 \phi_2^* \phi_0 \right] u_0 \\
& + \left[\beta_0 \phi_0 \phi_{-2} + \sqrt{6}\beta_1 (\phi_{-1})^2 \right] v_0 \\
& + \left[(\beta_0 + 4\beta_1) \phi_{-1}^* \phi_{-2} + 2\sqrt{6}\beta_1 \phi_0^* \phi_{-1} \right. \\
& \left. + \sqrt{6}\beta_1 \phi_1^* \phi_0 + \left(2\beta_1 - \frac{2}{5}\beta_2 \right) \phi_2^* \phi_1 \right] u_{-1} \\
& + [(\beta_0 + 4\beta_1) \phi_{-1} \phi_{-2}] v_{-1} + \mathcal{L}_5 u_{-2} \\
& + [(\beta_0 + 4\beta_1) (\phi_{-2})^2] v_{-2} = \omega u_{-2}, \tag{6.120}
\end{aligned}$$

$$\begin{aligned}
& - \left[\left(\beta_0 - 4\beta_1 + \frac{2}{5}\beta_2 \right) \phi_2^* \phi_{-2}^* + \left(2\beta_1 - \frac{2}{5}\beta_2 \right) \phi_1^* \phi_{-1}^* + \frac{\beta_2}{5} (\phi_0^*)^2 \right] u_2 \\
& - \left[\left(\beta_0 - 4\beta_1 + \frac{2}{5}\beta_2 \right) \phi_2 \phi_{-2}^* \right] v_2 \\
& - \left[(\beta_0 - 2\beta_1) \phi_1^* \phi_{-2}^* + \sqrt{6}\beta_1 \phi_0^* \phi_{-1}^* \right] u_1 \\
& - \left[(\beta_0 - 2\beta_1) \phi_1 \phi_{-2}^* + \left(2\beta_1 - \frac{2}{5}\beta_2 \right) \phi_2 \phi_{-1}^* \right] v_1 \\
& - \left[\beta_0 \phi_0^* \phi_{-2}^* + \sqrt{6}\beta_1 (\phi_{-1}^*)^2 \right] u_0 \\
& - \left[\beta_0 \phi_0 \phi_{-2}^* + \sqrt{6}\beta_1 \phi_1 \phi_{-1}^* + \frac{2}{5}\beta_2 \phi_2 \phi_0^* \right] v_0 \\
& - [(\beta_0 + 4\beta_1) \phi_{-1}^* \phi_{-2}^*] u_{-1} \\
& - \left[(\beta_0 + 4\beta_1) \phi_{-1} \phi_{-2}^* + 2\sqrt{6}\beta_1 \phi_0 \phi_{-1}^* \right. \\
& \left. + \sqrt{6}\beta_1 \phi_1 \phi_0^* + \left(2\beta_1 - \frac{2}{5}\beta_2 \right) \phi_2 \phi_1^* \right] v_{-1} \\
& - [(\beta_0 + 4\beta_1) (\phi_{-2}^*)^2] u_{-2} - \mathcal{L}_5 v_{-2} = \omega v_{-2}, \tag{6.121}
\end{aligned}$$

where:

$$\begin{aligned}\mathcal{L}_1 = & -\frac{1}{2}\nabla^2 + V(\vec{r}) - 2p + 4q + 2(4\beta_1 + \beta_0)n_2 \\ & + (4\beta_1 + \beta_0)n_1 + \beta_0n_0 + (\beta_0 - 2\beta_1)n_{-1} \\ & + \left(\beta_0 - 4\beta_1 + \frac{2}{5}\beta_2\right)n_{-2} - \mu,\end{aligned}\quad (6.122)$$

$$\begin{aligned}\mathcal{L}_2 = & -\frac{1}{2}\nabla^2 + V(\vec{r}) - p + q + (\beta_0 + 4\beta_1)n_2 \\ & + 2(\beta_0 + \beta_1)n_1 + (\beta_0 + 3\beta_1)n_0 \\ & + \left(\beta_0 - \beta_1 + \frac{2}{5}\beta_2\right)n_{-1} + (\beta_0 - 2\beta_1)n_{-2} - \mu,\end{aligned}\quad (6.123)$$

$$\begin{aligned}\mathcal{L}_3 = & -\frac{1}{2}\nabla^2 + V(\vec{r}) + \beta_0n_2 \\ & + (\beta_0 + 3\beta_1)n_1 + \left(2\beta_0 + \frac{2}{5}\beta_2\right)n_0 \\ & + (\beta_0 + 3\beta_1)n_{-1} + \beta_0n_{-2} - \mu,\end{aligned}\quad (6.124)$$

$$\begin{aligned}\mathcal{L}_4 = & -\frac{1}{2}\nabla^2 + V(\vec{r}) + p + q + (\beta_0 - 2\beta_1)n_2 \\ & + \left(\beta_0 - \beta_1 + \frac{2}{5}\beta_2\right)n_1 + (\beta_0 + 3\beta_1)n_0 \\ & + 2(\beta_0 + \beta_1)n_{-1} + (\beta_0 + 4\beta_1)n_{-2} - \mu,\end{aligned}\quad (6.125)$$

$$\begin{aligned}\mathcal{L}_5 = & -\frac{1}{2}\nabla^2 + V(\vec{r}) + 2p + 4q + \left(\beta_0 - 4\beta_1 + \frac{2}{5}\beta_2\right)n_2 \\ & + (\beta_0 - 2\beta_1)n_1 + \beta_0n_0 + (\beta_0 + 4\beta_1)n_{-1} + 2(\beta_0 + 4\beta_1)n_{-2} - \mu.\end{aligned}\quad (6.126)$$

Here, we are again using the notation $n_\nu = |\phi_\nu|^2$ where $\nu = -2, -1, 0, 1, 2$.

The implementation of these equations in code is done in the exact same way as was done for the spin one case, however, now instead of $6L^2$ equations, we will have $10L^2$ equations and as a result the M matrix will have a dimension of $10L^2 \times 10L^2$ where each $L^2 \times L^2$ block is filled in in the same way as was described for the spin one Bogoliubov equations. We will also need an expression for the chemical potential in this case also. We will just list the chemical potential here as the procedure for finding it is the same as in the spin one case, only now using the five time-independent Gross-Pitaevskii equations instead.

$$\mu = \int \left\{ \sum_{m=-2}^2 \left(\frac{1}{2} |\nabla \phi_m|^2 + (V - pm + qm^2) |\phi_m|^2 \right) + \beta_0 n^2 + \beta_1 |\vec{F}|^2 + \beta_2 |A_{00}|^2 \right\} \quad (6.127)$$

Remember that here, $n = \sum_{m=-2}^2 |\phi_m|^2$ and we are using the spin matrices defined in equations (3.95) to (3.97) and equation (3.86) as opposed to the spin one versions.

7 Results

Now that we have reviewed the theory of spinless and spinor Bose-Einstein condensates and the vortices that can be hosted within them; as well as the code we have developed to simulate these systems in the ground state. We will now look at test cases to show the working of this code. We will first start with simulating a vortex in the ferromagnetic phase of a spin one condensate, linking back to what we expect from theory discussed in section (5). Once we have done this, we will analyse our Bogoliubov code for a spin one condensate and show how our code reproduces the excitation spectra of a zero potential system in the ferromagnetic phase. We will then give an example of how these codes can easily be run by a user. After this, we will consider the same codes for a spin two condensate; first showing how we can hold vortices in our systems and maintain the long range behaviour. We will analyse our Bogoliubov code and show how our codes reproduce the excitation spectra of a zero potential system in the cyclic and biaxial-nematic phases. After, we will look at Bogoliubov excitations with the vortices in both the cyclic and biaxial-nematic phase as background.

7.1 Spin One Vortex Simulation

Recall in section (5), we looked at an example in the ferromagnetic phase of a spin one condensate where we saw that a vortex with an even winding in the phase of the wavefunction was unstable and decayed to a uniform configuration with no vortex. We also saw that an odd winding vortex of winding greater than one decayed into the singly quantized vortex, that is, a vortex of winding one in the complex phase of the wavefunction. In this section, we will demonstrate these results using our spin one ground state code, thus giving a nice test case to demonstrate our code working correctly.

Before we look at this, we first need to consider the different length scales of importance for this system. These length scales will determine how we set certain parameters for our code. The discussion here also holds for a spin two condensate and so will also be important for the sections to come as well as this one.

The system we will look at is a condensate in a harmonic potential. We have seen earlier that our code is setup for a two dimensional condensate. In section (6.1.1), we obtained a dimensionless form of the Gross-Pitaevskii equations for a condensate in a harmonic potential in three-dimensions. In particular we obtained a dimensionless form for the interaction parameters of the system which we include here again for convenience:

$$\beta_m = \frac{c_m N}{\omega r_s^3 \hbar}. \quad (7.1)$$

Here, c_m is the physical interaction parameter; N is the number of particles in the system; ω is the harmonic trap frequency, r_s is the characteristic length of the harmonic trap which has been defined in section (6.1.1) and \hbar is the reduced Planck constant.

It is these dimensionless interaction parameters that we would like to know how to set for the system we are looking at. One of the main governing factors of how we set these will be the healing length of the condensate. As mentioned earlier, the healing length, ξ , describes the length scale over which the condensate varies and as a result we would like it to be a reasonable size in terms of both lattice spacings in our grid and the characteristic length of our harmonic potential.

To understand how the healing length relates to these other length scales, let's first remind ourselves of the healing length:

$$\xi_m = \frac{\hbar}{\sqrt{2Mc_m n}} \quad (7.2)$$

Here, we have written the healing length in a slightly different way to before. We are now writing the healing lengths in terms of the interaction parameters c_m , instead of U_0 in the spinless case. This means that we now have different healing lengths for the different interactions in the system.

We can determine what the healing length is in terms of the dimensionless interaction parameters β_m by rearranging equation (7.1) for c_m and then substituting this into (7.2):

$$\xi_m = \frac{\hbar}{\sqrt{2M \left(\frac{\beta \omega r_s^3 \hbar}{N} \right) n}}. \quad (7.3)$$

To continue we need an expression for the particle density n . If we assume that the particles are all contained in the harmonic trap, then we can take the volume of the system to be approximately r_s^3 . Note that this is for three-dimensions, we will consider our two dimensional case soon. This means that we get an expression for the particle density as $n = N/r_s^3$. Substituting this into (7.3), we get:

$$\xi_m = \frac{\hbar}{\sqrt{2M\beta\omega\hbar}} \quad (7.4)$$

With this expression we can now determine how the healing length relates to the characteristic length scale of the harmonic oscillator, r_s :

$$\begin{aligned} \frac{\xi}{r_s} &= \sqrt{\frac{M\omega}{\hbar}} \frac{\hbar}{\sqrt{2M\beta\omega\hbar}} \\ &= \frac{1}{\sqrt{2\beta}} \end{aligned} \quad (7.5)$$

As mentioned, this expression is for a three-dimensional system. However, this expression will also hold for a two dimensional system where we restrict excitations in the z-direction by increasing the trap frequency in that direction as discussed in [37]. We will not do the dimension reduction here but have a similar procedure described for a system on a torus in

section (6.1.1).

When the dimension reduction and scaling to dimensionless variables occurs for this system, we get the following for the dimensionless interaction parameter:

$$\beta_m = \frac{c_m N}{\omega r_s^2 r_z \hbar}. \quad (7.6)$$

Here, r_z is the characteristic length of the harmonic trap in the z-direction which we can think of as being thin as one way of understanding how the system is effectively two dimensional now. If we now substitute this into the healing length expression (7.2) but with the particle density now as $n = \frac{N}{r_s^2 r_z}$, we will get the same expression for the healing length as compared to the characteristic length of the trap now in two dimensions.

The last length scale we need to account for is the lattice spacing length, h of our finite grid. For our purposes, this length is controlled by the number of lattice spacings, L , we can take in one direction of the two-dimensional grid. In order for our code to run in a reasonable time, we find that the maximum value we can take for this is $L = 100$. This number could be possibly increased if running on better hardware or if the user is willing to wait longer for improved accuracy.

We will make a rough estimate relating the healing length to the characteristic length of the trap in the following way. We expect the width of the trap to be roughly of length r_s in the non-interacting system. Therefore we will take our grid to look at eight units of r_s across which means that the boundaries of our lattice are $a = -4$ and $b = 4$. This means that there is about twelve lattice spacings per characteristic length r_s . Since we have a relation between the characteristic length and the healing length by setting the dimensionless interaction parameter β_m given by (7.5), we can set each β_m in such a way that the healing length is smaller than the characteristic length of the trap, r_s but still has enough lattice spacings per healing length to model the system appropriately.

For our spin one system in the ferromagnetic phase, we will take the following parameters of β_0 and β_1 to achieve this:

$$\begin{aligned} \beta_0 &= 10, \\ \beta_1 &= -4. \end{aligned} \quad (7.7)$$

With these parameters we get healing lengths of $\xi_0 \approx 2.8$ and $\xi_1 \approx 4.42$ in terms of the number of lattice spacings they take up.

We can now use these parameters in our code to setup an even and odd winding vortex as an initial condition in the ferromagnetic phase of the spin one condensate and demonstrate their stability within our code. First, let's think about how to set up this initial condition. Our starting point will be to set the spin components in accordance to the general order parameter for a spin one ferromagnetic condensate given by (5.19). This is a good base for

our initial condition, however, it will not suffice by itself as we need to model our initial condition to be a good approximation to the ground state in the regime we are looking at in order for our code to walk down to the ground state in the current regime. To do this, we should smooth the wavefunction of each component with a gaussian function which will bring the wavefunction to zero at the boundary (in line with the zero boundary conditions used here). This gaussian also approximates the ground state of a particle in an isotropic harmonic oscillator well so should make it easier for our code to converge to the correct state. Finally, we would like to keep a vortex in the system if it is stable. To do this, we need to use a pinning potential in the centre of the trap as used in [21]. For our purposes, we will just add a large value to the potential if we are within a specified radius of the centre of the trap. To account for this in the initial condition, we need to ensure that the function goes to zero at the centre of the trap. We are doing this, to account for the pinning potential which should keep the density at zero in the centre. It is worth noting that as we have seen, not all vortices in spinor condensates have zero density at their core, however, this will be our first approach for implementing a vortex in these systems. From this, we should be able to see the winding of the vortex far from the core. After, we will look at how we can inspect the core of a vortex. Taking all of this into consideration, we get the following initial condition for vortices in the ferromagnetic phase:

$$\phi_{1,init} = r^5 e^{-\frac{r^2}{\sigma^2}} e^{i(\phi' - \alpha)} \cos \frac{\beta^2}{2} \quad (7.8)$$

$$\phi_{0,init} = \frac{r^5}{\sqrt{2}} e^{-\frac{r^2}{\sigma^2}} \sin \beta \quad (7.9)$$

$$\phi_{-1,init} = r^5 e^{-\frac{r^2}{\sigma^2}} e^{i(\phi' + \alpha)} \sin \frac{\beta^2}{2}, \quad (7.10)$$

where $\phi' = n_w \varphi$, $\alpha = -n_w \varphi$ for an even winding vortex and $\phi' = (n_w + 1)\varphi$, $\alpha = -n_w \varphi$ for an odd winding vortex with φ being the polar angle and $n_w \in \mathbb{Z}$. We can control the width of the gaussian initial condition by setting σ to an appropriate value. We will set β to $\pi/64$. This means that at the start, most of the particles should be in the $m = 1$ component of the condensate and so we can set the initial winding of the vortex within this component using ϕ' and α .

We will first look at an even winding vortex. To do this we will set ϕ' and α as specified above for an even winding vortex and we will set $n_w = 1$. This means that we will have set an initial winding of two in the phase of the $m = 1$ component. We include the non-zero density and phase plots for the initial condition. Here the non-zero densities occur in the $m = 1$ and $m = 0$ components. We can ignore the phase on the $m = -1$ component as there are no particles present there in the initial condition. The phase of the $m = 0$ component is zero in the initial condition. As a result, we only present the density of the $m = 1$ and $m = 0$ components, along with the phase of the $m = 1$ component in figures (24), (25) and

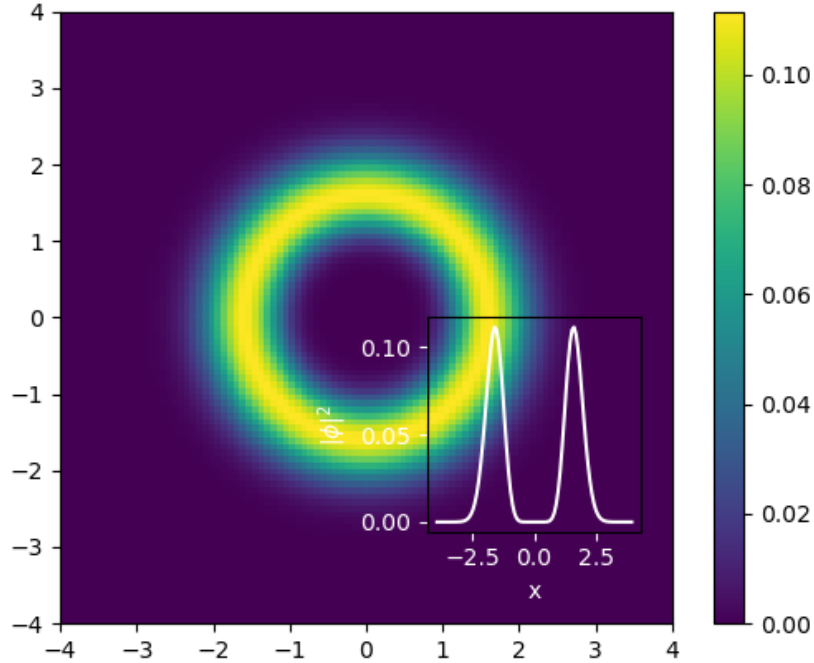


Figure 24: Initial density of the $m = 1$ component with a spin two vortex as the initial condition. Inset figure shows a cross section at $y = 0$.

(26).

Although we can see that the phase of the condensate has a winding value of two in figure (26), it is really the winding at some distance from the core that we are interested in. As a result, we also include a plot of the spherical harmonic representation of the condensate around a loop of radius $1.8r_s$ where r_s is the characteristic trap length that we have chosen to scale by earlier. This is shown in figure (27).

When we pass this into our spin one ground state code, it works to converge to a local minimum. We show the final densities of each component in figures (28), (29) and (30), and the spherical harmonic representation of the final state around a loop of radius $1.8r_s$ in figure (31).

We see that the vortex of even winding has disappeared from our code. This agrees with the theory discussed in section (5) where we saw that a vortex of even winding is unstable and decays to the uniform state in the spin one ferromagnetic phase.

We can do the same analysis again for an odd winding vortex. Here we take a vortex of winding one and show that our spin one gradient descent code finds a local minimum where we keep this winding in the system. We change ϕ' accordingly in the initial condition

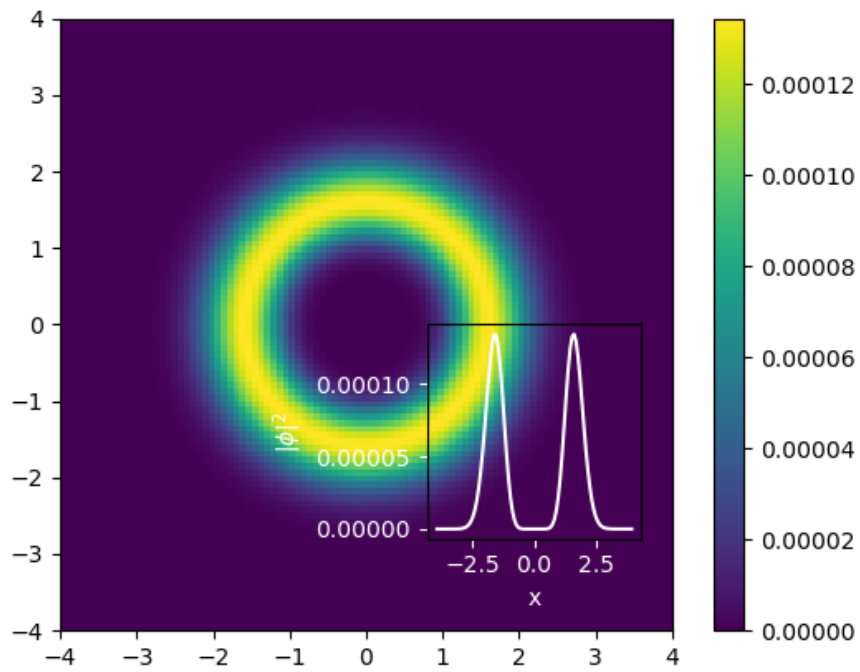


Figure 25: Initial density of the $m = 0$ component with a spin two vortex as the initial condition. Inset figure shows a cross section at $y = 0$.

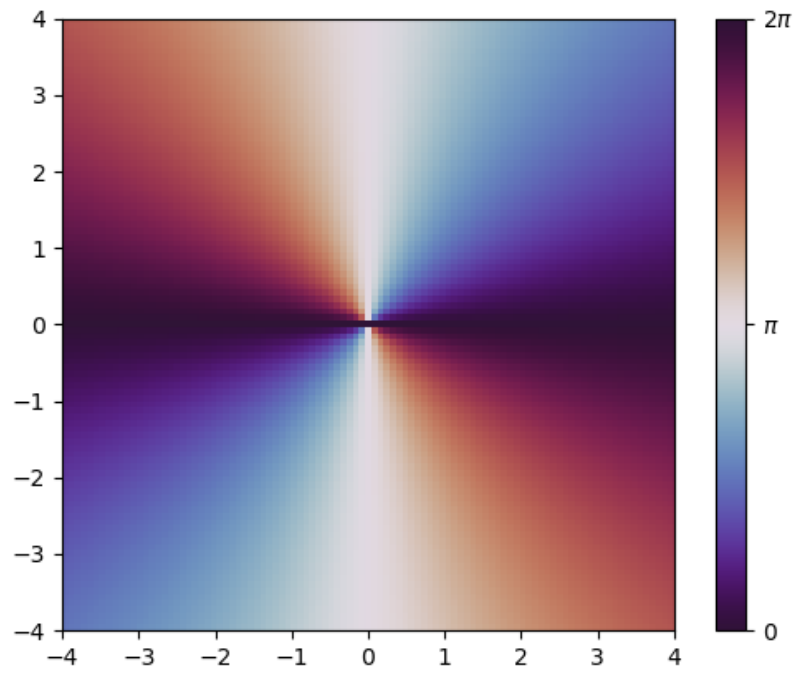


Figure 26: Initial phase of the $m = 1$ component with a spin two vortex as the initial condition.

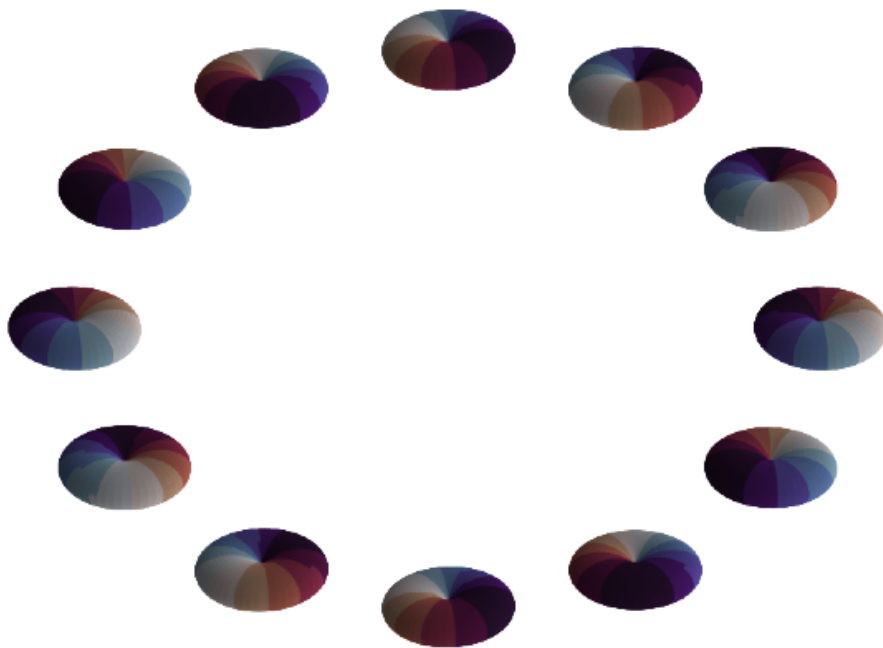


Figure 27: Spherical harmonic representation of the condensate around a loop of radius $1.8r_s$. These spherical harmonic plots characterise the ferromagnetic phase. We can see that a winding value of two is occurring. The colour scale characterising the phase of the condensate is the same as that in figure (26).

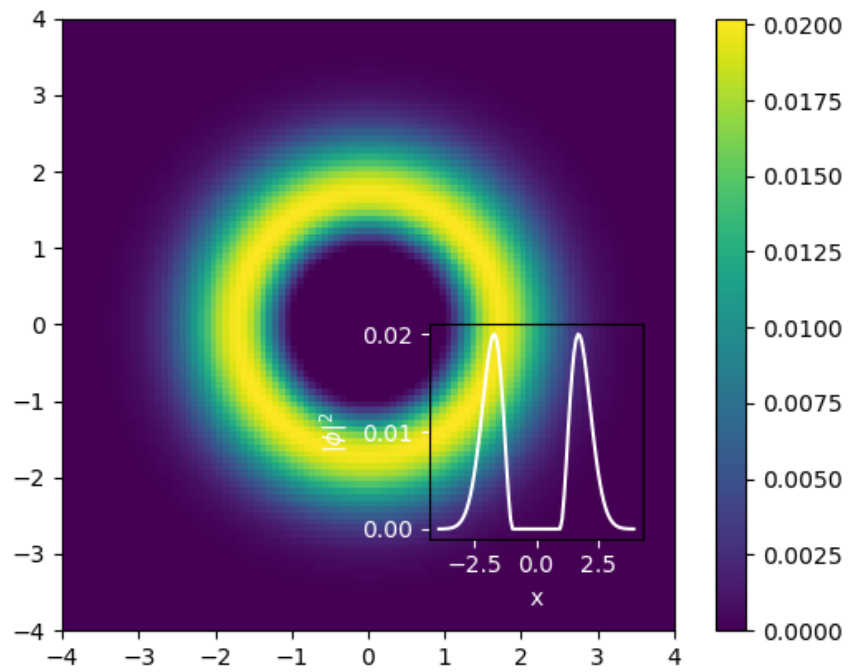


Figure 28: Final density of the $m = 1$ component with a spin two vortex as the initial condition. Inset figure shows a cross section at $y = 0$.

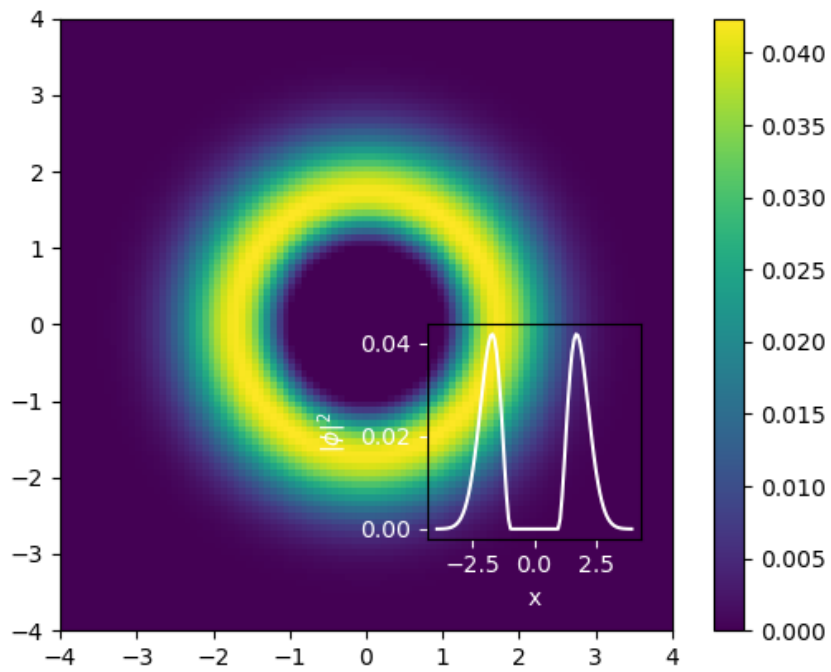


Figure 29: Final density of the $m = 0$ component with a spin two vortex as the initial condition. Inset figure shows a cross section at $y = 0$.

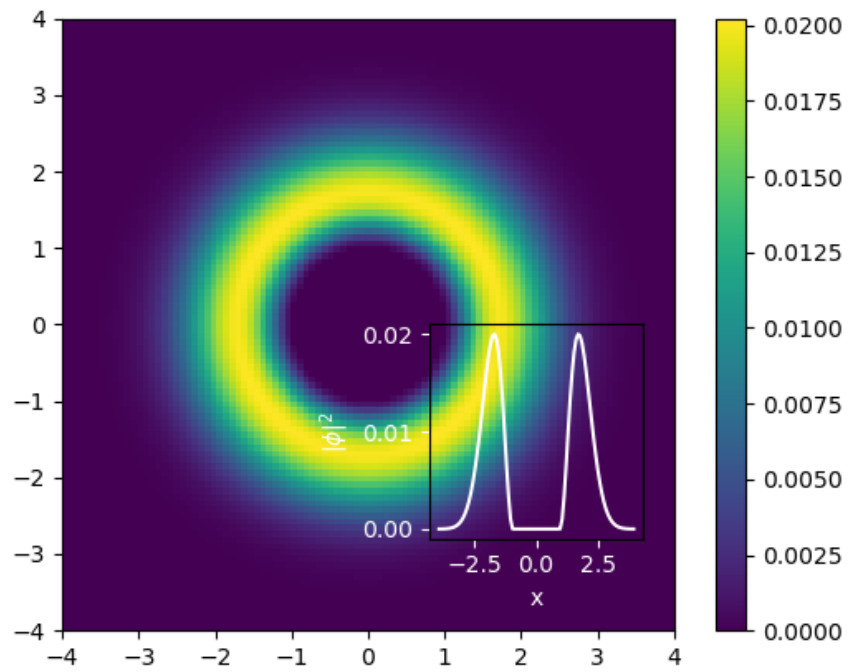


Figure 30: Final density of the $m = -1$ component with a spin two vortex as the initial condition. Inset figure shows a cross section at $y = 0$.

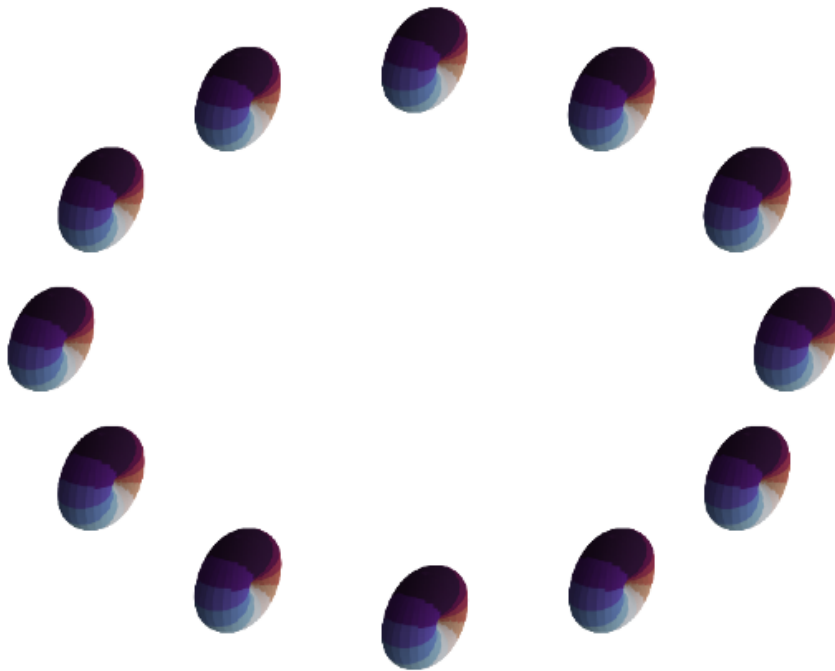


Figure 31: Spherical harmonic representation for the final state of the condensate with an initial winding of 2. These are taken around a loop of radius $1.8r_s$. These spherical harmonic plots characterise the ferromagnetic phase, however, we can see that there is no longer a winding present away from the core. The colour scale characterising the phase of the condensate is the same as that in figure (26).

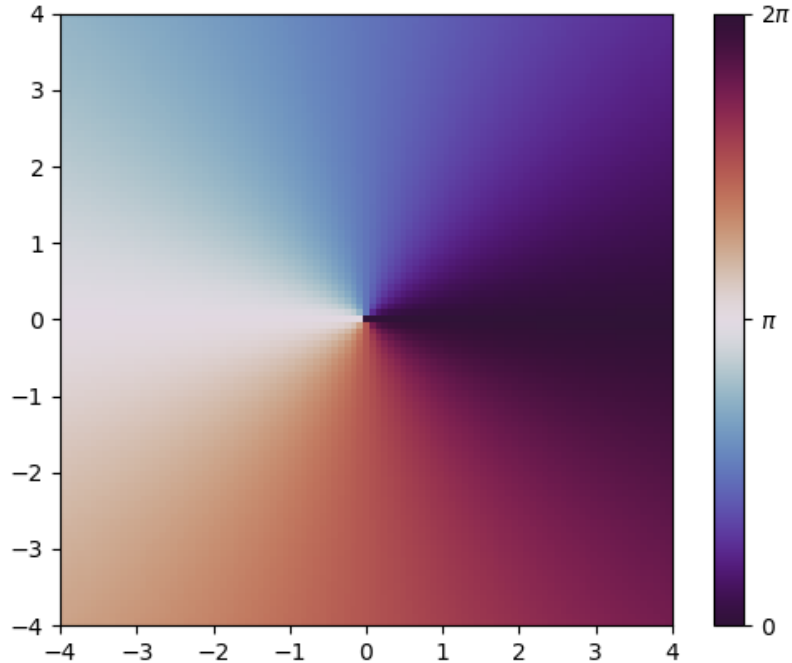


Figure 32: Initial phase of the $m = 1$ component with a spin one vortex as the initial condition.

and set $n_w = 0$ in order to obtain a winding of one in the initial condition of the $m = 1$ component. The initial density profiles are the same as those shown in figures (24) and (25), however the winding of the phase here is now set to one which can be seen in the phase of the $m = 1$ component of the condensate shown in figure (32).

When we pass this into the ground state code for a spin one condensate, we get densities for the $m = 1$ and $m = 0$ components of the converged state shown in figures (33) and (34). The density of the $m = -1$ component of the converged state remains zero.

We have also included the spherical harmonic representation of the final converged state around a loop of radius $1.8r_s$ to demonstrate that we have managed to keep this vortex in the system. This is shown in figure (35).

Finally, we saw that the vortex of winding one in the ferromagnetic phase is meant to have a polar core. Currently we will not see that in our code as the pinning potential we are using causes the density at the core of the vortex to go to zero. However, we can pass the final state of the system with a winding one vortex as the initial condition of the gradient descent code with the pinning potential turned off to see if a polar core appears. We will check this after a small number of gradient descent steps compared to the total number of

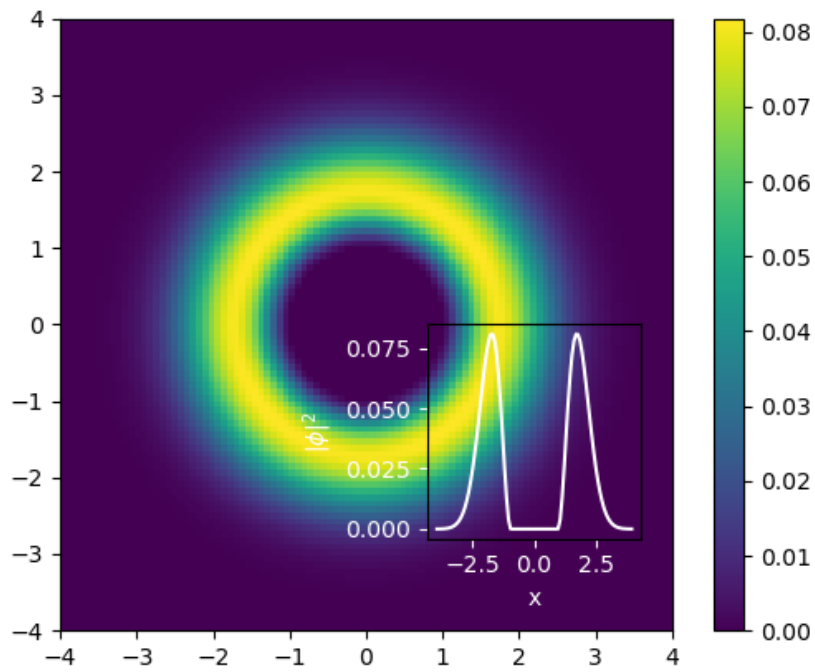


Figure 33: Final density of the $m = 1$ component with a spin one vortex as the initial condition. Inset figure shows a cross section at $y = 0$.

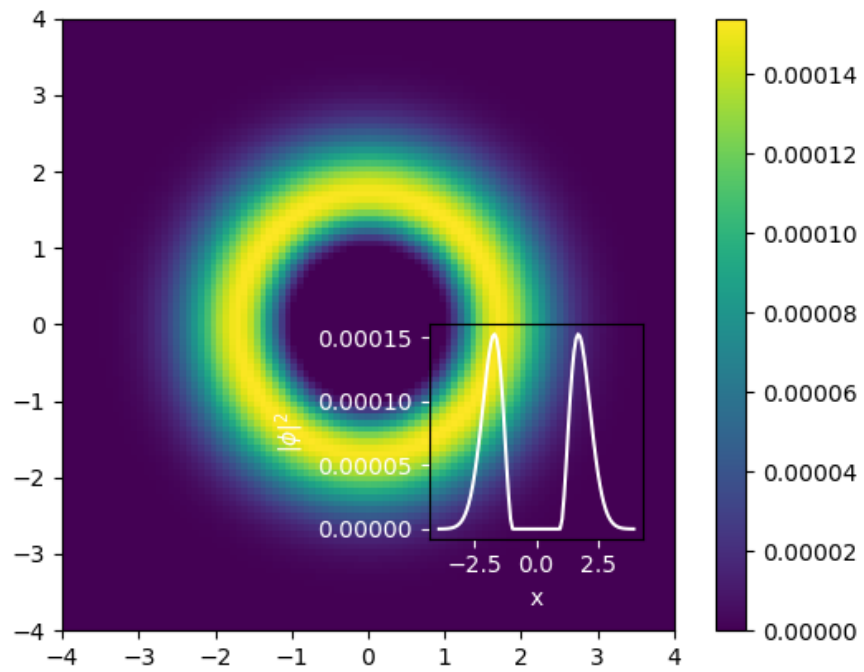


Figure 34: Final density of the $m = 0$ component with a spin one vortex as the initial condition. Inset figure shows a cross section at $y = 0$.

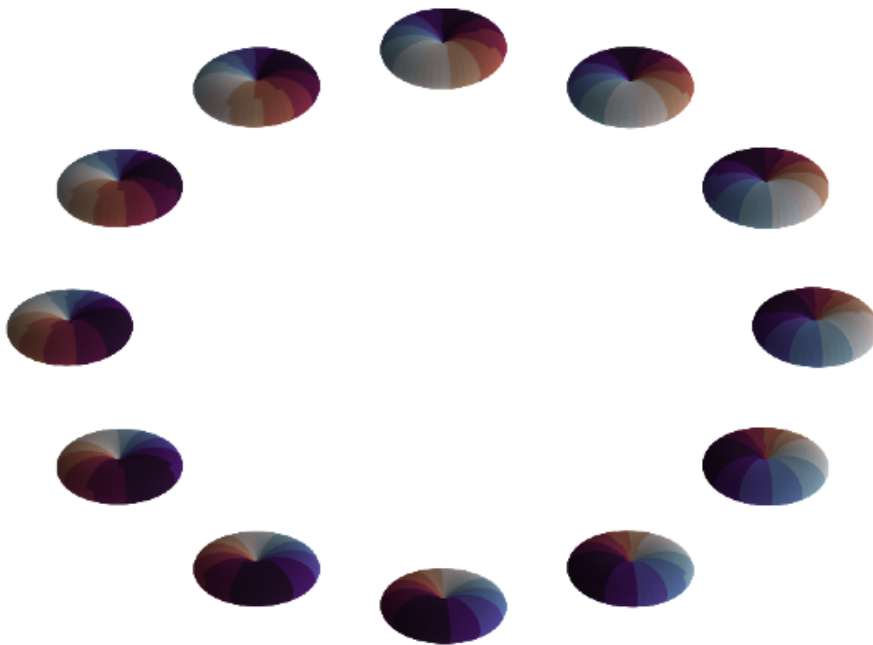


Figure 35: Spherical harmonic representation for the final state of the condensate with an initial winding of 1. These are taken around a loop of radius $1.8r_s$. These spherical harmonic plots characterise the ferromagnetic phase. We can clearly see that a winding of one is still present here. The colour scale characterising the phase of the condensate is the same as that in figure (26).

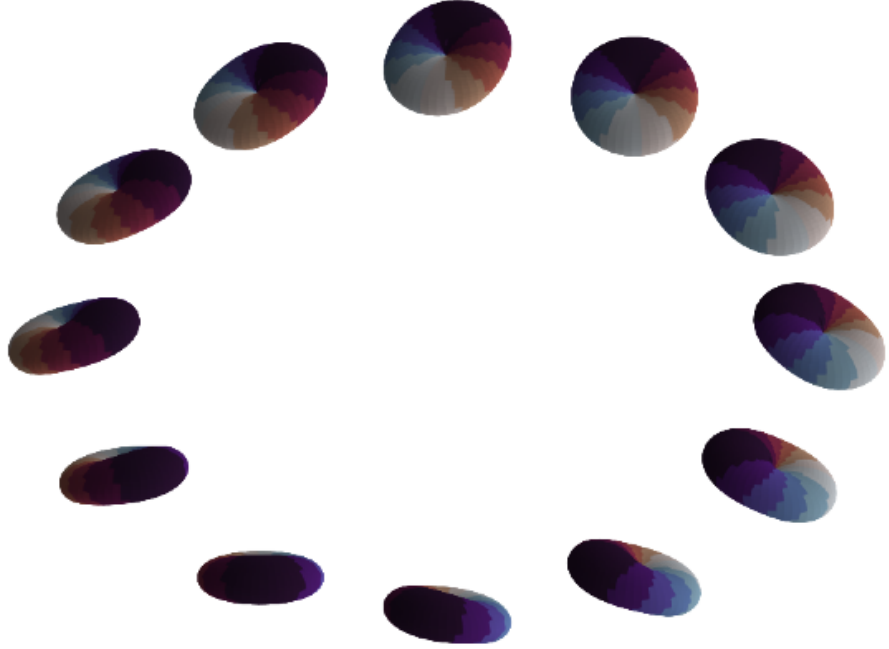


Figure 36: Spherical harmonic representation for the state of the condensate 75 gradient descent steps after lifting the pinning on a winding one vortex. These are taken around a loop of radius $1.8r_s$. These spherical harmonic plots characterise the ferromagnetic phase. We can clearly see that a winding of one is still present here, although it is certainly less stable. The colour scale characterising the phase of the condensate is the same as that in figure (26).

steps taken as the code may work to get rid of this polar core to further minimize the energy over a longer period of steps.

If we look at the frames from this run after 75 gradient descent steps, we get the situation shown using spherical harmonic plots in figures (36) and (37) for a loop at radius $1.8r_s$ from the core and a loop at radius $0.1r_s$ from the core respectively. The densities of each component are also shown in figures (38) to (40).

We can see from all of these plots that the particles at the core of the condensate are in a polar phase, and those further from the core are still in the ferromagnetic phase. We can see that the winding of the vortex far from the core is still present, although it is less stable than before the pinning was lifted. This polar core with ferromagnetic winding is the predicted feature of this vortex as discussed in section (5) and so our results agree with theory.

If we look at the converged state of the condensate after lifting the pinning potential with

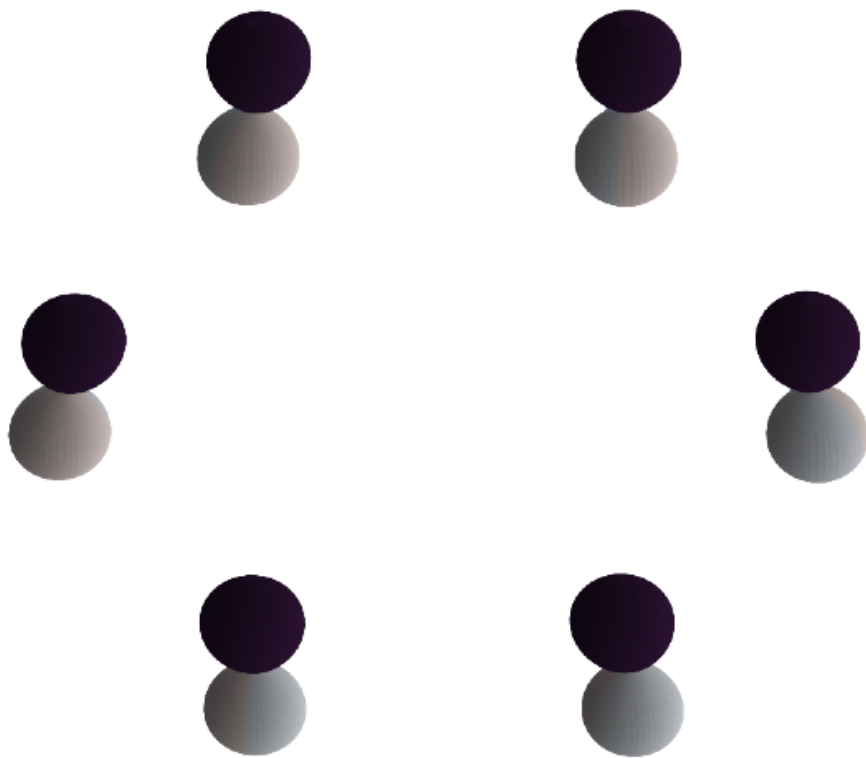


Figure 37: Spherical harmonic representation for the state of the condensate 75 gradient descent steps after lifting the pinning on a winding one vortex. These are taken around a loop of radius $0.1r_s$. These spherical harmonic plots characterise the polar phase. The colour scale characterising the phase of the condensate is the same as that in figure (26).

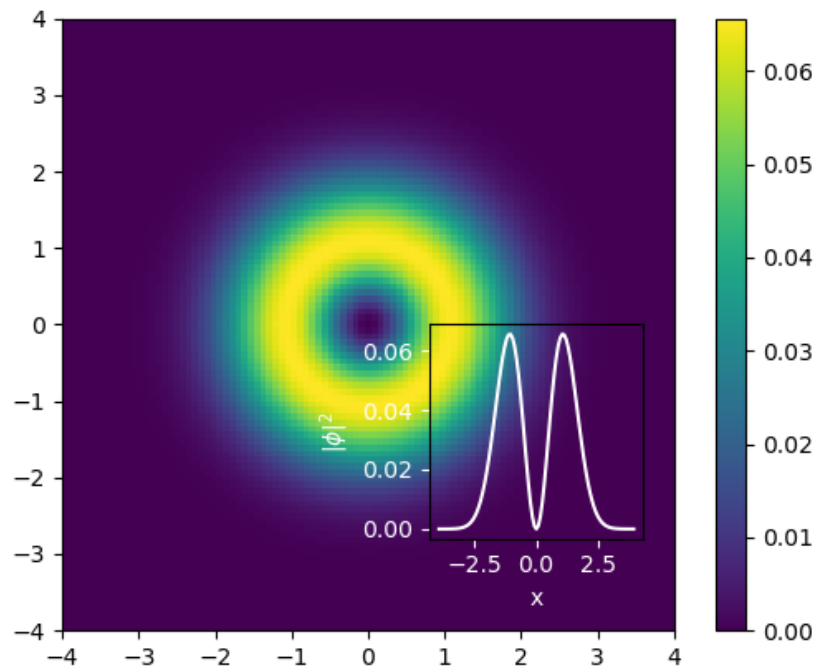


Figure 38: Density of the $m = 1$ component 75 gradient descent steps after lifting the pinning on a winding one vortex. Inset figure shows a cross section at $y = 0$.

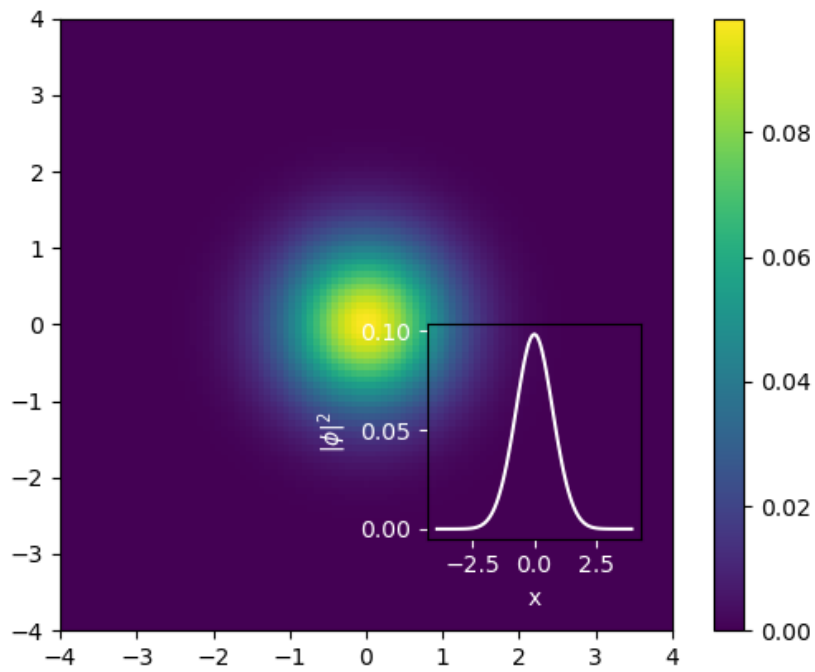


Figure 39: Density of the $m = 0$ component 75 gradient descent steps after lifting the pinning on a winding one vortex. Inset figure shows a cross section at $y = 0$.

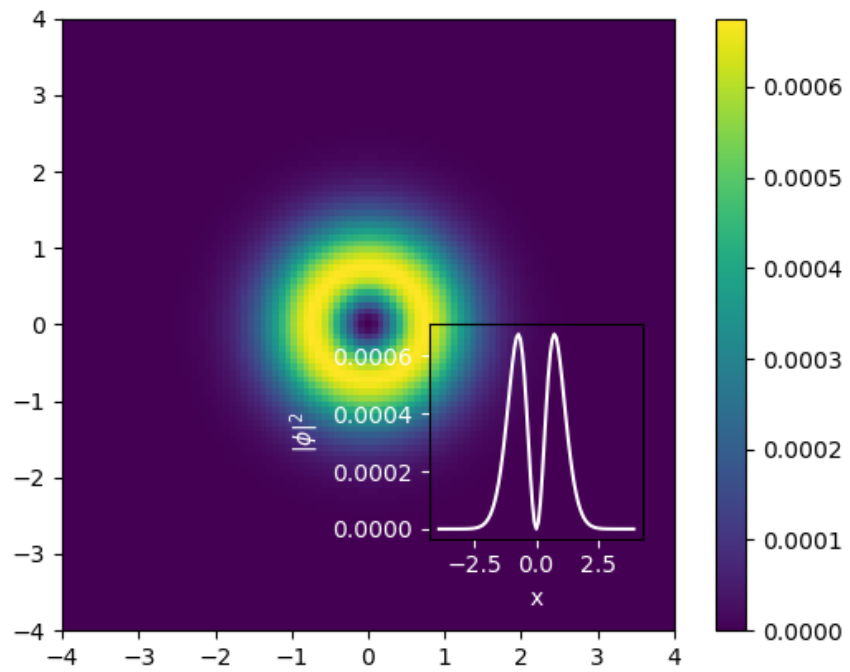


Figure 40: Density of the $m = -1$ component 75 gradient descent steps after lifting the pinning on a winding one vortex. Inset figure shows a cross section at $y = 0$.

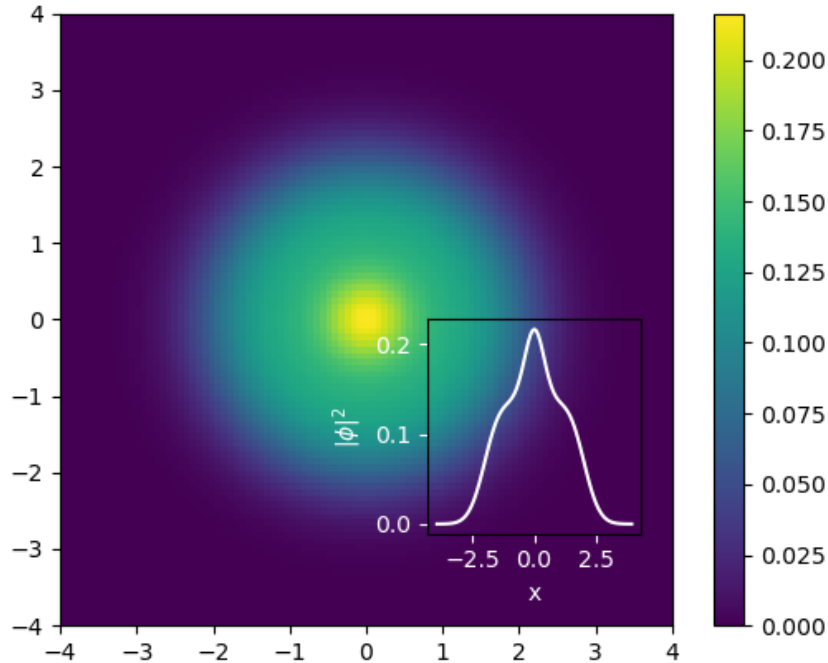


Figure 41: Energy density of the condensate 75 gradient descent steps after lifting the pinning on a winding one vortex. We can see from the peak in the center of the condensate that there is extra energy here which is due to the presence of a vortex.

a winding one vortex present, we end up back in the ferromagnetic state and the vortex has been lost from the system. We can look at snapshots of the energy density of the condensate after 75 gradient descent steps and at the final state as another indication of the presence of a vortex that then moves out of our system once our code has converged. These are shown in figures (41) and (42) respectively.

7.2 Spin One Bogoliubov Spectrum

Earlier, we showed the derivation of the spin one Bogoliubov equations along with a description of how our code solves these equations to give us the excitations of the ground state along with the eigenfrequencies corresponding to these. Here, we will look at this spectrum of frequencies for the ferromagnetic phase of a spin one condensate and show that our code is giving expected results.

First we need to derive what this spectrum is for the ferromagnetic phase. To do this we will first restrict the spin one Bogoliubov equations, given by equations (6.96) to (6.101) to the ferromagnetic phase. This means taking $\eta = (1, 0, 0)$ as the normalized spinor for the

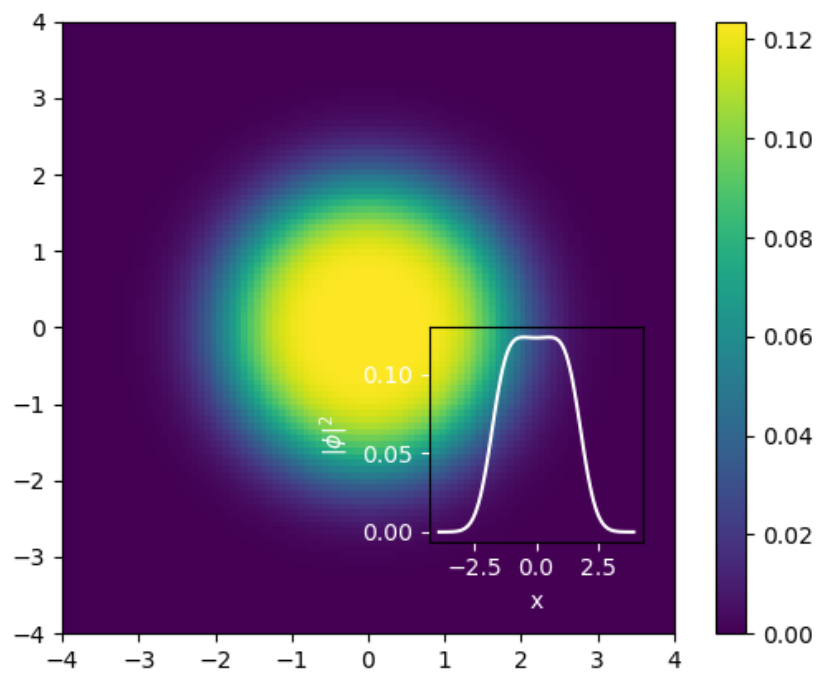


Figure 42: Energy density of the converged state of the condensate after lifting the pinning on a winding one vortex. We can see that the energy has smoothed out which is evidence that we have lost the vortex from our system.

ferromagnetic phase, where $\phi = \sqrt{n}\zeta$ and n is the particle density, and subbing this ϕ into the spin one Bogoliubov equations. When we do this, we get the following:

$$\mathcal{L}_1 u_1 + (\beta_0 + \beta_1) n v_1 = \omega u_1, \quad (7.11)$$

$$-(\beta_0 + \beta_1) n u_1 - \mathcal{L}_1 v_1 = \omega v_1, \quad (7.12)$$

$$\mathcal{L}_2 u_0 = \omega u_0, \quad (7.13)$$

$$-\mathcal{L}_2 v_0 = \omega v_0, \quad (7.14)$$

$$\mathcal{L}_3 u_{-1} = \omega u_{-1}, \quad (7.15)$$

$$-\mathcal{L}_3 v_{-1} = \omega v_{-1}, \quad (7.16)$$

where:

$$\mathcal{L}_1 = -\frac{1}{2}\nabla^2 + q - p + 2(\beta_0 + \beta_1)n - \mu, \quad (7.17)$$

$$\mathcal{L}_2 = -\frac{1}{2}\nabla^2 + (\beta_0 + \beta_1)n - \mu \quad (7.18)$$

$$\mathcal{L}_3 = -\frac{1}{2}\nabla^2 + q + p + (\beta_0 - \beta_1)n - \mu. \quad (7.19)$$

For $\phi = \sqrt{n}(1, 0, 0)^T$ which is the case here, the chemical potential given by (6.106) becomes:

$$\begin{aligned} \mu &= \int \left\{ (\beta_0 + \beta_1) |\phi_1|^4 + (q - p) |\phi_1|^2 \right\} dx dy \\ &= \int \left\{ (\beta_0 + \beta_1) n^2 + (q - p) n \right\} dx dy \\ &= (\beta_0 - \beta_1) n^2 (b - a)^2 + (q - p) n (b - a)^2 \\ &= (\beta_0 + \beta_1) n + q - p, \end{aligned} \quad (7.20)$$

where we have used that in this case, the particle density is $n = 1/(b - a)^2$ where we integrated over both directions of our lattice which has side length $(b - a)$.

Looking at equations (7.11) to (7.16), we notice that they now decouple into equations that are easier to solve. More specifically, we can determine the eigenfrequencies ω corresponding to different eigenmodes.

The first of these spectra is obtained by simultaneously solving equations (7.11) and (7.12) which in matrix form is:

$$\begin{pmatrix} \hat{\mathcal{L}}_1 & (\beta_0 + \beta_1)n \\ -(\beta_0 + \beta_1)n & -\hat{\mathcal{L}}_1 \end{pmatrix} \begin{pmatrix} \hat{u}_1 \\ \hat{v}_1 \end{pmatrix} = \omega \begin{pmatrix} \hat{u}_1 \\ \hat{v}_1 \end{pmatrix}. \quad (7.21)$$

Note that we have Fourier transformed the equations in order to describe the spectrum in

momentum space. We will look at what form $\hat{\mathcal{L}}_1$ takes in a moment.

The spectrum, ω for this set of equations is:

$$\omega = \sqrt{\hat{\mathcal{L}}_1^2 - (\beta_0 + \beta_1)^2 n^2} \quad (7.22)$$

To expand this out, we need to inspect the form of $\hat{\mathcal{L}}_1$. The only term in \mathcal{L}_1 given by (7.17) that gets modified by the Fourier transform is the derivative term $-\frac{1}{2}\nabla^2$. This term will go to ϵ_k where:

$$\epsilon_k = \frac{1}{2} \left(\frac{2\pi k_x}{(b-a)} \right)^2 + \frac{1}{2} \left(\frac{2\pi k_y}{(b-a)} \right)^2. \quad (7.23)$$

We get momentum in both directions due to our system being in two-dimensions. k_x and k_y can take on any integer value including negative values and so we see we can get modes that are degenerate with different combinations of k_x and k_y .

We can now expand out $\hat{\mathcal{L}}_1$ in equation (7.22) in order to get an expression for the first spectrum of eigenfrequencies.

$$\begin{aligned} \omega &= \sqrt{(\epsilon_k + q - p + 2(\beta_0 + \beta_1)n - \mu)^2 - (\beta_0 + \beta_1)^2 n^2} \\ &= \sqrt{(\epsilon_k + (\beta_0 + \beta_1)n)^2 - (\beta_0 + \beta_1)^2 n^2} \\ &= \sqrt{\epsilon_k(\epsilon_k + 2(\beta_0 + \beta_1)n)}. \end{aligned} \quad (7.24)$$

This gives us an expression for the first set of eigenfrequencies that can be obtained in the ferromagnetic phase of a spin one condensate. To obtain the others, we use equations (7.13) to (7.16). Note that within these four equations, (7.13) and (7.14) will give the same magnitude for ω but with the opposite sign. This is the same scenario for equations (7.15) and (7.16). As a result, we will just give the spectra obtained from equations (7.13) and (7.15) here.

$$\omega = \epsilon_k + p - q, \quad (7.25)$$

$$\omega = \epsilon_k + 2p - 2\beta_1 n. \quad (7.26)$$

We can now check our spin one Bogoliubov code to see if it reproduces these spectra.

We have run our Bogoliubov code with periodic boundary conditions in zero potential in order to match the spectra listed above. Here we have chosen to keep β_0 fixed at 9 and are varying β_1 between -9 and -1 in order to stay within the ferromagnetic phase.

We can produce a scatter plot of the lowest momentum eigenvalues produced by our code and plot the expected spectra on top of these. This is shown in figure (43) where it can be seen that our results from the code match with the expected results.

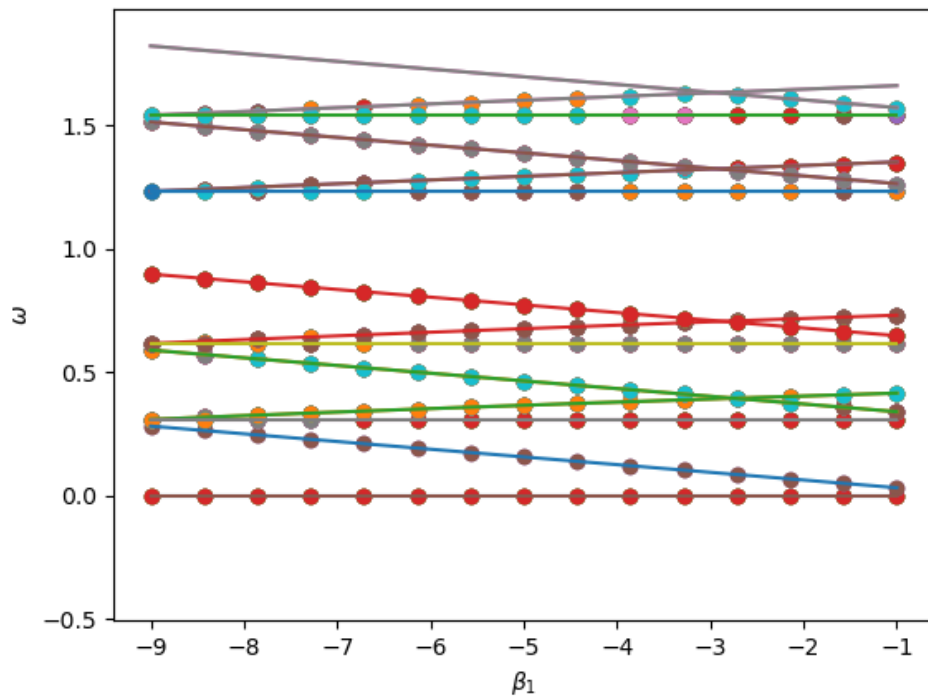


Figure 43: Scatter plot of the low lying eigenvalues for the ferromagnetic phase of a spin one condensate in zero potential. Exact results are plotted as lines on top. We see that these match.

```

Please choose an input file (options: ferromagnetic, polar, override, custom)
Note that we are only providing vortices in the ferromagnetic phase currently
|ferromagnetic

Please choose an initial condition (options: generic, vortex, contd)
vortex

Please choose a winding for the vortex
1

Please choose a value of sigma for the width of the Gaussian
1.0

Do you want to run this order parameter through the ground state code? (y or n)
y

Please select what run you are performing to append onto the end of your saved files
1

```

Figure 44: Example run of `interactiveRunGroundState.py` for a winding one vortex in a spin one condensate.

7.3 Running the spin one codes

We will now give a brief example of how the likes of the results shown in the previous two sections can be generated using our spin one codes. Recall that a detailed list of all code files contained within the spin one suite of codes can be found in section (6.1.5). Here, we will look at two files that have been set up to call these background files for the user by asking a series of questions about the type of run the user would like to perform as well as the parameters for this run. These two files are called **`interactiveRunGroundState.py`** and **`interactiveRunBogoliubov.py`**. First, let's look at an example run of **`interactiveRunGroundState.py`** and how it works.

When the user starts this code, they will be asked a series of questions that help set up the run they would like to perform. An example of this is shown for a winding one vortex in figure (44).

When this run finishes, the code will package all accepted steps of the gradient descent for each condensate component, along with a copy of the input file and text file containing the user's input to the code into a folder named `run[runNumber]` where `runNumber` is the number the user chose to identify this run.

This code file can also be used to load in a vortex state with the pinning potential turned off. An example of doing such a run for the winding one vortex saved in the folder **`run1`** is shown in figure (46).

When the file is run in this way, the data is saved in the same folder with the run number specified appended to the end of the files. As a result, ensure that the run number chosen is not one already existing in this folder or results will be overwritten. A user inputs file is

↑ ← masters > finalCode > spinOne > run1
↕ ↻ 🔍 Search run1

Name	Date modified	Type	Size
 phiMinusOne1	28/08/2022 13:00	File	17,004 KB
 phiOne1	28/08/2022 13:00	File	17,004 KB
 phiZero1	28/08/2022 13:00	File	16,927 KB
 spinOneInputFM	28/08/2022 12:58	Configuration sett...	1 KB
 userInputs1	28/08/2022 17:32	Text Document	1 KB

Figure 45: Output of code is packaged in a folder for the user.

```

Please choose an input file (options: ferromagnetic, polar, override, custom)
Note that we are only providing vortices in the ferromagnetic phase currently
custom

Please specify the folder you wish to load from (including / at the end)
run1/

Please type the exact name of the input file (including extension)
spinOneInputFM.ini

Please choose an initial condition (options: generic, vortex, contd)
contd

Please provide the number of run that you want to load in
1

Does this run have a pinning (if this run was run as a vortex and is
not being passed into ground state again, answer yes) y or n
n

Do you want to run this order parameter through the ground state code? (y or n)
y

Please select what run you are performing to append onto the end of your saved files
2

```

Figure 46: Example run of interactiveRunGroundState.py to load in a vortex and run through the gradient descent code with the pinning potential turned off.

Name	Date modified	Type	Size
phiMinusOne1	28/08/2022 13:00	File	17,004 KB
phiMinusOne2	31/08/2022 21:38	File	194,084 KB
phiOne1	28/08/2022 13:00	File	17,004 KB
phiOne2	31/08/2022 21:38	File	194,084 KB
phiZero1	28/08/2022 13:00	File	16,927 KB
phiZero2	31/08/2022 21:38	File	194,084 KB
spinOneInputFM	28/08/2022 12:58	Configuration sett...	1 KB
userInputs1	28/08/2022 17:32	Text Document	1 KB
userInputs2	31/08/2022 21:26	Text Document	1 KB

Figure 47: Output of continued run is packaged in the same folder as the input to this run.

again created for this run and saved in the same folder as the generated data. This can be seen in figure (47).

Note that it can easily be seen that **interactiveRunGroundState.py** can be used to load in a previous run to look at further by just answering no to running the ground state code again. From here, all relevant parameters for the relevant run will be loaded into the interactive python console and the user can use **groundStateTools.py** to further inspect the system loaded in.

In the same way that is shown above, we can wrap the Bogoliubov code in a helper file to run. This file is called **interactiveRunBogoliubov.py**. Here we will show some sample runs of this file to serve as instructions on usage. The first use for this file is to run a fresh Bogoliubov run with constant background in either the ferromagnetic or polar phase. Here, we show doing this for the ferromagnetic phase in figure (48) along with the saved files packaged in a folder in figure (49).

We can also load in eigenvalues and eigenvectors to inspect further using this code. An example of loading in the data generated in the previous example is shown in figure (50).

Finally, we can take an initial condition to be something other than constant background, for example we might take the vortex with pinning from earlier on which was saved in **run1**. The output for this run is shown in figure (51).

After running the code for a continued configuration, the data from the Bogoliubov code will be saved in the same folder as the input, along with a file detailing the users inputs to the code as shown in figure (52).

7.4 Spin Two Vortex Simulation

We now turn to showing how, with an appropriate choice of initial conditions, we can simulate a vortex in a spin two condensate with our ground state code. The converged state still contains the vortex we choose to simulate and as a result we can pass this as

```

Do you wish to load eigenvectors or run Bogoliubov? (load or run)
run

Please choose an input file (options: ferromagnetic, polar, custom)
ferromagnetic

Do you want a potential? (y or n)
n

Do you want a pinning potential? (y or n)
n

Please choose an initial condition (options: generic, vortex, contd)
generic

Please choose a number for this run
1

How many eigenvectors do you want to generate? (int)
100

```

Figure 48: Example run of interactiveRunBogoliubov.py to run the Bogoliubov code for a constant background in the ferromagnetic phase.

The screenshot shows a file explorer window with the following structure:

- Path: \ll masters > finalCode > spinOne > bogRun1
- Search bar: Search bogRun1
- Table of files:

Name	Date modified	Type	Size
eigVals1	01/09/2022 16:55	File	2 KB
eigVecs1	01/09/2022 16:55	File	91,885 KB
spinOneInputFM	01/09/2022 16:54	Configuration sett...	1 KB
userInputsBog1	01/09/2022 16:54	Text Document	1 KB

Figure 49: Output of a generic run is packaged in a new folder called bogRun[runNumber] where runNumber is specified by the user at the start of the code.

```
Do you wish to load eigenvectors or run Bogoliubov? (load or run)
load

Please choose a directory to load from (please append / at end)
bogRun1/

Please provide the number of run that you want to load in
1

Please choose an input file (options: ferromagnetic, polar, custom)
custom

Please specify the folder you wish to load from (including / at the end)
bogRun1/

Please type the exact name of the input file (including extension)
spinOneInputFM.ini

Do you want a potential? (y or n)
n

Do you want a pinning potential? (y or n)
n
```

Figure 50: Output to load in previously obtained results from the Bogoliubov code.

```
Do you wish to load eigenvectors or run Bogoliubov? (load or run)
run

Please choose an input file (options: ferromagnetic, polar, custom)
custom

Please specify the folder you wish to load from (including / at the end)
run1/

Please type the exact name of the input file (including extension)
spinOneInputFM.ini

Do you want a potential? (y or n)
y

Do you want a pinning potential? (y or n)
y

What value of pinning would you like? (float value)
500.0

Please choose an initial condition (options: generic, vortex, contd)
contd

Please provide the number of run that you want to load in
1

How many eigenvectors do you want to generate? (int)
100
```

Figure 51: Output of running `interactiveRunBogoliubov.py` for a non-constant initial condition that has already been passed through the ground state code.

Name	Date modified	Type	Size
eigVals1	01/09/2022 18:21	File	2 KB
eigVecs1	01/09/2022 18:21	File	91,885 KB
phiMinusOne1	28/08/2022 13:00	File	17,004 KB
phiMinusOne2	31/08/2022 21:38	File	194,084 KB
phiOne1	28/08/2022 13:00	File	17,004 KB
phiOne2	31/08/2022 21:38	File	194,084 KB
phiZero1	28/08/2022 13:00	File	16,927 KB
phiZero2	31/08/2022 21:38	File	194,084 KB
spinOneInputFM	28/08/2022 12:58	Configuration sett...	1 KB
userInputs1	28/08/2022 17:32	Text Document	1 KB
userInputs2	01/09/2022 12:34	Text Document	1 KB
userInputsBog1	01/09/2022 18:21	Text Document	1 KB

Figure 52: Output from a continued configuration is saved in the same folder as the input.

background into our Bogoliubov code to study excitations above this vortex state. As discussed in section (7.1), we must consider the different length scales present in order to determine suitable values for the dimensionless interaction parameters of the system. We get the same expression for the healing length in terms of the characteristic oscillator length as in the spin one case. This expression was given by equation (7.5). Using this we can choose suitable values for our interaction parameters β_0 , β_1 and β_2 . We keep the same setup for our grid as in the spin one case of a lattice with boundaries $a = -4$ and $b = 4$. With this, in order to ensure the healing length is smaller than the characteristic length scale of the harmonic oscillator while still keeping enough lattice spacings per healing length, we take the following interaction parameter values:

$$\begin{aligned}
 \beta_0 &= 20, \\
 \beta_1 &= 10, \\
 \beta_2 &= 10.
 \end{aligned}
 \tag{7.27}$$

These parameters give healing lengths of $\epsilon_0 \approx 1.98$, $\epsilon_1 \approx 2.8$ and $\epsilon_2 \approx 2.8$ in terms of the number of lattice spacings they take up.

Now that we have determined what we will set the parameters of our code to, we need to consider the initial condition to pass into our ground state code for a vortex state in a spin two condensate. We have seen in section (5.3.3) that we can imprint a vortex in our system by using the representative order parameter of a spin two condensate and vary the euler angles associated with a particular vortex around a closed loop from zero to the final value of these euler angles. However, this in itself will not be sufficient as an initial condition as

we also need to consider smoothing the wavefunction of the condensate so that it is a good starting approximation of the lowest energy state in that we hope our gradient descent code will converge to. Furthermore, as in the case of a spin one condensate, we will need to use a pinning potential to keep the vortex in place. For this, we again increase the potential by some constant value if we are within some specified radius of the center of the harmonic trap.

This means that we must think about how we will smooth the wavefunction. For our purposes, we will do this in the following way. We first find the ground state of a condensate with a pinning potential of 500 in the center of a harmonic trap with no interactions turned on. The initial condition for this configuration is chosen to be the representative order parameter of the phase of the wavefunction within which the vortex we wish to study occurs. This initial condition is then smoothed with a generic gaussian function in order to bring our initial state for this run closer to the ground state of a condensate in a harmonic trap. We then feed the final state of this run as the initial condition for the same system but with interactions turned on, where the interactions are set in such a way that cause the condensate to sit in the phase of interest. Once we find the final state of this run, we take it's density and use this as the smoothing function for our vortex initial condition which we then feed into our ground state code. That is, the initial condition for our vortex state is the smoothing density found from a system with a pinning potential present, but no vortex; multiplied by the representative order parameter of a particular phase of the spin two condensate which varies according to the euler angles that describe the vortex we are interested in.

We can now look at some of these vortices to see that our ground state code keeps them within our system. We have found that we can keep the long distance behaviour or winding of a vortex within our system, however, due to the small system sizes that we have been able to run, we cannot comment on the core behaviour of these vortices. Further work could be done in the future to run this code for larger system sizes and as a result, study the behaviour of the vortex cores.

In section (6.3), we saw that in order to setup a vortex as an initial condition within our system, we need to know the axis and angle of rotation corresponding to this vortex, as well as the gauge angle. Once we know this, our code can find the corresponding Euler angles and from this build the wavefunction that will serve as our initial condition for the ground state code. We also saw in section (6.3) that since we have the $SU(2)$ form of these vortices, we can use (5.28) to find the axis and angle of rotation. We already know the gauge angle of each vortex in the cyclic and biaxial nematic phases from section (5.3.3), so we have all the information we need to setup our initial condition for each vortex.

Below, we provide the information we need to setup different types of vortices within a spin two condensate for the cyclic and biaxial-nematic phases. Here, we will list elements within each conjugacy class. We will omit vortices from conjugacy classes (1) and (2) as these are just the identity and integer spin vortices. In each of these we set $n_w = 0$. We

also list the gauge angle as ϕ , and the angle of rotation as θ .

Cyclic vortex parameters

- (3) $i\sigma_y$: $\phi = 0$, $\theta = \pi$ about (0,1,0).
- (4) $\phi = \frac{2\pi}{3}$
- (a) $\tilde{\sigma}$: $\theta = \frac{2\pi}{3}$ about (-1,-1,-1).
- (b) $-i\sigma_x\tilde{\sigma}$: $\theta = \frac{2\pi}{3}$ about (1,1,-1).
- (5) $\phi = \frac{2\pi}{3}$
- (a) $-\tilde{\sigma}$: $\theta = \frac{4\pi}{3}$ about (1,1,1).
- (b) $i\sigma_x\tilde{\sigma}$: $\theta = \frac{4\pi}{3}$ about (-1,-1,1).
- (6) $\phi = \frac{4\pi}{3}$
- (a) $-\tilde{\sigma}^2$: $\theta = \frac{2\pi}{3}$ about (1,1,1).
- (b) $-i\sigma_y\tilde{\sigma}^2$: $\theta = \frac{2\pi}{3}$ about (-1,-1,1).
- (7) $\phi = \frac{4\pi}{3}$
- (a) $\tilde{\sigma}^2$: $\theta = \frac{4\pi}{3}$ about (-1,-1,-1).
- (b) $i\sigma_y\tilde{\sigma}^2$: $\theta = \frac{4\pi}{3}$ about (1,1,-1).

Biaxial-Nematic vortex parameters

- (3) $-i\sigma_x$: $\phi = 0$, $\theta = \pi$ about (1,0,0).
- (4) $-i\sigma_z$: $\phi = 0$, $\theta = \pi$ about (0,0,1).
- (5) $\phi = \pi$
- (a) $\tilde{\sigma}$: $\theta = \frac{\pi}{2}$ about (0,0,-1).
- (b) $-i\sigma_z\tilde{\sigma}$: $\theta = \frac{\pi}{2}$ about (0,0,1).
- (6) $\phi = \pi$
- (a) $-\tilde{\sigma}$: $\theta = \frac{3\pi}{2}$ about (0,0,1).
- (b) $i\sigma_z\tilde{\sigma}$: $\theta = \frac{3\pi}{2}$ about (0,0,-1).
- (7) $\phi = \pi$
- (a) $i\sigma_x\tilde{\sigma}$: $\theta = \pi$ about (-1,-1,0).
- (b) $i\sigma_y\tilde{\sigma}$: $\theta = \pi$ about (1,-1,0).

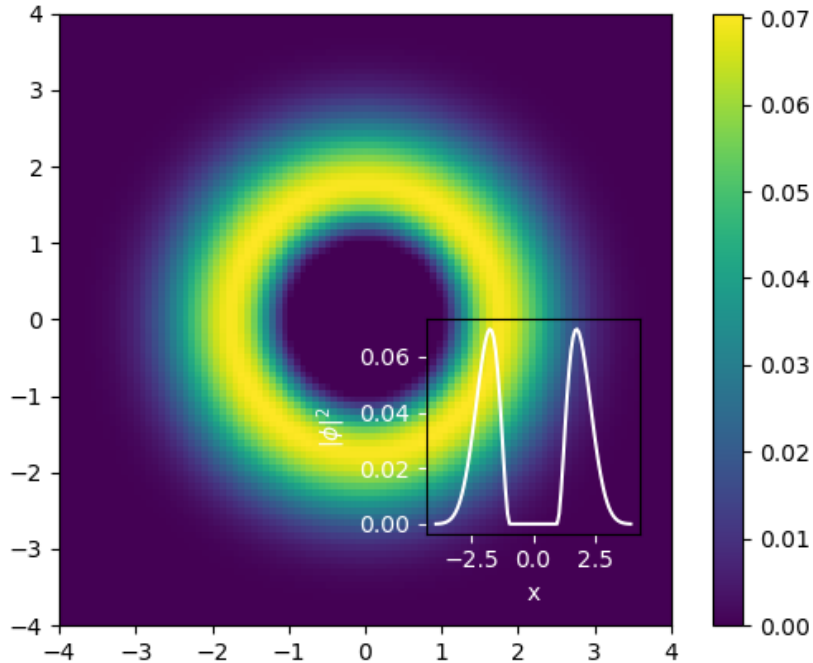


Figure 53: Density of vortex 7(a) in the cyclic phase. Inset is a cross section of this density at $y = 0$.

Now that we have listed all the relevant parameters, we need to setup a vortex within our code. Let's look at some examples of our code holding the long range behaviour of the vortex once it has been fed in as an initial condition to our ground state code.

We will first look at the example 7(a) within the cyclic phase vortices. We expect this vortex to rotate by an angle of $\frac{4\pi}{3}$ about the (-1,-1,-1) axis and for the gauge angle to shift by $\phi = \frac{4\pi}{3}$. When we construct the relevant initial condition for this vortex and pass it into the ground state code, we get the density and winding for the final state after gradient descent as shown in figures (53) and (54).

We saw earlier that vortices in the same conjugacy class should be indistinguishable as far as homotopy theory is concerned. We can investigate this by looking at the energy of the condensate at each accepted gradient descent step for vortices in the same conjugacy class in the cyclic phase. This is shown in figure (55).

As a further demonstration of our code, we show another example of a vortex state being stabilized within our ground state code. This time, we take an example from the biaxial-nematic phase. Figure (56) shows the winding of this vortex after being passed through the ground state code. The density is the same as that of vortex 7(a) in the cyclic phase as

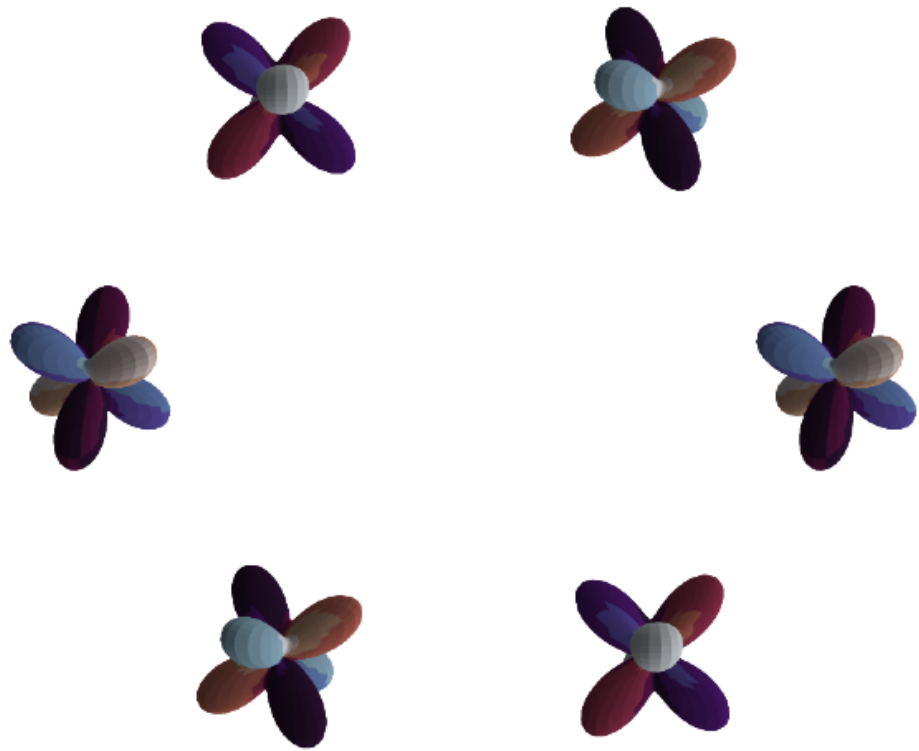


Figure 54: Winding of vortex 7(a) in the cyclic phase at a radius of $2r_s$ where r_s is the characteristic length of the harmonic trap. We can see from this that the vortex is still present and in the cyclic phase. Note that the axis of rotation was rotated onto the z-axis before being passed into the ground state code.

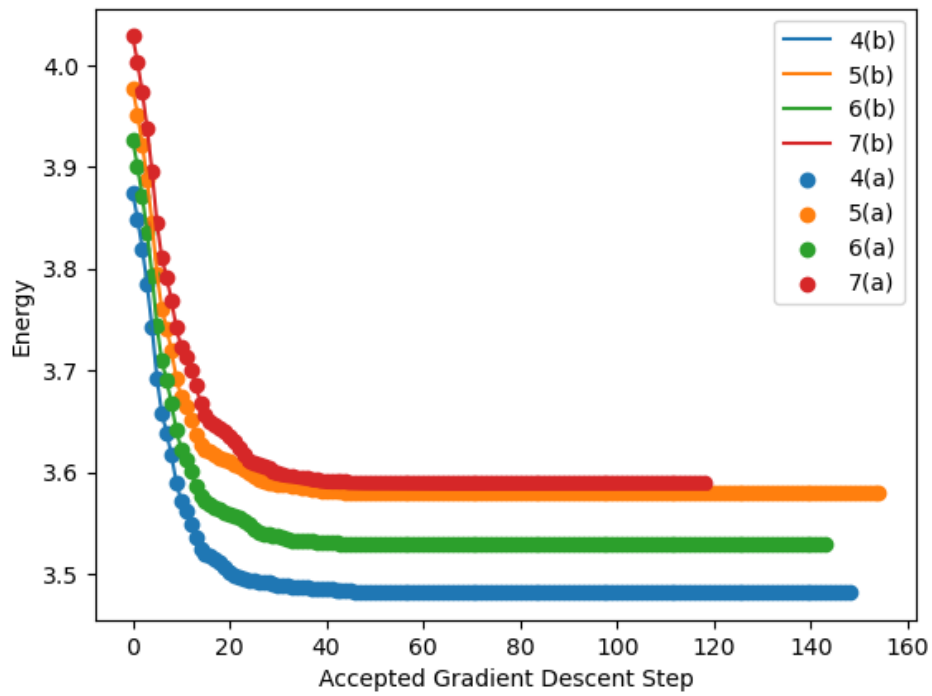


Figure 55: Comparison of the energies for the different vortices present in the cyclic phase of a spin two condensate. We see that the energies of vortices in the same conjugacy class line up.

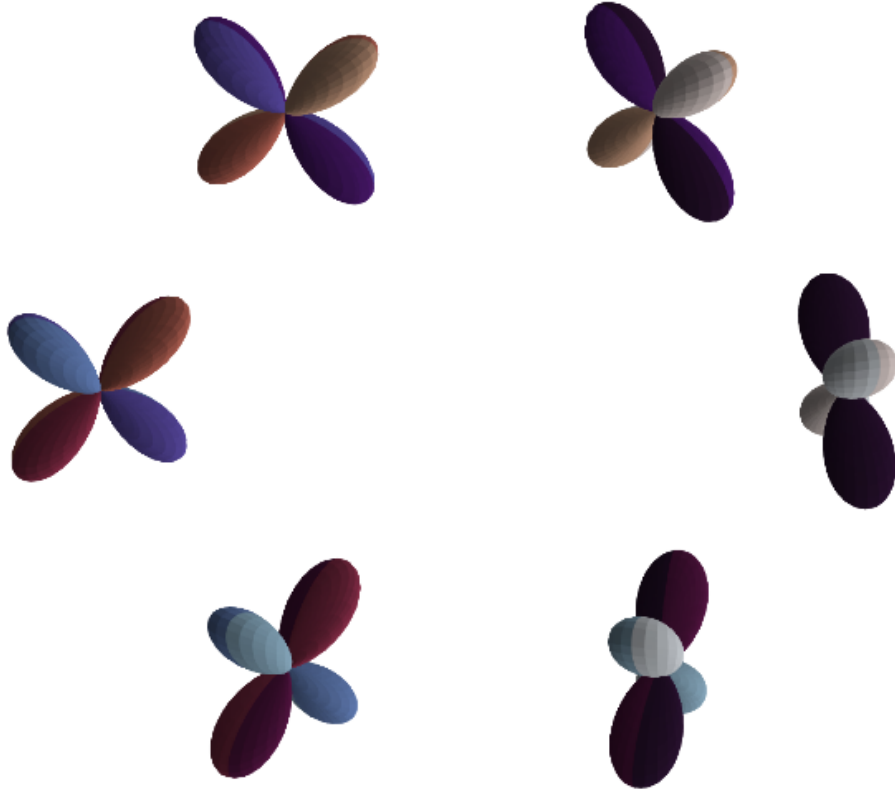


Figure 56: Winding of the vortex 7(a) in the biaxial-nematic phase at a radius of $2r_s$ where r_s is the characteristic length of the harmonic trap. We can see from this that the vortex is still present and in the correct phase. Note that the axis of rotation was rotated onto the z -axis before being passed into the ground state code.

shown in figure (53).

7.5 Spin Two Bogoliubov Spectrum

As in the spin one case, here we will compare the eigenvalues that our spin two code produces with expected results from the literature. We will do this for both the cyclic phase and biaxial-nematic phase in a zero potential system.

Cyclic Phase For the cyclic phase, we feed the background $\zeta = (1/2, 0, 1/\sqrt{2}, 0, -1/2)$ into our Bogoliubov code. This means that we are taking each component of the condensate to be constant everywhere in space.

From [42] we know that this regime should have the following spectra:

$$\begin{aligned}
\omega_1 &= \sqrt{\epsilon_k(\epsilon_k + 4\beta_1 n)}, \\
\omega_2 &= \sqrt{\epsilon_k(\epsilon_k + 2\beta_0 n)}, \\
\omega_3 &= \epsilon_k + \frac{2}{5}\beta_2 n,
\end{aligned} \tag{7.28}$$

where ϵ_k is given by (7.23).

Here we verify these spectra by running our spin two Bogoliubov code for varying values of β_1 and β_2 , while keeping β_0 fixed at $\beta_0 = 20$. We do this simultaneously by introducing a new variable λ that varies between zero and one and then vary β_1 and β_2 according to the following:

$$\begin{aligned}
\beta_1 &= 10 + 30\lambda, \\
\beta_2 &= 10 + 30\lambda.
\end{aligned} \tag{7.29}$$

If we produce a scatter plot of the lowest momentum eigenvalues produced by our code and plot the expected spectra on top of these, we see that they agree as in figure (57).

Biaxial-Nematic Phase

For the biaxial-nematic phase, we feed the background $\zeta = (1/\sqrt{2}, 0, 0, 0, 1/\sqrt{2})$ into our Bogoliubov code; again taking each component to be these constants everywhere in space. From [43], we know that this regime should have the following spectra for zero potential. Note that here we have used (3.38) to convert from the strength of interaction parameters, g_F , which are used to express the spectra in [43].

$$\begin{aligned}
\omega_1 &= \sqrt{\epsilon_k \left(\epsilon_k + 2\beta_0 n + \frac{2}{5}\beta_2 n \right)}, \\
\omega_2 &= \sqrt{\epsilon_k \left(\epsilon_k + 8\beta_1 n - \frac{2}{5}\beta_2 n \right)}, \\
\omega_3 &= \sqrt{\epsilon_k \left(\epsilon_k - \frac{2}{5}\beta_2 n \right)}, \\
\omega_4 &= \sqrt{\epsilon_k \left(\epsilon_k + 2\beta_1 n - \frac{2}{5}\beta_2 n \right)},
\end{aligned} \tag{7.30}$$

where ϵ_k is given by (7.23).

Just as in the cyclic phase, we can verify these spectra with our Bogoliubov code. We will again take a parameter λ that varies between zero and one, and use it to vary β_1 and

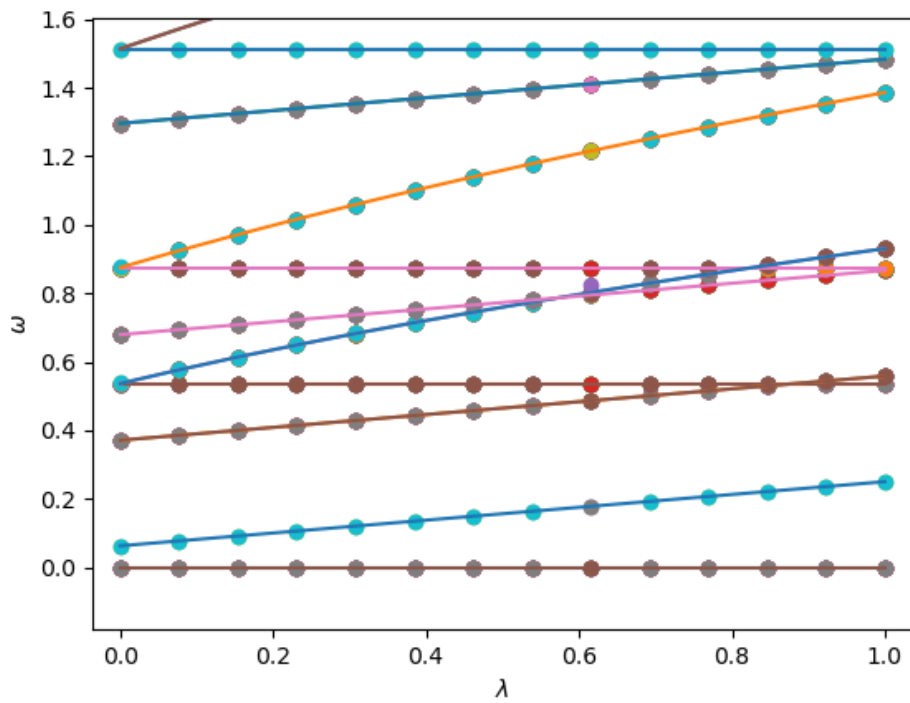


Figure 57: Scatter plot of the low lying eigenvalues for the cyclic phase of a spin two condensate in zero potential. Exact results are plotted as lines on top. We see that these match.

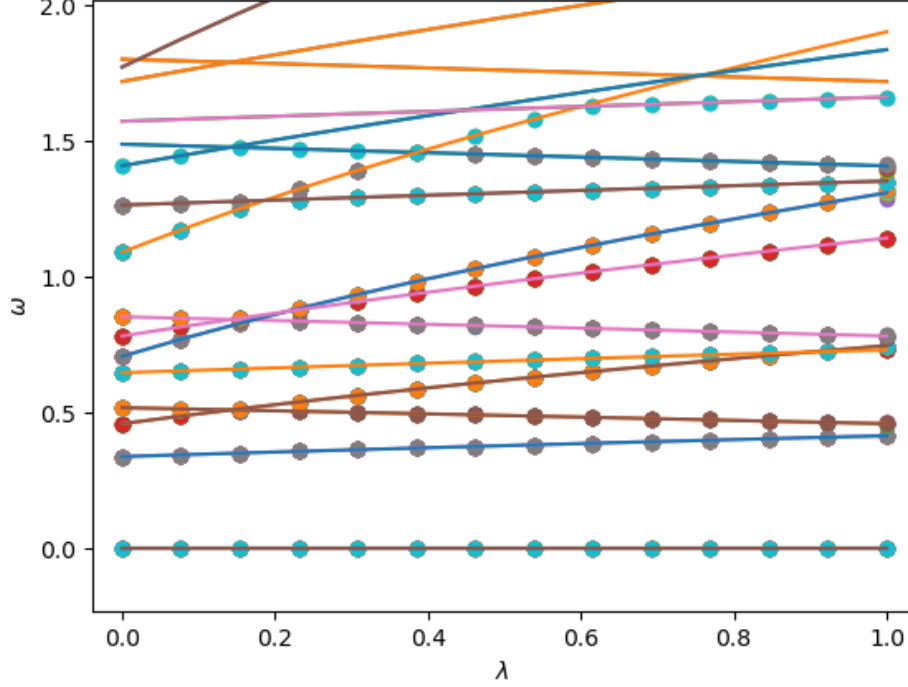


Figure 58: Scatter plot of the low lying eigenvalues for the biaxial-nematic phase of a spin two condensate in zero potential. Exact results are plotted as lines on top. We see that these match.

β_2 in the following way:

$$\beta_1 = 10 + 30\lambda, \tag{7.31}$$

$$\beta_2 = -(10 + 30\lambda). \tag{7.32}$$

We run our Bogoliubov code for each of these values of β_1 and β_2 while again keeping β_0 fixed at $\beta_0 = 20$ and then plot them against the exact spectra to get the plot shown in figure (58). We again see that our results agree with the expected results, which serves as a further verification of the proper functionality of our Bogoliubov code.

7.6 Bogoliubov Excitations of Vortex States

We can now combine our ground state and Bogoliubov code to look at elementary excitations of vortices in the ground state of a spin two condensate. We are particularly interested in

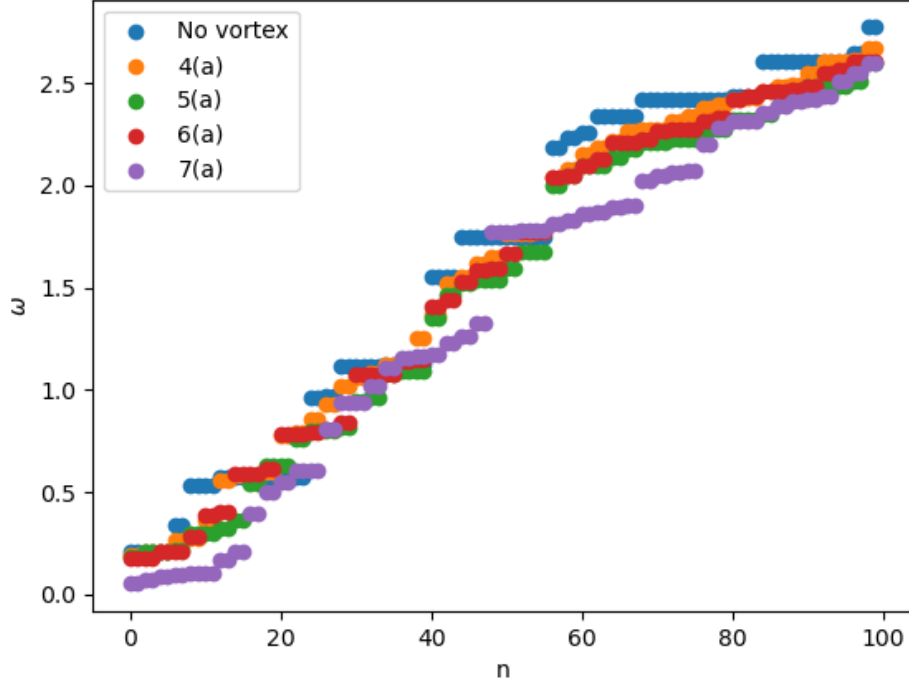


Figure 59: Spectra for vortices in the cyclic phase as well as a state with no vortex (pinning potential present) for comparison.

whether we can distinguish vortex types from each other as well as from a state with no vortex present. The best way of determining this is by looking at the Bogoliubov spectra for each vortex as well as for the state with a pinning potential but no vortex present. We will first look at this for the cyclic phase vortices before looking at the biaxial-nematic phase.

Cyclic phase vortices By generating vortex ground states as in section (7.4) and feeding these into our Bogoliubov code, we obtain the Bogoliubov spectrum for this state. We run this for the same parameters as mentioned in section (7.4) and generate the first hundred modes. If we plot these spectra for one vortex in each conjugacy class as well as a state with a pinning potential present but no vortex, we get the plot for the eigenvalues like in figure (59).

In order to get a better comparison between these spectra, we can split them out by just adding a different constant to each one. If we do this we can see more detail of each spectra as in figure (60).

We see from figure (59) that we can indeed distinguish the different types of vortices in the cyclic phase by looking at their excitation spectra. From figure (60), we see that there

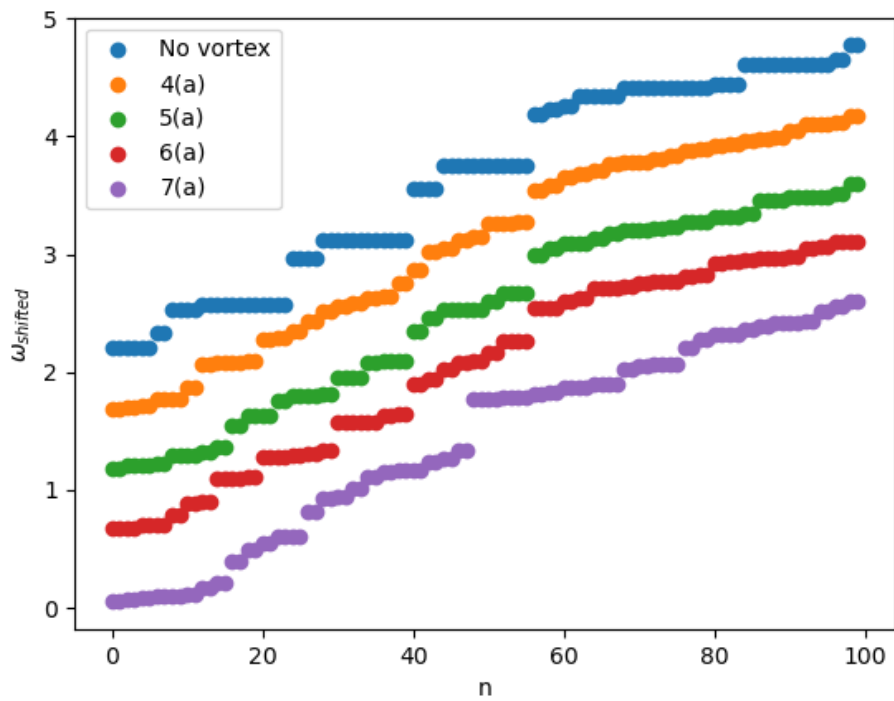


Figure 60: Spectra for vortices in the cyclic phase as well as a state with no vortex (pinning potential present) for comparison. These spectra have been shifted by different constants in order to gain a better comparison of each of their shape.

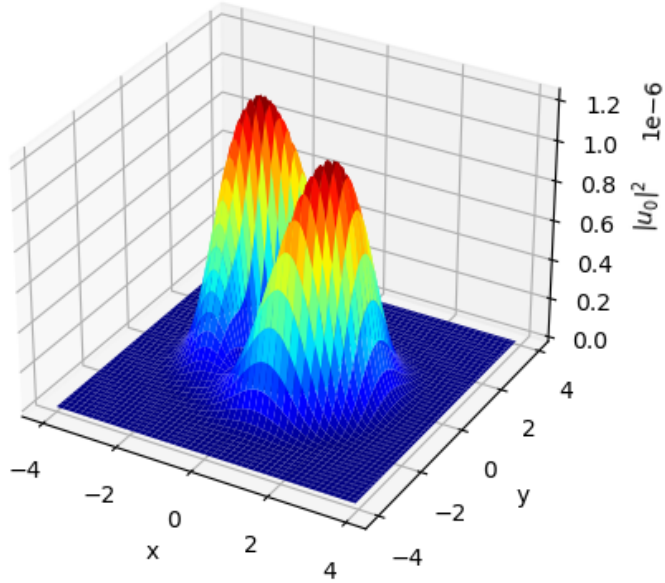


Figure 61: $u_0(\vec{r})$ component of mode 8 for a state with no vortex as in fig (60).

is much more degeneracy in the eigenvalues of the state with no vortex compared to the vortex states. This suggests that there is a symmetry present for the system with no vortex that is broken when a vortex is introduced. Although we have not determined in general what this symmetry is or why exactly it is broken by the vortex states, which may be due to lattice effects in our code; we do have an example from the Bogoliubov modes generated that shows a rotational symmetry in the non-vortex state. Here we just show this for u_0 for mode 8 and 9. We see from figures (61) and (62) that these two modes are a rotation of each other which shows the symmetry present as both have the same eigenvalue as displayed in the third band of eigenvalues for the non-vortex state in figure (60). We note that the same rotation occurs for all other non-zero components of these two modes.

Biaxial-Nematic Phase Vortices We now do the same analysis for the biaxial-nematic phase and look at the low lying spectra of vortex states listed in section (7.4). Figures (63) and (64) show the original spectra for these states and the spectra of these states shifted for ease of comparison.

Again, we can see that the vortices in the biaxial-nematic phase can be distinguished from each other by looking at their Bogoliubov spectra. We also again see that the degeneracy of

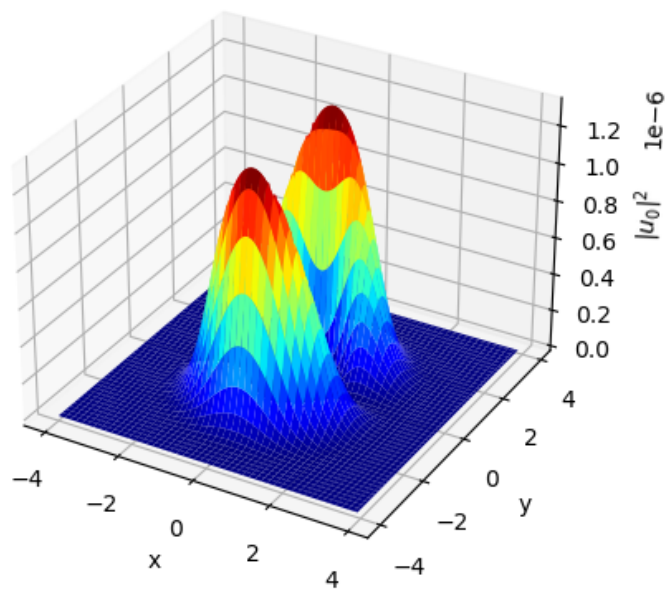


Figure 62: $u_0(\vec{r})$ component of mode 9 for a state with no vortex as in fig (60). We see that this is a rotation of u_0 of mode 8 in fig (61).

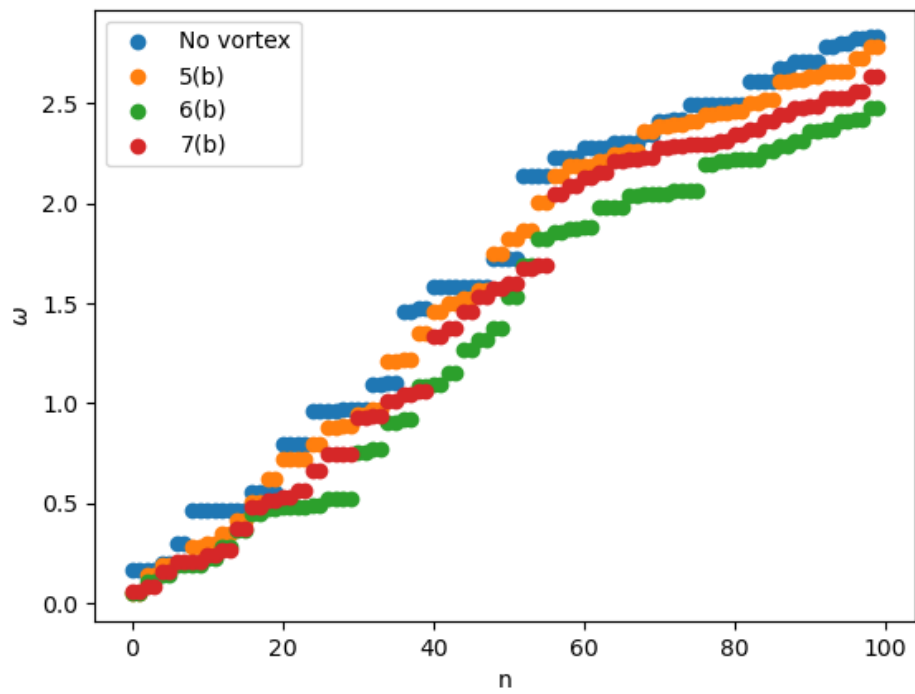


Figure 63: Spectra for vortices in the biaxial-nematic phase as well as a state with no vortex (pinning potential present) for comparison.

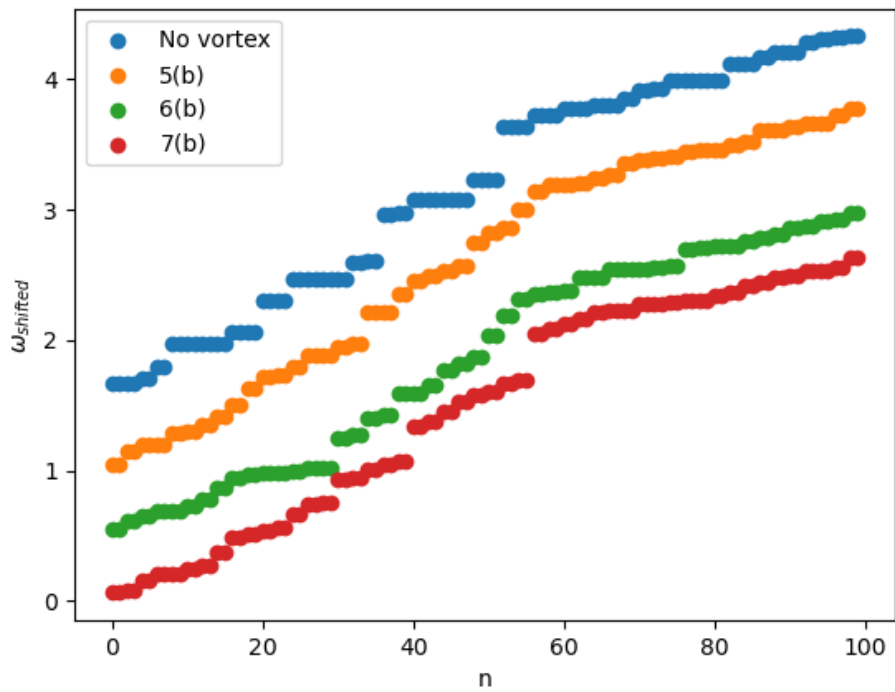


Figure 64: Spectra for vortices in the biaxial-nematic phase as well as a state with no vortex (pinning potential present) for comparison. These spectra have been shifted by different constants in order to gain a better comparison of each of their shape.

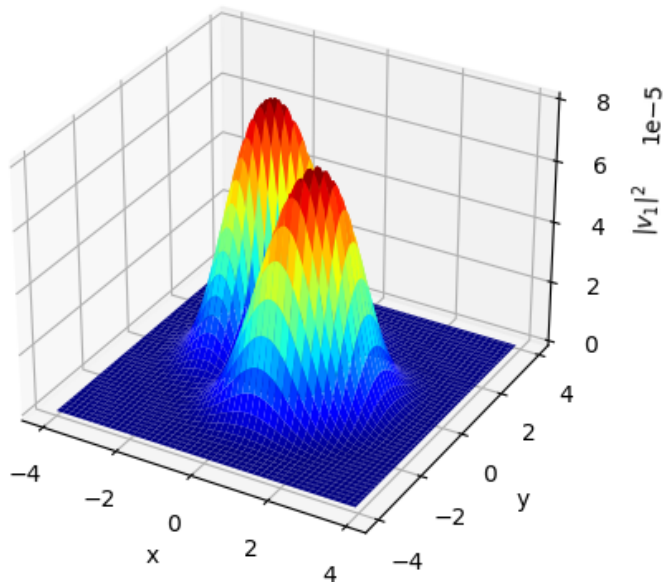


Figure 65: $|v_1|^2$ for mode 12 of the non-vortex state in the biaxial-nematic phase.

a state with no vortex is higher than that for vortex states. This again suggests some sort of symmetry is broken when looking at the vortex states. In a similar fashion to what was done in the analysis of the cyclic phase, we can see that some of the symmetry present for the non-vortex state is rotational. We do not include plots here as it is not instructive after seeing this for the cyclic phase.

We know that rotational symmetry is not the only cause of the degeneracy as we can look at other modes with the same eigenvalues and see that they are not just simple rotations of each other. This can be seen by looking at modes 12 and 14 of the non-vortex state in the biaxial-nematic phase. Figures (65) and (66) show the absolute value of the v_1 component of mode 12 and 14 for the non-vortex state in the biaxial-nematic phase. Although a rotation does occur between these two configurations, we see that this is not the only change that has occurred as the amplitudes of the two configurations are different which would suggest a rotation in spin space has also occurred.

A possible trajectory to pursue from this is to look at exactly what the symmetry we are seeing in the non-vortex states of the cyclic and biaxial-nematic phases is and why this is broken when we introduce a vortex into the system.

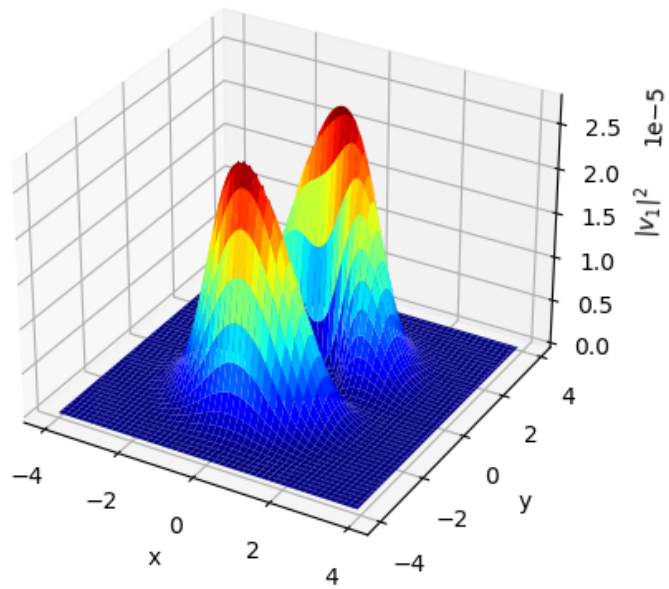


Figure 66: $|v_1|^2$ for mode 14 of the non-vortex state in the biaxial-nematic phase. It appears that a rotation in space and a spin rotation has occurred in order to get to this state from the configuration shown in fig (65)

```

What phase would you like to look at? (cyclic or binem)
binem

Please enter the x-axis of the vortex
-1

Please enter the y-axis of the vortex
-1

Please enter the z-axis of the vortex
0

Please enter the angle of rotation of the vortex
(as a fraction of pi radians, eg for 4*pi/3 enter 4 followed by a space and then 3).
1 1

Please enter the value for the gauge angle of the vortex
(in the same format as that entered for the angle of rotation).
1 1

Do you want to generate a smoothing function or load one in? (generate or load)
generate

What number would you like to give to this run?
6

Please enter how many generations you wish to run before computing the smoothing density.
2

Would you like to save all generations? (y or n)
y

```

Figure 67: User input to `interactiveGroundState.py` for producing vortex 7(a) in the ground state of the biaxial-nematic phase.

7.7 Running the spin two codes

Now that we have seen results generated by our spin two ground state and Bogoliubov codes, we will now give an example of how a user can run these codes to produce such results. The example we will provide will be that of vortex 7(a) of the biaxial-nematic phase. We will first show how this vortex is produced in our ground state code and then show how we can run Bogoliubov on top of this. The two files to do this are listed as `interactiveGroundState.py` and `interactiveBogoliubov.py`.

Let's first look at generating vortex 7(a) in the ground state of the system using `interactiveGroundState.py`. The user will be asked a series of questions such as what phase of the wavefunction they would like to be in and what parameters they would like to set to characterise the vortex. These parameters can be found in section (7.4). An example of user input for this scenario is shown in figure (67).

Note that for the gauge angle and angle of rotation, the input format is not conventional and so we will just briefly describe it here. If the user would like to enter an angle of $\frac{4\pi}{3}$, this is entered as `4 3`. That is, the number 4, followed by a space, followed by the number

3. Due to this format, if the user wants an angle of π , this must be input as **1 1**. Similarly for an angle of zero, this must be input as **0 1**.

As mentioned earlier, in order to smooth the wavefunction for a vortex, we must generate wavefunctions for the system with a pinning potential in the center of the condensate without and with interactions. Within **interactiveGroundState.py**, the user has the choice to generate these wavefunctions before generating the vortex or load in a previously generated wavefunction to use for smoothing the vortex wavefunction. If the user chooses to generate new wavefunctions, these wavefunctions will be saved, starting with the number 90 and increasing by one as we slowly turn on the interactions, where the pinning potential is turned on in all cases. The user can specify how slowly to turn the interactions to the final value by specifying to run more generations of wavefunctions before calculating the smoothing density. As a result of this, the user is encouraged not to save their own configuration runs with these numbers as it will lead to unexpected results.

Once this code finishes running. The output for this configuration, along with a user input text file and the configuration file used, will be saved in a folder called **run5**. If we wish to run Bogoliubov on top of this vortex, we can run **interactiveBogoliubov.py**, specifying that we wish to work in the directory where our vortex configuration sits, which in this case is **run5**. We do not show output for running this file as the steps to do so are self-explanatory when running. If the user chooses to run **interactiveBogoliubov.py** on top of the already generated vortex in **run5**, the eigenvalues and eigenvectors for this will be stored in the same folder. An example of the contents stored in this folder after running both files is shown in figure (68).

7.8 Limitations of our code

It is worth noting that there are limitations to our code. The first of these is that since we are only able to run for a certain amount of lattice spacings before the code will not run in a reasonable amount of time on our hardware, we can only look at very small system sizes. As a result of this, the parameters that we use to obtain vortices in our system are very sensitive and making certain changes to these may lead to unexpected results. More work could be done in the future to look at whether our code would be more versatile if we could run for larger system sizes and more lattice spaces.

Another limitation worth mentioning is that there are particular vortices that we seemed to be unable to fully hold in the ground state using our code. An example of such a vortex is vortex (3) in the cyclic phase. The result we obtain for this vortex after running through the ground state can be seen in figure (69).

We also came across an example seen in vortices in conjugacy class (6) of the biaxial-nematic phase where the Bogoliubov spectrum contained complex eigenvalues which is a sign of instability [44]. Figure (70) shows the real and imaginary part of the Bogoliubov spectrum for vortex 6(b) of the biaxial nematic phase.

↑ This PC > Documents > masters > finalCode > spinTwo > run6

Name	Date modified	Type	Size
eigVals	27/10/2022 21:54	File	2 KB
eigVecs	27/10/2022 21:54	File	156,251 KB
phiMinusOne6	27/10/2022 21:32	File	17,464 KB
phiMinusOne90	27/10/2022 21:27	File	15,779 KB
phiMinusOne91	27/10/2022 21:29	File	9,498 KB
phiMinusTwo6	27/10/2022 21:32	File	17,464 KB
phiMinusTwo90	27/10/2022 21:27	File	15,779 KB
phiMinusTwo91	27/10/2022 21:29	File	9,498 KB
phiOne6	27/10/2022 21:32	File	17,464 KB
phiOne90	27/10/2022 21:27	File	15,779 KB
phiOne91	27/10/2022 21:29	File	9,498 KB
phiTwo6	27/10/2022 21:32	File	17,464 KB
phiTwo90	27/10/2022 21:27	File	15,779 KB
phiTwo91	27/10/2022 21:29	File	9,498 KB
phiZero6	27/10/2022 21:32	File	17,464 KB
phiZero90	27/10/2022 21:27	File	15,779 KB
phiZero91	27/10/2022 21:29	File	9,498 KB
spinTwoInputBinem	27/10/2022 21:23	Configuration sett...	1 KB
userInputs	27/10/2022 21:23	Text Document	1 KB

Figure 68: Output from `interactiveGroundState.py` and `interactiveBogoliubov.py` is stored in a separate folder specified at runtime.

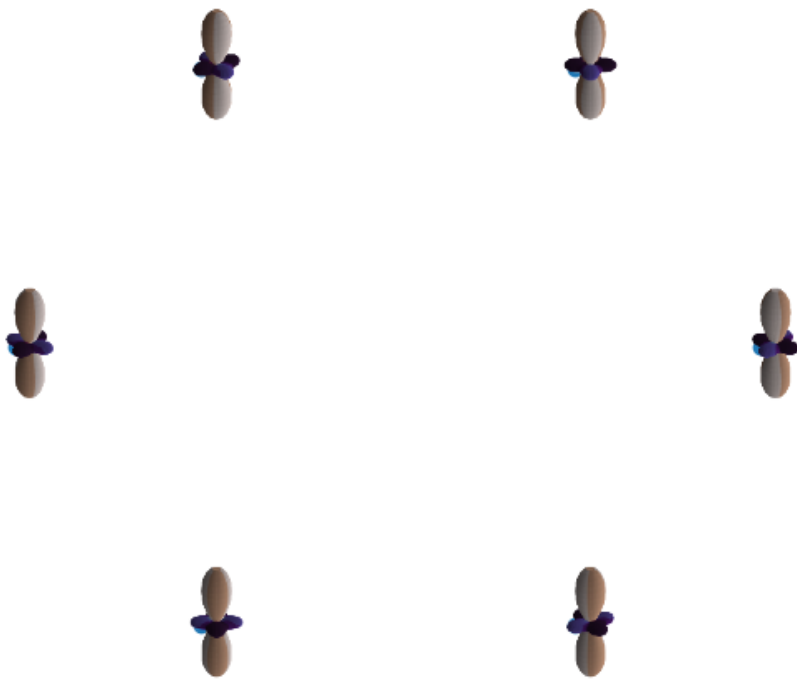


Figure 69: Example of the end state we obtain for vortex (3) in the cyclic phase. We can see that the vortex has not been held properly here. Note that this is after 2000 iterations of our ground state code.

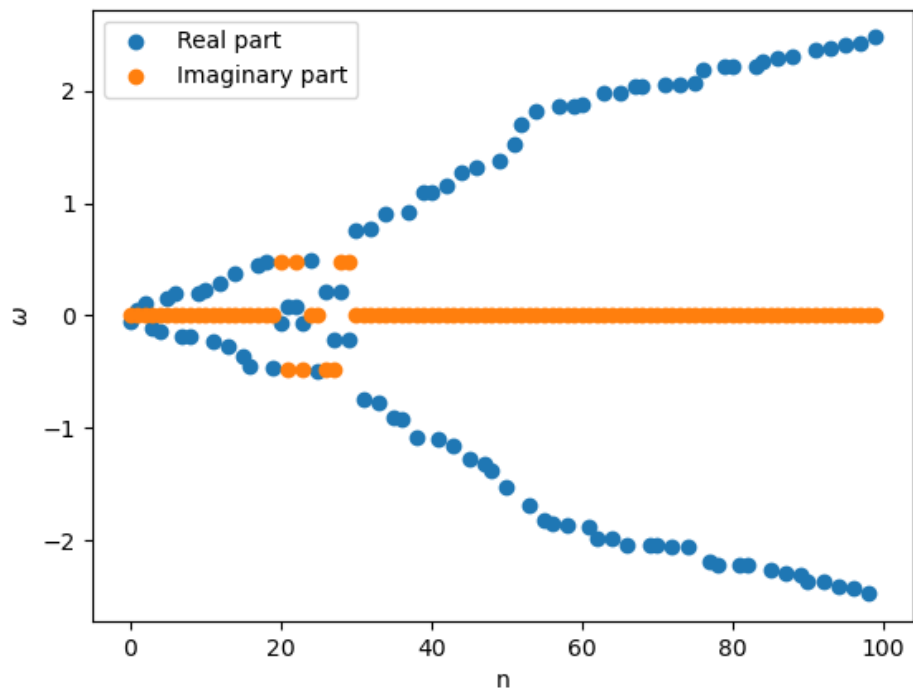


Figure 70: The real and imaginary parts of the eigenvalues for each mode, n , in the spectrum of vortex 6(b) of the biaxial-nematic phase.

We note that these vortices that are mentioned above are the only ones that we have seen issues with and all others seem to be held well by our code and have all real eigenvalues in their Bogoliubov spectra. As a result, the results that we discuss in the previous section are still valid.

Conclusion

Throughout this thesis, with the aim of developing our own codes, we have looked at the different types of vortices that can be hosted in spinor condensates, as well as reviewing the basic physics and mean-field description of a Bose-Einstein condensate. We discussed how the variety of vortices present in a condensate increases as we look at higher spin, with only an integer winding vortex present in a spinless system, compared to the non-abelian vortices with both phase and spin variation present in spin two. The link made between non-abelian vortices in a spin two condensate and quantum computation in [21] was the initial inspiration for looking at these vortices. We hope that the information provided in this thesis on how these vortices are described in a condensate will give others the knowledge needed to use these in fields such as the aforementioned; as well as encourage others into what is an interesting field of research.

Alongside the theory mentioned above, we have also developed codes to simulate the ground state of a spin one and spin two condensate, as well as codes to look at the Bogoliubov excitations of these returned states. With a particular interest in vortex states as mentioned, we also spent time developing methods for imprinting vortices as initial conditions for our ground state codes. These codes have been published on a public repository and a detailed description of how these codes were developed, including the options available for running them, has been included in this thesis. As well as this, we have provided results showing the output of our code, including examples of non-abelian vortices that have been held in the ground state by our code in both the cyclic and biaxial-nematic phase. We have also discussed the limitations we found within our codes; the studying of which would be worth investigating further.

Putting together both our ground state and Bogoliubov code in spin two, we were able to show that we can use the spectra of the elementary excitations of vortex states to distinguish the class of vortex present in a condensate. We also saw that the degeneracy of a state with a pinning potential with no vortex present was higher than the same state with a vortex present and provided an example of some of the symmetry that this points to. Studying this symmetry in more detail, as well as looking at why this symmetry seems to be broken when we introduce a vortex into the system would be an interesting avenue of further research.

We note that codes have been previously developed in Fortran and subsequently in C for simulating spinless condensates in fully anisotropic traps [45, 46]. Since we started this research, codes have been published in Fortran in order to look at spin-orbit coupled spin one and spin two condensates [47, 48]. We hope that our code will fit into this landscape to be used for initial exploration of systems of interest before moving to more complex codes. Providing codes in a higher level language such as python will provide accessibility. Furthermore, the integration of vortices into our code, as well as the ability to look at Bogoliubov excitations on top of these vortex states should also serve as useful functionality for users.

In recent years, research surrounding Bose-Einstein condensates has only continued to increase, with recent developments such as looking at condensates in micro-gravity [49], as well as emerging fields such as quantum turbulence [50, 51] and overlapping condensates of different atom species [52] only adding to the excitement surrounding this field of research. As a result, we hope that the codes developed as part of this thesis, along with the thesis itself will serve as a suitable introduction into this field and provide early career researchers with simple tools that can be used to investigate these systems further.

References

- [1] A. Einstein. *Quantentheorie des einatomigen idealen Gases. Zweite Abhandlung*, pages 245–257. John Wiley & Sons, Ltd, 2005.
- [2] Bose. Plancks Gesetz und Lichtquantenhypothese. *Zeitschrift fur Physik*, 26(1):178–181, December 1924.
- [3] W Ketterle, M R Andrews, K B Davis, D S Durfee, D M Kurn, M O Mewes, and N J van Druten. Bose–einstein condensation of ultracold atomic gases. *Physica Scripta*, 1996(T66):31, jan 1996.
- [4] M. H. Anderson, J. R. Ensher, M. R. Matthews, C. E. Wieman, and E. A. Cornell. Observation of bose-einstein condensation in a dilute atomic vapor. *Science*, 269(5221):198–201, 1995.
- [5] K. B. Davis, M. O. Mewes, M. R. Andrews, N. J. van Druten, D. S. Durfee, D. M. Kurn, and W. Ketterle. Bose-einstein condensation in a gas of sodium atoms. *Phys. Rev. Lett.*, 75:3969–3973, Nov 1995.
- [6] C. C. Bradley, C. A. Sackett, J. J. Tollett, and R. G. Hulet. Evidence of bose-einstein condensation in an atomic gas with attractive interactions [phys. rev. lett. 75, 1687 (1995)]. *Phys. Rev. Lett.*, 79:1170–1170, Aug 1997.
- [7] Gordon Baym and C. J. Pethick. Ground-state properties of magnetically trapped bose-condensed rubidium gas. *Phys. Rev. Lett.*, 76:6–9, Jan 1996.
- [8] Klaus Kirsten and David J. Toms. Bose-einstein condensation of atomic gases in a general harmonic-oscillator confining potential trap. *Physical Review A*, 54(5):4188–4203, nov 1996.
- [9] Masahito Ueda and Anthony J. Leggett. Macroscopic quantum tunneling of a bose-einstein condensate with attractive interaction. *Physical Review Letters*, 80(8):1576–1579, feb 1998.
- [10] C. W. Gardiner, P. Zoller, R. J. Ballagh, and M. J. Davis. Kinetics of bose-einstein condensation in a trap. *Physical Review Letters*, 79(10):1793–1796, sep 1997.
- [11] Stenger, J., Inouye, S., Stamper-Kurn, D. et al. Spin domains in ground-state bose–einstein condensates. *Nature*, 396:345–348, 1998.
- [12] Tomoya Isoshima, Kazushige Machida, and Tetsuo Ohmi. Spin-domain formation in spinor bose-einstein condensation. *Physical Review A*, 60(6):4857–4863, dec 1999.
- [13] K. W. Madison, F. Chevy, W. Wohlleben, and J. Dalibard. Vortex formation in a stirred bose-einstein condensate. *Physical Review Letters*, 84(5):806–809, jan 2000.

- [14] M. R. Matthews, B. P. Anderson, P. C. Haljan, D. S. Hall, C. E. Wieman, and E. A. Cornell. Vortices in a bose-einstein condensate. *Physical Review Letters*, 83(13):2498–2501, sep 1999.
- [15] An-Chun Ji, W. M. Liu, Jun Liang Song, and Fei Zhou. Dynamical creation of fractionalized vortices and vortex lattices. *Physical Review Letters*, 101(1), jul 2008.
- [16] Liang-Liang Xu, Yong-Kai Liu, Shiping Feng, and Shi-Jie Yang. Fractional spin-vortex states in $F = 2$ spinor bose-einstein condensates. *Physics Letters A*, 383(21):2515–2518, 2019.
- [17] Michikazu Kobayashi, Yuki Kawaguchi, and Masahito Ueda. Vortex tiling in a spin-2 spinor bose-einstein condensate, 2009.
- [18] Sang Won Seo, Seji Kang, Woo Jin Kwon, and Yong il Shin. Half-quantum vortices in an antiferromagnetic spinor bose-einstein condensate. *Physical Review Letters*, 115(1), jul 2015.
- [19] Y. Xiao, M. O. Borgh, L. S. Weiss, A. A. Blinova, J. Ruostekoski, and D. S. Hall. Controlled creation and decay of singly-quantized vortices in a polar magnetic phase. *Communications Physics*, 4(1), mar 2021.
- [20] Y. Xiao, M. O. Borgh, A. Blinova, T. Ollikainen, J. Ruostekoski, and D. S. Hall. Topological superfluid defects with discrete point group symmetries. *Nature Communications*, 13(1), aug 2022.
- [21] T. Mawson, T. C. Petersen, J.K. Slingerland, and T.P. Simula. Braiding and fusion of non-abelian vortex anyons. *Physical Review Letters*, 123(14), oct 2019.
- [22] Sumathi Rao. An anyon primer, 1992.
- [23] Simon Trebst, Matthias Troyer, Zhenghan Wang, and Andreas W. W. Ludwig. A short introduction to fibonacci anyon models. *Progress of Theoretical Physics Supplement*, 176:384–407, 2008.
- [24] N. E. Bonesteel, L. Hormozi, G. Zikos, and S. H. Simon. Braid topologies for quantum computation. *Physical Review Letters*, 95(14), sep 2005.
- [25] <https://github.com/nfox66/becSuite>.
- [26] C.J Pethick and H. Smith. *Bose-Einstein Condensation in Dilute Gases*. Cambridge University Press, Cambridge, UK, 2002.
- [27] Yuki Kawaguchi and Masahito Ueda. Spinor bose-einstein condensates. *Physics Reports*, 520(5):253–381, nov 2012.

- [28] Masahito Ueda and Masato Koashi. Theory of spin-2 bose-einstein condensates: Spin correlations, magnetic response, and excitation spectra. *Phys. Rev. A*, 65:063602, May 2002.
- [29] Tetsuo Ohmi and Kazushige Machida. Bose-einstein condensation with internal degrees of freedom in alkali atom gases. *Journal of the Physical Society of Japan*, 67(6):1822–1825, jun 1998.
- [30] Tin-Lun Ho. Spinor bose condensates in optical traps. *Phys. Rev. Lett.*, 81:742–745, Jul 1998.
- [31] Keiji Murata, Hiroki Saito, and Masahito Ueda. Broken-axisymmetry phase of a spin-1 ferromagnetic bose-einstein condensate. *Physical Review A*, 75(1), jan 2007.
- [32] Ronald Y. Dong. *Nuclear Magnetic Resonance of Liquid Crystals*, chapter Back Matter, pages 255–260. Springer New York, NY, 1985.
- [33] N. D. Mermin. The topological theory of defects in ordered media. *Rev. Mod. Phys.*, 51:591–648, Jul 1979.
- [34] Gordon W. Semenoff and Fei Zhou. Discrete symmetries and $1/3$ -quantum vortices in condensates of $F = 2$ cold atoms. *Physical Review Letters*, 98(10), mar 2007.
- [35] Mark Friesen Yun-Pil Shim, Jianjia Fei, Sangchul Oh, Xuedong Hu. Single-qubit gates in two steps with rotation axes in a single plane. arxiv.org/abs/1303.0297, 2013.
- [36] Weizhu Bao and Yongyong Cai. Review article: Mathematical models and numerical methods for spinor bose-einstein condensates. *Communications in Computational Physics*, 24(4), 2018.
- [37] M. D. Lee, S. A. Morgan, M. J. Davis, and K. Burnett. Energy-dependent scattering and the gross-pitaevskii equation in two-dimensional bose-einstein condensates. *Phys. Rev. A*, 65:043617, Apr 2002.
- [38] Maresuke Shiraishi. *Probing the Early Universe with the CMB Scalar, Vector and Tensor Bispectrum*, chapter Back Matter, pages 155–164. Springer Tokyo, 2013.
- [39] Ian R. Cole. Modelling CPV. 6 2015.
- [40] Kuei Sun, Chunlei Qu, Yong Xu, Yongping Zhang, and Chuanwei Zhang. Interacting spin-orbit-coupled spin-1 bose-einstein condensates. *Physical Review A*, 93(2), feb 2016.
- [41] Yali Gao and Yongyong Cai. Numerical methods for bogoliubov-de gennes excitations of bose-einstein condensates. *Journal of Computational Physics*, 403:109058, 2020.

- [42] Gong-Ping Zheng, Lei-Kuan Xu, Shuai-Feng Qin, Wen-Tian Jian, and J.-Q. Liang. An order-by-disorder process in the cyclic phase of spin-2 condensate with a weak magnetic field. *Annals of Physics*, 334:341–350, 2013.
- [43] J-P Martikainen and K-A Suominen. Collective excitations in an $F = 2$ bose-einstein condensate. *Journal of Physics B: Atomic, Molecular and Optical Physics*, 34(21):4091–4101, oct 2001.
- [44] Y. Nakamura, M. Mine, M. Okumura, and Y. Yamanaka. Condition for emergence of complex eigenvalues in the bogoliubov–de gennes equations. *Physical Review A*, 77(4), apr 2008.
- [45] P. Muruganandam and S.K. Adhikari. Fortran programs for the time-dependent gross–pitaevskii equation in a fully anisotropic trap. *Computer Physics Communications*, 180(10):1888–1912, 2009.
- [46] Dušan Vudragović, Ivana Vidanović, Antun Balaž, Paulsamy Muruganandam, and Sadhan K. Adhikari. C programs for solving the time-dependent gross–pitaevskii equation in a fully anisotropic trap. *Computer Physics Communications*, 183(9):2021–2025, 2012.
- [47] Pardeep Kaur, Arko Roy, and Sandeep Gautam. Fortress: Fortran programs for solving coupled gross–pitaevskii equations for spin–orbit coupled spin-1 bose–einstein condensate. *Computer Physics Communications*, 259:107671, 2021.
- [48] Paramjeet Banger, Pardeep Kaur, Arko Roy, and Sandeep Gautam. Fortress ii: Fortran programs for solving coupled gross-pitaevskii equations for spin-orbit coupled spin-2 bose-einstein condensate, 2020.
- [49] Aveline, D.C, Williams, J.R., Elliott, E.R et al. Observation of bose-einstein condensates in an earth-orbiting research lab. *Nature*, 582:193–197, 2020.
- [50] L. Madeira, A. Cidrim, M. Hemmerling, M. A. Caracanhas, F. E. A. dos Santos, and V. S. Bagnato. Quantum turbulence in bose–einstein condensates: Present status and new challenges ahead. *AVS Quantum Science*, 2(3):035901, 2020.
- [51] Áttis V. M. Marino, Lucas Madeira, André Cidrim, F. E. A. dos Santos, and Vanderlei S. Bagnato. Momentum distribution of vinen turbulence in trapped atomic bose–einstein condensates. *The European Physical Journal Special Topics*, 230(4):809–812, apr 2021.
- [52] Claire Warner, Aden Z. Lam, Niccolò Bigagli, Henry C. Liu, Ian Stevenson, and Sebastian Will. Overlapping bose-einstein condensates of Na and Cs. *Physical Review A*, 104(3), sep 2021.